



UNIVERSITÀ DEGLI STUDI DI PALERMO

Biologia Cellulare e Scienze e Tecnologie del Farmaco - Indirizzo Scienze Farmaceutiche
Dipartimento di Scienze e Tecnologie Biologiche Chimiche e Farmaceutiche (STEBICEF)
Settore Scientifico Disciplinare - SSD:CHIM/08

Synthesis and antiproliferative activity of thiazolyl-bis-pyrrolo[2,3-*b*]pyridines, indolyl-thiazolyl-pyrrolo[2,3-*b*]pyridines and indolyl-thiazolyl-pyrrolo[2,3-*c*]pyridines, nortopsentin analogues

IL DOTTORE
Doct. **GLORIA DI VITA**

IL COORDINATORE
Chiar.mo Prof. PATRIZIA DIANA

IL TUTOR
Chiar.mo Prof. GIROLAMO CIRINCIONE

INDEX

THIAZOLYL-BIS-PYRROLO[2,3-*b*]PYRIDINES, INDOLYL-THIAZOLYL-PYRROLO[2,3-*b*]PYRIDINES AND INDOLYL-THIAZOLYL-PYRROLO[2,3-*c*]PYRIDINES

- INTRODUCTION 2
- RESULTS AND DISCUSSION: CHEMISTRY 25
- RESULTS AND DISCUSSION: BIOLOGY 41
- EXPERIMENTAL SECTION 59
- REFERENCES 94

SYNTHESIS OF NAPHTHALENE DIIMIDE DERIVATIVES AS G-QUADRUPLEX LIGANDS (SCHOOL OF PHARMACY, UCL, LONDON)

- INTRODUCTION 97
- RESULTS AND DISCUSSION: CHEMISTRY 113
- RESULTS AND DISCUSSION: BIOLOGY 117
- EXPERIMENTAL SECTION 122
- REFERENCES 130

DISCOVERY OF NEW G-QUADRUPLEX BINDING CHEMOTYPES (SCHOOL OF PHARMACY, UCL, LONDON)

- INTRODUCTION 133
- RESULTS AND DISCUSSION 133
- EXPERIMENTAL SECTION 136
- REFERENCES 137

INTRODUCTION

Cancer is a devastating malignancy and it is one of the principal causes of death in the World affecting 8.2 million people in 2012 (WHO data). Currently tumors are the second leading cause of death in industrialized countries, preceded only by cardiovascular diseases. Surgical excision, radiation therapy and cancer chemotherapy are the three main therapeutic approaches on which it is based anticancer therapy. Although for some types of tumor surgery and radiotherapy are the elective therapeutic choice, chemotherapy is increasingly used.

The ability to treat tumors with a chemotherapy drug approach goes back to the first half of the twentieth century, when it was discovered the cytotoxic effect of nitrogen mustards on hematopoietic cells. Since the continuous search for new molecules with antineoplastic action, the better understanding of their molecular mechanisms, resulted in continuous improvements in the prognosis and quality of life of cancer patients.

But the heterogeneity and complexity of neoplastic diseases are a limit to the efficacy of classical chemotherapy, based on the effect cytostatic / cytotoxic of the drugs, basically due to mechanisms that interfere with DNA synthesis, required for the proliferation.

The occurrence of serious side effects common to most “Classic” antineoplastic drugs is due to the mechanism of action. They are cytotoxic against not only the malignant cells, but also against all those in active proliferation; in some cases the cytotoxic action depends on the phase of the cell cycle in which the cell is located (cycle specific drugs) while in others it is entirely independent (not cycle specific drugs). In the first case, the antineoplastic effect will be influenced by the interval of exposure of tumor cells to the drug and the route of administration chosen will be the continuous infusion. In the second case, the antineoplastic effect will be due to the maximum reachable concentration and the drug administration will preferably be in bolus.

Furthermore, the neoplastic cells may be more or less sensitive to anticancer agents, but above all they can develop resistance that in some cases affect the clinical outcome of therapy. Notwithstanding the difficulties mentioned, cancer chemotherapy continues to progress and to induce encouraging clinical results: the better understanding of the mechanisms of action, the pharmacokinetic studies and the identification of analogues of classical chemotherapy less toxic, have allowed an improvement of prognosis of patients with cancer. For these reasons the search for new anticancer drugs is one of the main objectives of scientific research [1].

Anticancer drugs can be generally divided in (Fig.1) [1]:

- Alkylating agents: (nitrosoureas, nitrogen mustards, alkyl sulfonate, ethylenimine, triazenes) they act via a reactive alkyl group that form covalent bonds with nucleic acids. There follows cross-linkings of the two strands of DNA, preventing replication or DNA breakage.
- Platinum coordination complexes: (cisplatin, carboplatin, oxaliplatin) they act through the cross linking of DNA molecules. The DNA adducts formed by the platinum-containing complexes inhibit DNA replication and lead to strand breaks, causing apoptosis, inhibition of RNA and protein synthesis.
- Antimetabolites: (antifolates, purine and pyrimidine analogues) molecules, similar to the nucleotides, that interfere with one or more enzymes or their reactions that are necessary for DNA synthesis. They affect DNA synthesis by acting as a substitute to the actual metabolites that would be used in the normal metabolic pathway causing alterations or block.
- Microtubule damaging agents: (vincristine, vinblastine, paclitaxel, docetaxel) molecules that interfere with microtubule functions. They prevent the proper functioning of the mitotic spindle resulting in a non-cell division and subsequent apoptosis.
- Topoisomerase inhibitors: agents designed to interfere with the action of topoisomerase enzymes (topoisomerase I and II), which are involved in the changes in DNA structure by catalyzing the breaking and rejoining of the phosphodiester backbone of DNA strands during replication and transcriptase. Topoisomerase inhibitors are divided according to which type of enzyme is inhibited: topoisomerase I inhibitors such as irinotecan and topotecan; topoisomerase II inhibitors such as etoposide.
- Antibiotics: (anthracyclines, mitomycin) their activity is related to DNA intercalation, blocking synthesis of DNA and RNA, alteration of membrane fluidity and ion transport, semiquinone free radical an oxygen radical generation.
- Proteasome inhibitors: (bortezomib) they block the chymotrypsin-like activity of 26S, cellular complexes that break down proteins. The inhibition of proteasome alters the homeostatic mechanism of the cellular protein catabolism, resulting in cell death.
- Unarmed monoclonal antibody: (tastuzumab, rituximab) they bind only to cancer cell-specific antigens and induce an immunological response against the target cancer cell. Some monoclonal antibody can be used for the delivery of a toxin or radioisotopes. Monoclonal antibody therapy can be used only for type of tumors in which antigens (and the respective antibodies) have been recognized.

- Tyrosine protein-kinase inhibitors: (imatinib, gefitinib) they are a class of chemotherapeutic agents that inhibit or block the enzyme tyrosine kinase. This is can be done in two different ways: competitive ATP inhibition at the catalytic binding site of tyrosine kinase, preventing the autophosphorylation of tyrosine residues; occupation of the extracellular site of the ligand with a monoclonal antibody, preventing the activation of the receptor.
- Hormonal drugs: they are used for some kind of cancers that are hormone sensitive or hormone dependent and need hormones to grow or develop. Cancers that can be hormone sensitive are breast, prostate, ovarian and endometrial cancer.

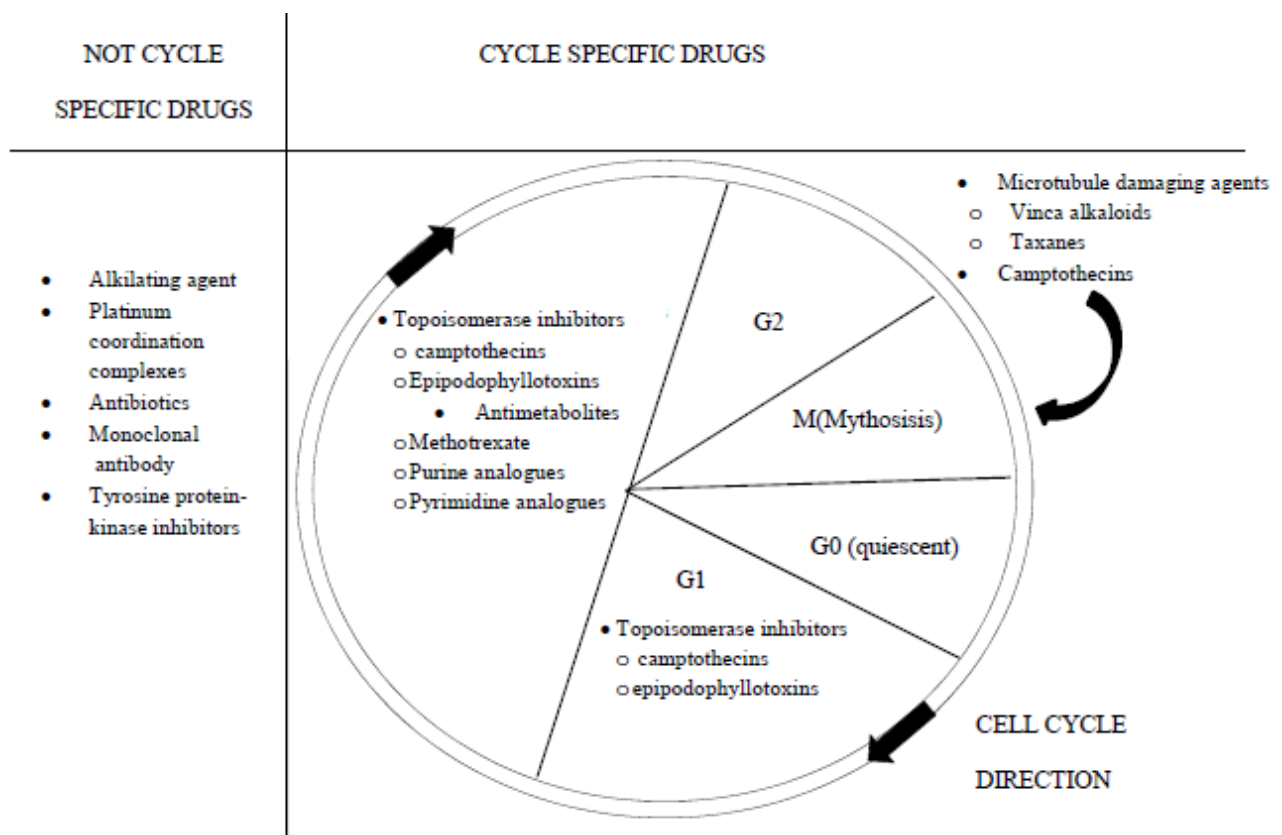


Figure 1. Anticancer drug classification.

One of the rarest forms of cancer is mesothelioma (or malignant mesothelioma) a tumor type that develops from cells of the mesothelium. About 43.000 people worldwide die from this cancer every year.

The mesothelium is a thin layer that covers and lines several internal organs of the body. This membrane protects them thanks to the production of a particular liquid lubricant that facilitates the movements. The mesothelium has different names depending on the different localization: in the

chest is called pleura, in the abdominal cavity is called peritoneum and it is called pericardium in the heart sac.

Mesothelioma is an extremely aggressive primary neoplasia of the serosal lining of the pleura, peritoneum, pericardium or tunica vaginalis [2]. It is a slow-growing solid tumor and it is classified into three classes in relation to its histological morphology: epithelial, biphasic and sarcomatoid. [3] There are four types of mesothelioma, each named for the area of the body where the cancer forms. There are pleural (lungs), peritoneal (abdomen), pericardial (heart) and testicular mesothelioma (Fig.2). Pleural and peritoneal are the most common types, comprising nearly 90 percent of all diagnoses.

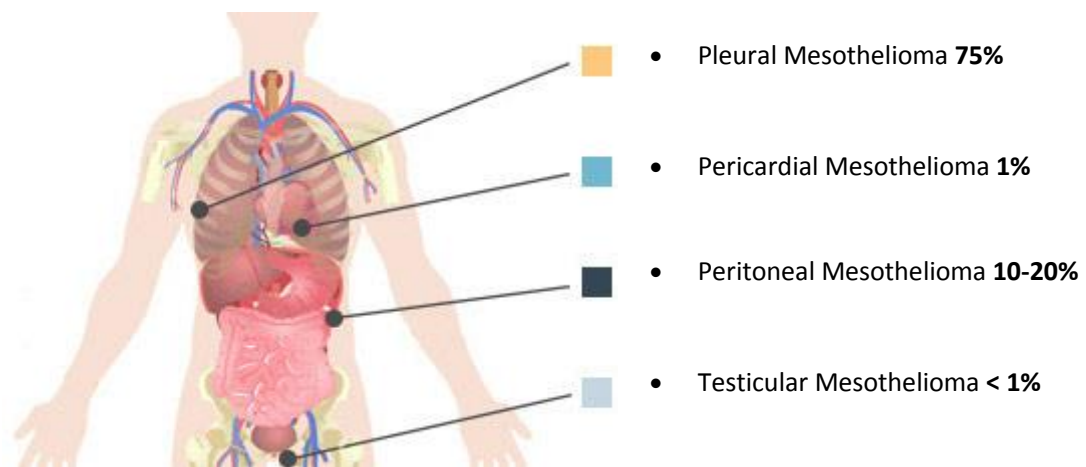


Figure 2. Types of mesothelioma.

Pleural mesothelioma, is an aggressive type of cancer that develops in the lining of the lungs and it is often diagnosed at a very advanced stage. Peritoneal mesothelioma develops in the peritoneum, the membrane that lines the abdominal cavity and it is the second-most predominant type (Fig.3).

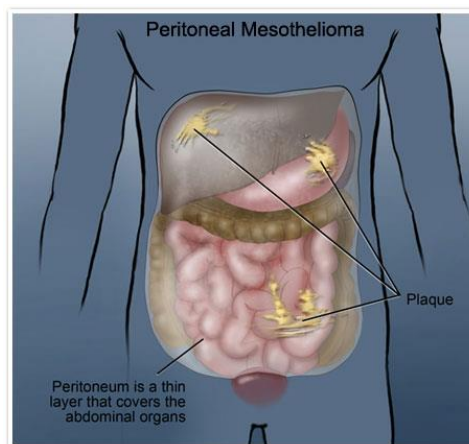


Figure 3. Peritoneal mesothelioma.

The rarest types of the cancer are pericardial and testicular mesothelioma. Pericardial mesothelioma develops in the lining of the heart, while testicular mesothelioma starts in the lining of the testicles.

Several papers showed a strong relationship between a prolonged exposure to asbestos (usually in the workplace), erionite, simian virus 40 (SV40), several genes (p16^{INK4a}, p14^{ARF}, NF2, LATS2, SAV, CTNNB1) and the development of mesothelioma [3].

Diffuse Malignant Peritoneal Mesothelioma (DMPM) is a rare, aggressive and lethal form of mesothelioma that was first recognized and described a century ago. It is a diffuse primary malignant condition arising from mesothelial cells that line the peritoneal cavity and accounts for approximately 10-30 % of all forms of malignant mesothelioma [4]. It is characterized by a difficult diagnosis, different presentations and variable course. In spite of different therapeutic approaches, such as palliative surgery, systemic or intra-peritoneal chemotherapy [5], DMPM has a poor prognosis with a median overall survival that usually does not go beyond 1 year. The failure of conventional therapies towards the neoplastic cells has motivated the exploration of alternative therapeutic protocols.

Prognosis depends on clinical presentation, the completeness of cytoreduction and gender (female patients survive longer than male patients). The practice of intraperitoneal chemotherapy may improve the life expectancy of the patients. In recent years, treatment of these patients was similar to that of patients with ovarian cancer and now includes cytoreductive surgery, heated intraoperative intraperitoneal chemotherapy with cisplatin and doxorubicin, and early postoperative intraperitoneal paclitaxel. Adjuvant intraperitoneal paclitaxel and second-look cytoreduction follow these perioperative treatments. This combined treatment approach with debulking surgery and intraperitoneal chemotherapy has resulted in a median survival of 50 to 60 months [6].

In selected series, the introduction of an innovative strategy combining aggressive cytoreductive surgery (CRS) and hyperthermic intraperitoneal chemotherapy (HIPEC) using cisplatin or mitomycin C has improved median survival up to 40-92 months [7, 8, 9].

The median survival was improved between 8.7 and 26.7 months in patients that have received systemic pemetrexed with platinum compounds or gemcitabine [10, 11].

Recent studies on the molecular biology of DMPM have revealed new understandings about the potentially important role of the phosphatidylinositol 3-kinase/mammalian target of rapamycin and epidermal growth factor receptor pathways in this type of cancer, which can evolve into new therapeutic opportunities for patients with DMPM [9].

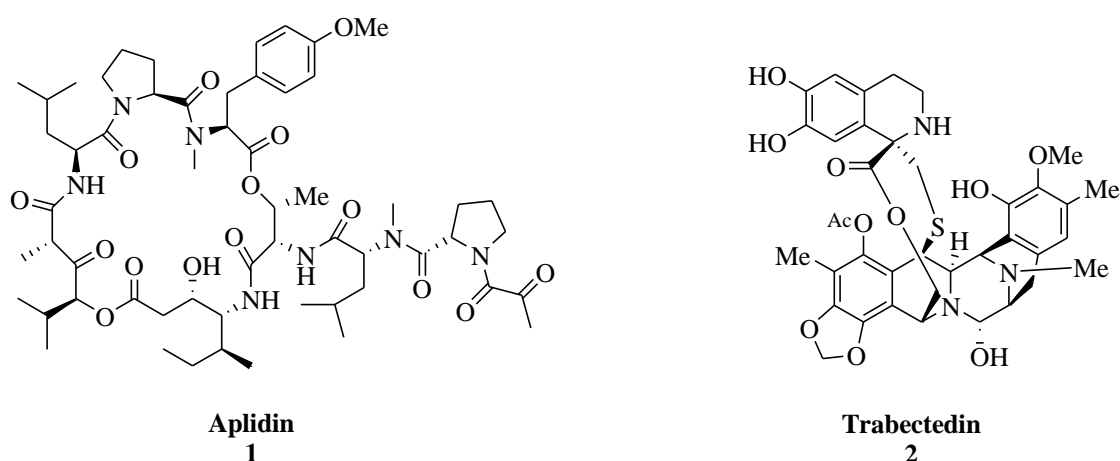
For patients who do not respond to treatment, lack of therapeutic options leads to a poor prognosis [11]. Furthermore, not much is known about the pathogenesis of this disease. These considerations have moved the exploration of novel effective therapeutic strategies which are able to halt the disease progression.

In recent years, attention has been paid to the discovery of new bioactive compounds based on natural products scaffolds as possible novel cancer therapeutic agents. The application of natural compounds is having particular success mainly due to biotechnological advances and novel approaches such as high-throughput screening and combinatorial synthesis, although the clinical use of natural compounds was known, as reported in the medical scripts since ancient Egypt [12]. This is due to the wide diversity of structural features of the natural compounds and their potent panel of biological properties.

There are many organisms in the ocean that produce a huge variety of compounds to help them survive extreme conditions of temperature and pressure and to defend them against predators. Several screenings were carried out for the identification of numerous of anti-cancer alkaloids from cyanobacteria, fungi, sponges, algae and tunicates [13].

However, the limited number of drugs that have reached clinical trials or employed in clinical use is due to the considerable difficulties that occur in the development of drugs from marine sources.

Nevertheless these difficulties, the two alkaloids aplidin **1** and trabectedin **2** have reached phase II clinical trials for the cure of many solid and hematologic tumors [12, 13].



Marine organisms are an exceptional source of compounds and metabolites having useful biological activities, such as antimicrobial, anti-inflammatory, antimalarial, antioxidant, anti-HIV and anticancer activity and they can be considered as potential new drug suitable for the treatment of human diseases (Fig.4) [14].

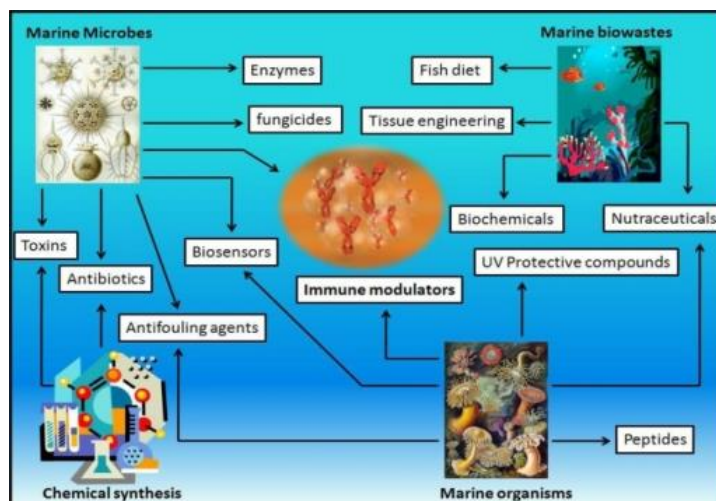
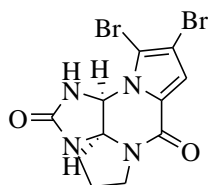


Figure 4. Marine drugs biological activities.

Marine alkaloids include pyridoacridine, indole, pyrrole, pyridine, isoquinoline, guanidine, macrocyclic and steroidal alkaloids [15].

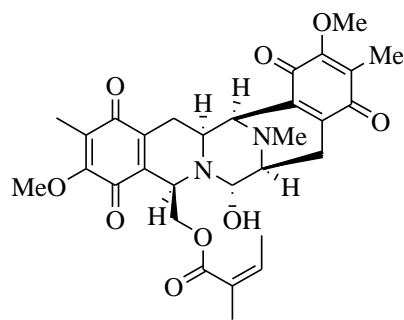
Dibromophakellstatin **3**, a tetracyclic pyrrole-imidazole alkaloid isolated from the marine sponge *Phakellia mauritiana*, displayed inhibitory activity against a panel of human cancer cell lines: ovary (OVCAR-3), brain (SF-295), kidney (A-498), lung (H-460), colon (KM20L2) and melanoma (SK-MEL-5) with ED₅₀ values of 0.46, 1.5, 0.21, 0.62, 0.11 and 0.11 $\mu\text{g}/\text{mL}$, respectively [16].



Dibromophakellstatin

3

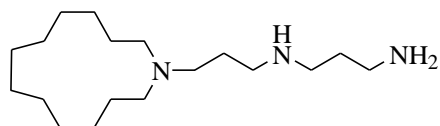
Jorumycin **4**, isoquinoline alkaloid, was isolated from the mantle and the mucus of the pacific nudibranch *Jorunna funebris* and was active against NIH 3T3 tumor cells (100% of inhibition at 50 ng/mL) and also revealed cytotoxic activity against P388, A-549, HT-29 and MEL-28 cells with GI₅₀ value of 12.5 $\mu\text{g}/\text{mL}$ each [17].



Jorumycin

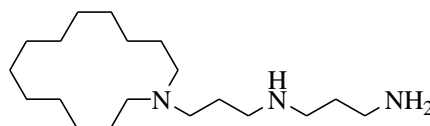
4

Motuporamines A-C **5-7**, macrocyclic alkaloids isolated from the marine sponge *Xestospongia exigua*, showed anti-invasive and anti-angiogenic activity because repressed *in vitro* invasion of basement membranes by many tumor cells such as MDA-231 breast carcinoma and PC-3 prostate carcinoma cells [12].



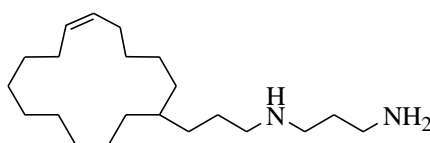
Motuporamine A

5



Motuporamine B

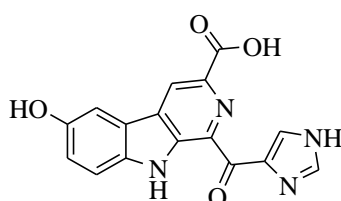
6



Motuporamine C

7

Hytricarboline **8**, 1-imidazolyl-3-carboxy-6-hydroxy- β -carboline alkaloid, isolated from a marine sponge *Hyrrios reticulates*, exhibited selective activity against non-small cell lung (H522-T1), melanoma (MDA-MB-435) and lymphoma (U937) with GI₅₀ values of 1.2, 3.0 and 1.5 μ g/mL, respectively. It also causes 57% inhibition of HeLa cells at 230 μ M [18].



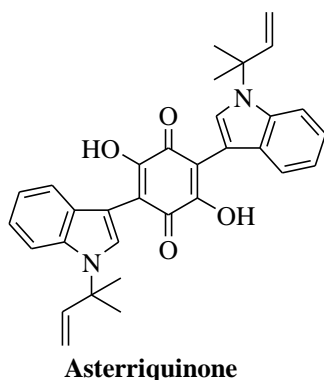
Hytricarboline

8

In particular, marine bisindole alkaloids, consisting of 2 indole units connected to each other, through their 3 position, by a spacer such as carbocycles, heterocycles differently sized or linear

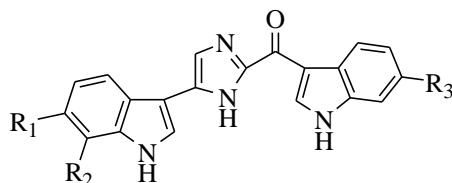
chains, have received considerable attention because of their broad spectrum of biological activities as antitumor, antiviral, antimicrobial and anti-inflammatory agent.

Asterriquinone **9**, characterized by a quinone moiety, is an antitumor metabolite isolated from *Aspergillus terreus* IFO 6123, and showed an inhibitory affect against Ehrlich carcinoma, ascites hepatoma AH13 and mouse P-338 leukemia [19, 20].



9

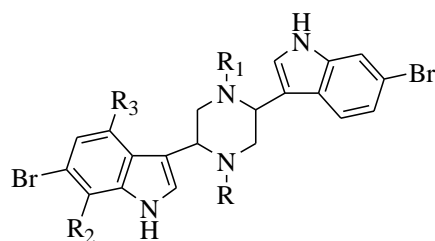
Topsentin **10** and bromotopsentin **11**, isolated from the Mediterranean sponge *Topsentia genitrix*, containing 2-acyl imidazole moiety between two indole units, showed antitumor properties. Topsentin **10** showed antiproliferative activity against cultured human and murine tumor cells. It presented *in vitro* activity against P388 with GI₅₀ value of 3 $\mu\text{g/mL}$, human tumor cell (HCT-8, A-549, T47D) with GI₅₀ value of 20 $\mu\text{g/mL}$ and *in vivo* activity against P388 and B16 melanoma. Bromotopsentin **11** showed anti-proliferative activity against human non small cell bronchopulmonary carcinoma cells (NSCLC-N6) with GI₅₀ value of 12 $\mu\text{g/mL}$ [15].



10 Topsentin R₁ = R₂ = H, R₃ = OH

11 Bromotopsentin R₁ = Br, R₂ = H, R₃ = OH

Dragmacidins, isolated from deep-water sponges, including *Dragmacidon*, *Halicortex*, *Spongsorites* and *Hexadela*, are composed by different spacers and different related properties. Dragmacidin **12**, dragmacidins A-C **13-15**, having a saturated six-membered heterocyclic link piperazine, showed modest antifungal, antiviral and cytotoxic activity.



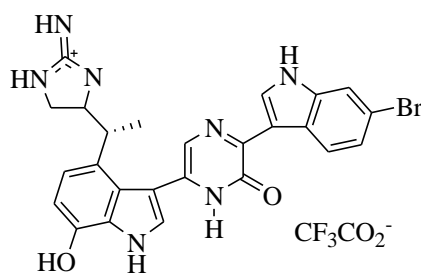
12 Dragmacidin R = H, R₁ = Me, R₂ = Br, R₃ = OH

13 Dragmacidin A R = R₂ = R₃ = H, R₁ = Me

14 Dragmacidin B R = R₁ = Me, R₂ = R₃ = H

15 Dragmacidin C R = R₁ = R₂ = R₃ = H

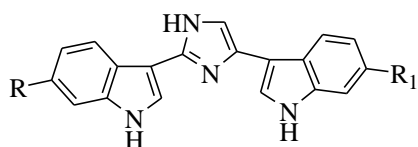
Dragmacidin D **16**, structurally composed by a pyrazinone moiety, showed a potent inhibition against protein phosphates, in particular against protein phosphatase 1 (PP1) and was a selective inhibitor of neural oxide synthase (nNOS), which is involved in neurodegenerative diseases [21]. It was found to be active against human lung tumor cell lines and inhibited *in vitro* growth of the P-388 murine and A-549 with GI₅₀ values of 1.4 and 4.5 μg/ml, respectively [15].



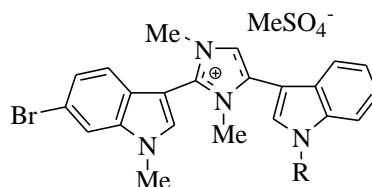
Dragmacidin D

16

Nortopsentins A-C **17-19**, group of bisindole alkaloids having a characteristic five membered ring as spacer, the imidazole, were first isolated by Howard from *Spongosorites ruetzleri* and *Halichondria*. The subsequent catalytic hydrogenation of nortopsentine A-C **17-19** led to nortopsentin D **20**, while the methylation of nortopsentine B **18** with dimethyl sulfate in the presence of potassium carbonate in acetone afforded trimethyl and tetramethyl nortopsentins B **21-22**, as MeSO₄⁻ salt. Nortopsentin A-C exhibited *in vitro* cytotoxicity against P388 leukemia cells with GI₅₀ of 7.6, 7.8, 1.7, μg/ml, respectively. They also showed antifungal activity against *Candida albicans* (MIC 3.1, 6.2, 12.5 μg/ml). The *N*-methylated derivatives of nortopsentin B **21-22** showed *in vitro* a significant improvement in the cytotoxicity against P-388 cells to that of the parent compound (0.9 and 0.34 μg/ml) [22, 23, 24].



- 17 Nortopsentin A** R = R₁ = Br
18 Nortopsentin B R = Br, R₁ = H
19 Nortopsentin C R = H, R₁ = Br
20 Nortopsentin D R = R₁ = H

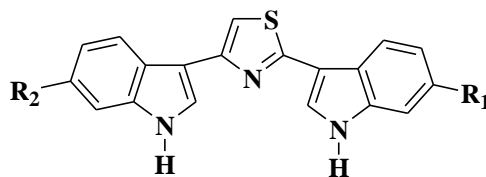


- 21 Trimethylnortopsentin B** R = H
22 Tetramethylnortopsentin B R = Me

Due to the considerable biological activities shown and its low availability, nortopsentin has become an attractive field in medicinal chemistry.

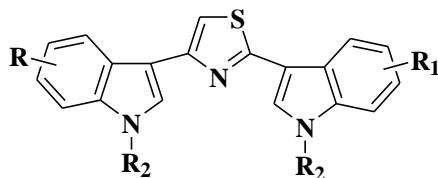
Between the several analogues reported in the literature, significant is the cytotoxic activity shown by 2,4-bis(3-indolyl)thiazoles **23-26**, analogues of nortopsentins in which the imidazole central ring of the natural compound was replaced by a thiazole one.

These compounds **23-26** showed cytotoxic activity against a wide number of human cancer cell lines, as shown in table 1 [23].



- 23** R₁ = R₂ = H
24 R₁ = H, R₂ = Br
25 R₁ = Br, R₂ = H
26 R₁ = R₂ = Br

Considering these interesting results, the authors have synthesized new derivatives with a bis-indolyl-thiazole structure, modifying the substituents on the indole portion in order to increase the cytotoxic activity [24].



| | R | R ₁ | R ₂ | | R | R ₁ | R ₂ |
|-----------|------|----------------|----------------|-----------|-------|----------------|----------------|
| 23 | H | H | H | 28 | 5-Br | 5-Br | H |
| 24 | H | 6-Br | H | 29 | 6-Br | 6-OMe | H |
| 25 | 6-Br | H | H | 30 | 6-Br | 5-Br | H |
| 26 | 6-Br | 6-Br | H | 31 | 6-OMe | 6-Br | H |
| 27 | H | 5-Br | H | 32 | 5-Br | 6-Br | H |
| | | | | 33 | H | H | Me |

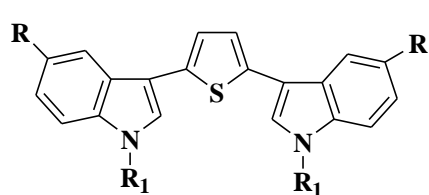
Table 1. Cancer cell growth inhibitory activity of compounds **23-33** *in vitro*.

| Cell Line | Cytotoxicity (GI ₅₀ in μ M) | | | | | | | | | | |
|-----------------------------------|--|------|------|------|------|------|------|------|------|------|------|
| | 23 | 24 | 25 | 26 | 27 | 28 | 29 | 30 | 31 | 32 | 33 |
| Leukemia | | | | | | | | | | | |
| CCRF-CEM | ND | 14.6 | 10.9 | 10.1 | 2.11 | 2.40 | 27.7 | 2.58 | 2.66 | 2.99 | >100 |
| HL-60(TB) | ND | ND | ND | 0.95 | 2.43 | 2.76 | ND | 3.76 | 4.13 | 3.86 | >100 |
| K-562 | 3.27 | 18.8 | 5.61 | 4.69 | 1.96 | 1.94 | 15.2 | 2.13 | 1.74 | 2.25 | 11.2 |
| MOLT-4 | 5.31 | 19.9 | 31.2 | 5.80 | 1.41 | 1.75 | 23.0 | 1.55 | 2.95 | 2.26 | 14.1 |
| RPMI82226 | ND | 19.4 | 12.2 | 11.4 | 1.97 | 1.95 | 27.1 | 2.24 | 2.03 | 1.84 | 20.8 |
| Non-small cell lung cancer | | | | | | | | | | | |
| NCI-226 | >100 | 14.4 | 24.4 | 3.3 | 2.10 | 3.14 | 45.4 | 2.48 | 2.24 | 7.23 | 32.2 |
| NCIH322M | >100 | 16.7 | 18.9 | 18.4 | 2.01 | 1.99 | 70.8 | 2.51 | 3.09 | 2.99 | 24.5 |
| NCI-H460 | >100 | 16.1 | 7.31 | 16.4 | 2.55 | 1.93 | 23.2 | 2.31 | 1.58 | 2.00 | 26.5 |
| EKVX | >100 | 15.6 | 29.5 | 28.6 | ND | ND | 32.1 | 0.48 | 0.29 | 0.55 | ND |
| Colon cancer | | | | | | | | | | | |
| HCT-15 | >100 | 15.2 | 17.8 | 8.50 | 1.81 | 2.51 | 7.54 | 2.70 | 0.81 | 2.84 | >100 |
| SW-620 | >100 | 16.5 | 25.6 | 12.5 | 1.52 | 2.14 | 7.00 | 3.57 | 5.50 | 2.89 | 59.4 |
| CNS cancer | | | | | | | | | | | |
| SF-295 | 33.6 | 14.6 | 9.23 | 4.81 | 1.98 | 2.71 | 73.5 | 4.56 | ND | ND | 23.5 |
| SF-268 | ND | 18.3 | 32.1 | ND | 1.52 | 2.44 | 26.0 | 2.69 | 13.8 | 1.80 | 58.2 |
| SNB-19 | >100 | 17.8 | 41.8 | 17.2 | 2.11 | 3.75 | >100 | 2.60 | 10.5 | 3.34 | 42.6 |
| U21 | >100 | 17.9 | 28.1 | 15.3 | 2.10 | 2.30 | 25.0 | 3.34 | 5.07 | 3.00 | 32.4 |
| Ovarian cancer | | | | | | | | | | | |
| IGROV1 | 8.14 | 13.0 | 30.5 | 14.4 | 1.85 | 1.70 | 81.5 | 2.96 | 4.61 | 2.43 | 27.0 |
| OVCAR-5 | >100 | 16.1 | 37.1 | 23.6 | 1.96 | 2.14 | 42.7 | 2.16 | 3.44 | 2.35 | 95.9 |
| Renal cancer | | | | | | | | | | | |
| 786-0 | >100 | 18.0 | 19.9 | 15.9 | 2.28 | 1.95 | 27.4 | 1.50 | 3.89 | 2.21 | 17.2 |
| A498 | >100 | 17.0 | 25.7 | 23.2 | 1.92 | 2.48 | 89.4 | 2.19 | 7.43 | 2.40 | 12.6 |
| RXF 393 | ND | 22.4 | 7.62 | 18.4 | 1.81 | 1.69 | 11.9 | 2.42 | 2.03 | 1.66 | 14.1 |
| Prostate cancer | | | | | | | | | | | |
| PC-3 | >100 | 15.6 | 16.9 | 15.3 | 2.02 | 2.57 | 10.4 | 4.16 | 3.49 | 2.81 | 21.9 |
| DU-145 | >100 | 18.8 | 14.9 | 18.4 | 2.29 | 2.61 | >100 | 3.74 | 5.46 | 2.03 | 42.9 |
| Breast cancer | | | | | | | | | | | |
| MCF7 | >100 | 16.7 | 27.2 | 6.46 | 2.13 | 2.70 | 54.1 | 0.88 | 4.36 | 3.82 | 45.5 |
| MDAMB435 | 33.1 | 14.9 | 25.6 | 4.34 | 2.53 | 2.27 | 7.70 | 4.54 | 14.6 | 3.97 | 26.4 |
| MDA-N | 83.0 | 19.2 | 31.5 | 2.94 | 1.88 | 2.09 | 8.27 | 2.86 | 6.84 | 3.77 | 24.9 |
| T-47D | >100 | 24.8 | 23.9 | 16.2 | 3.27 | 2.90 | 59.3 | 3.33 | 4.12 | 1.76 | 28.1 |
| BT-549 | >100 | 18.3 | 73.8 | 41.1 | 2.71 | 10.6 | 67.3 | 1.24 | 1.46 | 1.41 | 56.3 |
| Melanoma | | | | | | | | | | | |
| LOX IWVI | 21.8 | 15.5 | 6.55 | 11.3 | 1.97 | 1.69 | 64.1 | 2.32 | 2.41 | 1.87 | 36.4 |
| MALME3M | >100 | 16.9 | >100 | ND | 1.28 | 1.72 | 1.72 | 1.45 | 1.50 | 2.83 | 19.0 |
| M14 | >100 | 14.2 | 32.4 | 10.6 | 1.61 | 1.63 | >100 | 2.86 | 5.49 | 2.77 | 26.7 |
| SKMEL2 | >100 | ND | 37.5 | 68.8 | 1.81 | 1.98 | 19.1 | 3.25 | 7.30 | 2.91 | 38.8 |
| SKMEL28 | >100 | 14.2 | 7.74 | 32.0 | 3.02 | 3.05 | >100 | 9.84 | 1.36 | 4.96 | 61.5 |
| SKMEL5 | ND | 14.9 | 23.7 | 28.5 | 1.76 | 1.63 | >100 | 2.82 | 5.13 | 3.36 | 26.9 |

ND= not determined

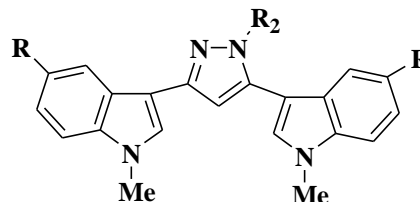
The synthesized compounds were evaluated for cytotoxicity in the National Cancer Institute (NCI, Bethesda MD) against approximately a panel of 60 human tumor cell lines (Tab. 2). All compounds, with the exception of compound **23**, showed cytotoxic activity in a wide range of human tumor cell lines. The position of bromine in the indole ring plays an important role for the cytotoxicity. Compounds **27**, **28**, with a bromine atom in position 5, exhibited an increased activity than derivatives **24**, **25**, with a bromine atom in position 6. Compounds dibrominated at 5',6' (**30**) and 5',6' (**32**) position showed a greater anti-proliferative activity than 6-6'dibrominated derivative **26**. The introduction of a methyl group in the indole moiety lead to 2,4-bis-(*N*-methylindolyl)thiazole **33** in which we can observe a decrease of the activity against the most active cell lines.

In the research lab where I carried out my PhD thesis, different analogues of nortopsentin has been synthesized, in which the imidazole ring of the natural compound was replaced by other five-membered heterocycles, such as thiophene **34** [25], pyrazole **35** [26], furan **36** [27], isoxazole **37** [27], and pyrrole **38** [28]. Some of them showed remarkable antiproliferative activity in cancer cells, often with IC₅₀ values at submicromolar level.



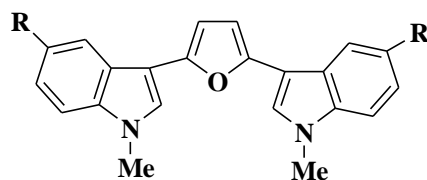
2,5-bis(3'-indolyl)thiophenes

34



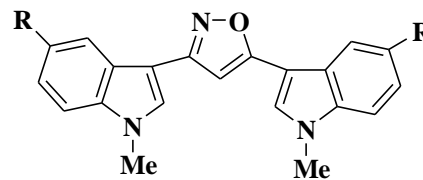
3,5-bis(3'-indolyl)pyrazoles

35



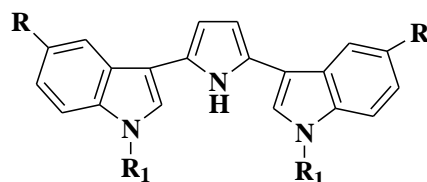
2,5-bis(3'-indolyl)furans

36



3,5-bis(3'-indolyl)isoxazoles

37



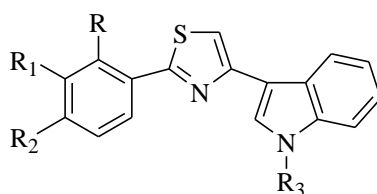
2,5-bis(3'-indolyl)pyrroles

38

Furthermore, considering the interesting antitumor activity of 2,4-bis(3'-indolyl)thiazole reported in literature, different analogues of nortopsentin in which the heterocyclic core of the system is constituted by a thiazole ring have been synthesized.

In particular 3-(2-phenyl-1,3-thiazol-4-yl)-1*H*-indoles **39**, 3-(2-phenyl-1,3-thiazol-4-yl)-1*H*-7-azaindoles **40** and 3-[2-(1*H*-indol-3-yl)-1,3-thiazol-4-yl]-1*H*-4-azaindoles **41** have been reported.

Derivatives **39**, in which one indole ring has been substituted by a phenol one, tested at a single concentration (10^{-5} M), did not exhibited considerable anti-proliferative activity [29].

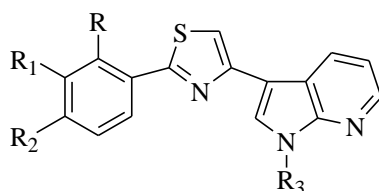


3-(2-phenyl-1,3-thiazol-4-yl)-1*H*-indoles

39

R = H
 R₁ = H,
 R₂ = H, Me, OMe, Cl, Br, F
 R₃ = H, Me

Instead 3-(2-phenyl-1,3-thiazol-4-yl)-1*H*-7-azaindoles **40**, in which the indole ring of the derivatives **39** has been substituted with a 7-azaindole one, showed anti-proliferative activity against a wide range of human tumor cell lines with GI₅₀ values from micromolar to nanomolar concentrations. They were also able to inhibit the activity of cyclin-dependent kinase I (CDK1) with GI₅₀ values less than 1 μM [29].

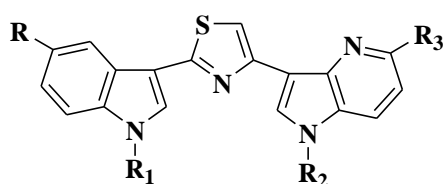


3-(2-phenyl-1,3-thiazol-4-yl)-1H-7-azaindoles

40

R = H, Cl, F
 R₁ = H, Me, F
 R₂ = H, Me, OMe, Cl, Br, F
 R₃ = H, Me

Further studies led to the synthesis of 3-[2-(1H-indol-3-yl)-1,3-thiazol-4-yl]-1H-4-azaindoles **41** in which the indole ring of the 2,4-bis(3-indolyl)thiazole derivatives, reported in literature, has been substituted with a 4-azaindole one. Some of them reduced the growth of four cell lines with different histologic origin (breast cancer MDA-MB-231, pancreatic carcinoma Mia PaCa-2, androgen-independent prostate cancer PC3, diffuse malignant peritoneal mesothelioma STO) with GI₅₀ values of 4.1-49.1 μM. Studies to understand the mechanism of action revealed that they acted as CDK1 inhibitor (GI₅₀ value of 0.64-0.87 μM) causing a cell cycle arrest at G₂/M phase [30].

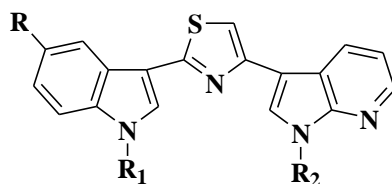


3-[2-(1H-indol-3-yl)-1,3-thiazol-4-yl]-1H-4-azaindoles

41

R = H, Me, OMe, Cl, Br, F
 R₁ = H, Me, Boc
 R₂ = H, Me
 R₃ = H, OMe

Thereafter the attention was focused on the synthesis of indolyl-7-azaindolyl thiazoles **42a-n**, **43a-j**, **44a-j** in which 4-azaindole ring has been replaced by a 7-azaindole one (Tab.2) [31].



3-[2-(1H-indol-3-yl)-1,3-thiazol-4-yl]-1H-7aza-indoles

42a-n
43a-j
44a-j

Table 2. 3-[2-(1H-Indol-3-yl)-1,3-thiazol-4-yl]-1H-7-azaindoles **42a-n, 43a-j, 44a-j.**

| Compd | R | R ₁ | R ₂ | Yield% | Compd | R | R ₁ | R ₂ | Yield |
|-------|-----|----------------|----------------|--------|-------|-----|----------------|----------------|-------|
| 42a | H | Me | H | 85 | 43d | Cl | Boc | H | 90 |
| 42b | Me | Me | H | 70 | 43e | Br | Boc | H | 80 |
| 42c | OMe | Me | H | 90 | 43f | H | Boc | Me | 92 |
| 42d | Cl | Me | H | 78 | 43g | Me | Boc | Me | 53 |
| 42e | Br | Me | H | 60 | 43h | OMe | Boc | Me | 90 |
| 42f | F | Me | H | 95 | 43i | Cl | Boc | Me | 90 |
| 42g | H | Me | Me | 75 | 43j | Br | Boc | Me | 72 |
| 42h | Me | Me | Me | 60 | 44a | H | H | H | 99 |
| 42i | OMe | Me | Me | 85 | 44b | Me | H | H | 95 |
| 42j | Cl | Me | Me | 57 | 44c | OMe | H | H | 99 |
| 42k | Br | Me | Me | 55 | 44d | Cl | H | H | 99 |
| 42l | F | Me | Me | 91 | 44e | Br | H | H | 54 |
| 42m | F | H | H | 87 | 44f | H | H | Me | 71 |
| 42n | F | H | Me | 60 | 44g | Me | H | Me | 99 |
| 43a | H | Boc | H | 85 | 44h | OMe | H | Me | 90 |
| 43b | Me | Boc | H | 60 | 44i | Cl | H | Me | 99 |
| 43c | OMe | Boc | H | 90 | 44j | Br | H | Me | 90 |

All the synthesized indolyl-azaindolyl thiazoles **42a-n, 43a-j** and **44a-j** were submitted to the National cancer Institute (NCI; Bethesda MD) in order to evaluate their biological activity as antitumor agents. Biological screening were performed according to the NCI protocol, at the 10^{-5} M dose for the *in vitro* disease-oriented antitumor screenings against a panel of about 60 human tumor cell lines derived from 9 human cancer cell types, that have been grouped in disease sub-panel including leukemia, non-small cell lung cancer, colon cancer, central nervous system cancer, melanoma, ovarian cancer, renal cancer, prostate cancer and breast cancer cell lines. Compounds **42a, 42d, 42f, 42g, 42l-n, 43f, 44b-f** selected by the NCI for full evaluation at five concentration levels (10^{-4} - 10^{-8} M), showed antiproliferative activity with GI_{50} at micro to sub-micromolar range (Tab.3).

Table 3. In *vitro* inhibition of cancer cell lines growth by compounds **42a**, **42d**, **42f**, **42g**, **42l-n**, **43f**, **44b-f**.

| Compd | N° of cell line tested | N° of active cell lines | GI ₅₀ (μM) | |
|------------|------------------------|-------------------------|-----------------------|--------|
| | | | Range | MG_MID |
| 42a | 59 | 56 | 0.84-0.60 | 0.70 |
| 42d | 59 | 59 | 0.85-0.66 | 0.73 |
| 42f | 60 | 60 | 0.87-0.72 | 0.75 |
| 42g | 59 | 59 | 0.83-0.72 | 0.76 |
| 42l | 55 | 55 | 0.82-0.72 | 0.77 |
| 42m | 23 | 14 | 0.80-0.69 | 0.69 |
| 42n | 58 | 58 | 0.82-0.63 | 0.75 |
| 43f | 59 | 59 | 0.78-0.68 | 0.72 |
| 44b | 48 | 3 | 0.82-0.74 | 0.61 |
| 44c | 58 | 58 | 0.79-0.62 | 0.73 |
| 44d | 59 | 59 | 0.77-0.71 | 0.74 |
| 44e | 59 | 59 | 0.77-0.70 | 0.74 |
| 44f | 60 | 60 | 0.86-0.70 | 0.79 |

The five most active compounds **42f**, **42g**, **42l**, **42n**, **44f** were further tested by Istituto Nazionale dei Tumori (Fondazione IRCCS, Milano) against in 2 additional cell lines: STO and Meso II, derived from human Diffuse Malignant Peritoneal Mesothelioma (DMPM), a tumor type not included in the NCI panel. After 72 hours of exposure to increasing concentrations of each compound, compounds **42f**, **44f** and **42l** showed a dose-dependent inhibition of cell proliferation in both cellular models and they did not interfere with the proliferation of normal cells (W138) (Tab.4).

Table 4. Cytotoxic activity of compounds **42f**, **42g**, **42l**, **42n**, **44f** in DMPM and normal cells.

| Compd | GI ₅₀ (μM) ^(a) | | |
|------------|--------------------------------------|------------|------------|
| | STO | MesoII | WI38 |
| 42f | 0.49±0.07 | 25.12±3.06 | >100 |
| 44f | 0.33±0.07 | 4.11±0.22 | >100 |
| 42g | 0.61±0.14 | 16.77±1.99 | 18.76±3.21 |
| 42l | 0.43±0.11 | 4.85±0.64 | >100 |
| 42n | 0.54±0.09 | 13.27±0.74 | 15.44±3.87 |

^a Data are reported as GI₅₀ values (concentration of drug required to inhibit growth by 50%) determined by MTS assay after 72 h of continuous exposure to each compound. The data represents mean values ± SD of at least three independent experiments.

The antitumoral activity of compounds **42f**, **44f** and **42l** was investigated on STO cells xenotransplanted in athymic nude mice and after the treatment with each compound it was possible to observe a marked tumor growth inhibition (Fig.5).

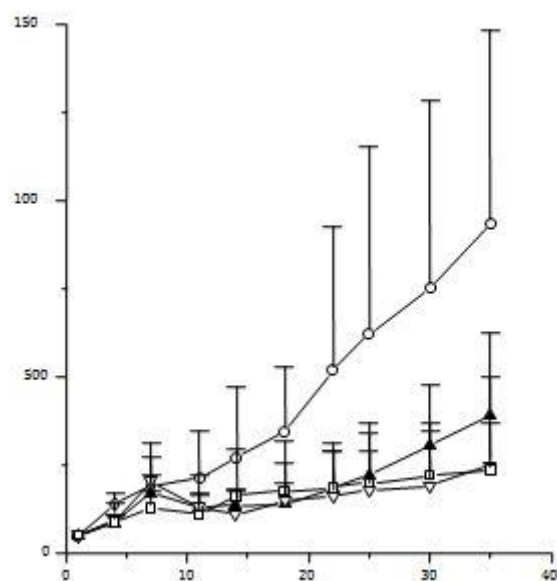


Figure 5. Activity of **42f**, **44f**, and **42l** derivatives on STO cells xenotransplanted on athymic mice. Drugs were administered ip at 25 (**42f** and **42l**) or 50 (**44f**) mg/kg qd×4–5/w×3w, starting from the day after the injection. **p < 0.01, *p < 0.05.

In particular, a statistically significant tumor volume inhibition (TVI) compared with the control (73%, 75%, 58% for **42f**, **42l**, **44f** compounds, respectively) it was observed (Tab. 5). Two complete responses were observed in each treatment group, with the disappearance of tumor induced by treatment.

Table 5. Activity of derivatives **42f**, **44f**, **42l** on STO cells xenotransplanted on athymic mice.

| Compd | TVI (%) ^a | CR ^b | BWL (%) ^c | TOX ^d |
|------------|----------------------|-----------------|----------------------|------------------|
| 42f | 73* | 2/8 | 4 | 0/8 |
| 42l | 75** | 2/8 | 1 | 0/8 |
| 44f | 58* | 2/8 | 7 | 0/8 |

^aTumor volume inhibition (%) in treated vs control mice, determined 17 days after the end of drug treatment (day 35). ^bComplete response, disappearance of tumor induced by treatment. ^cBWL, body weight loss induced by treatment (%). ^dToxic death on treated animals. **p < 0.01, *p < 0.05.

As many nortopsentin analogues exhibited the cellular effects by inhibiting of kinase activity, in order to study the mechanism of action, compounds **42f**, **42l** and **44f** were tested on several protein kinases (CDK1, CDK5, EGFR, FGFR1, RET, MET, KIT, JAK2, PKCA, PKCB, CHKI, MAPK12, GSK, PKA, GSK3 α , GSK3 β). Results showed that those compounds markedly repressed CDK1 activity with GI₅₀ values (0.89±0.07, 0.75±0.03, 0.86±0.04) comparable to those reported for CDK1

inhibitors roscovitine and purvalanol A (0.73 ± 0.06 , and 0.59 ± 0.08 , respectively) and they decreased CDK1 activity in a time-dependent way. These compounds were also active against GSK3 β protein, but only at very high concentration (Tab.6).

Table 6. *In vitro* Kinase inhibitory activity of derivatives **42f**, **42l**, **44f**.

| Protein kinase | GI ₅₀ (μ M) ^(a) | | | | |
|--------------------------------|--|-----------------|-----------------|----------------|----------------|
| | 42f | 42l | 44f | Roscovitine | Purvalanol A |
| CDK1 | 0.89 ± 0.07 | 0.75 ± 0.03 | 0.86 ± 0.04 | 0.73 ± 0.06 | 0.59 ± 0.08 |
| GSK-3β | 42.18 ± 3.28 | 40.18 ± 2.94 | 35.68 ± 1.69 | >50 | >50 |

^a Concentration of drug required to inhibit by 50% (GI₅₀) the activity of CDK1 e GSK-3 β . Values represent the mean values \pm SD of three independent experiments.

Moreover, it was study the phosphorylation status of histone H1, a specific substrate for CDK1, in STO cell lines, in order to confirm the ability of these 3 derivatives to inhibit CDK1 activity in living cells; the obtained results showed a substantial and time dependent reduction of kinase activity (Fig.6 A-B).

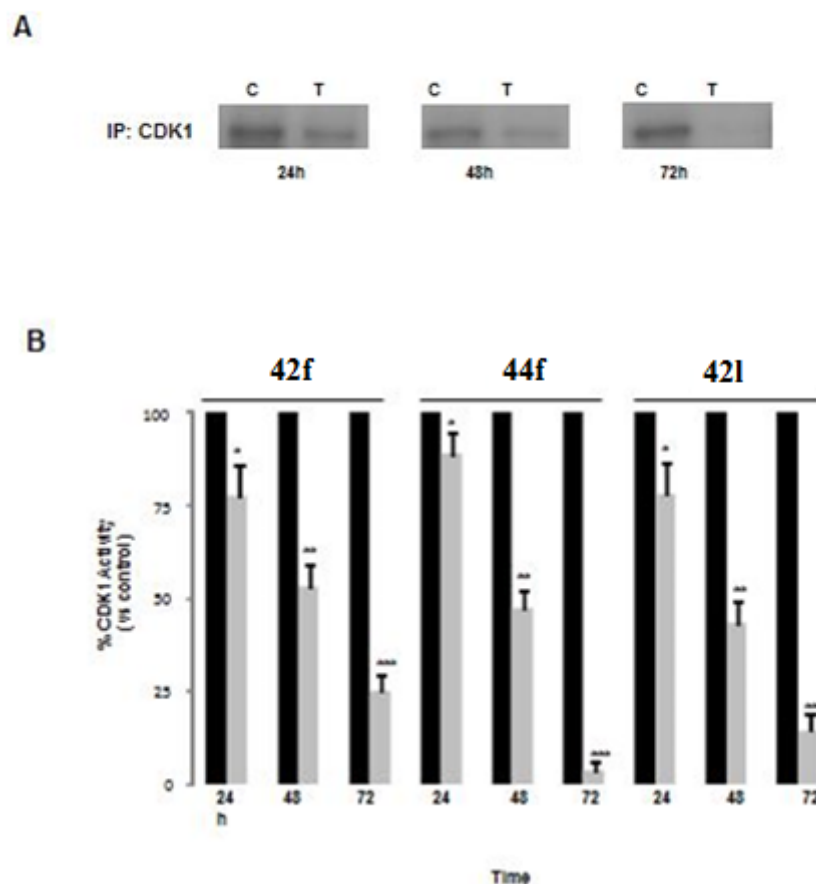


Figure 6. Effect of **42f**, **44f**, and **42l** derivatives on CDK1 kinase activity in DMPM cells. (A) Representative kinase assay illustrating the CDK1 activity in STO cells at different intervals after exposure to 1% (v/v) DMSO (control cells; C) or to derivative

44f (GI₅₀; T). (B) Densitometric quantification of CDK1 activity in STO cells exposed to derivatives **42f**, **44f**, and **42l** for 24, 48, and 72 h. CDK1 activity was achieved by immunoprecipitation. Data are reported as the percentage of CDK1 activity in cells exposed to derivatives **42f**, **44f**, and **42l** (gray column) compared with DMSO-treated cells (black column) and represent the mean values \pm SD of at least three independent experiments. ***p < 0.001, **p < 0.01, *p < 0.05.

These compounds were also tested in STO and Meso II cells to observe the importance of nortopsentin analogue treatment on cell cycle progression. Compound **42f**, **44f**, **42l** induced a time-dependent accumulation of cells in the G₂/M phase, and a concomitant decrease of the percentage of cells in the G₁ phase. It was also observe a marched growth in the number of cells with apoptotic morphology (as chromatin condensation and DNA morphology) and a significant increase in the activity of caspase 9 and 3 (Fig. 7).

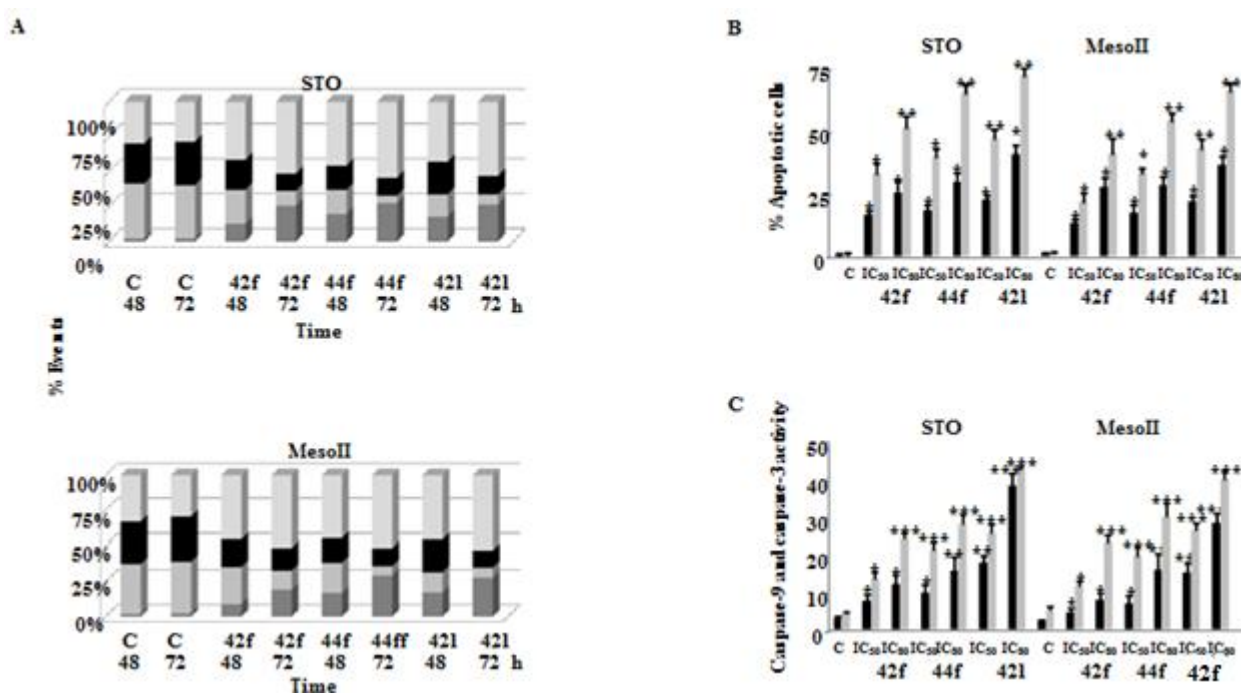


Figure 7. Effect of **42f**, **44f**, and **42l** derivatives on cell-cycle progression and apoptosis induction. (A) STO and MesoII cells were exposed to 1% (v/v) DMSO (control cells; C) or to derivatives **42f**, **44f**, and **42l** (GI₅₀) for 48 and 72 h. Data are reported as the percentage of cells in sub-G₁ (dark gray), G₁ (light gray), S (black), and G₂/M (white) phases and represent the mean values of three independent experiments; SDs were always within 5%. (B) The percentage of cells with apoptotic morphology was assessed by fluorescence microscopy after exposure of DMPM cells to 1% (v/v) DMSO (control cells; C) or to derivatives **42f**, **44f**, and **42l** at 48 h (black column) and 72 h (gray column) after treatment. Data are expressed as mean values \pm SD of at least three independent experiments. ***p < 0.001, *p < 0.01. (C) The catalytic activity of caspases was assessed after 72 h of exposure of the DMPM cells to 1% (v/v) DMSO (control cells; C) or to derivatives **42f**, **44f**, and **42l**. Caspase-9 (black column) and caspase-3 (gray column) catalytic activity was determined in vitro by hydrolysis of the fluorogenic substrates (LEHD-pNA and DEVD-pNA, respectively). Data are expressed as mean values \pm SD of at least three independent experiments. ***p < 0.001, **p < 0.01, *p < 0.02.

It was previously demonstrated that DMPM chemo-resistance was principally caused by the dysregulation of apoptotic pathway, through the over-expression of members of the inhibitors of apoptosis protein family (IAP), such as survivin [32], a multifunctional protein involved in cell

division and in the suppression of apoptosis and selectively overexpressed in most human cancers [33]. It has been demonstrated that to carry out its functions, survivin needs to be physically associated with CDK1 and phosphorylated on the Thr³⁴ residue by CDK1/Cyclin B1 complex [33, 34].

It was investigated the effect of these compounds on survivin activation. Immunoblotting experiments demonstrated that 1*H*-pyrrolo[2,3-*b*]pyridine derivatives induced apoptosis in DMPM cells through a relevant and time-dependent decrease of levels of the active form of survivin, phosphorylated in THr³⁴ (Fig. 8).

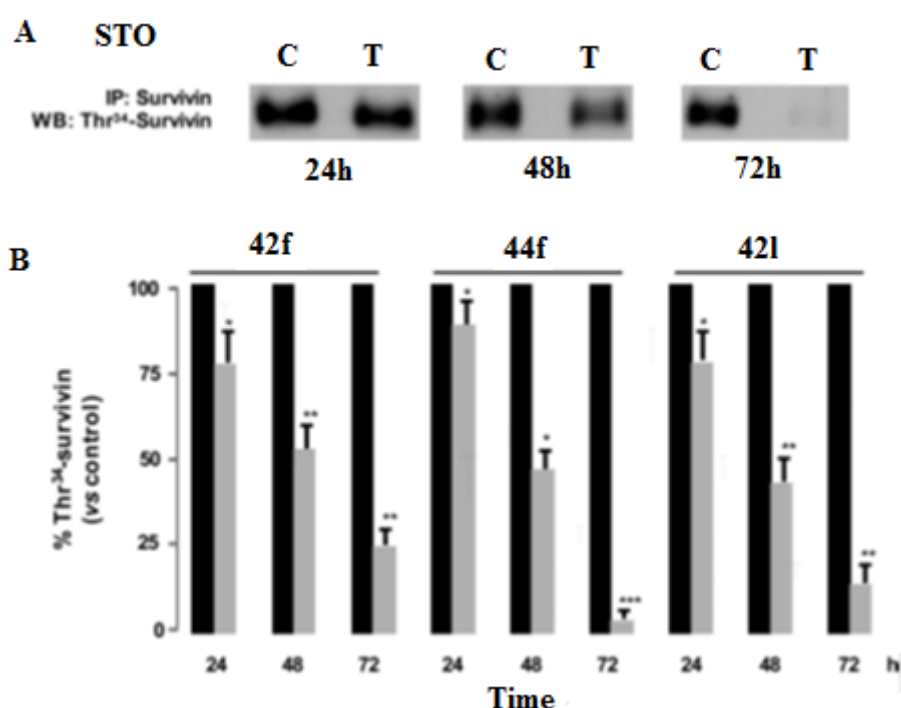


Figure 8. Effect of **42f**, **44f**, and **42l** derivatives on survivin phosphorylation. (A) Representative Western blotting illustrating the survivin phosphorylation status in STO cells after exposure to 1% (v/v) DMSO (control cells; C) or to derivative **44f**, (GI₅₀; T). (B) Densitometric quantification of surviving phosphorylation levels in STO cells exposed to **42f**, **44f**, and **42l** for 24, 48, and 72 h. The phosphorylation of survivin on the Thr³⁴ residue was evaluated on STO cells treated with 1% (v/v) DMSO (control cells; black column) or to derivatives **42f**, **44f**, and **42l** (IC₅₀; gray column) by Western immunoblotting. Survivin was immunoprecipitated using the antihuman survivin antibody and analyzed with the antibody to phosphorylated Thr³⁴. Data are expressed as mean values ± SD of at least three independent experiments. ***p < 0.001, **p < 0.01, *p < 0.05.

The cytotoxic effect of the most active compound **44f** was also investigated in DMPM cells alone or in combination with the taxan paclitaxel. At the beginning STO and MesoII cells were treated only with the taxan for 24 h and then for 72 h they were exposure also to compound **44f**. At all concentrations, it was observed a synergistic cytotoxic effect to inhibit DMPM cell survival. After the combination of two drugs, an inhibition of cell proliferation bigger than that estimated by simple

addition/amount of the effects of the two agents it was detected (Fig. 9A). A higher catalytic activity of caspase-3 was identified in cells treated with the two compounds than in those exposed to each single agent (Fig. 9B).

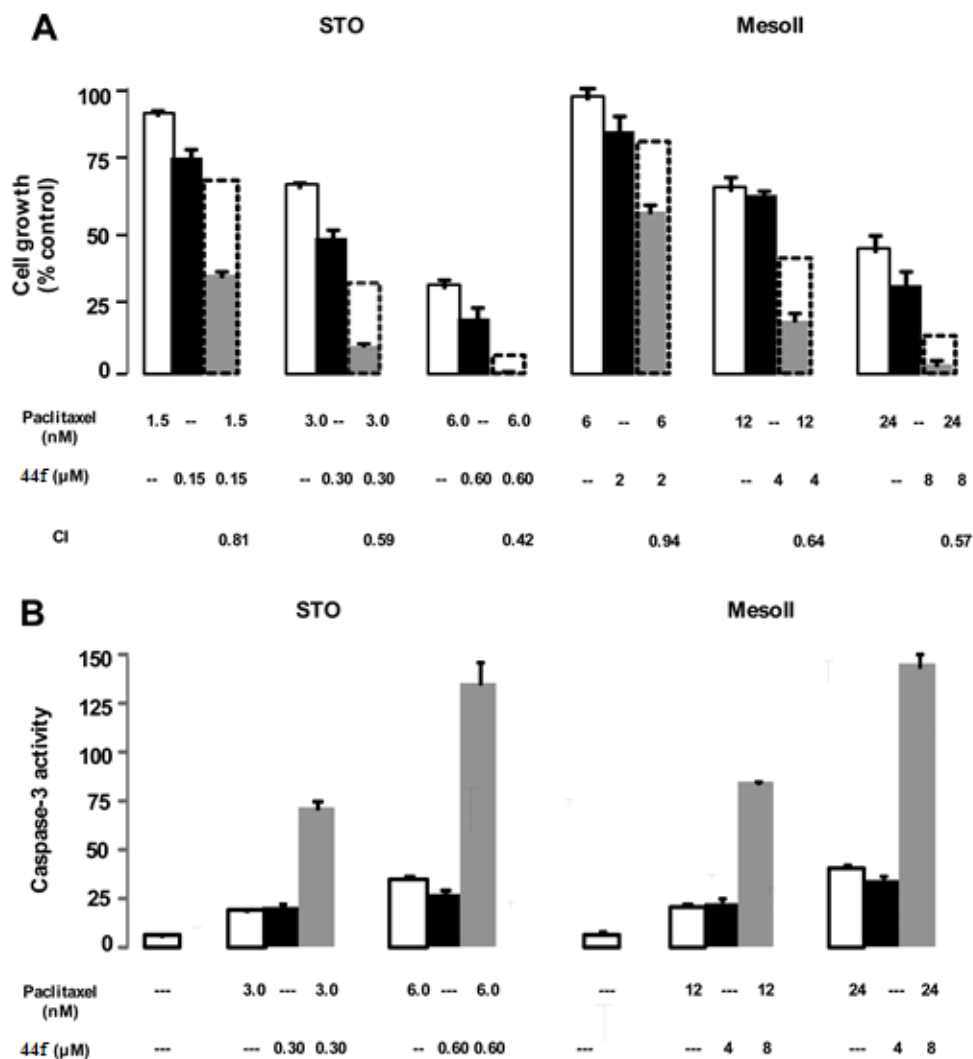
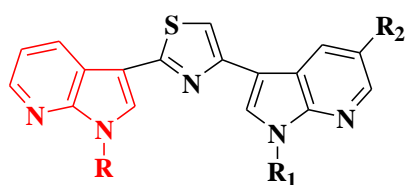


Figure 9. Cytotoxic effect of **44f** derivative in combination with paclitaxel in DMPM cells. (A) The cytotoxic effect of paclitaxel and **44f** derivative, alone or in combination, was assessed by MTS assay. The dashed lines represent the expected additive effect of the combination, calculated as the product of the effects of the individual drugs. Data are expressed as mean values \pm SD of at least three independent experiments. CI was calculated according to Chou and Talalay.⁴⁷ (B) Caspase-3 catalytic activity was determined in vitro by the hydrolysis of the specific fluorogenic substrate (DEVD-pNA). Data are expressed as mean values \pm SD of at least three independent experiments. * $p < 0.001$.

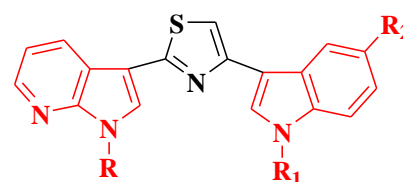
Considering the interesting results shown by indolyl-7-azaindolyl thiazoles of type **42-44**, the aim of my PhD project was the synthesis of new biologically active their analogues. In particular, three new series have been synthesized:

- [3,3'-(1,3-thiazole-2,4-diyl)bis(1*H*-pyrrolo[2,3-*b*]pyridines)] **45** in which two 7-azaindole rings are linked to the thiazole central ring;
- [3-[4-(1*H*-indol-3-yl)-1,3-thiazol-2-yl]-1*H*-pyrrolo[2,3-*b*]pyridines] **46, 47, 48** in which the indole and 7-azaindole moieties, respectively in position 2 and 5, have been switched;
- [7-chloro-3-[2-(1*H*-indol-3-yl)-1,3-thiazol-4-yl]-1*H*-pyrrolo[2,3-*c*]pyridines] **49, 50, 51** in which the 7-azaindole unit is replaced by a 6-azaindole moiety.



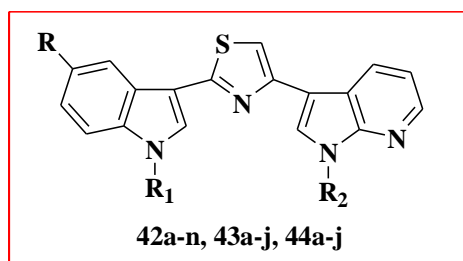
3,3'-(1,3-thiazole-2,4-diyl)bis1*H*-pyrrolo[2,3-*b*]pyridines

45



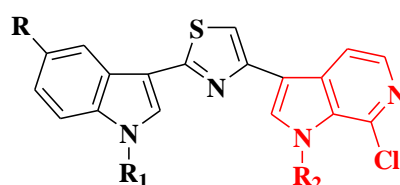
3-[4-(1*H*-indol-3-yl)-1,3-thiazol-2-yl]-1*H*-pyrrolo[2,3-*b*]pyridines

46, 47, 48



42a-n, 43a-j, 44a-j

3-[2-(1*H*-indol-3-yl)-1,3-thiazol-4-yl]-1*H*-pyrrolo[2,3-*b*]pyridines



7-chloro-3-[2-(1*H*-indol-3-yl)-1,3-thiazol-4-yl]-1*H*-pyrrolo[2,3-*c*]pyridine

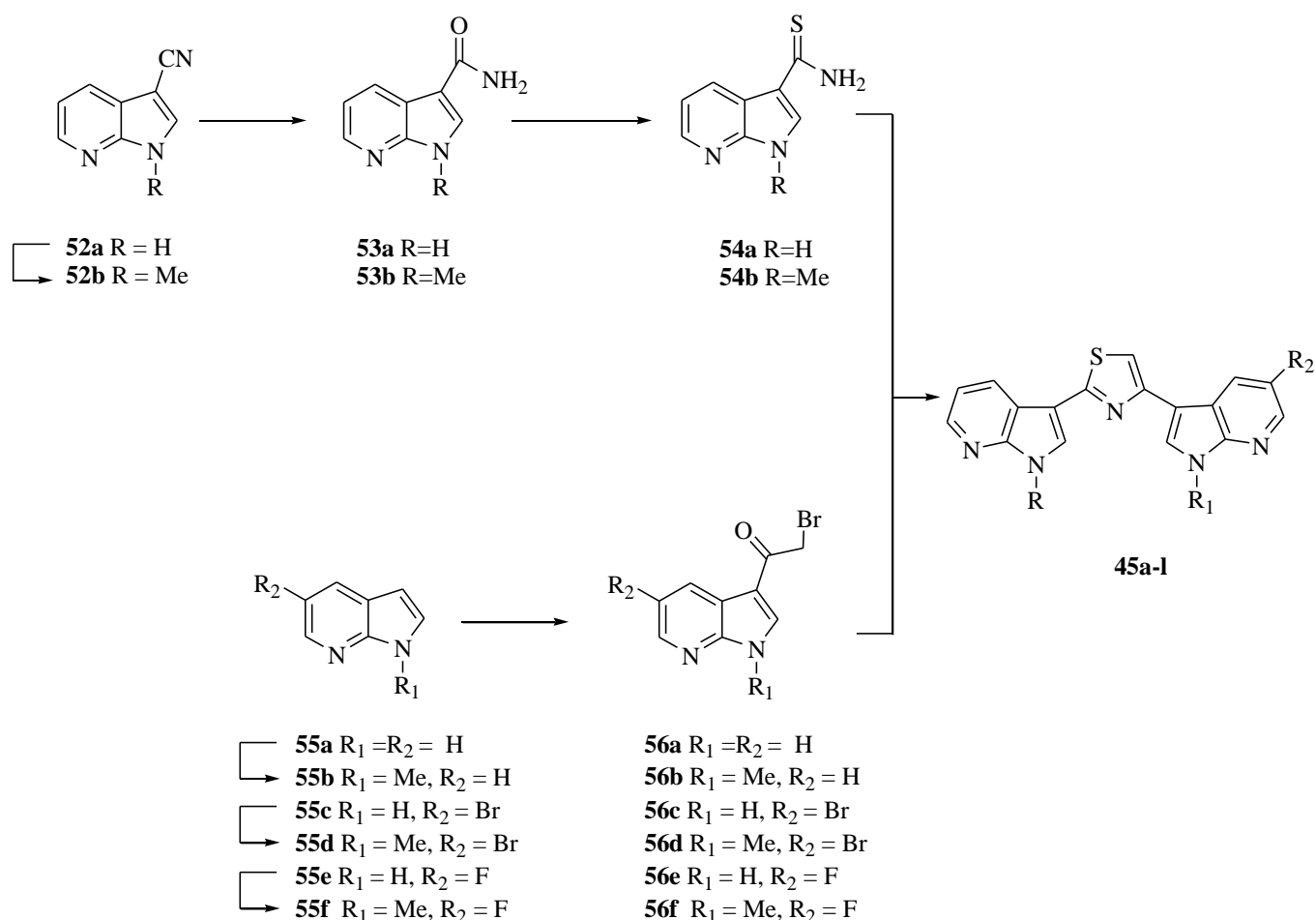
49, 50, 51

RESULTS AND DISCUSSIONS: CHEMISTRY

The synthetic pathway involves the synthesis of thiazole derivatives **45-51** (Tab. 7-9), by a Hantzsch reaction between two key intermediates: thioamides of type **54**, **78**, **79**, **80** and 3-haloacetyl compounds of type **56**, **67**, **85**, **86** at reflux in ethanol (Scheme 1, 9,18).

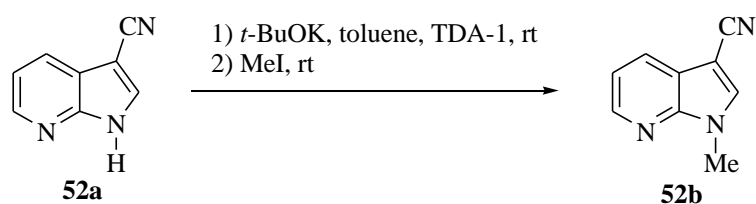
For the preparation of 3,3'-(1,3-thiazole-2,4-diyl)bis(1*H*-pyrrolo[2,3-*b*]pyridines **45a-l** we focused on the synthesis of carbothioamides **54a,b** and 3-bromoacetyl compounds **56a-f** (Scheme 1).

Scheme 1. Synthesis of 3,3'-(1,3-thiazole-2,4-diyl)bis(1*H*-pyrrolo[2,3-*b*]pyridines **45a-l**.



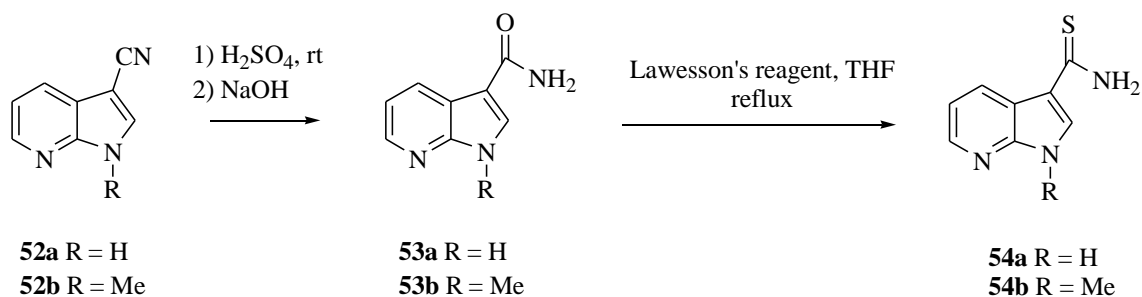
Carbothioamides **54a,b** were obtained starting from 3-cyano-7azaindoles **52a,b** (Scheme 2). Derivative **52b**, was obtained in good yields (85%) from the 7-azaindole **52a**, using potassium *t*-butoxide as base, tris[2-(2-methoxyethoxy)ethyl]amine (TDA-1) (1 or 2 drops) as phase transfer catalyst and methyl iodide as methylating agent in toluene at room temperature.

Scheme 2.



3-Cyano-7azaindoles **52a,b** were reacted with concentrated sulfuric acid at room temperature for 15-60 minutes and the subsequent alkalization with concentrated sodium hydroxide afforded the corresponding carboxamides **53a,b** in high yields (95-99%). 3-Carboxythioamides **54a,b** were conveniently prepared in excellent yields (88-99%) from the corresponding carboxamides **53a,b** using 2,4-bis(4-methoxyphenyl)-1,3,2,4-dithiadiphosphetane-2,4-disulfide (Lawesson's Reagent) in tetrahydrofuran under reflux for 30 minutes (Scheme 3) [35].

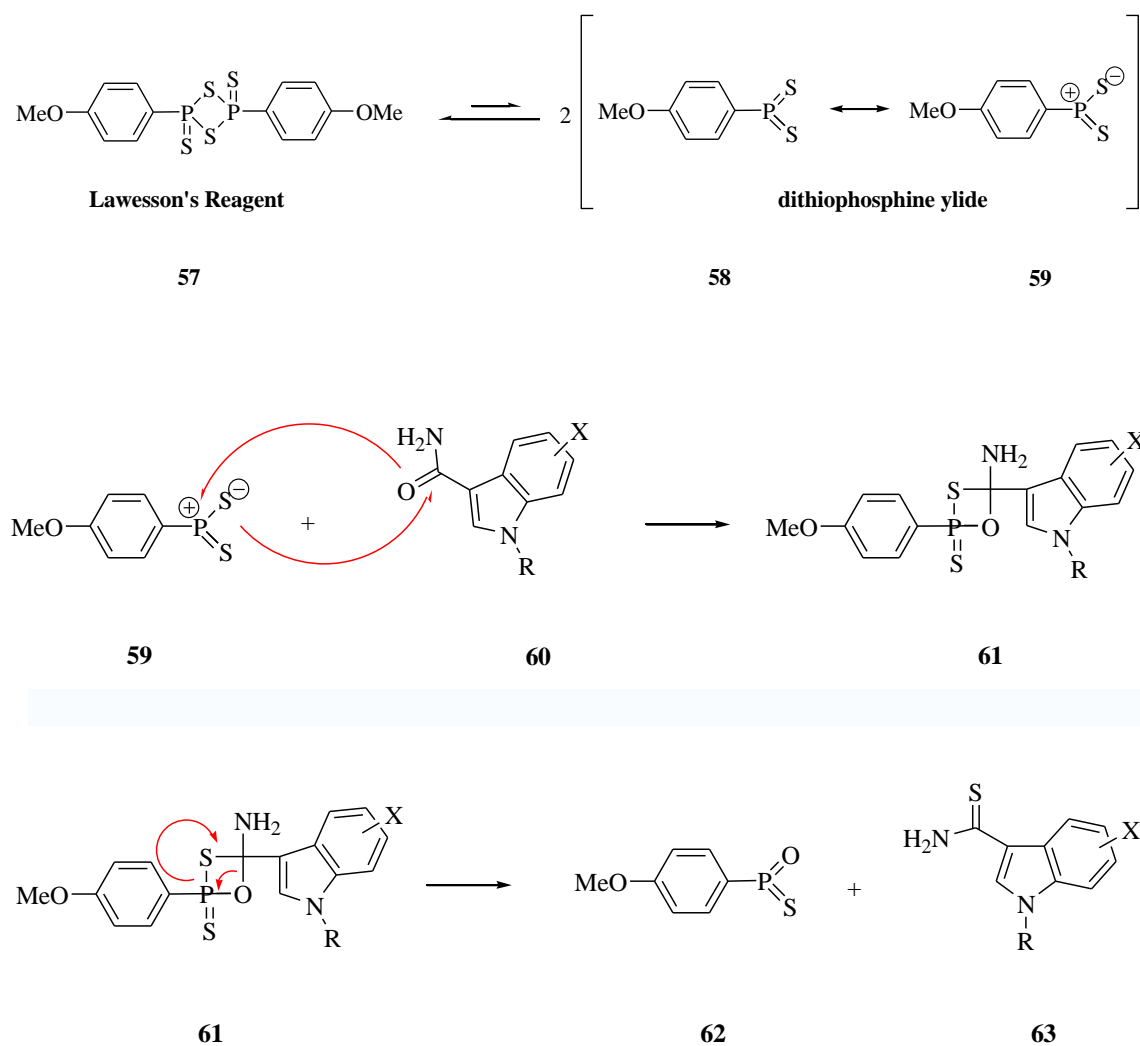
Scheme 3.



Lawesson's reagent [2,4-bis(4-methoxyphenyl)-1,3,2,4-dithiadiphosphetane-2,4-disulfide] **57** is constituted by a four membered central ring in which there are alternating sulfur and phosphorus atoms. It is a mild and convenient thionating agent for ketons, esters and amides that allows the preparation of thioketons, thioesters and thioamides in good yields.

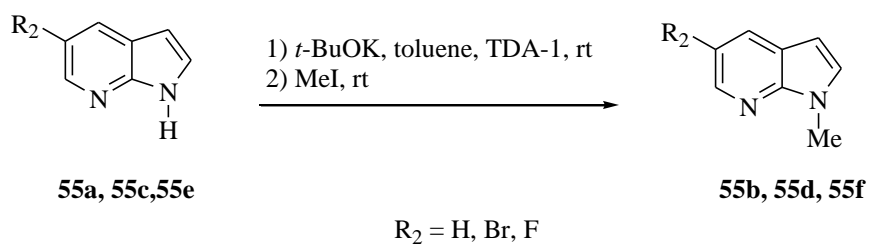
In solution Lawesson's reagent is in equilibrium with two more reactive dithiophosphine ylides **58** and **59**. The reaction of the ylide **59** with a carbonyl group **60** gives a thioxaphosphetane intermediate **61**. Then through Wittig rearrangement, the thioxaphosphetane intermediate **61** decomposes and generates the stable phenyl (thioxo) phosphine oxide **62** and the corresponding thioamide **63** (Scheme 4).

Scheme 4.



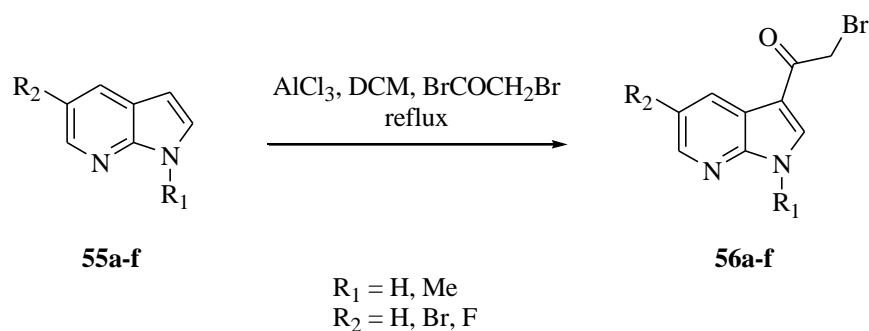
The variously substituted 7-azaindoles **55a,c,e** were converted into the corresponding *N*-methyl derivatives **55b,d,f** (60-96%) using potassium *tert*-butoxide, TDA-1 and methyl iodide (Scheme 5) [27, 29].

Scheme 5.



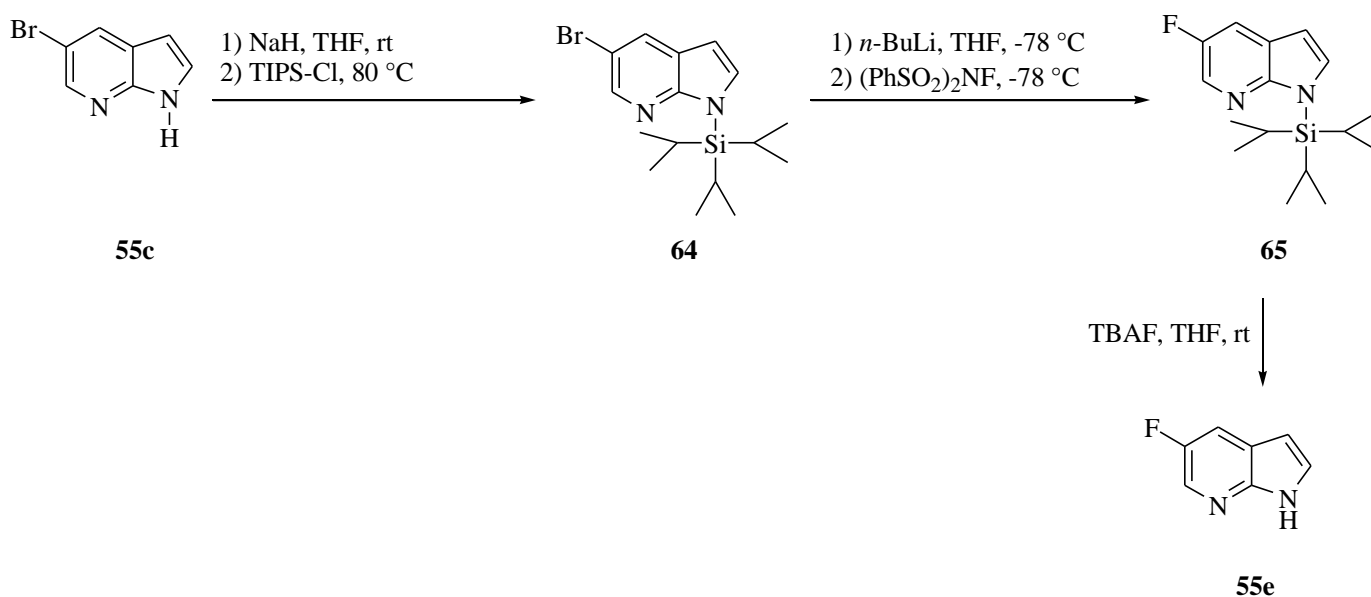
3-Bromoacetyl-7-azaindoles **56a-f** were efficiently synthesized (70-92%) by acylation of derivatives **55a-f** with bromoacetyl bromide in the presence of aluminium chloride in dichloromethane at reflux (Scheme 6) [29].

Scheme 6.



5-Fluoro-7-azaindole **55e** was prepared starting from the commercial available 5-bromo-7-azaindole **55c**. 5-Bromo 7-azaindole **55c** was reacted with triisopropylsilyl chloride in the presence of sodium hydride in tetrahydrofuran to afford with a quantitative yield 5-bromo-1-[tri(propan-2-yl)silyl]-1*H*-pyrrolo[2,3-*b*]pyridine **64**. The subsequent introduction of a fluorine atom by addition of *n*-butyl lithium (solution 2.5 M in tetrahydrofuran) and *N*-fluorobenzenesulfonimide at -78°C under a nitrogen atmosphere gave 5-fluoro-1-[tri(propan-2-yl)silyl]-1*H*-pyrrolo[2,3-*b*]pyridine **65** (yield 70%). After the deprotection of derivative **65** with tetrabutylammonium fluoride (TBAF) in tetrahydrofuran at room temperature, 5-fluoro 7-azaindole **55e** was isolated (yield 80%) (Scheme 7) [36].

Scheme 7.



Reaction of thioamides **54a,b** and 3-bromoacetyl-7-azaindole compounds **56a-f** in ethanol at reflux for 30 minutes gave, after crystallization, the desired bis-7-azaindolyl thiazoles **45a-l** (Scheme 8) from good to excellent yields (60-94%) (Tab. 7).

Scheme 8.

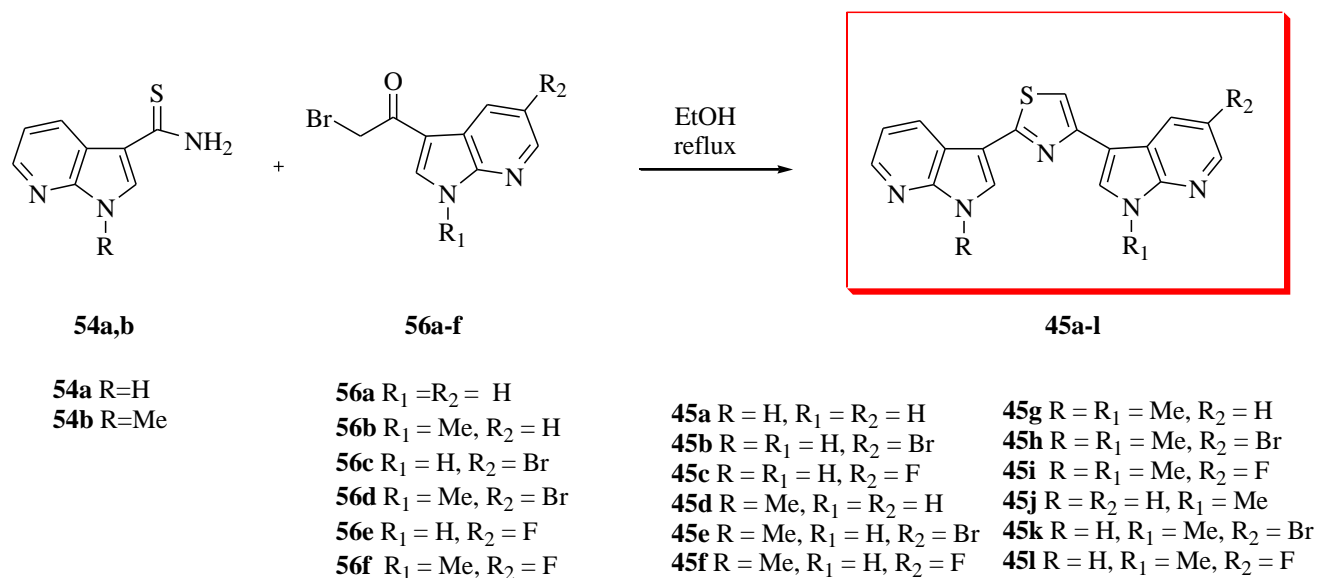
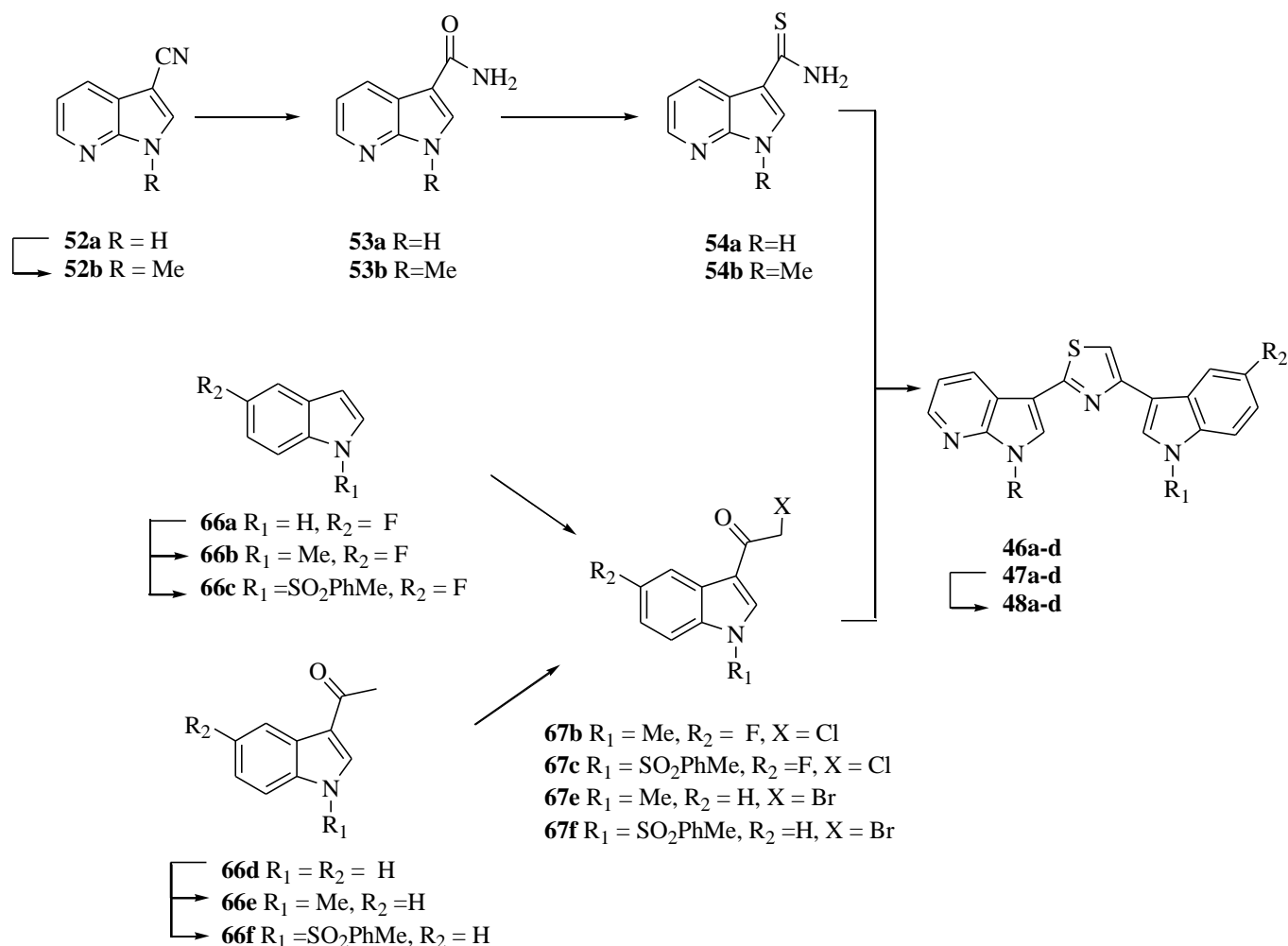


Table 7. Substituted 3,3'-(1,3-thiazole-2,4-diyl)bis(1*H*-pyrrolo[2,3-*b*]pyridines **45a-l**.

| Compd | R | R ₁ | R ₂ | Yield% | Compd | R | R ₁ | R ₂ | Yield% |
|------------|----|----------------|----------------|--------|------------|----|----------------|----------------|--------|
| 45a | H | H | H | 63 | 45g | Me | Me | H | 60 |
| 45b | H | H | Br | 60 | 45h | Me | Me | Br | 90 |
| 45c | H | H | F | 75 | 45i | Me | Me | F | 60 |
| 45d | Me | H | H | 90 | 45j | H | Me | H | 85 |
| 45e | Me | H | Br | 94 | 45k | H | Me | Br | 80 |
| 45f | Me | H | F | 90 | 45l | H | Me | F | 72 |

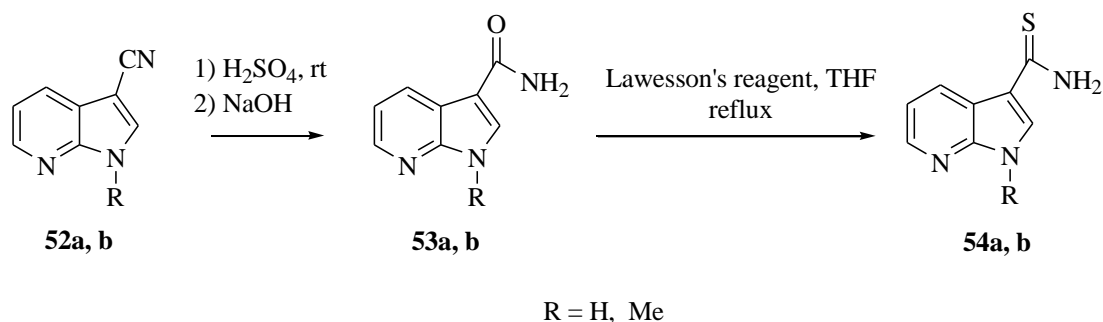
Derivatives 3-[4-(1*H*-indol-3-yl)-1,3-thiazol-2-yl]-1*H*-pyrrolo[2,3-*b*]pyridines **46a-d**, **47a-d**, **48a-d** were conveniently prepared by the same cyclization between the key intermediates: carbothioamides **54a,b** and 3-haloacetyl compounds **67b, c, e, f** (Scheme 9).

Scheme 9. Synthesis of 3-[4-(1*H*-indol-3-yl)-1,3-thiazol-2-yl]-1*H*-pyrrolo[2,3-*b*]pyridines **46a-d**, **47a-d**, **48a-d**.



Thioamides **54a,b** were obtained from the corresponding 3-cyano-7azaindoles **52a,b**, through the formation of carboxamides **53a,b** (Scheme 10) [29, 35].

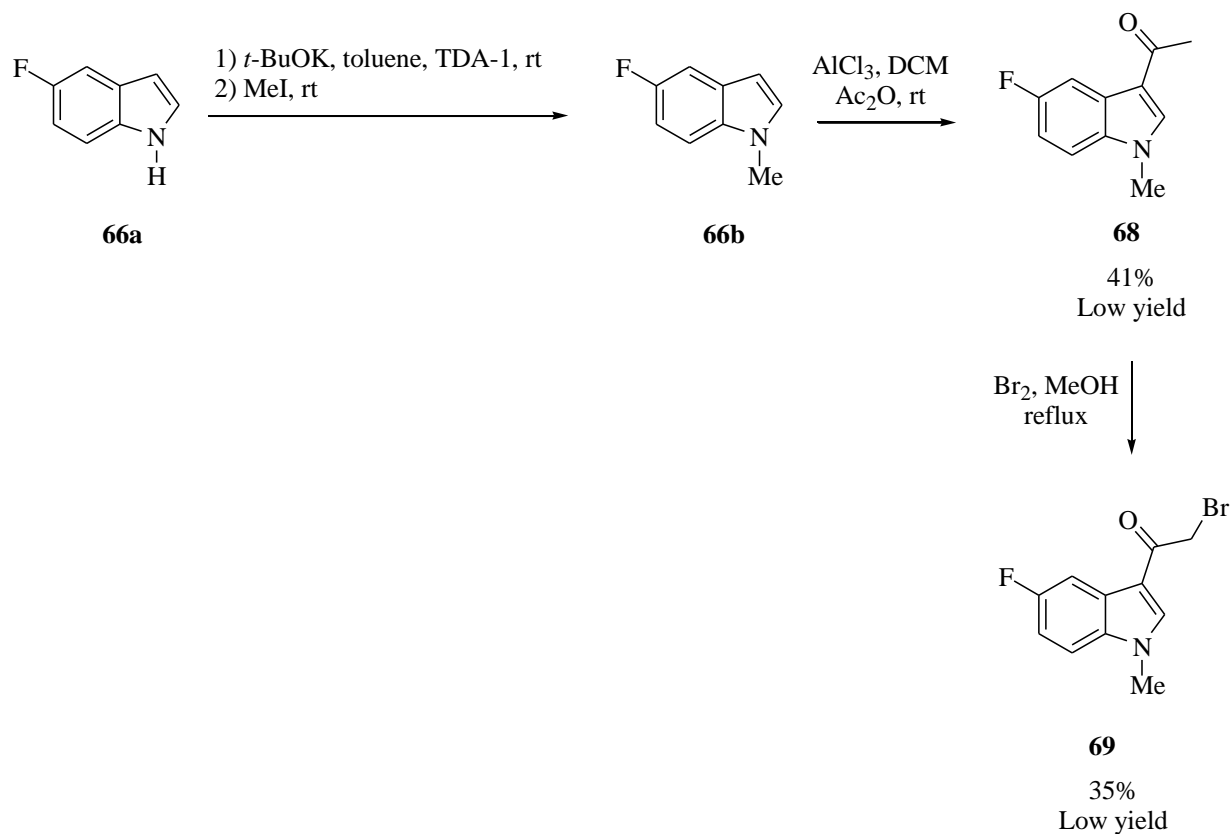
Scheme 10.



For the synthesis of 5-fluoro-3-haloacetylindole intermediates it was initially synthesized derivative **66b** by methylation of 5-fluoro indole **66a** using potassium *t*-butoxide, TDA-1 and methyl iodide

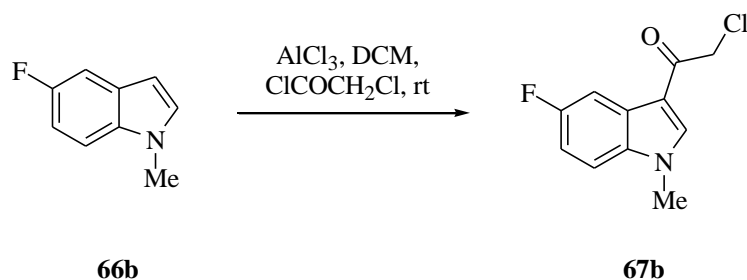
(yield 98%) [31]. The subsequent acylation of *N*-methyl derivative **66b** with acetic anhydride in the presence of aluminium chloride at room temperature in dichloromethane under nitrogen atmosphere gave the intermediate **68** (yield 41%), which reacted with bromine in methanol at reflux to give 3-bromoacetyl indole **69** but in very low yield (35%) (Scheme 11).

Scheme 11.



It was therefore decided to synthesize 3-chloro acetyl indole **67b** starting from 5-fluoro-1-methylindole **66b** with chloroacetyl chloride in presence of aluminium chloride in dichloromethane at room temperature (yield 50%) (Scheme 12).

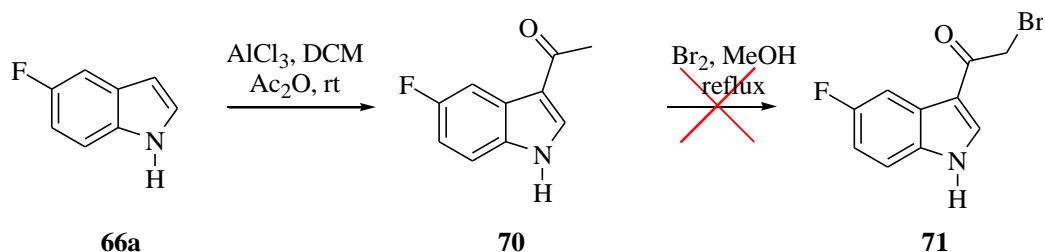
Scheme 12.



In the meantime, 5-fluoro indole **66a** was placed to react with acetic anhydride in the presence of aluminium chloride at reflux under nitrogen atmosphere to obtain 3-acetyl indole **70** (yield 55%).

However, the following bromination with bromine in methanol did not afford to the desired 3-bromoacetyl indole **71** (Scheme 13).

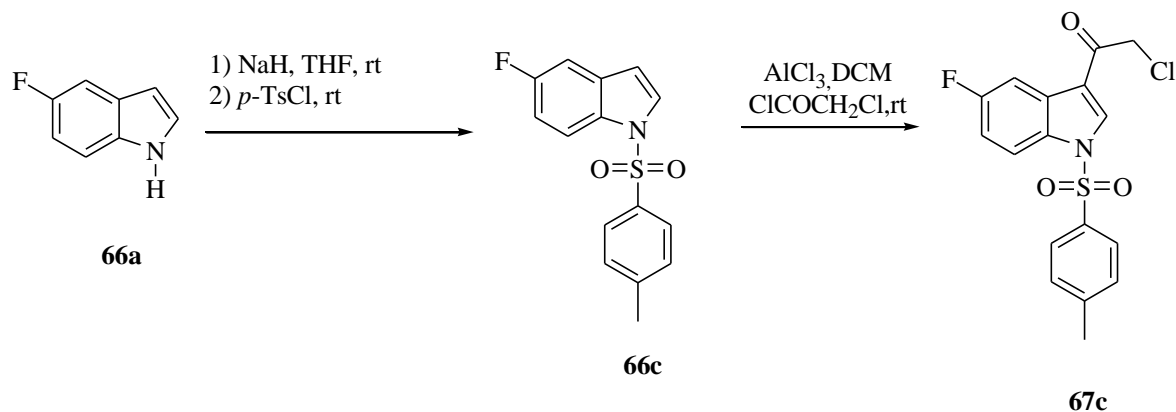
Scheme 13.



So it was necessary to change the reaction pathway and to protect the amino function of 5-fluoroindole with a *p*-toluenesulfonyl group.

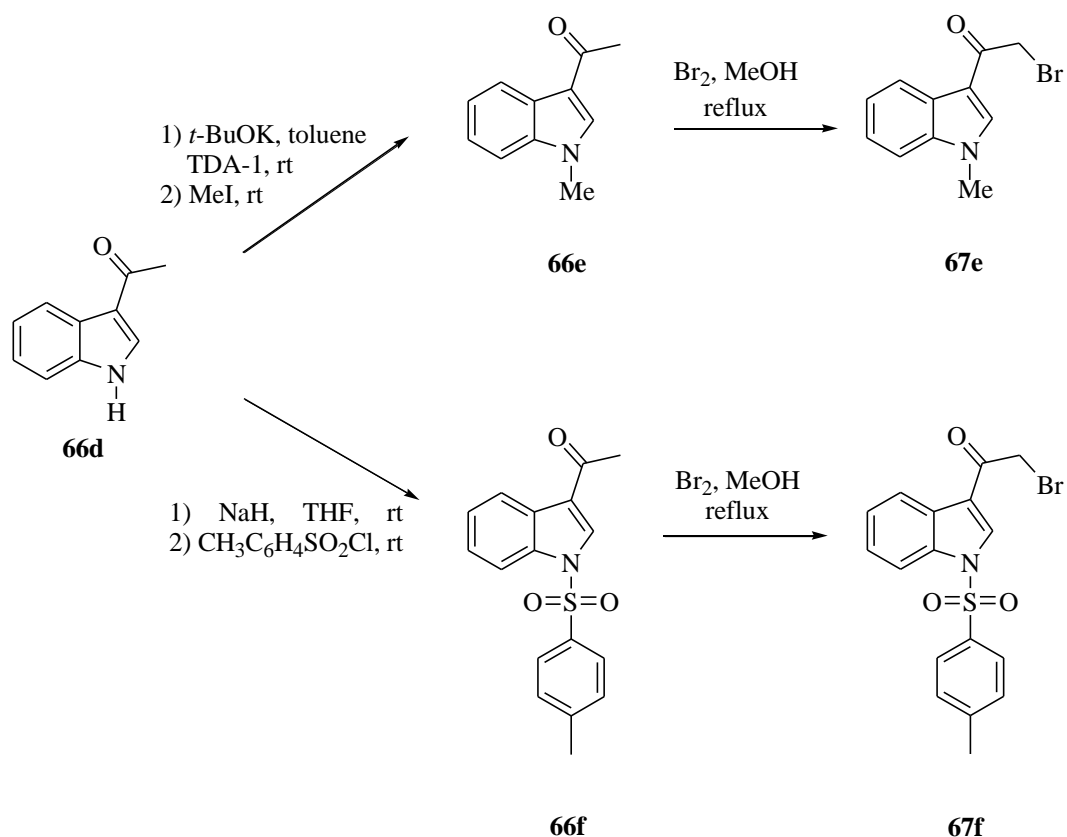
In fact, the reaction of 5-fluoroindole **66a** using sodium hydride and *p*-toluenesulfonyl chloride in tetrahydrofuran at room temperature gave desired compound **66c** with an excellent yield (96%). Derivative **67c** was obtained in good yield (55%) from the corresponding protected indole **66c** by reaction with chloroacetyl chloride and aluminium chloride in dichloromethane (Scheme 14).

Scheme 14.



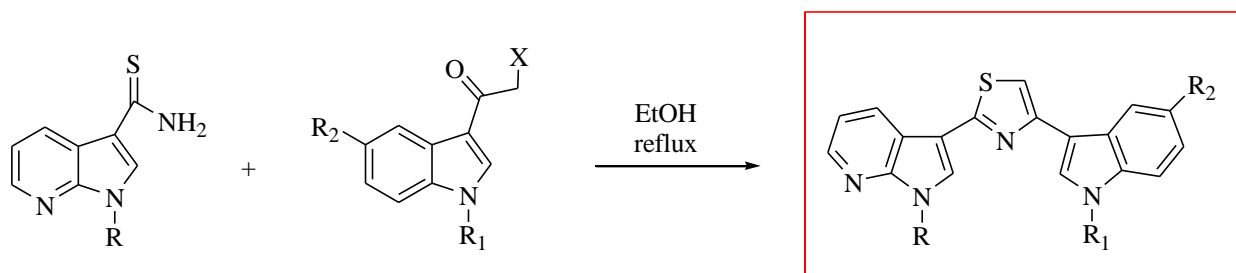
Acetyl indoles **66e,f** were brominated using bromine in methanol at reflux to yield 3-bromoacetyl indoles **67e,f** in good yields (70% and 40%, respectively) [29]. Derivatives **66e,f** were obtained from the commercial available 3-acetyl indole **66d**, which was subjected to a methylation reaction in the presence of *t*-butoxide, TDA-1 and methyl iodide to give compound **66e** (yield 80%) [31]; or protected using sodium hydride and *p*-toluenesulfonyl chloride in tetrahydrofuran at room temperature to give **66f** (yield 90%) (Scheme 15).

Scheme 15.



Thioamides **54a,b** and 3-bromo or 3-chloro acetylindole compounds **67b, c, e, f** were reacted in ethanol at reflux for 30 minutes. After crystallization with ethanol provided the desired 3-[4-(1*H*-indol-3-yl)-1,3-thiazol-2-yl]-1*H*-pyrrolo[2,3-*b*]pyridines **46a-d, 47a-d**, in good yields (30-97%) (Scheme 16) (Tab. 8).

Scheme 16.



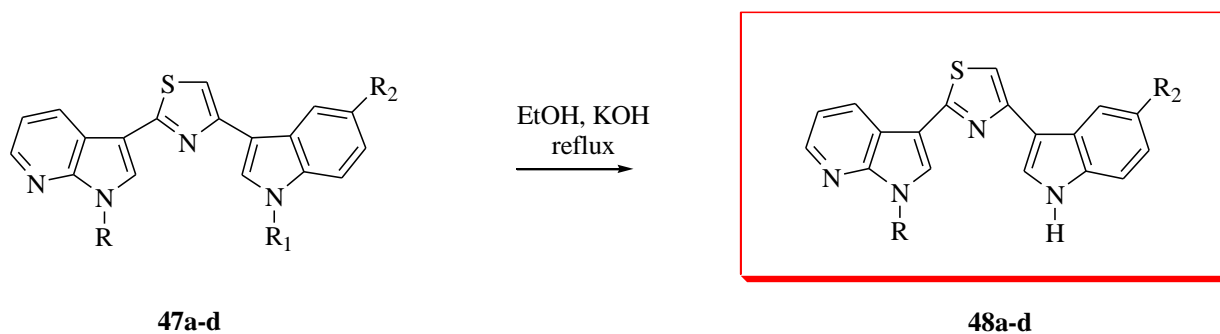
54a R=H
54b R=Me

67b R₁ = Me, R₂ = F, X = Cl
67c R₁ = SO₂PhMe, R₂ = F, X = Cl
67e R₁ = Me, R₂ = H, X = Br
67f R₁ = SO₂PhMe, R₂ = H, X = Br

46a R = H, R₁ = Me, R₂ = F
46b R = R₁ = Me, R₂ = F
46c R = R₂ = H, R₁ = Me
46d R = R₁ = Me, R₂ = H
47a R = H, R₁ = SO₂PhMe, R₂ = F
47b R = Me, R₁ = SO₂PhMe, R₂ = F
47c R = R₂ = H, R₁ = SO₂PhMe
47d R = Me, R₁ = SO₂PhMe, R₂ = H

The alkaline hydrolysis of *N*-tosil compounds **47a-d** with potassium hydroxide in ethanol at reflux afforded the corresponding *NH* compounds **48a-d** from moderate to excellent yields (40-98%) (Scheme 17) (Tab. 8).

Scheme 17.



47a R = H, R₁ = SO₂PhMe, R₂ = F
47b R = Me, R₁ = SO₂PhMe, R₂ = F
47c R = H, R₁ = SO₂PhMe, R₂ = H
47d R = Me, R₁ = SO₂PhMe, R₂ = H

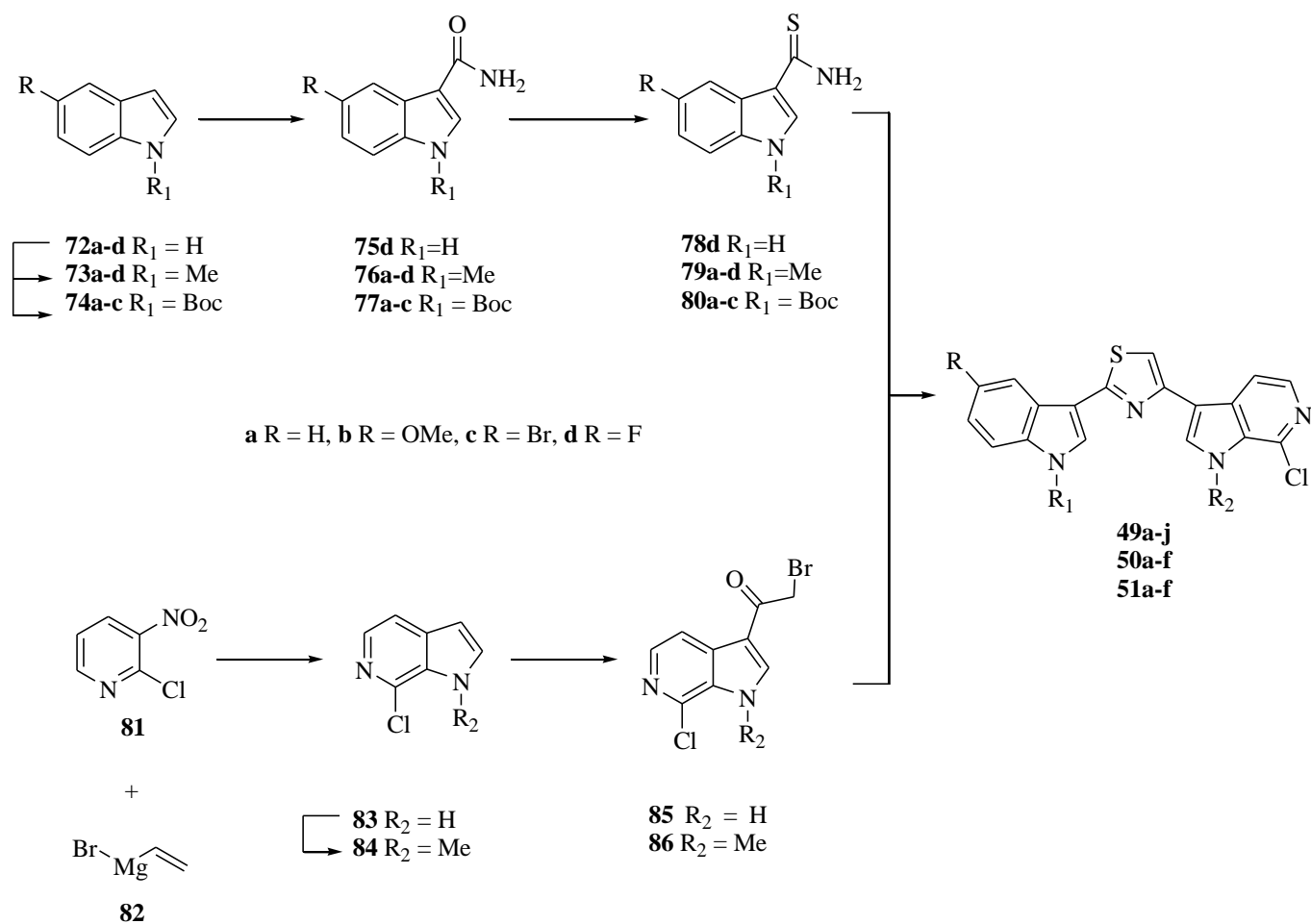
48a R = R₁ = H, R₂ = F
48b R = Me, R₁ = H, R₂ = F
48c R = R₁ = R₂ = H
48d R = Me, R₁ = R₂ = H

Table 8. Substituted 3-[4-(1*H*-indol-3-yl)-1,3-thiazol-2-yl]-1*H*-pyrrolo[2,3-*b*]pyridines **46a-d**, **47a-d**, **48a-d**.

| Compd | R | R ₁ | R ₂ | Yield% | Compd | R | R ₁ | R ₂ | Yield% |
|------------|----|----------------------|----------------|--------|------------|----|----------------------|----------------|--------|
| 46a | H | Me | F | 97 | 47c | H | SO ₂ PhMe | H | 90 |
| 46b | Me | Me | F | 30 | 47d | Me | SO ₂ PhMe | H | 50 |
| 46c | H | Me | H | 60 | 48a | H | H | F | 98 |
| 46d | Me | Me | H | 60 | 48b | Me | H | F | 40 |
| 47a | H | SO ₂ PhMe | F | 97 | 48c | H | H | H | 98 |
| 47b | Me | SO ₂ PhMe | F | 40 | 48d | Me | H | H | 98 |

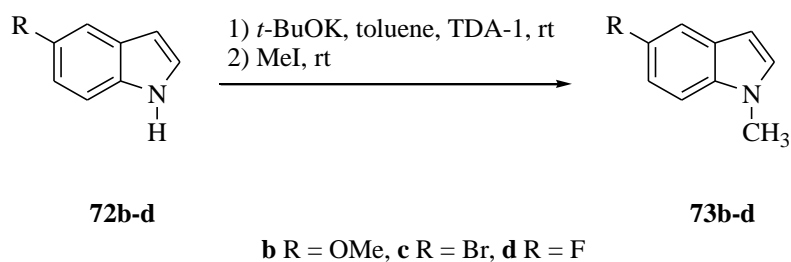
The synthesis of 7-chloro-3-[2-(1*H*-indol-3-yl)-1,3-thiazol-4-yl]-1*H*-pyrrolo[2,3-*c*]pyridines **49a-j**, **50a-f**, **51a-f** involve a Hantzsch reaction between thioamides **78d**, **79a-d**, **80a-c** and 6-azaindoles **85**, **86** (Scheme 18).

Scheme 18. Synthesis of 7-chloro-3-[2-(1*H*-indol-3-yl)-1,3-thiazol-4-yl]-1*H*-pyrrolo[2,3-*c*]pyridine **49a-j**, **50a-f**, **51a-f**.



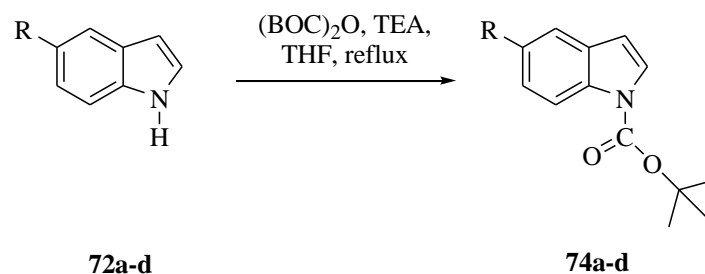
The first step for the synthesis of carbothioamides **78d**, **79a-d** and **80a-c** was the functionalization of the indolyl moiety. In particular, the methylation of the variously substituted indoles **72b-d** (**73a** is commercial available), gave methylated derivatives **73b-d** in excellent yields (96-98%) (Scheme 19) [27].

Scheme 19.



Moreover, the indoles **72a-d** were also protected as *N-tert*-butylcarboxylate using di-*tert*-butyl dicarbonate and triethylamine in tetrahydrofuran under reflux to obtain derivatives **74a-d** in very good to quantitative yields (90-100%) (Scheme 20) [30, 31].

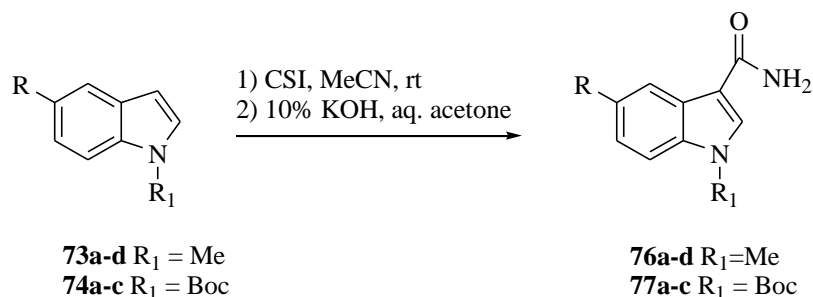
Scheme 20.



a R = H, **b** R = OMe, **c** R = Br, **d** R = F

All the indoles **73a-d**, **74a-d** were converted into the corresponding carboxamide derivatives by the reaction with chloroacetyl isocyanate (CSI) in acetonitrile, followed by alkaline hydrolysis of the chlorosulfonyl group. The reaction was carried out at room temperature and gave carboxamide derivatives **76a-d** and **77a-c** in good yields (40-60%) (Scheme 21) [30, 31].

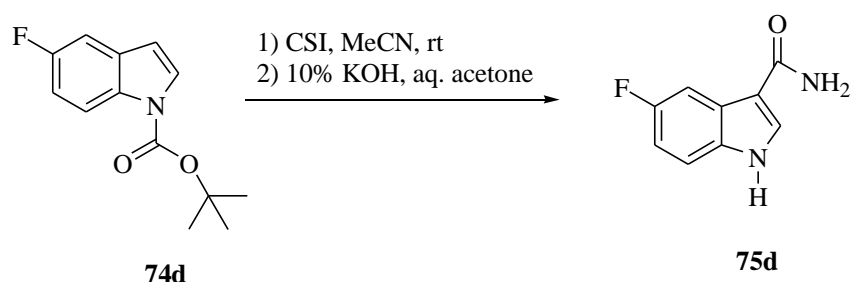
Scheme 21.



a R = H, **b** R = OMe, **c** R = Br, **d** R = F

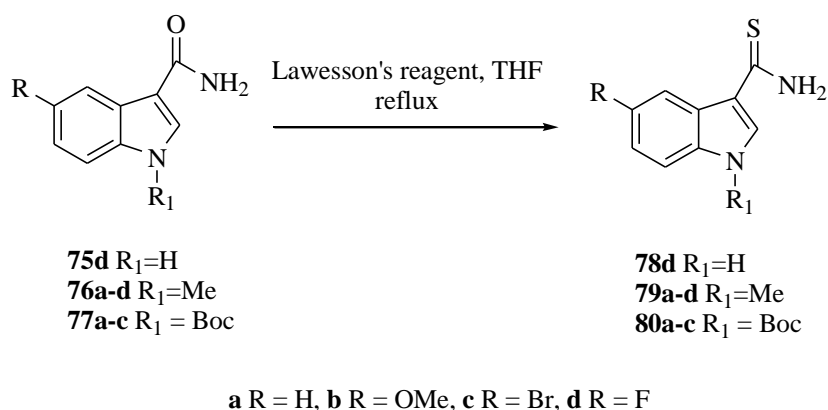
For compound **74d** the reaction with chloroacetyl isocyanate at room temperature did not work and it was necessary force the reaction conditions, increasing the temperature and only under reflux it was possible to isolate the unprotected carboxamide in moderate yield (40%) **75d** (Scheme 22).

Scheme 22.



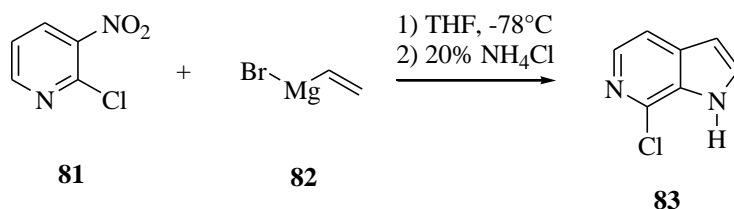
The subsequent treatment of carboxamides **75d**, **76a-d**, **77a-c** with Lawesson's reagent in tetrahydrofuran under reflux afforded the thioamides **78d**, **79a-d** and **80a-c** (90-98%) (Scheme 23) [30,31].

Scheme 23.



Starting from the commercial 2-chloro-3-nitropyridine **81** and vinylmagnesium bromide **82** in tetrahydrofuran at -78 °C under nitrogen atmosphere it was possible to obtain, after acid workup, the 6-azaindole **83** (Scheme 24) [37].

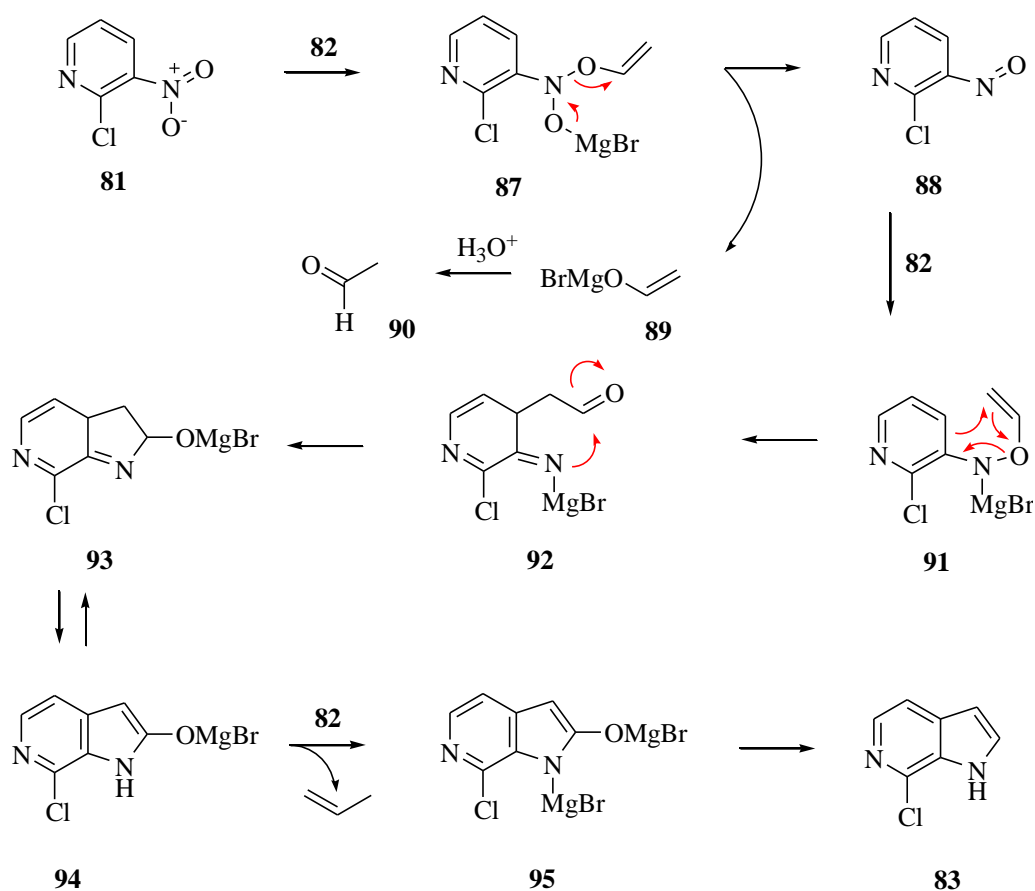
Scheme 24.



This reaction is carried out through the Bartoli indole synthesis, an organic reaction where a substituted nitroarene is converted to an indole ring using an excess of a vinyl Grignard reagent, followed by an acid workup. The mechanism begins by the addition of the Grignard reagent **82** onto the nitroarene **81** to form intermediate **87**. This intermediate spontaneously decomposes to form a

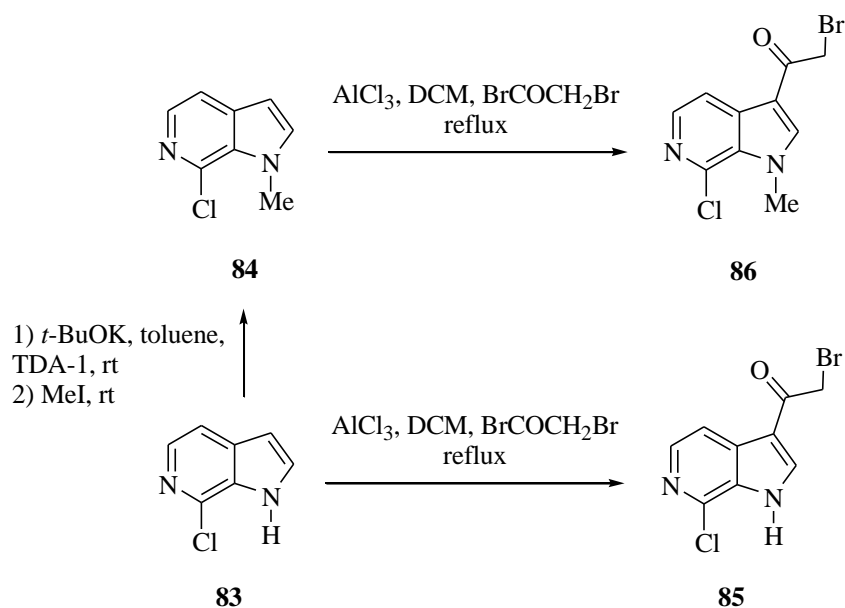
nitrosoarene **88** and a magnesium salt **89**. Upon reaction workup, the magnesium salt **89** will liberate a carbonyl compound **90**. Reaction of the compound **88** with a second equivalent of the Grignard reagent **82** forms intermediate **91**. The steric bulk of the ortho group causes a [3,3]-sigmatropic rearrangement (Claisen) forming the intermediate **92**. Cyclization and tautomerization give intermediate **94**, which will react with a third equivalent of the Grignard reagent **82** to give a dimagnesium indole salt **95**, which upon elimination of water gives the indole **83** (Scheme 25) [38].

Scheme 25.



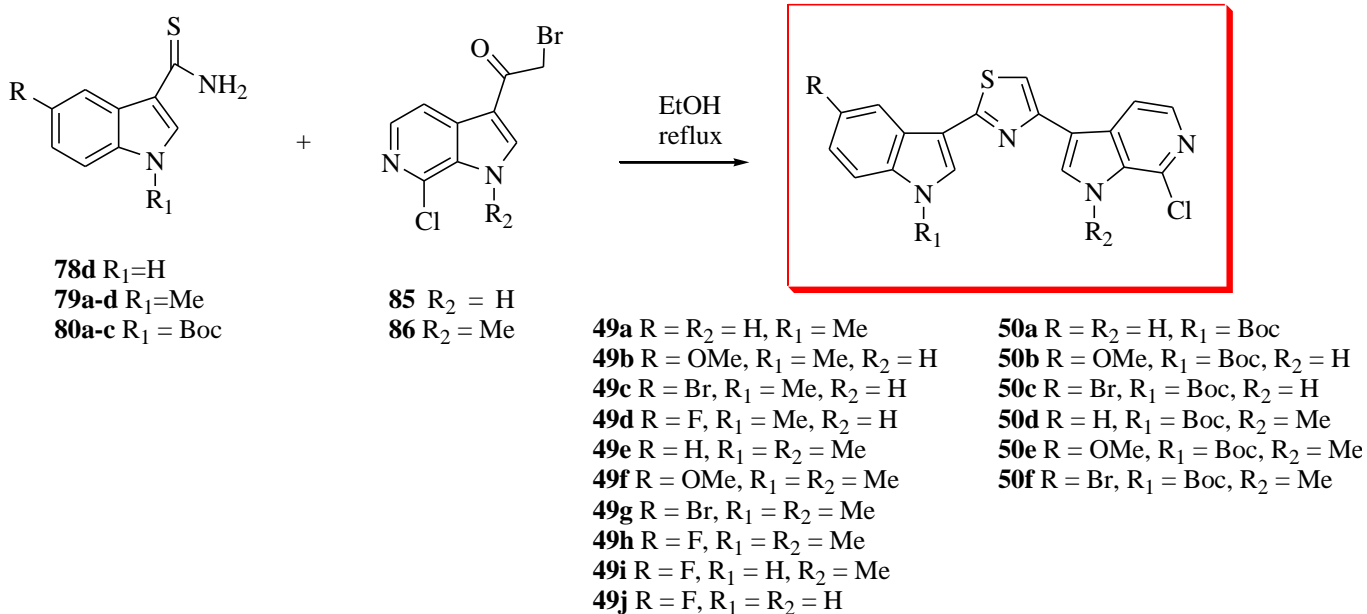
The 6-azaindole **83** obtained was converted into the corresponding *N*-methyl derivative **84** (70%). Compound **83** and **84** were transformed into the corresponding 3-bromoacetyl-6-aza-indoles **85**, **86** (88-98%) by reaction with bromoacetyl bromide in the presence of aluminium chloride in dichloromethane under reflux for 40 minutes (Scheme 26).

Scheme 26.



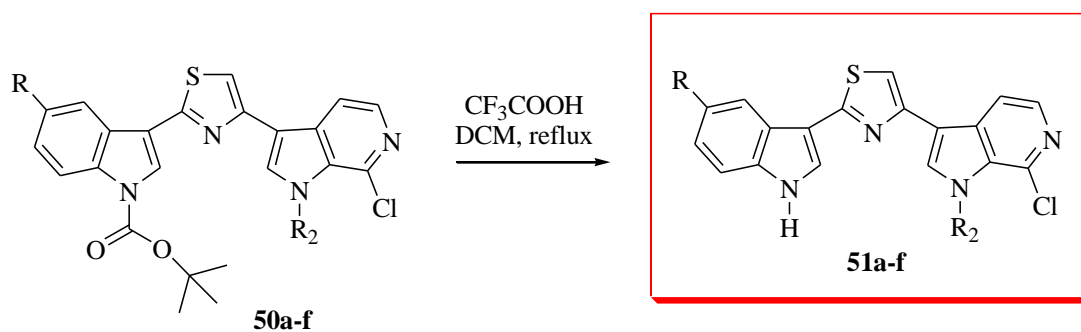
Reaction of all thioamides **78d**, **79a-d**, **80a-c** and 3-bromoacetyl-6-azaindole compounds **85,86** in ethanol under reflux provided, after crystallization, the desired indolyl-6-azaindolyl thiazoles **49a-j** and **50a-f** (65-98%) (Scheme 27) (Tab. 9).

Scheme 27.



The subsequent hydrolysis of *N*-Boc compounds **50a-f** with trifluoroacetic acid in dichloromethane at reflux afforded, after neutralization, the corresponding *N*-unprotected thiazoles **51a-f** (62-99%) (Scheme 28) (Tab. 9).

Scheme 28.



50a R = H, R₂ = H
50b R = OMe, R₂ = H
50c R = Br, R₂ = H
50d R = H, R₂ = Me
50e R = OMe, R₂ = Me
50f R = Br, R₂ = Me

51a R = H, R₂ = H
51b R = OMe, R₂ = H
51c R = Br, R₂ = H
51d R = H, R₂ = Me
51e R = OMe, R₂ = Me
51f R = Br, R₂ = Me

Table 9. Substituted 7-chloro-3-[2-(1*H*-indol-3-yl)-1,3-thiazol-4-yl]-1*H*-pyrrolo[2,3-*c*]pyridine **49a-j**, **50a-f**, **51a-f**.

| Compd | R | R ₁ | R ₂ | Yield% | Compd | R | R ₁ | R ₂ | Yield% |
|------------|-----|----------------|----------------|--------|------------|-----|----------------|----------------|--------|
| 49a | H | Me | H | 98 | 50b | OMe | Boc | H | 77 |
| 49b | OMe | Me | H | 65 | 50c | Br | Boc | H | 77 |
| 49c | Br | Me | H | 93 | 50d | H | Boc | Me | 91 |
| 49d | F | Me | H | 97 | 50e | OMe | Boc | Me | 92 |
| 49e | H | Me | Me | 96 | 50f | Br | Boc | Me | 91 |
| 49f | OMe | Me | Me | 79 | 51a | H | H | H | 93 |
| 49g | Br | Me | Me | 98 | 51b | OMe | H | H | 62 |
| 49h | F | Me | Me | 95 | 51c | Br | H | H | 98 |
| 49i | F | H | Me | 82 | 51d | H | H | Me | 75 |
| 49j | F | H | H | 66 | 51e | OMe | H | Me | 73 |
| 50a | H | Boc | H | 84 | 51f | Br | H | Me | 99 |

RESULTS AND DISCUSSIONS: BIOLOGY

All the synthesized thiazoles **45a-l**, **46a-d**, **47a-d**, **48a-d**, **49a-j**, **50a-f** and **51a-f** (Tab. 7-9) were submitted to the National Cancer Institute (NCI, Bethesda MD) in order to evaluate their antitumor activity.

Biological screening were performed on derivatives **45a-l**, **46c,d**, **47c,d**, **48c,d**, **49a-j**, **50a-f**, **51a-f**, according to the NCI protocol, at the 10^{-5} M dose for the *in vitro* disease-oriented antitumor screenings against a panel of about 60 human tumor cell lines derived from 9 human cancer cell types, that have been grouped in disease sub-panel including leukemia, non-small cell lung cancer, colon cancer, central nervous system cancer, melanoma, ovarian cancer, renal cancer, prostate cancer and breast cancer cell lines (Tab. 10).

Table 10. Mean Growth Percent of compounds **45a-l**, **46c-d**, **47c-d**, **48c-d**, **49a-j**, **50a-f**, **51a-f**.

| Mean Growth Percent | | | | | | | | | | |
|---------------------|------------|------------|------------|------------|------------|------------|------------|------------|------------|------------|
| Compd | 45a | 45b | 45c | 45d | 45e | 45f | 45g | 45h | 45i | 45j |
| | 96.25 | 73.88 | 81.60 | 60.08 | 68.77 | 98.94 | 93.30 | 87.69 | 75.71 | 86.53 |
| Compd | 45k | 45l | 46c | 46d | 47c | 47d | 48c | 48d | 49a | 49b |
| | 31.86 | 69.34 | 72.28 | 28.74 | 94.54 | 53.02 | 89.28 | 29.80 | 91.91 | 76.64 |
| Compd | 49c | 49d | 49e | 49f | 49g | 49h | 49i | 49j | 50a | 50b |
| | 84.71 | 96.96 | 87.56 | 92.20 | 91.54 | 77.46 | 65.01 | 36.21 | 90.88 | 68.50 |
| Compd | 50c | 50d | 50e | 50f | 51a | 51b | 51c | 51d | 51e | 51f |
| | 88.11 | 58.74 | 89.46 | 73.58 | 41.11 | 37.10 | 17.34 | 66.84 | 38.95 | 56.23 |

Compounds **45k**, **46d**, **48d** and **51c** satisfied the criteria set by the NCI for activity in this assay and were selected for further screenings at 5 concentrations at 10-fold dilution (10^{-4} - 10^{-8} M) on the full panel (Tab. 11). The antitumor activity of compounds was given by three parameters for each cell line: GI_{50} (GI_{50} is the molar concentration of the compound that inhibits 50% net cell growth), TGI (TGI is the molar concentration of the compound leading to total inhibition of net cell growth), and LC_{50} (LC_{50} is the molar concentration of the compound that induces 50% net cell death). The average values of mean graph midpoint (MG_MID) were calculated for each of these parameters.

Table 11. *In vitro* inhibition of cancer cell line growth by compounds **45k**, **46d**, **48d**, **51c** (μM)^a.

| Cell lines | GI ₅₀ (μM) | | | |
|-----------------------------------|------------------------------------|------|-----------------|------|
| | 45k | 46d | 48d | 51c |
| Leukemia | | | | |
| CCRF-CEM | 6.81 | 0.40 | 0.43 | 3.16 |
| HL-60(TB) | >100 | 0.30 | 0.32 | 2.64 |
| K-562 | 8.76 | 0.07 | 0.12 | 2.73 |
| MOLT-4 | >100 | 0.67 | 0.66 | 3.02 |
| RPMI-8226 | >100 | 0.46 | 0.65 | 4.03 |
| SR | ND ^b | 0.06 | 0.14 | 1.27 |
| Non-Small Cell Lung Cancer | | | | |
| A549/ATCC | 2.59 | 0.56 | 0.71 | 3.83 |
| EKVK | 1.27 | 0.91 | 0.91 | 3.11 |
| HOP-62 | 2.39 | 0.81 | 0.94 | 2.11 |
| HOP-92 | 5.03 | 0.35 | 0.31 | 2.43 |
| NCI-H226 | 1.97 | 0.74 | 0.65 | 2.40 |
| NCI-H23 | 2.80 | 0.72 | 0.67 | 2.42 |
| NCI-H322M | >100 | 0.76 | ND ^b | 3.54 |
| NCI-H460 | 2.98 | 0.30 | 0.37 | 2.16 |
| NCI-H522 | 4.86 | 0.04 | 0.05 | 2.28 |
| Colon Cancer | | | | |
| COLO-205 | ND ^b | 0.19 | 0.19 | 1.80 |
| HCC-2998 | >100 | 1.13 | 1.18 | 2.22 |
| HCT-116 | 2.91 | 0.38 | 0.39 | 2.35 |
| HCT-15 | 13.7 | 0.17 | 0.29 | 1.40 |
| HT29 | 6.75 | 0.25 | 0.19 | 2.66 |
| KM12 | 5.70 | 0.21 | 0.40 | 2.15 |
| SW-620 | 4.46 | 0.22 | 0.30 | 1.92 |
| CNS Cancer | | | | |
| SF-268 | 6.01 | 2.44 | 0.94 | 4.06 |
| SF-295 | 3.01 | 0.25 | 0.31 | 2.48 |
| SF-539 | 27.7 | 0.18 | 0.25 | 1.87 |
| SNB-19 | 6.74 | 0.63 | 0.64 | 3.25 |

| | | | | |
|------------------------|-----------------|-------|-------|-----------------|
| SNB-75 | 2.18 | 0.16 | 0.14 | 2.37 |
| U251 | 2.70 | 0.41 | 0.43 | 2.05 |
| Melanoma | | | | |
| LOX IMVI | 4.26 | 0.54 | 0.51 | 1.63 |
| MALME-3M | 3.01 | 1.04 | 0.75 | ND ^b |
| M14 | 4.06 | 0.27 | 0.29 | 2.22 |
| MDA-MB-435 | 3.17 | 0.04 | 0.03 | 3.43 |
| SK-MEL-2 | 19.8 | 0.58 | 0.41 | 4.09 |
| SK-MEL-28 | ND ^b | 1.20 | 0.77 | 1.85 |
| SK-MEL-5 | 2.05 | 0.24 | 0.27 | 2.61 |
| UACC-257 | ND ^b | 13.00 | 14.20 | 2.68 |
| UACC-62 | 3.47 | 0.30 | 0.42 | 2.19 |
| Ovarian Cancer | | | | |
| IGROV1 | 2.21 | 1.33 | 1.18 | 2.51 |
| OVCAR-3 | 2.91 | 0.10 | 0.25 | 3.45 |
| OVCAR-4 | 2.03 | 7.22 | 0.52 | 3.25 |
| OVCAR-5 | >100 | 1.41 | 2.39 | 3.14 |
| OVCAR-8 | 3.72 | 0.66 | 0.82 | 3.65 |
| NCI/ADR-RES | 3.88 | 0.09 | 0.15 | 2.71 |
| SK-OV-3 | 3.25 | 0.57 | 0.52 | 2.78 |
| Renal Cancer | | | | |
| 786-0 | 9.65 | 0.97 | 0.72 | 1.37 |
| A498 | 10.9 | 0.50 | 0.37 | 1.56 |
| ACHN | 2.35 | 0.72 | 0.51 | 2.02 |
| CAKI-1 | 1.56 | 0.38 | 0.44 | 1.96 |
| RXF393 | 2.05 | 0.33 | 0.52 | 1.48 |
| SN12C | ND ^b | 12.10 | 5.48 | 3.35 |
| TK-10 | 3.77 | 0.60 | 0.99 | 4.16 |
| UO-31 | ND ^b | 0.90 | 0.69 | 0.93 |
| Prostate Cancer | | | | |
| PC-3 | 4.35 | 0.46 | 0.56 | 3.86 |
| DU-145 | 3.51 | 0.39 | 0.57 | 1.76 |
| Breast Cancer | | | | |
| MCF7 | 6.77 | 0.33 | 0.37 | 2.20 |

| | | | | |
|-----------------|------|-----------------|-----------------|------|
| MDA-MB-231/ATCC | 3.02 | 2.82 | 1.29 | 1.68 |
| HS 578T | 2.43 | 0.59 | 0.66 | 3.70 |
| BT-549 | 20.5 | 0.47 | 0.44 | 4.70 |
| T-47D | 1.80 | ND ^b | ND ^b | 3.12 |
| MDA-MB-468 | 0.81 | 0.28 | 0.23 | 1.18 |

^aData obtained from NCI's in vitro disease-oriented tumor cells screen

^bND = Not Determined

An evaluation of the data reported in table 12 pointed out that all derivatives resulted active at micromolar to nanomolar concentration, against most of the tested cell lines, as it has been confirmed by the range of GI₅₀ value of 0.81-27.7, 0.04-13.00, 0.03-14.20, 0.93-4.70 μ M, respectively for compounds **45k**, **46d**, **48d**, **51c**.

The indolyl-thiazolyl-pyrrolo[2,3-*b*]pyridine **46d**, **48d** and indolyl-thiazolyl-pyrrolo[2,3-*c*]pyridine **51c** resulted more active than thiazolyl-bis-pyrrolo[2,3-*b*]pyridine derivative **45k** in terms either of GI₅₀ (mean value 1.09, 0.86, 2.59 and 5.26 μ M, respectively) and percentage of sensitive cell lines out of the total number of cell lines investigated (100%, 100%, 100% and 89%, respectively).

Derivative **45k** showed selectivity with respect to MDA-MB-468 (GI₅₀ 0.81 μ M) of breast cancer subpanel, EKVK (GI₅₀ 1.27 μ M) of non small cell lung, and CAKI-1 (GI₅₀ 1.56 μ M) of renal cancer subpanel.

Derivative **46d** was shown to be selective with respect to the leukemia subpanel having all the subpanel cell lines GI₅₀ in the range 0.06-0.67 μ M. The most sensitive cell lines are K-562 (GI₅₀ 0.07 μ M) and SR (GI₅₀ 0.06 μ M) of leukemia, NCI-H522 (GI₅₀ 0.04 μ M) of non-small cell lung cancer, MDA-MB-435 (GI₅₀ 0.04 μ M) of melanoma, OVCAR-3 and NCI/ADR-RES (GI₅₀ 0.10, 0.09 μ M, respectively) of ovarian cancer.

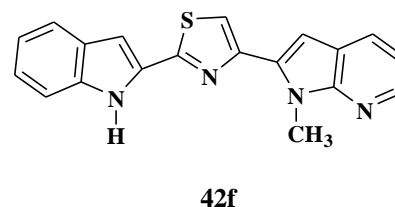
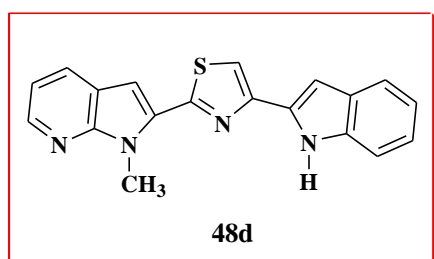
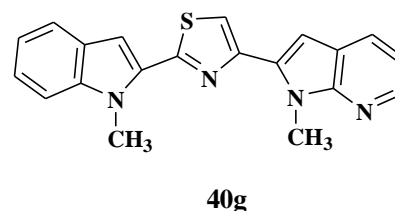
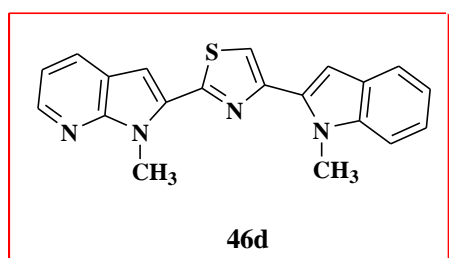
Derivative **48d** was shown to be selective with respect to the non-small cell lung cancer subpanel having all the subpanel cell lines GI₅₀ in the range 0.05-0.94 μ M. The most sensitive cell lines are K-562 (GI₅₀ 0.12 μ M) and SR (GI₅₀ 0.14 μ M) of leukemia, NCI-H522 (GI₅₀ 0.05 μ M) of non-small cell lung cancer, SNB-75 (GI₅₀ 0.14 μ M) of CNS cancer, MDA-MB-435 (GI₅₀ 0.03 μ M) of melanoma, NCI/ADR-RES (GI₅₀ 0.15 μ M) of ovarian cancer.

Derivative **51c** was shown to be selective with respect to the renal cancer subpanel having all the subpanel cell lines GI₅₀ in the range 0.93-4.16 μ M. The most sensitive cell lines are UO-31 (GI₅₀ 0.93 μ M), 786-0 (GI₅₀ 1.37 μ M), RXF393 (GI₅₀ 1.48 μ M), and A498 (GI₅₀ 1.56 μ M). Cell lines sensitive to derivative **51c** were also SR (GI₅₀ 1.27 μ M) of leukemia, HCT-15 (GI₅₀ 1.40 μ M) of colon cancer, and MDA-MB-468 (GI₅₀ 1.18 μ M) of breast cancer subpanel.

Table 12. Overview of compounds **45k**, **46d**, **48d** and **51c**.

| Compd | N° of cell line | N° of active cell | GI ₅₀ (μM) | |
|------------|-----------------|-------------------|-----------------------|--------|
| | tested | lines | Range | MD_MID |
| 45k | 54 | 48 | 0.81-27.7 | 5.26 |
| 46d | 59 | 59 | 0.04-13.00 | 1.09 |
| 48d | 58 | 58 | 0.03-14.20 | 0.86 |
| 51c | 59 | 59 | 0.93-4.70 | 2.59 |

Comparing the antiproliferative activity of the most active derivatives of 7-azaindoly thiazole **46d**, **48d** and 6-azaindoly thiazole **51c** with analogues of the previous series, already published [31] (**40g**, **42f**, **42e**) (Scheme 29), we can observe that all compounds were active against the total number of cell lines investigated (Tab. 13). As show in the table 13, it is possible to observe that the switching of the indole and 7-azaindole rings (**46d**, **48d**) led to a comparable antiproliferative activity than compounds **40g** and **42g**. Conversely, the substitution of the 7-aza-indole moiety (**42e**) with a 6-aza-indole one (**51c**) cause a reduction of the antitumoral activity, as it is possible to observe by GI₅₀ values reported.

Scheme 29.

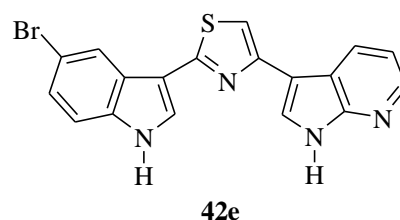
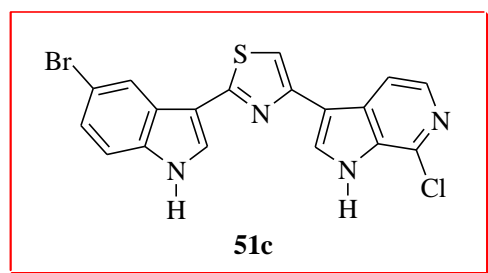


Table 13. Overview of compounds **46d**, **48d**, **51c**, **40g**, **42f**, **42e**.

| Compd. | N° of cell line tested | N° of active cell lines | GI ₅₀ (μM) | |
|------------|------------------------|-------------------------|-----------------------|--------|
| | | | Range | MD_MID |
| 42f | 58 | 58 | 0.72-0.84 | 0.79 |
| 48d | 58 | 58 | 0.03-14.20 | 0.86 |
| 40g | 58 | 58 | 0.72-0.83 | 0.76 |
| 46d | 59 | 59 | 0.04-13.00 | 1.09 |
| 42e | 59 | 59 | 0.69-0.77 | 0.74 |
| 51c | 59 | 59 | 0.93-4.16 | 2.59 |

The antiproliferative activity of all the synthesized thiazoles **45a-l**, **46a-d**, **47a-d**, **48a-d**, **49a-j**, **50a-f** and **51a-f** was further examined by Istituto Nazionale dei Tumori (Fondazione IRCCS, Milano) in two additional cell lines, STO and MesoII, derived from human DMPM, a tumor type non included in the NCI panel.

Cells were exposed to increasing concentrations (from 0.01 to 50 μM) of each compound for 72 hours after which time the amount of proliferation was determined by the MTS assay.

The MTS assay is a cell-based assay often used for screening collections of compounds to determine if the test molecules have effects on cell proliferation or show direct cytotoxic effects that can lead to cell death. It is a chromogenic assay that involves the biological reduction by viable cells of the tetrazolium compound 3-(4,5-dimethylthiazol-2-yl)5-(3-carboxymethoxyphenyl)-2-(4-sulfophenyl)2*H*-tetrazolium (or MTS), which is negatively charged and do not readily penetrate cells. NADH in metabolically active viable cells can reduce tetrazolium compounds into brightly colored formazan products (Fig. 10).

Figure 10. Intermediate electron acceptor pheazine ethyl sulfate (PES) transfers electron from NADH in the cytoplasm to reduce MTS in the culture medium into an aqueous soluble formazan.

to facilitate the reduction of the tetrazolium into the colored formazan product, that is directly soluble in cell culture medium.

With the exception of derivative **45e** and **45k** (GI_{50} 49.5±1.1, 34.5±5.3, respectively in MesoII cells), any thiazolyl-bis-pyrrolo[2,3-*b*]pyridine derivative showed antiproliferative activity against STO and MesoII cells (Tab. 14).

Table 14. Cytotoxic activity of thiazole derivatives **45a-l** in STO and MesoII cell lines.

| Compd | GI_{50} (μ M) ^a | | Compd | GI_{50} (μ M) ^a | |
|------------|-----------------------------------|-------------------|------------|-----------------------------------|----------|
| | STO | MesoII | | STO | MesoII |
| 45a | > 5.0 | > 50.0 | 45g | > 5.0 | > 50.0 |
| 45b | N.A. ^b | N.A. ^b | 45h | > 5.0 | > 50.0 |
| 45c | > 5.0 | > 50.0 | 45i | > 5.0 | > 50.0 |
| 45d | > 5.0 | > 50.0 | 45j | > 5.0 | > 50.0 |
| 45e | > 5.0 | 49.5±1.1 | 45k | > 5.0 | 34.5±5.3 |
| 45f | > 5.0 | > 50.0 | 45k | > 5.0 | > 50.0 |

(a) Data are reported as IC_{50} values (concentration of drug required to inhibit growth by 50%) determined by the MTS assay after 72 hours of continuous exposure to each compound. Data represent mean values ± SD of at least three independent experiments.

(b) N.A.: not assessed because the compound was insoluble.

Respect to indolyl-thiazolyl-pyrrolo[2,3-*c*]pyridines, compounds **49j** and **51f** showed comparable antiproliferative activity against both cellular models with GI_{50} values of 4.5±0.2, 29.0±1.0 and 4.9±0.1, 28.7±0.2 μ M, respectively. Compound **49a** and **49c** exhibited comparable inhibitory activity in STO cells (GI_{50} values of 3.7±0.1, 3.3±0.2 μ M, respectively); compounds **49i**, **50a**, **50b**, **50c**, **51c** and **51e** were active against MesoII cells (GI_{50} values of 27.6±1.1, 33.2±1.2, 31.1±1.2, 31.2±0.3, 16.7±0.1, 46.1±2.1, respectively) (Tab. 15).

Table 15. Cytotoxic activity of thiazole derivatives **49a-j**, **50a-f**, **51a-f**.

| Compd | GI_{50} (μ M) ^a | | Compd | GI_{50} (μ M) ^a | |
|------------|-----------------------------------|--------|------------|-----------------------------------|----------|
| | STO | MesoII | | STO | MesoII |
| 49a | 3.7±0.1 | > 50.0 | 50b | > 5.0 | 31.1±1.2 |
| 49b | > 5.0 | > 50.0 | 50c | > 5.0 | 31.2±0.3 |

| | | | | | |
|------------|---------|----------|------------|-------------------|-------------------|
| 49c | 3.3±0.2 | > 50.0 | 50d | > 5.0 | > 50.0 |
| 49d | > 5.0 | > 50.0 | 50e | > 5.0 | > 50.0 |
| 49e | > 5.0 | > 50.0 | 50f | N.A. ^b | N.A. ^b |
| 49f | > 5.0 | > 50.0 | 51a | > 5.0 | > 50.0 |
| 49g | > 5.0 | > 50.0 | 51b | N.A. ^b | N.A. ^b |
| 49h | > 5.0 | > 50.0 | 51c | > 5.0 | 16.7±0.1 |
| 49i | > 5.0 | 27.6±1.1 | 51d | > 5.0 | > 50.0 |
| 49j | 4.5±0.2 | 29.0±1.0 | 51e | > 5.0 | 46.1±2.1 |
| 50a | > 5.0 | 33.2±1.2 | 51f | 4.9±0.1 | 28.7±0.2 |

(a) Data are reported as IC₅₀ values (concentration of drug required to inhibit growth by 50%) determined by the MTS assay after 72 hours of continuous exposure to each compound. Data represent mean values ± SD of at least three independent experiments.

(b) N.A.: not assessed because the compound was insoluble.

Indolyl-thiazolyl-pyrrolo[2,3-*b*]pyridines **46a-d**, **47a-d** and **48a-d**, exhibited better antiproliferative activity. As indicated by the drug concentration required to inhibit growth by 50% (GI₅₀ values which ranged from 0.08 to 3.9 μM), compounds **46d**, **48b** and **48d** presented good inhibitory affect in both cellular models. In particular, compounds **46d**, **48b** and **48d** induced the best growth inhibitory effect against STO cells (GI₅₀ values of 0.08±0.01, 0.4±0.02, 0.4±0.1 μM, respectively).

Table 16. Cytotoxic activity of thiazole derivatives **46a-d**, **47a-d**, **48a-d**.

| Compd | GI ₅₀ (μM) ^a | | | | |
|------------|------------------------------------|-------------------|------------|----------|---------|
| | STO | MesoII | Compd | STO | MesoII |
| 46a | 3.4±0.1 | > 50.0 | 47c | > 5.0 | > 50.0 |
| 46b | N.A. ^b | N.A. ^b | 47d | 4.3±0.2 | > 50.0 |
| 46c | > 5.0 | > 50.0 | 48a | > 5.0 | > 50.0 |
| 46d | 0.08±0.01 | 3.2±0.1 | 48b | 0.4±0.02 | 3.9±0.2 |
| 47a | 3.5±0.2 | > 50.0 | 48c | > 5.0 | > 50.0 |
| 47b | N.A. ^b | N.A. ^b | 48d | 0.4±0.1 | 4.3±0.1 |

(a) Data are reported as IC₅₀ values (concentration of drug required to inhibit growth by 50%) determined by the MTS assay after 72 hours of continuous exposure to each compound. Data represent mean values ± SD of at least three independent experiments.

(b) N.A.: not assessed because the compound was insoluble.

Compounds **45k**, **46d**, **48d** and **51c**, which were selected for screenings at 5 concentrations at 10-fold dilution (10^{-4} - 10^{-8} M) on the full panel by the NCI, were further tested in order to elucidate the mechanism of action. About compounds **46d** and **48d**, biological assays are currently under investigation.

Instead, selective toxicity of compounds **45k** and **51c** towards tumor cells was investigated. To this aim human HTC-116 colorectal carcinoma cells, against which both compounds exhibited a comparable antiproliferative effects (GI_{50} 2.91 and 2.35 μ M, Table 11), and intestinal normal-like differentiated Caco-2 cells were exposed to the compounds for 24 h and viability compared using by colorimetric MTT assay.

NADH-dependent cellular oxidoreductase enzymes, present in the cytosolic compartment of the cells, may, under defined conditions, reflect the number of viable cells present. These enzymes are capable of reducing the water soluble tetrazolium dye MTT 3-(4,5-dimethylthiazol-2-yl)-2,5-diphenyltetrazolium bromide to its insoluble formazan crystals, which has a purple color (Fig. 12). A solubilization solution (usually dimethyl sulfoxide, an acidified ethanol solution, a solution of the detergent sodium dodecyl sulfate in diluted hydrochloric acid, acidified isopropanol, dimethylformamide, or combinations of detergent and organic solvent) is added to dissolve the insoluble purple formazan product into a colored solution. The absorbance of this colored solution can be quantified by measuring at a certain wave length (usually 570 nm) using a plate reading spectrophotometer. Viable cells with active metabolism convert MTT into a purple colored formazan product. When cells die, they lose the ability to convert MTT into formazan [39, 40].

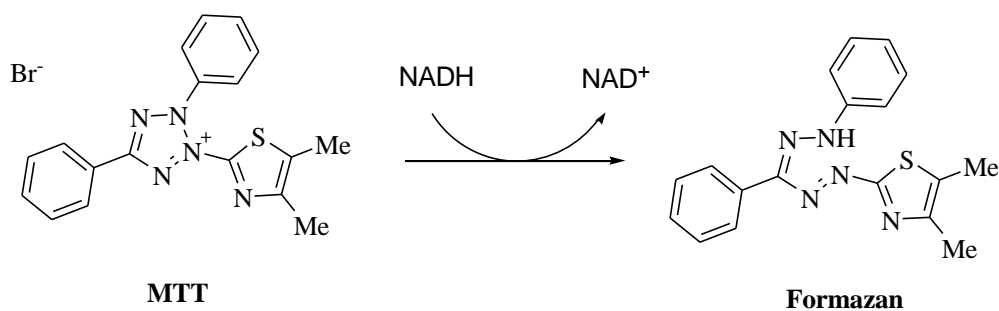
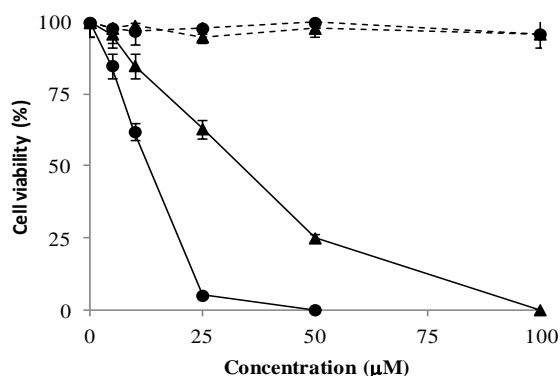


Figure 12. Structures of MTT and colored formazan product.

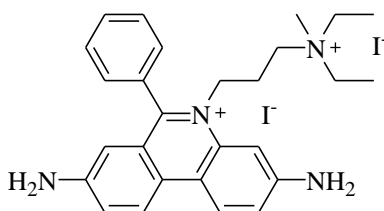
While both derivatives **45k** and **51c**, in the range 5 to 100 μ M, dose-dependently inhibited the intestinal HCT-116 cell proliferation, they did not affect the differentiated Caco-2 cell viability, suggesting tumor cells as the main target of their cytotoxic action (Fig. 13). GI_{50} values of **45k** and **51c** calculated after 24 h treatment of HCT-116 cells, were 33.55 ± 2.31 μ M and 13.15 ± 0.95 μ M, respectively.

Figure 13. Effect of **45k** (triangle) and **51c** (circle) on the viability of human intestinal cell lines either tumoral (HCT-116; full line) or normal-like (differentiated Caco-2; dashed line). Cells were treated with the compounds **45k** and **51c** and cell survival was measured after 24 h by MTT assay in comparison to cells treated with vehicle alone (control). Values are the mean of three separate experiments in triplicate.



It was next determined alterations in the cell cycle caused by derivatives **45k** and **51c** in colorectal cancer cells. Flow cytometry analysis of nuclear DNA content after 24 h treatment of HCT-116 cells was determined using propidium iodide (PI) **96**, in order to distinguish cells in different phases of the cell cycle. Drug concentrations were chosen on the basis that they represent values above and below the respective GI_{50} values.

Propidium iodide (PI) **96** is a fluorescent molecule that binds nucleic acid with little or no sequence preference. Because PI binds RNA as well as DNA, RNaseA (ribonuclease A) is also used to digest cellular RNA and thus decrease background RNA staining from the experiment. Since PI is membrane impermeant, a detergent is used to both fix and permeabilize cells.



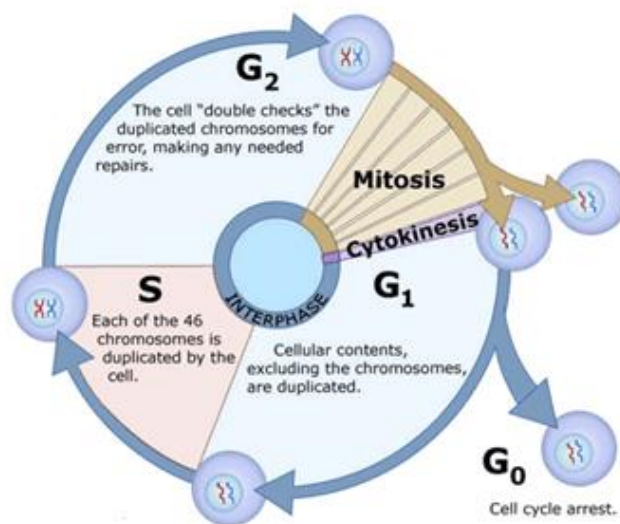
Propidium Iodide
96

This dye binds in a stoichiometric way the amount of DNA present in the cell. In this way, as the DNA content of cells duplicates during the S phase of the cell cycle, the relative amount of cells in the G₀ phase and G₁ phase (before S phase), in the S phase, and in the G₂ phase and M phase (after S phase) can be determined. In eukaryotic cells, the cell cycle, the complex sequence of events by

which cells grow and divide, includes a series of four distinct phases. The G₁, S, and G₂ phases of the cell cycle are collectively referred to as interphase; the mitosis phase involves the separation of nuclear chromosomes, followed by cytokinesis (division of the cytoplasm forming two distinct cells). At the end of the mitotic cell cycle, two distinct cells are produced, which contains identical genetic material (Fig. 14).

During the G₁ phase, the period prior to the synthesis of DNA, the cell increases in mass and organelle number in preparation for cell division. During the S phase, the cell synthesizes DNA and the chromosome content is doubled. The G₂ phase is the period after DNA synthesis but before the start of mitosis and the cell synthesizes additional proteins. Once a cell has completed the cell cycle, it goes back into the G₁ phase and repeats the cycle again. Cells in the body can also be placed in a non-dividing state called the Gap phase (G₀) at any point in their life.

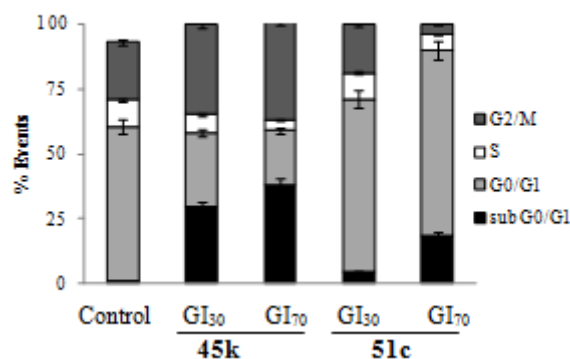
Figure 14. Cell cycle.



So cells that are in S phase will have more DNA than cells in G₁. They will take up proportionally more dye and will fluoresce more brightly because they have doubled their DNA content. The cells in G₂/M will be approximately twice as bright as cells in G₁.

Compared to control cells, **45k** caused a dose-dependent accumulation of cells in G₂/M phase, paralleled by a reduction in the percentage of cells in the G₁ phase and by a significant increase of cells in the sub-G₁ phase, which is representative of cells with fragmented DNA. On the other hand, **51c** induced a dose-dependent accumulation of cells in G₁ phase accompanied by a decrement in the percentage of cells in G₂/M phases. Moreover, accumulation of sub-G₁ population was significantly higher than control ($p < 0.05$) only at high concentration of the drug (Fig. 15). These results indicated that the two compounds caused arrest of the HCT-116 cancer cell growth involving different check points of the cell cycle.

Figure 15. Effect of **45k** and **51c** on the cell cycle distribution of HCT-116 cells. Flow cytometric analysis of propidium iodide-stained cells after 24 h treatment with the compounds or vehicle alone (control). The percentage of cells in the different phases of the cycle was calculated by Expo32 software. Values are the mean \pm SD of three separate experiments in triplicate.



To determine whether HCT-116 cells undergo apoptosis upon treatment with the nortopsentin analogues, cells were treated with **45k** or **51c** for 24 h, stained with both propidium iodide (PI) **96** and Annexin V-fluorescein isothiocyanate (FITC), and analyzed by flow cytometry.

The apoptotic program is characterized by certain morphologic features, including loss of plasma membrane, condensation of the cytoplasm and nucleus, and inter-nucleosomal cleavage of DNA.

In apoptotic cells, the membrane phospholipid phosphatidylserine (PS) is translocated from the inside to the outside of the plasma membrane, and PS is exposed to the external cellular environment. Annexin V is a 35-36 kDa Ca^{2+} dependent phospholipid-binding protein that has high affinity for PS, and binds to cells with exposed PS. Annexin V can be conjugated with fluorochromes including FITC (Fluorescein isothiocyanate). Since this complex binds with high affinity PS, it can be used as a sensitive probe for flow cytometric analysis of cells that are undergoing apoptosis. In particular, the externalization of PS happens in the earlier stages of apoptosis, so Annexin V-FITC staining can be used to identify apoptosis at an earlier stage.

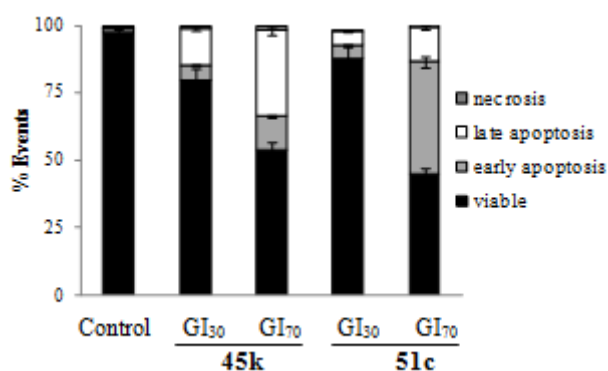
Staining with FITC Annexin V is typically used in combination with a vital dye such as propidium iodide (PI) **96**, in order to distinguish early, late apoptosis or necrosis. Indeed PI **96** does not enter viable cells, but in dead and damaged cells the membrane become permeable to PI. We can distinguish:

- viable cells in which PI and annexin V-FITC are negative;
- early apoptosis cells in which PI is negative and annexin V-FITC is positive;
- late apoptosis cells in which PI and annexin V-FITC are positive;

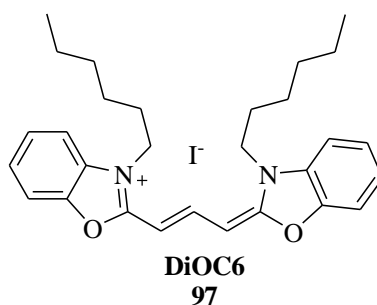
- necrotic cells in which PI is positive and annexin V-FITC is negative.

In figure 16 we can observe that neither compound caused cell necrosis. Rather, while the percentage of cells in late apoptosis increased at the increase of the **45k** doses, apoptotic effects of **51c** were evident only at high concentrations (GI_{70}), when cells in early apoptosis appeared significantly increased with respect to control ($p < 0.05$).

Figure 16. Effect of **45k** and **51c** on apoptosis of HCT-116 cells. Percentage of Annexin V/propidium iodide (PI) double-stained cells, as determined by flow cytometry after 24 h treatment with the compounds or vehicle alone (control). The percentage of cells in the different phases of apoptosis was calculated by Expo32 software. Values are the mean \pm SD of three separate experiments in triplicate.



Mitochondria play a critical role in regulating the apoptotic machinery. Mitochondrial membrane potential ($\Delta\psi_m$) is an important parameter of mitochondrial function and an indicator of cell health. Loss of $\Delta\psi_m$ suggests the leak of mitochondrial membrane integrity, signal of the beginning of the proapoptotic pathway. It was then examined mitochondrial membrane potential ($\Delta\psi_m$) loss using DiOC6 (3,3'-dihexyloxacarbocyanine iodide) **97**, a cationic lipophilic fluorescent mitochondria-specific and voltage-dependent dye, after treatment with compounds **45k** and **51c**.

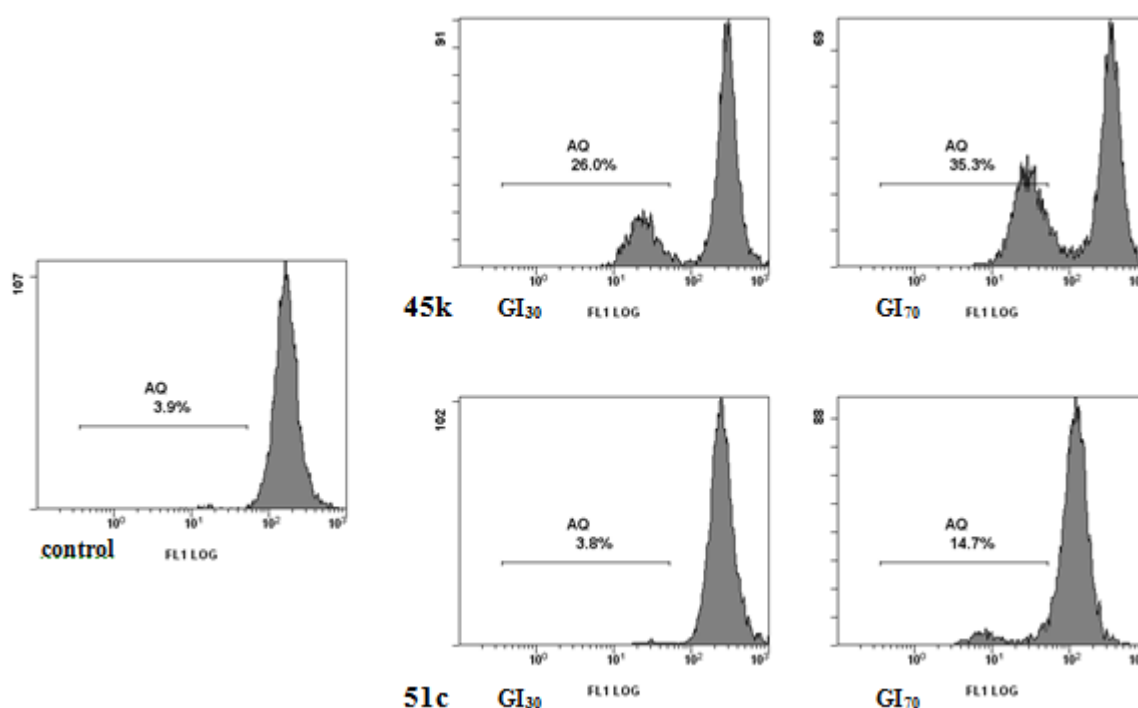


DiOC6 **97** accumulates in mitochondria matrix to its large negative membrane potential, and it can be useful to monitor the mitochondrial membrane potential using flow cytometric detection.

Changes on mitochondrial membrane potential are indicated by a reduction in the DiOC6-induced fluorescence intensity.

As indicated by the decrement in DiOC6 green-associated fluorescence, treatment of HCT-116 cells with **45k**, for 24 h, induced a remarkable dose-dependent dissipation of $\Delta\psi_m$ (Fig.17).

Figure 17. Effects of compounds **45k** and **51c** on mitochondrial transmembrane potential in HCT-116 cells. The $\Delta\psi_m$ was detected by fluorescence intensity of 3,3'-dihexyloxycarbocyanine iodide-treated cells, as determined by flow cytometry. Control, cells treated with vehicle. Representative images of three experiments with comparable results.

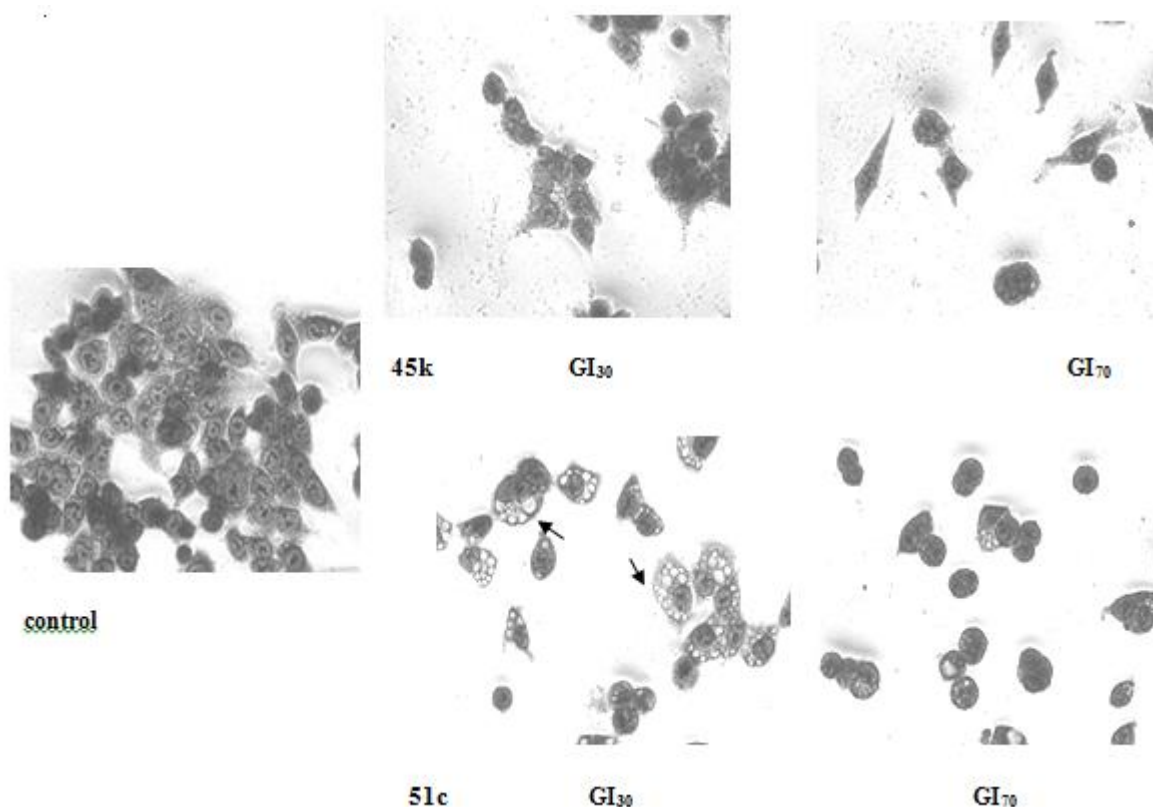


On the other hand, incubation with **51c** did not cause mitochondrial dysfunction at GI₃₀, whereas induced a significant increase in $\Delta\psi_m$ loss at higher concentrations. Overall our findings indicated that, although the thiazole derivatives inhibited the HCT-116 tumor cell growth, they may elicit different molecular pathways of programmed cell death.

Morphology of HCT-116 cells treated for 24 h with compounds **45k** and **51c** was assessed by microscopy analysis after Giemsa staining. Both compounds caused an evident dose-dependent reduction of the cell population with respect to control (Fig. 18). However, whereas **45k** caused highly condensate cells, as a sign of their apoptotic fate, more complex alterations were observed after treatment with **51c**. Low concentration of drug (GI₃₀) caused evident expansion of whole cytoplasm, with a massive accumulation of multiple-membrane bounded vacuoles without apparent

loss of nuclear material, a morphology characteristic of autophagic cell death. On the other hand, when HCT-116 cells were treated with higher concentration of **51c** (GI₇₀), vacuolization was less evident and cells with condensed morphology prevailed, indicating evolution of the cell fate towards apoptosis.

Figure 18. Compound **51c** induces accumulation of acid vacuoles in HCT-116 cells. (A) Micrographs of Giemsa-stained cells in 40x magnification. Control, cells treated with vehicle. Representative images of three experiments with comparable results.

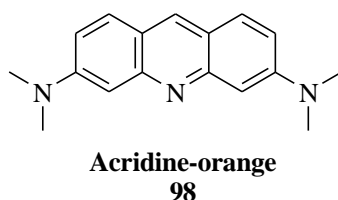


Then, it was performed FACS analysis of acridine-orange stained acid vacuoles (AVO) using the red to green ratio as an indicator of acid vacuolar organelle accumulation [41].

Several studies proposed two types of programmed cell death [42]. Type I or apoptosis, is mediated by a cascade of caspases and factors released by the mitochondria. It is characterized by typical morphological and biochemical features such as chromatin margination and condensation, early nuclear collapse. Type II programmed cell death is characterized by increased autophagy and early destruction of the cytoplasm [43]. In particular this response is dominated by the appearance and accumulation of acidic vesicular organelles [44].

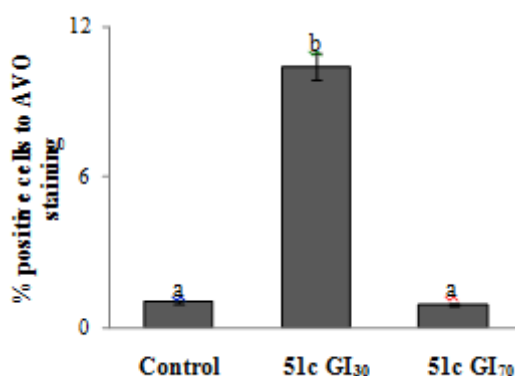
Acridine-orange (AO) **98** is a fluorescent molecule used to identify apoptotic cell death or autophagy. Being cell-permeable, it can interact with DNA emitting green fluorescence or

accumulate in acidic organelles in which it becomes protonated forming aggregates that emit bright red fluorescence. In acridine-orange stained cells, the cytoplasm and nucleolus fluoresce bright green, whereas acidic compartments fluorescence bright red. The intensity of the red fluorescence is proportional to the amount of acidity and/or volume of the cellular acidic compartment. By comparing the red/green fluorescence ratio it is possible to quantify change in the degree of acidity or the fractional volume of their cellular acidic compartment.



As shown in Figure 19, treatment of the cells with **51c** (GI₃₀), for 24 h, led to a 10-fold increase of the bright red to green fluorescence intensity ratio of acrydine orange, indicating an elevated induction of cell vacuolization associated to autophagy. Instead, the treatment of cells with the highest drug concentration did not significantly modify the percent of cells with AVO with respect to control, supporting the concept of a different cell death.

Figure 19. Compound **51c** induces accumulation of acid vacuoles in HCT-116 cells. The percentage of bright red (FL3) fluorescence-positive cells after AO staining and FACS analysis. Results are the mean±SD of two triplicate experiments. Mean values with unlike superscript letters were significantly different (P<0.05; Bonferroni's test).



Newly synthesized nortopsentin analogues showed cytotoxicity towards a broad spectrum of human cancer cell lines included in the NCI panel. In particular, compounds **45k**, **46d**, **48d** and **51c** exhibited the best results and were selected for further screenings at 5 concentrations at 10-fold dilution (10^{-4} - 10^{-8} M) on the full panel.

These derivatives resulted active at micromolar to nanomolar concentration, against most of the tested cell lines, as it has been confirmed by the range of GI₅₀ value of 0.81-27.7, 0.04-13.00, 0.03-14.20, 0.93-4.70 μ M, respectively for compounds **45k**, **46d**, **48d**, **51c**.

The antiproliferative activity of all compounds **45a-l**, **46a-d**, **47a-d**, **48a-d**, **49a-j**, **50a-f** and **51a-f**, was further examined by Istituto Nazionale dei Tumori (Fondazione IRCCS, Milano) in two additional cell lines, STO and MesoII, derived from human DMPM, a tumor type not included in the NCI panel. Results showed that only some of them impaired the growth of both experimental models of DMPM.

Compounds **45k**, **46d**, **48d** and **51c**, which showed the best results on the full panel by the NCI, were tested in order to explain the mechanism of action. About compounds **46d** and **48d**, biological assays are currently in progress.

Importantly, compounds **45k** and **51c** did not appreciably impair vitality of intestinal normal like cells. Investigating mechanisms underlying the antiproliferative effect in HCT-116 colon cancer cells, it was showed that **45k** caused a dose-dependent increase of the apoptotic cell population, activating the mitochondria-mediated pathway and inducing cell cycle arrest at the G2/M phase.

On the other hand **51c** elicited distinct responses in accordance with the dose. Concentrations lower than its GI₅₀, induced antiproliferative effects and morphological changes with massive accumulation of autophagic vacuoles without apparent signs of apoptosis. The observed arrest of cell cycle at G1 phase supports the autophagic fate of the cells [45].

Evolution of the cells toward apoptotic death following treatment with higher drug concentrations, suggests that **51c** may orchestrate a potential axis of autophagy and apoptosis in HCT-116 cells which can facilitate cellular destruction. The autophagy-signaling cascade induced by **51c** in HCT-116 cells is currently under investigation. Modulating autophagy appears of great interest in cancer. Indeed, current evidence suggests that autophagic cell death can be induced as an alternative to apoptosis with therapeutic purpose in cancer cells that are resistant to apoptosis. Compound **51c** may candidate as a lead compound for nortopsentin derivatives with autophagic activity.

EXPERIMENTALE SECTION

CHEMISTRY

General methods

All melting points were taken on a Buchi-Tottoly capillary apparatus and are uncorrected. IR spectra were determined in bromoform with a Shimadzu FT / IR 8400S spectrophotometer. ^1H and ^{13}C NMR spectra were measured at 200 and 50.0 MHz, respectively, on DMSO- d_6 or CDCl_3 solution, using a Bruker Avance II series 200 MHz spectrometer. Compounds **46a**, **46b**, **49d-f**, **h**, **j**, **50e,f** were characterized only by ^1H NMR spectra, for their poor solubility, the ^{13}C spectra were not performed. Chromatography column was performed with MERK silica gel 230-400 mesh ASTM or FLASH40i Biotage chromatography or with Buchi Sepacore chromatography module (prepacked cartridge reference).

Synthesis of 1-methyl-1H-pyrrolo[2,3-b]pyridine-3-carbonitrile (52b)

To a cold solution of **52a** (1.0 g, 7.0 mmol) in anhydrous toluene (20 mL), potassium *t*-butoxide (1.1 g, 9.5 mmol) and TDA-1 (1 or 2 drops) were added at 0 °C. The reaction mixture was stirred at room temperature for 6 h and then methyl iodide (7.0 mmol, 0.44 mL) was added at 0 °C. TLC analysis (DCM/ethyl acetate 9/1) revealed that methylation was complete after 1 h. The solvent was evaporated under reduced pressure. The residue was treated with water, extracted with DCM, dried (Na_2SO_4), evaporated and purified by column chromatography using DCM/ethyl acetate (9/1) as eluent. White solid; yield: 85%; mp: 106.1-106.6 °C; IR 2224 (CN) cm^{-1} ; ^1H NMR (200 MHz, DMSO- d_6) δ : 3.90 (s, 3H, CH_3), 7.35 (dd, 1H, $J = 4.7, 8.0$ Hz, H-5), 8.15 (dd, 1H, $J = 1.5, 8.0$ Hz, H-4), 8.47 (dd, 1H, $J = 1.5, 4.7$ Hz, H-6), 8.48 (s, 1H, H-2); ^{13}C NMR (50 MHz, DMSO- d_6) δ : 31.6 (q), 81.9 (s), 115.3 (s), 118.1 (d), 119.2 (s), 127.6 (d), 138.4 (d), 144.8 (d), 146.4 (s). Anal. Calcd for $\text{C}_9\text{H}_7\text{N}_3$: C, 68.78; H, 4.49; N, 26.74. Found: C, 68.61; H, 4.21; N, 26.92.

Synthesis of carboxamides (53a,b) [35]

A solution of appropriate carbonitrile derivatives **52a,b** (6.3 mmol) in concentrated sulphuric acid (3.3 mL) was stirred at room temperature for 15-60 min. The solution was slowly poured into ice and basified with concentrated NaOH. The residue was extracted with ethyl acetate dried (Na_2SO_4) and concentrated under reduced pressure to afford desired carboxamides **53a,b**.

1H-Pyrrolo[2,3-b]pyridine-3-carboxamide (53a)

Conditions: room temperature for 60 min. Brown solid; yield: 95%; mp: 273-274 °C; IR 3389, 3335 (NH_2), 3021 (NH), 1636 (CO) cm^{-1} ; ^1H NMR (200 MHz, DMSO- d_6) δ : 7.16 (dd, 1H, $J = 4.7,$

7.9 Hz, H-5), 7.52 (bs, 2H, NH₂), 8.16 (d, 1H, *J* = 2.5 Hz, H-2), 8.27 (dd, 1H, *J* = 1.7, 4.7 Hz, H-6), 8.46 (dd, 1H, *J* = 1.7, 7.9 Hz, H-4), 12.10 (bs, 1H, NH); ¹³C NMR (50 MHz, DMSO-*d*₆) δ: 109.3 (s), 116.8 (d), 118.5 (s), 128.6 (d), 129.2 (d), 143.3 (d), 148.4 (s), 165.8 (s). Anal. Calcd for C₈H₇N₃O: C, 59.62; H, 4.38; N, 26.07. Found: C, 59.46; H, 4.59; N, 26.25.

1-Methyl-1*H*-pyrrolo[2,3-*b*]pyridine-3-carboxamide (53b)

Conditions: room temperature for 15 min. White solid; yield: 99%; mp: 218-219 °C; IR 3347, 3326 (NH₂), 1614 (CO) cm⁻¹; ¹H NMR (200 MHz, DMSO-*d*₆) δ: 3.85 (s, 3H, CH₃), 7.20 (dd, 1H, *J* = 4.7, 7.9 Hz, H-5), 7.48 (bs, 2H, NH₂), 8.17 (s, 1H, H-2), 8.33 (dd, 1H, *J* = 1.7, 4.7 Hz, H-6), 8.45 (dd, 1H, *J* = 1.7, 7.9 Hz, H-4); ¹³C NMR (50 MHz, DMSO-*d*₆) δ: 31.2 (q), 108.2 (s), 117.0 (d), 118.7 (s), 129.4 (d), 132.3 (d), 143.2 (d), 147.4 (s), 165.5 (s). Anal. Calcd for C₉H₉N₃O: C, 61.70; H, 5.18; N, 23.99. Found: C, 61.55; H, 5.44; N, 24.19.

Synthesis of 1*H*-pyrrolo[2,3-*b*]pyridine-3-carbothioamides (54a,b) [35]

A mixture of Lawesson's reagent (0.33 g, 0.8 mmol) and appropriate carboxamides **53a,b** (1.3 mmol) in THF (10 mL) was heated under reflux for 30 min. The solution was cooled to room temperature and the solvent was removed under reduced pressure. The residue was purified by column chromatography using ethyl acetate as eluent to give desired carbothioamides **54a,b**.

1*H*-Pyrrolo[2,3-*b*]pyridine-3-carbothioamide (54a)

Yellow solid; yield: 88%; mp: 220-222 °C; IR 3306, 3180 (NH₂), 3020 (NH), 1590 (CS); ¹H NMR (200 MHz, DMSO-*d*₆) δ: 7.22 (dd, 1H, *J* = 4.7, 8.0 Hz, H-5), 8.23 (d, 1H, *J* = 2.7 Hz, H-2), 8.29 (dd, 1H, *J* = 1.5, 4.7 Hz, H-6), 8.99 (dd, 1H, *J* = 1.5, 8.0 Hz, H-4), 9.00 (s, 1H, SH), 9.10 (s, 1H, NH), 12.30 (bs, 1H, NH); ¹³C NMR (50 MHz, DMSO-*d*₆) δ: 114.7 (s), 117.1 (d), 118.8 (s), 127.6 (d), 130.3 (d), 143.5 (d), 148.9 (s), 193.0 (s). Anal. Calcd for C₈H₇N₃S: C, 54.22; H, 3.98; N, 23.71. Found: C, 54.02; H, 4.08; N, 23.91.

1-Methyl-1*H*-pyrrolo[2,3-*b*]pyridine-3-carbothioamide (54b)

Yellow solid; yield: 99%; mp: 232-233 °C; IR 3336, 3182 (NH₂), 1540 (CS) cm⁻¹; ¹H NMR (200 MHz, DMSO-*d*₆) δ: 3.86 (s, 3H, CH₃), 7.26 (dd, 1H, *J* = 4.7, 8.0 Hz, H-5), 8.28 (s, 1H, H-2), 8.33 (dd, 1H, *J* = 1.6, 4.7 Hz, H-6), 8.93 (dd, 1H, *J* = 1.6, 8.0 Hz, H-4), 8.97 (s, 1H, SH), 9.16 (bs, 1H, NH); ¹³C NMR (50 MHz, DMSO-*d*₆) δ: 31.3 (q), 113.7 (s), 117.4 (d), 118.7 (s), 130.3 (d), 131.8 (d), 143.3 (d), 147.8 (s), 192.6 (s). Anal. Calcd for C₉H₉N₃S: C, 56.52; H, 4.74; N, 21.97. Found: C, 56.32; H, 4.59; N, 22.27.

Synthesis of 1-methyl-1*H*-pyrrolo[2,3-*b*]pyridines (55b, d, f)

To a cold solution of appropriate pyrrolo-pyridines **55a,c,e** (2.5 mmol) in anhydrous toluene (25 mL), potassium *t*-butoxide (0.38 g, 3.4 mmol) and TDA-1 (1 or 2 drops) were added at 0 °C. The reaction mixture was stirred at room temperature for 3 h and then methyl iodide (2.5 mmol, 0.2 mL) was added at 0 °C. TLC analysis (ethyl acetate) revealed that methylation was complete after 1 h. The solvent was evaporated under reduced pressure. The residue was treated with water, extracted with DCM, dried (Na₂SO₄), evaporated and purified by column chromatography using DCM/ethyl acetate (9/1) as eluent to give derivatives **55b, d, f**.

1-Methyl-1*H*-pyrrolo[2,3-*b*]pyridine (55b) [29]

Oil; yield: 96%; ¹H NMR (200 MHz, CDCl₃) δ: 3.87 (s, 3H, CH₃), 6.43 (d, 1H, *J* = 3.4 Hz, H-3), 7.03 (dd, 1H, *J* = 4.8, 7.8 Hz, H-5), 7.15 (d, 1H, *J* = 3.4 Hz, H-2), 7.88 (1H, dd, *J* = 1.5, 7.8 Hz, H-4), 8.33 (1H, d, *J* = 4.8 Hz, H-6); ¹³C NMR (50 MHz, CDCl₃) δ: 31.1 (q), 99.1 (d), 115.3 (d), 120.4 (s), 128.6 (d), 128.9 (d+s), 142.6 (d). Anal. Calcd for C₈H₈N₂: C, 72.70; H, 6.10; N, 21.20. Found: C, 72.55; H, 6.03; N, 21.38.

5-Bromo-1-methyl-1*H*-pyrrolo[2,3-*b*]pyridine (55d) [27]

Brown solid; yield: 85%; mp: 62-63 °C ; ¹H NMR (200 MHz, DMSO-*d*₆) δ: 3.83 (s, 3H, CH₃), 6.44 (d, 1H, *J* = 3.4 Hz, H-3), 7.60 (d, 1H, *J* = 3.4 Hz, H-2), 8.21 (d, 1H, *J* = 2.1, H-4), 8.33 (d, 1H, *J* = 2.1 Hz, H-6); ¹³C NMR (50 MHz, DMSO-*d*₆) δ: 31.0 (q), 98.5 (d), 110.7 (s), 121.7 (s), 130.3 (d), 131.8 (d), 142.2 (d), 145.7 (s). Anal. Calcd for C₈H₇BrN₂: C, 45.53; H, 3.34; N, 13.27. Found: C, 45.38; H, 3.24; N, 13.45.

5-Fluoro-1-methyl-1*H*-pyrrolo[2,3-*b*]pyridine (55f)

Brown solid; yield: 60%; mp: 72-74 °C; ¹H NMR (200 MHz, DMSO-*d*₆) δ: 3.83 (s, 3H, CH₃), 6.47 (d, 1H, *J* = 3.4 Hz, H-3) 7.63 (d, 1H, *J* = 3.4 Hz, H-2), 7.87 (dd, 1H, *J* = 2.7, 9.5 Hz, H-4), 8.24-8.27 (m, 1H, H-6); ¹³C NMR (50 MHz, DMSO-*d*₆) δ: 31.1 (q), 98.8 (d, *J*_{C3-F} = 4.5 Hz), 113.9 (d, *J*_{C4-F} = 20.5 Hz), 119.9 (s, *J*_{C3a-F} = 7.5 Hz), 130.4 (d, *J*_{C6-F} = 29.2 Hz), 132.3 (d), 144.3 (s), 155.0 (s, *J*_{C5-F} = 238.0 Hz). Anal. Calcd for C₈H₇FN₂: C, 63.99; H, 4.70; N, 18.66. Found: C, 63.69; H, 4.91; N, 18.48.

Synthesis of 2-bromo-1-(1*H*-pyrrolo[2,3-*b*]pyridin-3-yl)ethanones (56a-f)

To a solution of appropriate 7-azaindoles **55a-f** (2.5 mmol) in 10 mL of anhydrous DCM, anhydrous aluminium chloride (1.2 g, 8.8 mmol) was slowly added. The reaction mixture was heated under reflux and bromoacetyl bromide (2.5 mmol, 0.2 mL) in 2 mL of anhydrous DCM was

added dropwise. The resulting solution was allowed to stir under reflux for 40 min. After cooling, water and ice were slowly added and the obtained precipitate (for derivative **56a**) was filtered off or the oil residue (for derivatives **56b-f**) was extracted with DCM and purified by column chromatography using DCM/ethyl acetate (9/1) as eluent.

2-Bromo-1-(1H-pyrrolo[2,3-b]pyridin-3-yl)ethanone (56a) [29]

White solid; yield: 92%; mp: 280-282°C; IR 3556 (NH), 1678 (CO) cm^{-1} ; ^1H NMR (200 MHz, DMSO- d_6) δ : 4.71 (s, 2H, CH₂), 7.30 (dd, 1H, $J = 4.7, 7.8$ Hz, H-5), 8.37 (d, 1H, $J = 4.7$ Hz, H-6), 8.47 (d, 1H, $J = 7.8$ Hz, H-4), 8.65 (s, 1H, H-2), 12.70 (s, 1H, NH); ^{13}C NMR (50 MHz, DMSO- d_6) δ : 46.3 (t), 112.3 (s), 117.7 (s), 118.4 (d), 129.5 (d), 135.1 (d), 144.6 (d), 149.0 (s), 186.4 (s). Anal. Calcd for C₉H₇BrN₂O: C, 45.22; H, 2.95; N, 11.72. Found: C, 45.40; H, 2.82; N, 11.54.

2-Bromo-1-(1-methyl-1H-pyrrolo[2,3-b]pyridin-3-yl)ethanone (56b) [29]

White solid; yield: 80%; mp: 116-117°C; IR 1650 (CO) cm^{-1} ; ^1H NMR (200 MHz, DMSO- d_6) δ : 3.91 (s, 3H, CH₃), 4.65 (s, 2H, CH₂), 7.34 (dd, 1H, $J = 7.6, 4.7$ Hz, H-5), 8.40-8.48 (m, 2H, H-4, H-6), 8.70 (s, 1H, H-2); ^{13}C NMR (50 MHz, DMSO- d_6) δ : 31.7 (q), 32.9 (t), 110.8 (s), 118.1 (d), 118.7 (s), 129.8 (d), 138.7 (d), 144.4 (d), 148.1 (s), 186.1 (s). Anal. Calcd for C₁₀H₉BrN₂O: C, 47.46; H, 3.58; N, 11.07. Found: C, 47.22; H, 3.63; N, 11.25.

2-Bromo-1-(5-bromo-1H-pyrrolo[2,3-b]pyridin-3-yl)ethanone (56c)

Brown solid; yield: 75%; mp: 244-245 °C; IR 3019 (NH), 1655 (CO) cm^{-1} ; ^1H NMR (200 MHz, DMSO- d_6) δ : 4.72 (s, 2H, CH₂), 8.46 (d, 1H, $J = 2.2$ Hz, H-4), 8.57 (d, 1H, $J = 2.2$ Hz, H-6), 8.71 (d, 1H, $J = 3.2$ Hz, H-2), 13.0 (bs, 1H, NH); ^{13}C NMR (50 MHz, DMSO- d_6) δ : 33.1 (t), 111.7 (s), 113.8 (s), 119.4 (s), 131.2 (d), 136.9 (d), 144.8 (d), 147.4 (s), 186.6 (s). Anal. Calcd for C₉H₆Br₂N₂O: C, 34.00; H, 1.90; N, 8.81. Found: C, 33.87; H, 2.11; N, 8.99.

2-Bromo-1-(5-bromo-1-methyl-1H-pyrrolo[2,3-b]pyridin-3-yl)ethanone (56d)

Brown solid; yield: 70%; mp: 166-167 °C; IR 1653 (CO) cm^{-1} ; ^1H NMR (200 MHz, DMSO- d_6) δ : 3.89 (s, 3H, CH₃), 4.66 (s, 2H, CH₂), 8.49 (d, 1H, $J = 2.2$ Hz, H-4), 8.54 (d, 1H, $J = 2.2$ Hz, H-6), 8.74 (s, 1H, H-2); ^{13}C NMR (50 MHz, DMSO- d_6) δ : 31.9 (q), 32.9 (t), 110.2 (s), 114.2 (s), 119.6 (s), 131.4 (d), 139.9 (d), 144.6 (d), 146.5 (s), 186.1 (s). Anal. Calcd for C₁₀H₈Br₂N₂O: C, 36.18; H, 2.43; N, 8.44. Found: C, 36.02; H, 2.67; N, 8.64.

2-Bromo-1-(5-fluoro-1H-pyrrolo[2,3-b]pyridin-3-yl)ethanone (56e)

Brown solid; yield: 74%; mp: 206-207 °C; IR 3555 (NH), 1654 (CO) cm^{-1} ; ^1H NMR (200 MHz,

DMSO-*d*₆) δ : 4.71 (s, 2H, CH₂), 8.20 (dd, 1H, J = 2.8, 9.1 Hz, H-4), 8.37-8.39 (m, 1H, H-6), 8.73 (d, 1H, J = 3.3 Hz, H-2), 12.88 (bs, 1H, NH); ¹³C NMR (50 MHz, DMSO-*d*₆) δ : 33.7 (t), 112.2 (s, J_{C7a-F} = 3.9 Hz), 115.0 (d, J_{C4-F} = 21.5 Hz), 118.1 (s, J_{C3a-F} = 7.9 Hz), 133.0 (d, J_{C6-F} = 26.5 Hz), 137.4 (d), 145.7 (s), 156.4 (s, J_{C5-F} = 243.0 Hz), 186.5 (s). Anal. Calcd for C₉H₆BrFN₂O: C, 42.05; H, 2.35; N, 10.90. Found: C, 41.85; H, 2.56; N, 10.76.

2-Bromo-1-(5-fluoro-1-methyl-1H-pyrrolo[2,3-*b*]pyridin-3-yl)ethanone (56f)

Brown solid; yield: 74%; mp: 149-150 °C; IR 1668 (CO) cm⁻¹; ¹H NMR (200 MHz, DMSO-*d*₆) δ : 3.90 (s, 3H, CH₃), 4.65 (s, 2H, CH₂), 8.20 (dd, 1H, J = 2.8, 9.0 Hz, H-4), 8.42-8.44 (m, 1H, H-6), 8.78 (s, 1H, H-2); ¹³C NMR (50 MHz, DMSO-*d*₆) δ : 32.0 (q), 32.8 (t), 110.6 (s, J_{C7a-F} = 3.9 Hz), 115.3 (d, J_{C4-F} = 21.9 Hz), 118.3 (s, J_{C3a-F} = 7.9 Hz), 132.8 (d, J_{C6-F} = 29.3 Hz), 140.4 (d), 144.8 (s), 156.7 (s, J_{C5-F} = 243.5 Hz), 186.0 (s). Anal. Calcd for C₁₀H₈BrFN₂O: C, 44.31; H, 2.97; N, 10.33. Found: C, 44.14; H, 2.73; N, 10.53.

Synthesis of 5-bromo-1-[tri(propan-2-yl)silyl]-1H-pyrrolo[2,3-*b*]pyridine (64) [36]

Sodium hydride (0.12 g, 5 mmol) was added in small portion to a stirred solution of 5-bromo-7-azaindole **55c** (0.4g, 2.03 mmol) in tetrahydrofuran (6 mL) at room temperature. The resulting suspension was stirred at room temperature for 30 min. Triisopropylsilyl chloride (0.6 mL, 3.05 mmol) was added and the reaction mixture was heated at 80 °C for 3h. The solvent was evaporated under reduced pressure and the residue was dissolved in water, extracted with DCM, dried (Na₂SO₄) and purified by column chromatography using DCM as eluent. White solid, yield: 99%, mp: 55 -56 °C, ¹H NMR (200 MHz, DMSO-*d*₆) δ : 1.03 (s, 9H, 3xCH₃), 1.07 (s, 9H, 3xCH₃), 1.78-1.93 (m, 3H, 3xCH), 6.62 (d, 1H, J = 3.5 Hz, H-3), 7.55 (d, 1H, J = 3.5 Hz, H-2), 8.20 (d, 1H, J = 2.3 Hz, H-4), 8.27 (d, 1H, J = 2.3 Hz, H-6); ¹³C NMR (50 MHz, DMSO-*d*₆) δ : 11.4 (d), 17.8 (q), 102.9 (d), 111.49 (s), 123.9 (s), 130.1 (d), 133.6 (d), 142.1 (d), 151.7 (s). Anal. Calcd for C₁₆H₂₅BrN₂Si: C, 54.38; H, 7.13; N, 7.93. Found: C, 54.18; H, 7.38; N, 7.74.

Synthesis of 5-fluoro-1-[tri(propan-2-yl)silyl]-1H-pyrrolo[2,3-*b*]pyridine (65) [36]

To a stirred solution of compound **64** (0.74 g, 2.1 mmol) in tetrahydrofuran (18 mL) over a period of 10 minutes at -78 °C under nitrogen atmosphere, a solution of butyl lithium (2.5 M, 1.3 mL, 3.1 mmol) was added dropwise. The resulting solution was stirred at -78 °C for 1 h and solid *N*-fluorobenzenesulfonimide (0.82 g, 2.6 mmol), was added in one portion and stirred at -78 °C for 2h. The solvent was removed under reduced pressure. The crude was extracted with ethyl acetate. The organic extract was dried with Na₂SO₄, concentrated and purified by column chromatography using cyclohexane/ethyl acetate (9/1) as eluent. Yellow oil; yield: 70%, ¹H NMR (200 MHz,

DMSO-*d*₆) δ : 1.04 (s, 9H, 3xCH₃), 1.08 (s, 9H, 3xCH₃), 1.78-1.93 (m, 3H, 3xCH), 6.63 (d, 1H, *J* = 3.5 Hz, H-3), 7.58 (d, 1H, *J* = 3.5 Hz, H-2), 7.84 (dd, 1H, *J* = 2.8, 9.4 Hz, H-4), 8.21 (dd, 1H, *J* = 1.6, 2.8 Hz, H-6); ¹³C NMR (50 MHz, DMSO-*d*₆) δ : 11.4 (d), 17.8 (q), 103.4 (d, *J*_{C3-F} = 4 Hz), 113.6 (d, *J*_{C4-F} = 20.12 Hz), 122.3 (s, *J*_{C3a-F} = 7 Hz), 130.1 (d, *J*_{C6-F} = 28.7 Hz), 134.2 (d), 150.0 (s), 155.1 (s, *J*_{C5-F} = 245 Hz). Anal. Calcd for C₁₆H₂₅FN₂Si: C, 65.71; H, 8.62; N, 9.58. Found: C, 65.46; H, 8.81; N, 9.34.

Synthesis of 5-fluoro-1H-pyrrolo[2,3-*b*]pyridine (55e) [36]

Tetrabutylammonium fluoride (TBAF), 1M in tetrahydrofuran (0.6 mL) was added to a stirred solution of compound **65** (0.320 g, 1.09 mmol) in tetrahydrofuran (2.5 mL) at room temperature and stirred for 15 min. The solvent was evaporated and the crude was purified by column chromatography using cyclohexane/ethyl acetate (8/2) as eluent. White solid; yield: 80%, mp: 180-181 °C; IR 3453 (NH) cm⁻¹; ¹H NMR (200 MHz, DMSO-*d*₆) δ : 6.46 (d, 1H, *J* = 3.4 Hz, H-3), 7.58 (d, 1H, *J* = 3.4 Hz, H-2), 7.84 (dd, 1H, *J* = 2.4, 9.6 Hz, H-6), 8.20 (dd, 1H, *J* = 2.1, 2.5 Hz, H-4), 11.81 (bs, 1H, NH); ¹³C NMR (50 MHz, DMSO-*d*₆) δ : 99.9 (d, *J*_{C3-F} = 4.5 Hz), 113.5 (d, *J*_{C4-F} = 20.1), 119.7 (s, *J*_{C3a-F} = 7 Hz), 128.6 (d), 130.5 (d, *J*_{C6-F} = 30 Hz), 145.3 (s), 155.0 (s, *J*_{C5-F} = 238 Hz). Anal. Calcd for C₇H₅FN₂: C, 61.76; H, 3.70; N, 20.58. Found: C, 61.51; H, 3.99; N, 20.35.

Synthesis of substituted -(1,3-thiazole-2,4-diyl) bis(1H-pyrrolo[2,3-*b*]pyridines (45a-l)

A suspension of the appropriate pyrrolo[2,3-*b*]pyridine-carbothioamides **54a,b** (5 mmol) and proper 3-bromoacetyl-pyrrolo[2,3-*b*]pyridine compound **56a-f** (5 mmol) in anhydrous ethanol (20 mL) was heated under reflux for 30 min. The precipitate, obtained after cooling, was filtered off, dried and crystallized with ethanol to afford derivatives **45a-l**.

3,3'-(1,3-Thiazole-2,4-diyl)bis(1H-pyrrolo[2,3-*b*]pyridine (45a)

Yellow solid; yield: 63%; mp: 346-347 °C; IR 3410, 3166 (NH) cm⁻¹; ¹H NMR (200 MHz, DMSO-*d*₆) δ : 7.48 (dd, 1H, *J* = 5.0, 7.9 Hz, ArH), 7.60 (dd, 1H, *J* = 5.5, 7.9 Hz, ArH), 8.00 (s, 1H, ArH), 8.39 (s, 1H, ArH), 8.46 (s, 1H, ArH), 8.48 (d, 1H, *J* = 5.5 Hz, ArH), 8.55 (d, 1H, *J* = 5.0 Hz, ArH), 8.87 (d, 1H, *J* = 7.9 Hz, ArH), 9.11 (d, 1H, *J* = 7.9 Hz, ArH), 12.75 (bs, 1H, NH), 12.90 (bs, 1H, NH); ¹³C NMR (50 MHz, DMSO-*d*₆) δ : 109.6 (d), 110.5 (s), 116.3 (d), 117.3 (d), 118.7 (s), 125.8 (s), 126.9 (d), 127.9 (d), 129.6 (s), 131.4 (d), 134.8 (d), 137.2 (d), 141.5 (d), 143.2 (s), 145.9 (s), 147.9 (s), 149.2 (s). Anal. Calcd for C₁₇H₁₁N₅S: C, 64.34; H, 3.49; N, 22.07. Found: C, 64.54; H, 3.70; N, 22.23.

5-Bromo-3-[2-(1*H*-pyrrolo[2,3-*b*]pyridin-3-yl)-1,3-thiazol-4-yl]-1*H*-pyrrolo[2,3-*b*]pyridine (45b)

Yellow solid; yield: 60%; mp: 390-311 °C; IR 3334, 3350 (NH) cm⁻¹; ¹H NMR (200 MHz, DMSO-*d*₆) δ: 7.35 (dd, 1H, *J* = 4.8, 8.0 Hz, H-5'), 7.87 (s, 1H, H-5), 8.24 (d, 1H, *J* = 2.6 Hz, H-2''), 8.35 (d, 1H, *J* = 2.1 Hz, H-6''), 8.38-8.42 (2H, m, H-2', H-6'), 8.80 (dd, 1H, *J* = 1.2, 8.0 Hz, H-4'), 8.81 (d, 1H, *J* = 2.1 Hz, H-4''), 12.26 (bs, 1H, NH), 12.46 (bs, 1H, NH); ¹³C NMR (50 MHz, DMSO-*d*₆) δ: 108.2 (d), 109.5 (s), 109.8 (s), 111.5 (s), 117.1 (d), 118.3 (s), 118.7 (s), 126.8 (d), 127.5 (d), 130.3 (d), 130.9 (d), 131.6 (s), 142.0 (d), 143.0 (d), 147.0 (s), 149.0 (s), 161.0 (s). Anal. Calcd for C₁₇H₁₀BrN₅S: C, 51.53; H, 2.54; N, 17.67. Found: C, 51.30; H, 2.26; N, 17.86.

5-Fluoro-3-[2-(1*H*-pyrrolo[2,3-*b*]pyridin-3-yl)-1,3-thiazol-4-yl]-1*H*-pyrrolo[2,3-*b*]pyridine (45c)

Yellow solid; yield: 75%; mp: 373-374 °C; IR 3247, 3156 (NH) cm⁻¹; ¹H NMR (200 MHz, DMSO-*d*₆) δ: 7.37 (dd, 1H, *J* = 4.8, 7.9 Hz, H-5'), 7.83 (s, 1H, H-5), 8.27 (d, 1H, *J* = 2.6 Hz, H-2''), 8.31 (t, 1H, *J* = 1.7 Hz, H-6''), 8.36 (d, 1H, *J* = 2.2 Hz, H-2'), 8.41 (dd, 1H, *J* = 1.3, 4.8 Hz, H-6'), 8.48 (d, 1H, *J* = 1.7 Hz, H-4''), 8.80 (dd, 1H, *J* = 1.3, 7.9 Hz, H-4'), 12.19 (bs, 1H, NH), 12.49 (bs, 1H, NH); ¹³C NMR (50 MHz, DMSO-*d*₆) δ: 108.1 (d), 110.0 (s), 114.0 (d, *J*_{C-4''} = 21.2 Hz), 116.9 (s), 117.1 (s), 117.2 (d), 127.7 (d), 128.1 (d), 131.2 (d, *J*_{C-6''} = 28.6 Hz), 132.7 (d), 140.4 (d), 144.8 (s), 145.5 (s), 147.4 (s), 149.2 (s), 153.0 (s), 159.2 (s, *J*_{C-5''} = 149 Hz). Anal. Calcd for C₁₇H₁₀FN₅S: C, 60.88; H, 3.01; N, 20.88. Found: C, 60.58; H, 2.80; N, 21.04.

1-Methyl-3-[4-(1*H*-pyrrolo[2,3-*b*]pyridin-3-yl)-1,3-thiazol-2-yl]-1*H*-pyrrolo[2,3-*b*]pyridine (45d)

Yellow solid; yield: 90%; mp: 278-279 °C; IR 3450 (NH) cm⁻¹; ¹H NMR (200 MHz, DMSO-*d*₆) δ: 3.95 (s, 3H, CH₃), 7.39 (dd, 1H, *J* = 4.8, 7.9 Hz, ArH), 7.55 (dd, 1H, *J* = 5.4, 7.8 Hz, ArH), 7.93 (s, 1H, ArH), 8.33 (s, 1H, ArH), 8.44-8.53 (m, 3H, 3xArH), 8.69 (d, 1H, *J* = 7.9 Hz, ArH), 9.05 (d, 1H, *J* = 7.8 Hz, ArH), 12.80 (bs, 1H, NH); ¹³C NMR (50 MHz, DMSO-*d*₆) δ: 31.4 (q), 107.7 (s), 109.0 (d), 110.7 (s), 115.8 (s), 116.2 (d), 117.3 (d), 120.0 (s), 126.6 (d), 129.4 (d), 130.7 (d), 134.18 (d), 137.7 (d), 142.4 (s), 143.2 (d), 146.7 (s), 148.1 (s), 151.0 (s). Anal. Calcd for C₁₈H₁₃N₅S: C, 65.24; H, 3.95; N, 21.13. Found: C, 65.06; H, 4.19; N, 21.43.

3-[4-(5-Bromo-1*H*-pyrrolo[2,3-*b*]pyridin-3-yl)-1,3-thiazol-2-yl]-1-methyl-1*H*-pyrrolo[2,3-*b*]pyridine (45e)

Yellow solid; yield: 94%; mp: 311 °C; IR 3347 (NH) cm⁻¹; ¹H NMR (200 MHz, DMSO-*d*₆) δ: 3.94 (s, 3H, CH₃), 7.36 (dd, 1H, *J* = 4.7, 7.9 Hz, H-5'), 7.86 (s, 1H, H-5), 8.23 (d, 1H, *J* = 2.6 Hz,

H-2''), 8.39 (d, 1H, $J = 2.2$ Hz, H-6''), 8.41 (s, 1H, H-2'), 8.44 (dd, 1H, $J = 1.6, 4.7$ Hz, H-6'), 8.72 (dd, 1H, $J = 1.6, 7.9$ Hz, H-4'), 8.81 (d, 1H, $J = 2.2$ Hz, H-4''), 12.27 (bs, 1H, NH); ^{13}C NMR (50 MHz, DMSO- d_6) δ : 31.6 (q), 108.1 (d), 108.3 (s), 109.4 (s), 111.5 (s), 117.2 (d), 117.6 (s), 118.8 (s), 126.8 (d), 130.2 (d), 130.4 (d), 130.8 (d), 142.6 (d), 142.9 (d), 146.5 (s), 147.0 (s), 149.0 (s), 161.0 (s). Anal. Calcd for $\text{C}_{18}\text{H}_{12}\text{BrN}_5\text{S}$: C, 52.69; H, 2.95; N, 17.07. Found: C, 52.84; H, 3.19; N, 16.93.

3-[4-(5-Fluoro-1H-pyrrolo[2,3-b]pyridin-3-yl)-1,3-thiazol-2-yl]-1-methyl-1H-pyrrolo[2,3-b]pyridine (45f)

Yellow solid; yield: 90%; mp: 316 °C; IR 3377 (NH) cm^{-1} ; ^1H NMR (200 MHz, DMSO- d_6) δ : 3.94 (s, 3H, CH_3), 7.38 (dd, 1H, $J = 4.8, 7.9$ Hz, H-5'), 7.83 (s, 1H, H-5), 8.27 (d, 1H, $J = 2.7$ Hz, H-2''), 8.32 (t, 1H, $J = 1.7$ Hz, H-6''), 8.43-8.48 (m, 3H, H-2', H-4''), H-6'), 8.71 (dd, 1H, $J = 1.5, 7.9$ Hz, H-4'), 12.18 (bs, 1H, NH); ^{13}C NMR (50 MHz, DMSO- d_6) δ : 31.5 (q), 107.6 (d), 108.2 (s), 109.9 (s, $J_{\text{C}7''\text{-F}} = 4.2$ Hz), 114.1 (d, $J_{\text{C}4''\text{-F}} = 21.3$ Hz), 117.0 (s, $J_{\text{C}3''\text{-F}} = 7.3$ Hz), 117.3 (d), 117.6 (s), 127.5 (d), 127.6 (d), 130.4 (d, $J_{\text{C}6''\text{-F}} = 27.2$ Hz), 130.9 (d), 131.5 (d), 142.7 (d), 145.5 (s), 146.6 (s), 149.2 (s), 155.3 (s, $J_{\text{C}5''\text{-F}} = 239$ Hz), 160.9 (s). Anal. Calcd for $\text{C}_{18}\text{H}_{12}\text{FN}_5\text{S}$: C, 61.88; H, 3.46; N, 20.04. Found: C, 61.68; H, 3.72; N, 20.23.

3,3'-(1,3-Thiazole-2,4-diyl)bis(1-methyl-1H-pyrrolo[2,3-b]pyridine) (45g)

Yellow solid; yield: 60%; mp: 310-311 °C; ^1H NMR (200 MHz, DMSO- d_6) δ : 3.94 (s, 3H, CH_3), 3.98 (s, 3H, CH_3), 7.36-7.45 (m, 2H, 2xArH), 7.82 (s, 1H, ArH), 8.32 (s, 1H, ArH), 8.42 (s, 1H, ArH), 8.45-8.52 (m, 2H, 2xArH), 7.75 (dd, 1H, $J = 1.0, 7.9$ Hz, ArH), 8.81 (d, 1H, $J = 7.8$ Hz, ArH); ^{13}C NMR (50 MHz, DMSO- d_6) δ : 31.4 (q), 31.7 (q), 108.2 (d), 109.5 (s), 116.1 (d), 117.3 (d), 117.4 (s), 129.9 (d), 130.8 (d), 131.5 (d), 140.0 (d), 140.1 (d), 143.0 (d), 144.9 (s), 145.1 (s), 145.2 (s), 146.9 (s), 148.7 (s), 161.2 (s). Anal. Calcd for $\text{C}_{19}\text{H}_{15}\text{N}_5\text{S}$: C, 66.07; H, 4.38; N, 20.27. Found: C, 65.92; H, 4.20; N, 20.40.

5-Bromo-1-methyl-3-[2-(1-methyl-1H-pyrrolo[2,3-b]pyridin-3-yl)-1,3-thiazol-4-yl]-1H-pyrrolo[2,3-b]pyridine (45h)

Yellow solid; yield: 90%; mp: 308 °C; ^1H NMR (200 MHz, DMSO- d_6) δ : 3.92 (s, 3H, CH_3), 3.93 (s, 3H, CH_3), 7.36 (dd, 1H, $J = 4.7, 7.9$ Hz, H-5'), 7.85 (s, 1H, H-5), 8.31 (s, 1H, H-2''), 8.40 (s, 1H, H-2'), 8.42 (dd, 1H, $J = 1.6, 4.7$ Hz, H-6'), 8.45 (d, 1H, $J = 2.2$ Hz, H-6''), 8.73 (dd, 1H, $J = 1.6, 7.9$ Hz, H-4'), 8.79 (d, 1H, $J = 2.2$ Hz, H-4''); ^{13}C NMR (50 MHz, DMSO- d_6) δ : 31.2 (q), 31.5 (q), 107.9 (d), 108.2 (s), 108.3 (s), 111.7 (s), 117.2 (d), 117.5 (s), 118.7 (s), 130.0 (d), 130.4

(d), 130.5 (d), 130.6 (d), 130.7 (d), 142.9 (d), 146.0 (s), 146.7 (s), 148.6 (s), 161.0 (s). Anal Calcd for C₁₉H₁₄BrN₅S: C, 53.78; H, 3.33; N, 16.50. Found: C, 53.65; H, 3.08; N, 16.73.

5-Fluoro-1-methyl-3-[2-(1-methyl-1*H*-pyrrolo[2,3-*b*]pyridin-3-yl)-1,3-thiazol-4-yl]-1*H*-pyrrolo[2,3-*b*]pyridine (45i)

Yellow solid; yield: 60%; mp: 301-302°C; ¹H NMR (200 MHz, DMSO-*d*₆) δ: 3.92 (s, 3H, CH₃), 3.93 (s, 3H, CH₃), 7.37 (dd, 1H, *J* = 4.7, 7.9 Hz, H-5'), 7.81 (s, 1H, H-5), 8.35-8.49 (m, 5H, H-2', H-2'', H4'', H-6', H-6''), 8.72 (dd, 1H, *J* = 1.5, 7.9 Hz, H-4'); ¹³C NMR (50 MHz, DMSO-*d*₆) δ: 31.3 (q), 31.4 (q), 107.4 (d), 108.2 (s), 108.7 (s, *J*_{C7''-a-F} = 4.2 Hz), 114.2 (d, *J*_{C4''-F} = 21.7 Hz), 117.0 (s, *J*_{C3''-a-F} = 7.3 Hz), 117.2 (d), 117.4 (s), 130.0 (d), 130.8 (d), 131.0 (d, *J*_{C6''-F} = 27.1 Hz), 131.4 (d), 143.0 (d), 144.5 (s), 146.9 (s), 148.9 (s), 153.2 (s), 159.5 (s, *J*_{C5''-F} = 155.0 Hz). Anal. Calcd for C₁₉H₁₄FN₅S: C, 62.79; H, 3.88; N, 19.27. Found: C, 62.94; H, 4.15; N, 19.38.

1-Methyl-3-[4-(1*H*-pyrrolo[2,3-*b*]pyridin-3-yl)-1,3-thiazol-2-yl]-1*H*-pyrrolo[2,3-*b*]pyridine (45j)

Yellow solid; yield: 85%; mp: 303-304 °C; IR 3410 (NH) cm⁻¹; ¹H NMR (200 MHz, DMSO-*d*₆) δ: 3.96 (s, 3H, CH₃), 7.36 (dd, 1H, *J* = 4.8, 7.9 Hz, ArH), 7.42 (dd, 1H, *J* = 4.9, 7.9 Hz, ArH), 7.82 (s, 1H, ArH), 8.31 (s, 1H, ArH), 8.39 (s, 1H, ArH), 8.42-8.46 (m, 2H, 2xArH), 8.73 (dd, 1H, *J* = 1.4, 7.9 Hz, ArH), 8.87 (dd, 1H, *J* = 1.5, 7.9 Hz, ArH), 12.60 (bs, 1H, NH); ¹³C NMR (50 MHz, DMSO-*d*₆) δ: 31.44 (q), 108.0 (d), 109.3 (s), 109.8 (s), 116.2 (d), 117.2 (d), 118.2 (s), 118.5 (s), 127.5 (d), 129.6 (d), 130.2 (d), 130.8 (d), 131.5 (s), 140.7 (s), 141.4 (d), 141.6 (s), 142.3 (d), 148.9 (s). Anal. Calcd for C₁₈H₁₃N₅S: C, 65.24; H, 3.95; N, 21.13. Found: C, 65.09; H, 3.69; N, 21.36.

5-Bromo-1-methyl-3-[2-(1*H*-pyrrolo[2,3-*b*]pyridin-3-yl)-1,3-thiazol-4-yl]-1*H*-pyrrolo[2,3-*b*]pyridine (45k)

Yellow solid; yield: 80%; mp: 301 °C; IR 3174 (NH) cm⁻¹; ¹H NMR (200 MHz, DMSO-*d*₆) δ: 3.92 (s, 3H, CH₃), 7.35 (dd, 1H, *J* = 4.8, 7.9 Hz, H-5'), 7.86 (s, 1H, H-5), 8.32 (s, 1H, H-2''), 8.33 (d, 1H, *J* = 3.1 Hz, H-2'), 8.41 (dd, 1H, *J* = 1.4, 4.8 Hz, H-6'), 8.43 (d, 1H, *J* = 2.2 Hz, H-6''), 8.79 (dd, 1H, *J* = 1.4, 7.9 Hz, H-4'), 8.80 (d, 1H, *J* = 2.2 Hz, H-4''), 12.44 (bs, 1H, NH); ¹³C NMR (50 MHz, DMSO-*d*₆) δ: 31.2 (q), 108.4 (d), 109.9 (s), 111.7 (s), 117.1 (d), 118.6 (s), 118.7 (s), 127.9 (d), 130.4 (d), 130.7 (d), 132.1 (d), 141.0 (d), 141.1 (s), 142.9 (d), 145.4 (s), 146.0 (s), 148.6 (s), 160.9 (s). Anal. Calcd for C₁₈H₁₂BrN₅S: C, 52.69; H, 2.95; N, 17.07. Found: C, 52.93; H, 3.09; N, 17.23.

5-Fluoro-1-methyl-3-[2-(1*H*-pyrrolo[2,3-*b*]pyridin-3-yl)-1,3-thiazol-4-yl]-1*H*-pyrrolo[2,3-*b*]pyridine (451)

Yellow solid; yield: 72%; mp: 295-296 °C; IR 3434 (NH) cm⁻¹; ¹H NMR (200 MHz, DMSO-*d*₆) δ: 3.93 (s, 3H, CH₃), 7.38 (dd, 1H, *J* = 4.8, 7.9 Hz, H-5'), 7.83 (s, 1H, H-5), 8.36-8.50 (m, 5H, H-2', H-2'', H4'', H-6', H-6''), 8.81 (dd, 1H, *J* = 1.4, 7.9 Hz, H-4'), 12.50 (bs, 1H, NH); ¹³C NMR (50 MHz, DMSO-*d*₆) δ: 31.3 (q), 107.8 (d), 108.7 (s, *J*_{C3a''-F} = 4.1 Hz), 109.8 (s), 114.2 (d, *J*_{C6''-F} = 21.8 Hz), 116.9 (s), 117.1 (d), 117.2 (d), 118.3 (s), 127.7 (d), 130.8 (d), 131.5 (d, *J*_{C4-F''} = 14.1 Hz), 141.5 (d), 144.5 (s), 145.9 (s), 148.9 (s), 153.2 (s), 159.4 (s, *J*_{C5'-F'} = 152.0 Hz). Anal. Calcd for C₁₈H₁₂FN₅S: C, 61.88; H, 3.46; N, 20.04. Found: C, 62.04; H, 3.70; N, 20.19.

Synthesis of 5-fluoro-1-methyl-1*H*-indole (66b) [31]

To a cold solution of 5-fluoro-indole **66a** (5 mmol) in anhydrous toluene (50 mL), potassium *t*-butoxide (0.76 g, 6.8 mmol) and TDA-1 (1 or 2 drops) were added. The reaction mixture was stirred at room temperature for 5h, and then methyl iodide (0.31 mL, 5 mmol) was added. The reaction mixture was stirred at room temperature for 1h. The solvent was evaporated under reduced pressure. The residue, treated with water, was filtered off and extracted with DCM, dried (Na₂SO₄), and evaporated to afford the pure methyl derivative. Yellow solid; yield: 98%; mp: 55-56 °C; ¹H NMR (200 MHz, CDCl₃) δ: 3.72 (s, 3H, CH₃), 6.41 (d, 1H, *J* = 3.2 Hz, H-3), 6.89-7.05 (m, 2H, H-4, H-6), 7.15-7.28 (m, 2H, H-2, H-7). ¹³C NMR (50 MHz, CDCl₃) δ: 33.0 (q), 100.7 (d, *J*_{C3-F} = 4.9 Hz), 105.4 (d, *J*_{C7-F} = 5.6 Hz), 109.6 (d, *J*_{C4-F} = 23.3 Hz), 109.9 (d, *J*_{C6-F} = 10.8 Hz), 130.3 (d), 130.4 (sx2), 157.8 (s, *J*_{C5-F} = 233.0 Hz). Anal. Calcd for C₉H₈FN: C, 72.47; H, 5.41; N, 9.39. Found: C, 72.82; H, 5.21; N, 9.12.

Synthesis of 5-fluoro-1-[(4-methylphenyl)sulfonyl]-1*H*-indole (66c)

To a stirred ice-cooled solution of 5-fluoro-indole **66a** (1.0 g, 7.4 mmol) in tetrahydrofuran (5 mL) sodium hydride (60% dispersion in mineral oil, 0.39 g, 9.6 mmol) was added and the mixture was stirred at room temperature for 24 h. To the mixture was added *p*-toluenesulfonyl chloride (2.12 g, 11.1 mmol) and the mixture was stirred at room temperature for 4 h. The residue was evaporated under reduced pressure, treated with water, extracted with ethyl acetate. The organic phase was dried (Na₂SO₄), evaporated under reduced pressure and purified by column chromatography using petroleum ether/DCM (9/1) as eluent. White solid; yield: 96%; mp: 111 -112 °C; IR 1373, 1172 (SO₂) cm⁻¹; ¹H NMR (200 MHz, DMSO-*d*₆) δ: 2.32 (s, 3H, CH₃), 6.82-6.84 (m, 1H, H-7), 7.19 (td, 1H, *J* = 2.6, 9.2, 11.0 Hz, H-6), 7.39 (d, 2H, *J* = 8.7 Hz, H-3', H-5'), 7.45 (d, 1H, *J* = 2.6 Hz, H-3), 7.87 (d, 2H, *J* = 8.7 Hz, H-2', H-6'), 7.88-7.97 (m, 2H, H-2, H-4); ¹³C NMR (50 MHz, DMSO-*d*₆)

δ : 21.0 (q), 107.0 (d, $J_{C4-F} = 24.1$ Hz), 109.3 (d, $J_{C3-F} = 4.2$ Hz), 112.5 (d, $J_{C6-F} = 25.8$ Hz), 114.4 (d, $J_{C7-F} = 9.6$ Hz), 126.7 (dx2), 128.9 (d), 130.2 (dx2), 130.6 (s), 131.6 (s, $J_{C3a-F} = 10.4$ Hz), 133.9 (s), 145.6 (s), 158.9 (s, $J_{C5} = 237.7$ Hz). Anal. Calcd for: C₁₅H₁₂FNO₂S: C, 62.27; H, 4.18; N, 4.84. Found: C, 62.57; H, 4.38; N, 4.69.

Synthesis of 1-(1-methyl-1*H*-indol-3-yl)ethanone (66e) [29]

Potassium *t*-butoxide (1.0 g, 8.6 mmol) and TDA-1 (1–2 drops) were added to a cold solution of 3-acetylidole **66d** (1.0 g, 6.3 mmol) in anhydrous toluene (50 mL). The reaction mixture was stirred at room temperature for 8h and then methyl iodide (0.4 mL, 6.3 mmol) was added. Methylation was complete after 2h. The solvent was evaporated under reduced pressure. The residue was treated with water, extracted with DCM, dried, evaporated, and purified by column chromatography using DCM/ethyl acetate (9/1) as eluent. White solid; yield: 80%, mp: 108-109 °C; IR 1643 (CO) cm⁻¹; ¹H NMR (200 MHz, DMSO-*d*₆) δ : 2.44 (s, 3H, CH₃), 3.85 (s, 3H, CH₃), 7.19-7.32 (m, 2H, H-5, H-6), 7.52 (dd, 1H, $J = 6.4, 1.8$ Hz, H-7), 8.23 (dd, 1H, $J = 6.4, 1.8$ Hz, H-4), 8.29 (s, 1H, H-2); ¹³C NMR (50 MHz, DMSO-*d*₆) δ : 27.2 (q), 33.0 (q), 110.5 (d), 115.6 (s), 121.4 (d), 121.9 (d), 122.7 (d), 125.7 (s), 137.2 (s), 137.9 (d), 192.0 (s). Anal. Calcd for: C₁₁H₁₁NO: C, 76.28; H, 6.40; N, 8.09. Found: C, 76.41; H, 6.29; N, 7.87.

Synthesis of 1-{1-[(4-methylphenyl)sulfonyl]-1*H*-indol-3-yl}ethanone (66f)

To a cooled solution of 3-acetylidole **66d** (1.0 g, 6.3 mmol) in tetrahydrofuran (5 mL) sodium hydride (60% dispersion in mineral oil, 0.25 g, 6.3 mmol) was added and the mixture was stirred at room temperature for 1 h. *p*-Toluenesulfonyl chloride (1.2 g, 6.3 mmol) was added and the mixture was stirred at room temperature for 24 h. The reaction mixture was purified by column chromatography using DCM as eluent. White solid; yield: 90%; mp: 148-149 °C; IR 1382, 1299 (SO₂), 1662 (CO) cm⁻¹; ¹H NMR (200 MHz, DMSO-*d*₆) δ : 2.33 (s, 3H, CH₃), 2.60 (s, 3H, CH₃), 7.32-7.39 (m, 2H, H-5, H-6), 7.43 (d, 2H, $J = 7.8$ Hz, H-3', H-5'), 7.95 (d, 1H, $J = 7.5$ Hz, H-7), 8.04 (d, 2H, $J = 7.8$ Hz, H-2', H-6'), 8.19 (d, 1H, $J = 7.5$ Hz, H-4), 8.81 (s, 1H, H-2); ¹³C NMR (50 MHz, DMSO-*d*₆) δ : 21.0 (q), 27.8 (q), 113.0 (d), 120.7 (s), 122.3 (d), 124.8 (d), 125.6 (d), 127.0 (s), 127.2 (dx2), 130.5 (dx2), 133.5 (s), 134.0 (s), 134.2 (d), 146.2 (s), 193.9 (s). Anal. Calcd for: C₁₇H₁₅NO₃S: C, 65.16; H, 4.82; N, 4.47. Found: C, 65.28, H, 5.06, N, 4.37.

Synthesis of 2-chloro-1-(5-fluoro-1*H*-indol-3-yl)ethanones (67b, 67c)

To a stirred ice-cooled suspension of anhydrous aluminium chloride (1.14 g, 8.5 mmol), in DCM (18 mL), was added dropwise at 0 °C a solution of suitable indole **66b,c** (1.21 mmol) in DCM (5 mL) under nitrogen atmosphere. Then chloroacetyl chloride (0.3 mL, 3.63 mmol) was slowly added

to the reaction mixture. The resulting mixture was stirred at room temperature for 1 h and poured in stirred ice and water and extracted with DCM. The organic phase was dried (Na₂SO₄), evaporated under reduced pressure and purified by column chromatography using DCM as eluent.

2-Chloro-1-(5-fluoro-1-methyl-1H-indol-3-yl)ethanone (67b)

White solid; yield: 50 %; mp: 185-186 °C; IR 1653.07 (CO) cm⁻¹; ¹H NMR (200 MHz, DMSO-*d*₆) δ: 3.89 (s, 3H, CH₃), 4.84 (s, 2H, CH₂), 7.20 (td, 1H, *J* = 2.6, 9.2, 11.0 Hz, H-6), 7.62 (dd, 1H, *J* = 4.5, 9.2 Hz, H-7), 7.84 (dd, 1H, *J* = 2.6, 11 Hz, H-4), 8.51 (bs, 1H, H-2); ¹³C NMR (50 MHz, DMSO-*d*₆) δ: 33.7 (q), 46.2 (t), 106.1 (d, *J*_{C4-F} = 24.8 Hz), 111.3 (d, *J*_{C6-F} = 26.1), 112.3 (s), 112.4 (d, *J*_{C7-F} = 9.8), 126.4 (s, *J*_{C3a-F} = 11.0 Hz), 133.9 (s), 139.5 (d), 159.0 (s, *J*_{C5-F} = 236 Hz), 185.6 (s). Anal. Calcd for C₁₁H₉ClFNO: C, 58.55; H, 4.02; N, 6.21. Found: C, 58.85; H, 4.14; N, 6.01.

2-Chloro-1-{5-fluoro-1-[(4-methylphenyl)sulfonyl]-1H-indol-3-yl}ethanone (67c)

White solid; yield: 55%; mp: 155-156 °C; IR 1375, 1171 (SO₂), 1683 (CO) cm⁻¹; ¹H NMR (200 MHz, CDCl₃) δ: 2.39 (s, 3H, CH₃), 4.54 (s, 2H, CH₂), 7.13 (td, 1H, *J* = 2.6, 8.9, 11.0 Hz, H-6), 7.31 (d, 2H, *J* = 8.0 Hz, H-3', H-5'), 7.82 (d, 2H, *J* = 8.0 Hz, H-2', H-6'), 7.90 (dd, 1H, *J* = 4.9, 8.9 Hz, H-7), 7.98 (dd, 2H, *J* = 2.6, 11.0 Hz, H-4), 8.34 (s, 1H, H-2); ¹³C NMR (50 MHz, CDCl₃) δ: 21.7 (q), 45.8 (t), 108.9 (d, *J*_{C6-F} = 25.5 Hz), 114.1 (s), 114.2 (d), 114.5 (d, *J*_{C4-F} = 14.0 Hz), 117.9 (s, *J*_{C7a-F} = 4.5 Hz), 127.2 (dx2), 130.2 (s), 130.4 (dx2), 133.5 (d), 134.1 (s), 146.5 (s), 160.1 (s, *J*_{C5-F} = 241 Hz), 186.7 (s). Anal. Calcd for C₁₇H₁₃ClFNO₃S: C, 55.82; H, 3.58; N, 3.83. Found: C, 55.99; H, 3.36; N, 4.10.

Synthesis of 2-bromo-(1H-indol-3-yl)ethanones (67e, 67f)

To a cold suspension of the appropriate 3-acetylindoles **66e,f** (1.9 mmol) in anhydrous methanol (3 mL), bromine (0.1 mL, 1.9 mmol) was added dropwise. The mixture was heated at reflux for 2 h. After cooling the solvent was evaporated under reduced pressure. The residue was treated with water, made alkaline by adding NaHCO₃ and extracted with ethyl acetate. The organic phase was dried, evaporated under reduced pressure and purified by column chromatography using DCM as eluent.

2-Bromo-1-(1-methyl-1H-indol-3-yl)ethanone (67e) [29]

Brown solid; yield: 70%; mp: 205-206 °C; IR 1643 (CO) cm⁻¹; ¹H NMR (200 MHz, DMSO-*d*₆) δ: 3.37 (s, 3H, CH₃), 4.60 (s, 2H, CH₂), 7.27–7.33 (m, 2H, H-5, H-6), 7.59 (dd, 1H, *J* = 6.0, 1.9 Hz, H-7), 8.18 (dd, 1H, *J* = 6.0, 1.9 Hz, H-4), 8.50 (s, 1H, H-2); ¹³C NMR (50 MHz, DMSO-*d*₆) δ: 33.3

(q), 33.4 (t), 110.9 (d), 112.3 (s), 121.3 (d), 122.5 (d), 123.3 (d), 125.9 (s), 137.4 (s), 138.7 (d), 185.8 (s). Anal. Calcd for C₁₁H₁₀BrNO: C, 52.41; H, 4.00; N, 5.56. Found: C, 52.57; H, 4.11; N, 5.39.

2-Bromo-1-{1-[(4-methylphenyl)sulfonyl]-1*H*-indol-3-yl}ethanone (67f)

Solid; yield: 40%; mp: 134-135 °C; IR 1379, 1177 (SO₂), 1668 (CO) cm⁻¹; ¹H NMR (200 MHz, CDCl₃) δ: 2.38 (s, 3H, CH₃), 4.36 (s, 2H, CH₂), 7.29 (d, 2H, *J* = 8.2 Hz, H-3', H-5'), 7.36-7.40 (m, 2H, H-5, H-6), 7.83-7.87 (m, 2H, H-2', H-6'), 7.91-7.96 (1H, m, H-7), 8.28-8.34 (2H, m, H-2, H-4); ¹³C NMR (50 MHz, CDCl₃) δ: 21.7 (q), 31.4 (t), 113.1 (d), 123.1 (d), 124.3 (s), 125.1 (d), 126.1 (d), 127.2 (dx2), 127.5 (s), 130.4 (dx2), 132.8 (d), 134.2 (s), 134.8 (s), 146.2 (s), 187.0 (s). Anal. Calcd for C₁₇H₁₄BrNO₃S: C, 52.05; H, 3.60; N, 3.57. Found: C, 52.25; H, 3.70; N, 3.35.

Synthesis of 1-(5-fluoro-1-methyl-1*H*-indol-3-yl)ethanone (68)

To a cooled suspension of anhydrous aluminium chloride (1.58 g, 11.76 mmol) in DCM (25 mL) was added drop-wise a solution of **66b** (0.250 g, 1.68 mmol) in dichloromethane (5 mL), under a nitrogen atmosphere. To the reaction mixture was slowly added acetic anhydride (0.48 mL, 5.04 mmol). The resulting mixture was stirred at room temperature for 4 h and it was poured into ice water and extracted with DCM. The organic phase was dried over Na₂SO₄, evaporated under reduced pressure and purified by column chromatography using DCM as eluent. White solid; yield: 41%, mp: 110-111 °C, IR 1683 (CO) cm⁻¹; ¹H NMR (200 MHz, CDCl₃) δ: 2.50 (s, 3H, CH₃), 3.84 (s, 3H, CH₃), 7.05 (td, 1H, *J* = 2.5, 8.9, 11.5 Hz, H-6), 7.22-7.28 (m, 1H, H-7), 7.71 (s, 1H, H-2), 8.05 (dd, 1H, *J* = 2.6, 9.7 Hz, H-4). Anal. Calcd for C₁₁H₁₀FNO: C, 69.10; H, 5.27; N, 7.33. Found: C, 68.87; H, 5.53; N, 6.98.

Synthesis of 2-bromo-1-(5-fluoro-1-methyl-1*H*-indol-3-yl)ethanone (69)

To a cold suspension of the appropriate 3-acetylindole **68** (2.45 mmol) in anhydrous methanol (3 mL), bromine (0.1 mL, 2.45 mmol) was added dropwise. The mixture was heated at reflux for 2 h. After cooling the solvent was evaporated under reduced pressure. The residue was treated with water, made alkaline by adding NaHCO₃ and extracted with ethyl acetate. The organic phase was dried, evaporated under reduced pressure and purified by column chromatography using cyclohexane/ethyl acetate (8/2) as eluent. White solid; yield: 35%, mp: 200-201 °C; IR 1680 (CO) cm⁻¹; ¹H NMR (200 MHz, DMSO-*d*₆) δ: 3.89 (s, 3H, CH₃), 4.83 (s, 2H, CH₂), 7.19 (td, 1H, *J* = 2.6, 9.2, 11.8 Hz, H-6), 7.63 (dd, 1H, *J* = 4.4, 8.9 Hz, H-7), 7.84 (dd, 1H, *J* = 2.5, 9.7 Hz, H-4), 8.52 (s, 1H, H-2); ¹³C NMR (50 MHz, DMSO-*d*₆) δ: 33.7 (q), 46.2 (t), 106.1 (d, *J*_{C-F} = 24.8 Hz), 111.3 (d,

$J_{C6-F} = 26.0$ Hz), 112.4 (d, $J_{C7-F} = 9.4$ Hz), 126.3 (s), 126.5 (s), 133.9 (s), 139.5 (d), 159.0 (s, $J_{C5-F} = 235$ Hz), 185.6 (s). Anal. Calcd for $C_{11}H_9BrFNO$: C, 48.91; H, 3.36; N, 5.19. Found: C, 48.64; H, 3.57; N, 5.43.

Synthesis of 1-(5-fluoro-1*H*-indol-3-yl)ethanone (70) [46]

To a solution of ammonium chloride (8.8 mmol, 0.47 g) suspended in DCM (4 mL) was added dropwise acetic anhydride (4.4 mmol, 0.42 ml) at room temperature, and the mixture was stirred at room temperature for 15 min. Then, 5-fluoro indole **66a** (2.22 mmol, 0.300 g) in DCM (4 mL) was added dropwise and the mixture was stirred at room temperature for 2 h. $AlCl_3$ (4.4 mmol, 0.60 g) was added. Acetic anhydride (2.22 mmol, 0.21 ml) was added, and the mixture was stirred for 30 min. The mixture was poured into crushed ice and subjected to extractive workups with EtOAc. The organic phase was dried, evaporated under reduced pressure and purified by column chromatography using dichloromethane/ethyl acetate (93/7) as eluent. White solid; yield: 55%; mp: 200-201 °C; IR 1670 (CO) cm^{-1} ; 1H NMR (200 MHz, DMSO- d_6) δ : 2.50 (s, 3H, CH_3), 7.07 (td, 1H, $J = 2.7, 9.1, 11.7$ Hz, H-6), 7.48 (dd, 1H, $J = 4.5, 8.8$ Hz, H-4), 7.85 (dd, 1H, $J = 2.6, 9.9$ Hz, H-7), 8.38 (s, 1H, H-2), 12.06 (bs, 1H, NH). Anal. Calcd for $C_{10}H_8FNO$: C, 67.79; H, 4.55; N, 7.91. Found: C, 67.53; H, 4.74; N, 7.71.

Synthesis of substituted indolyl-thiazolyl-1*H*-pyrrolo[2,3-*b*]pyridines (46a-d), (47a-d)

A suspension of the appropriate pyrrolo[2,3-*b*]pyridine-carbothioamide **54a,b** (5 mmol) and halo-acetyl compounds **67b,c,e,f** (5 mmol) in 3 mL of anhydrous ethanol was heated under reflux for 30 minutes. The precipitate, obtained after cooling, was filtered off, dried and crystallized with ethanol to afford derivatives **46a-d** and **47a-d**.

3-[4-(5-Fluoro-1-methyl-1*H*-indol-3-yl)-1,3-thiazol-2-yl]-1*H*-pyrrolo[2,3-*b*]pyridine (46a)

Yellow solid; yield: 97%; mp: 237-238 °C; IR 3550 (NH) cm^{-1} ; 1H NMR (200 MHz, DMSO- d_6) δ : 3.90 (s, 3H, CH_3), 7.12 (t, 1H, $J = 8.2$ Hz, H-6''), 7.44 (dd, 1H, $J = 5.2, 7.4$ Hz, H-5'), 7.54 (dd, 1H, $J = 4.6, 8.2$ Hz, H-7''), 7.73 (s, 1H, H-2''), 7.94 (dd, 1H, $J = 9.7, 2.5$ Hz, H-4''), 8.16 (s, 1H, H-2'), 8.38 (s, 1H, H-5), 8.45 (d, 1H, $J = 3.7$ Hz, H-6'), 8.89 (d, 1H, $J = 7.4$ Hz, H-4'), 12.74 (s, 1H, NH). Anal. Calcd for $C_{19}H_{13}FN_4S$: C, 65.50; H, 3.76; N, 16.08. Found: C, 65.76; H, 3.55; N, 16.22.

3-[4-(5-fluoro-1-methyl-1*H*-indol-3-yl)-1,3-thiazol-2-yl]-1-methyl-1*H*-pyrrolo[2,3-*b*]pyridine (46b)

Yellow solid; yield: 30%; mp: 286-287 °C; ¹H NMR (200 MHz, DMSO-*d*₆) δ: 2.56 (s, 3H, CH₃), 4.03 (s, 3H, CH₃), 6.02 (dd, 1H, *J* = 4.3, 10.7 Hz, H-7''), 6.76 (td, 1H, *J* = 2.3, 9.5, 10.7 Hz, H-6''), 6.98 (dd, 1H, *J* = 5.0, 8.4 Hz, H-5'), 7.25 (dd, 1H, *J* = 2.3, 9.5 Hz, H-4''), 7.72 (d, 1H, *J* = 7.8 Hz, H-4'), 8.19-8.81 (m, 4H, H-2', H-2'', H-5, H-6'). Anal. Calcd for C₂₀H₁₅FN₄S: C, 66.28; H, 4.17; N, 15.46. Found: C, 66.53; H, 3.90; N, 15.23.

3-[4-(1-Methyl-1*H*-indol-3-yl)-1,3-thiazol-2-yl]-1*H*-pyrrolo[2,3-*b*]pyridine (46c)

Yellow solid; yield: 60%; mp: 274-275 °C, IR 3427 (NH) cm⁻¹; ¹H NMR (200 MHz, DMSO-*d*₆) δ: 3.90 (s, 3H, CH₃), 7.21-7.30 (m, 2H, H-5'', H-6''), 7.36 (dd, 1H, *J* = 4.9, 7.7 Hz, H-5'), 7.53 (d, 1H, *J* = 7.1 Hz, H-7''), 7.66 (s, 1H, H-2''), 8.05 (s, 1H, H-5), 8.19 (d, 1H, *J* = 7.1 Hz, H-4''), 8.30 (d, 1H, *J* = 2.0 Hz, H-2'), 8.40 (d, 1H, *J* = 4.9 Hz, H-6'), 8.79 (d, 1H, *J* = 7.7 Hz, H-4'), 12.40 (bs, 1H, NH); ¹³C NMR (50 MHz, DMSO-*d*₆) δ: 32.6 (q), 106.5 (d), 109.6 (s), 110.2 (d), 117.1 (d), 117.3 (s), 119.9 (d), 120.1 (d), 121.6 (d), 124.9 (s), 126.9 (d), 129.2 (d), 129.7 (d), 137.1 (s), 143.2 (d), 143.3 (s), 147.9 (s), 150.1 (s), 161.0 (s). Anal. Calcd for C₁₉H₁₄N₄S: C, 69.07; H, 4.27; N, 16.96. Found: C, 68.90; H, 4.46; N, 16.75.

1-Methyl-3-[4-(1-methyl-1*H*-indol-3-yl)-1,3-thiazol-2-yl]-1*H*-pyrrolo[2,3-*b*]pyridine (46d)

Yellow solid; yield: 60%; mp: 290-291 °C; ¹H NMR (200 MHz, DMSO-*d*₆) δ: 3.90 (s, 3H, CH₃), 3.94 (s, 3H, CH₃), 7.17-7.30 (m, 2H, H-5'', H-6''), 7.39 (dd, 1H, *J* = 4.7, 7.9 Hz, H-5'), 7.53 (dd, 1H, *J* = 1.4, 6.9 Hz, H-7''), 7.66 (s, 1H, H-2''), 8.05 (s, 1H, H-2'), 8.19 (dd, 1H, *J* = 1.4, 6.9 Hz, H-4''), 8.41 (s, 1H, H-5), 8.45 (dd, 1H, *J* = 1.3, 4.7 Hz, H-6'), 8.78 (dd, 1H, *J* = 1.3, 7.9 Hz, H-4'); ¹³C NMR (50 MHz, DMSO-*d*₆) δ: 31.4 (q), 32.6 (q), 106.5 (d), 108.3 (s), 110.0 (s), 110.2 (d), 117.2 (d), 117.5 (s), 119.9 (d), 120.1 (d), 121.6 (d), 124.9 (s), 129.3 (d), 129.8 (d), 130.5 (d), 137.0 (s), 143.1 (d), 147.0 (s), 150.1 (s), 160.7 (s). Anal. Calcd for C₂₀H₁₆N₄S: C, 69.74; H, 4.68; N, 16.27. Found: C, 69.50; H, 4.84; N, 16.06.

3-(4-{5-Fluoro-1-[(4-methylphenyl)sulfonyl]-1*H*-indol-3-yl}-1,3-thiazol-2-yl)-1*H*-pyrrolo[2,3-*b*]pyridine (47a)

Yellow solid; yield: 97%; mp: 257-258 °C; IR 1337 (NH), 1171, 1370 (SO₂); ¹H NMR (200 MHz, DMSO-*d*₆) δ: 2.31 (s, 3H, CH₃), 7.28-7.32 (m, 2H, ArH), 7.39-7.42 (m, 2H, H-3''', H-5'''), 7.94-7.98 (m, 2H, H-2''', H-6'''), 8.03-8.15 (m, 3H, ArH), 8.42-8.49 (m, 3H, ArH), 8.74 (d, 1H, *J* = 7.4 Hz, H-4'), 12.67 (s, 1H, NH); ¹³C NMR (50 MHz, DMSO-*d*₆) δ: 21.1 (q), 107.3 (d, *J*_{C4'-F} = 24.1 Hz), 109.3 (s), 112.6 (d, *J*_{C6'-F} = 26.8 Hz), 113.4 (d), 114.9 (d, *J*_{C7'-F} = 9.9 Hz), 117.2 (d), 117.4 (s),

117.5 (s), 117.6 (s), 126.3 (d), 126.9 (2xd), 127.8 (d), 128.8 (s), 129.0 (s), 130.2 (d), 130.4 (2xd), 131.1 (s), 133.6 (s), 142.3 (d), 145.9 (s), 146.9 (s), 159.4 (s, $J_{C5''-F} = 245.5$ Hz). Anal. Calcd for $C_{25}H_{17}FN_4O_2S_2$: C, 61.46; H, 3.51; N, 11.47. Found: C, 61.73; H, 3.25; N, 11.31.

3-(4-{5-Fluoro-1-[(4-methylphenyl)sulfonyl]-1H-indol-3-yl}-1,3-thiazol-2-yl)-1-methyl-1H-pyrrolo[2,3-*b*]pyridine (47b)

White solid; yield: 40%; mp: 230-231; IR 1299, 1380 (SO₂) cm⁻¹; ¹H NMR (200 MHz, DMSO-*d*₆) δ: 2.32 (s, 3H, CH₃), 3.94 (s, 3H, CH₃), 7.28-7.43 (m, 2H, ArH), 7.41 (d, 2H, $J = 7.8$ Hz, H-3'''), H5'''), 7.87-7.94 (m, 2H, H2''', H6'''), 7.99-8.13 (m, 3H, ArH), 8.42-8.48 (m, 3H, ArH), 8.60 (d, 1H, $J = 7.3$ Hz, H-4'); ¹³C NMR (50 MHz, DMSO-*d*₆) δ: 21.0 (q), 31.2 (q), 107.4 (d, $J_{C4''-F} = 25.2$ Hz), 107.8 (s), 112.0 (d), 113.1 (d, $J_{C6''-F} = 27.5$ Hz), 114.8 (d, $J_{C7''-F} = 9.1$ Hz), 116.9 (s), 117.4 (d), 117.5 (s, $J_{C7''-a} = 4.0$ Hz), 126.3 (d), 126.9 (2xd), 128.6 (d), 128.8 (s), 129.0 (s), 130.4 (d), 130.8 (2xd), 131.1 (s), 133.6 (s), 143.8 (d), 145.9 (s), 146.9 (s), 147.6 (s), 159.3 (s, $J_{C5''-F} = 246.5$ Hz). Anal. Calcd for $C_{26}H_{19}FN_4O_2S_2$: C, 62.13; H, 3.81; N, 11.15. Found: C, 61.98; H, 3.99; N, 10.90.

3-(4-{1-[(4-methylphenyl)sulfonyl]-1H-indol-3-yl}-1,3-thiazol-2-yl)-1H-pyrrolo[2,3-*b*]pyridine (47c)

Yellow solid; yield: 90%; mp: 260-261 °C; IR 1374, 1174 (SO₂), 3498 (NH) cm⁻¹; ¹H NMR (200 MHz, DMSO-*d*₆) δ: 2.30 (s, 3H, CH₃), 7.31-7.41 (m, 5H, ArH), 7.94-7.98 (m, 2H, ArH), 8.01-8.07 (m, 2H, ArH), 8.36-8.39 (m, 4H, ArH), 8.64 (d, 1H, $J = 7.7$ Hz, H-4'), 12.39 (s, 1H, NH); ¹³C NMR (50 MHz, DMSO-*d*₆) δ: 21.0 (q), 109.1 (s), 11.8 (d), 113.4 (d), 116.7 (s), 117.2 (d), 117.7 (s), 121.7 (d), 124.0 (d), 124.5 (d), 125.2 (d), 126.8 (dx2), 127.2 (d), 127.9 (s), 128.6 (d), 130.3 (dx2), 133.8 (s), 134.6 (s), 144.0 (d), 145.7 (s), 147.3 (s), 148.7 (s), 162.1 (s). Anal. Calcd for $C_{25}H_{18}N_4O_2S_2$: C, 63.81; H, 3.86; N, 11.91. Found: C, 63.55; H, 4.02; N, 11.76.

1-Methyl-3-(4-{1-[(4-methylphenyl)sulfonyl]-1H-indol-3-yl}-1,3-thiazol-2-yl)-1H-pyrrolo[2,3-*b*]pyridine (47d)

Yellow solid; yield: 50%; mp: 250-251 °C; IR 1374, 1174 (SO₂) cm⁻¹; ¹H NMR (200 MHz, DMSO-*d*₆) δ: 2.30 (s, 3H, CH₃), 3.94 (s, 3H, CH₃), 7.37-7.45 (m, 5H, ArH), 7.93-7.97 (m, 2H, ArH), 8.01-8.09 (m, 2H, ArH), 8.31-8.47 (m, 4H, ArH), 8.66 (d, 1H, $J = 7.5$ Hz, H-4'); ¹³C NMR (50 MHz, DMSO-*d*₆) δ: 21.0 (q), 31.4 (q), 108.0 (s), 112.0 (d), 113.4 (d), 117.2 (s), 117.4 (d), 117.6 (s), 121.7 (d), 124.0 (d), 124.6 (d), 125.2 (d), 126.8 (2xd), 127.8 (s), 129.3 (d), 130.3 (2xd), 130.9 (d), 133.8 (s), 134.6 (s), 145.7 (s), 147.1 (s), 147.4 (s), 148.2 (d), 161.6 (s). Anal. Calcd for: $C_{26}H_{20}N_4O_2S_2$: C, 64.44; H, 4.16, N, 11.56. Found: C, 64.19; H, 4.33; N, 11.25.

Synthesis of indolyl-thiazolyl-1*H*-pyrrolo[2,3-*b*]pyridines (48a-d)

To a suspension of the appropriate derivatives **47a-d** (0.60 mmol) in 2 mL of anhydrous ethanol, potassium hydroxide (0.1 g, 1.8 mmol) was added and the mixture was heated at reflux for 1-2 h. The precipitate, obtained after cooling, was filtered off, dried and crystallized with ethanol to afford derivatives **48a-d**.

3-[4-(5-Fluoro-1*H*-indol-3-yl)-1,3-thiazol-2-yl]-1*H*-pyrrolo[2,3-*b*]pyridine (48a)

Conditions: reflux for 1.5 h. Yellow solid; yield: 98 %; mp: 248-249 °C; IR 3550, 3600 (NH) cm⁻¹; ¹H NMR (200 MHz, DMSO-*d*₆) δ: 7.05 (t, 1H, *J* = 7.8 Hz, H-6''), 7.47-7.53 (m, 2H, H-5', H-7''), 7.78 (bs, 1H, H-2''), 7.92 (d, 1H, *J* = 8.9 Hz, H-4''), 8.19 (bs, 1H, H-2'), 8.47 (m, 2H, H-5, H-6'), 8.95 (d, 1H, *J* = 7.4 Hz, H-4'), 11.70 (s, 1H, NH), 12.93 (bs, 1H, NH); ¹³C NMR (50 MHz, DMSO-*d*₆) δ: 104.7 (d, *J*_{C4''-F} = 21.6 Hz), 107.3 (d), 109.7 (d, *J*_{C6''-F} = 26.1 Hz), 109.8 (s), 110.7 (s), 113.0 (d, *J*_{C7''-F} = 10.0 Hz), 117.2 (d), 119.0 (s), 124.6 (s, *J*_{3''a-F} = 10.5 Hz), 127.2 (d), 128.2 (d), 132.3 (d), 133.3 (s), 140.6 (d), 144.7 (s), 149.6 (s), 157.5 (s, *J*_{C5''-F} = 232 Hz), 160.5 (s). Anal. Calcd for C₁₈H₁₁FN₄S: C, 64.66; H, 3.32; N, 16.76. Found: C, 64.37; H, 3.04; N, 16.57.

3-[4-(5-Fluoro-1*H*-indol-3-yl)-1,3-thiazol-2-yl]-1-methyl-1*H*-pyrrolo[2,3-*b*]pyridine (48b)

Conditions: reflux for 1 h. Yellow solid; yield: 40%; mp: 243-244 °C; IR 3557 (NH) cm⁻¹; ¹H NMR (200 MHz, DMSO-*d*₆) δ: 3.93 (s, 3H, CH₃), 7.04 (td, 1H, *J* = 2.1, 9.1, 10.9 Hz, H-6''), 7.35 (dd, 1H, *J* = 4.6, 7.8 Hz, H-5'), 7.49 (dd, 1H, *J* = 4.6, 9.1 Hz, H-7''), 7.70 (s, 1H, H-2''), 7.96 (dd, 1H, *J* = 2.1, 10.9 Hz, H-4''), 8.11 (bs, 1H, H-2'), 8.38 (s, 1H, H-5), 8.42 (d, 1H, *J* = 4.6 Hz, H-6'), 8.69 (d, 1H, *J* = 7.8 Hz, H-4'), 11.64 (bs, 1H, NH); ¹³C NMR (50 MHz, DMSO-*d*₆) δ: 31.2 (q), 104.9 (d, *J*_{C4''-F} = 24 Hz), 106.5 (d), 108.3 (s), 109.7 (d, *J*_{C6''-F} = 26 Hz), 111.3 (s, *J*_{C7''a} = 4.5 Hz), 112.9 (d, *J*_{C7''-F} = 9.5 Hz), 117.0 (s), 117.2 (d), 124.8 (s, *J*_{C4''a-F} = 10.1 Hz), 126.8 (d), 129.0 (d), 130.2 (d), 133.3 (s), 143.7 (d), 147.6 (s), 150.2 (s), 157.4 (s, *J*_{C5''-F} = 231.9 Hz), 160.8 (s). Anal. Calcd for C₁₉H₁₃FN₄S: C, 65.50; H, 3.76; N, 16.08. Found: C, 65.36; H, 3.47; N, 15.82.

3-[4-(1*H*-Indol-3-yl)-1,3-thiazol-2-yl]-1*H*-pyrrolo[2,3-*b*]pyridine (48c)

Conditions: reflux for 2 h. Yellow solid; yield: 98 %; mp: 297-298 °C; IR 3557, 3676 (NH) cm⁻¹; ¹H NMR (200 MHz, DMSO-*d*₆) δ: 7.13-7.23 (m, 2H, H-5'', H-6''), 7.39 (dd, 1H, *J* = 4.9, 7.9 Hz, H-5'), 7.47-7.51 (m, 1H, H-7''), 7.68 (s, 1H, H-2''), 8.05 (d, 1H, *J* = 2.6 Hz, H-2'), 8.18 (dd, 1H, *J* = 2.7, 7.1 Hz, H-4''), 8.34 (s, 1H, H-5), 8.42 (dd, 1H, *J* = 1.5, 4.9 Hz, H-6'), 8.82 (dd, 1H, *J* = 1.5, 7.9 Hz, H-4'), 11.46 (bs, 1H, NH), 12.50 (s, 1H, NH); ¹³C NMR (50 MHz, DMSO-*d*₆) δ: 106.6 (d), 109.7 (s), 110.9 (s), 111.9 (d), 117.1 (d), 117.6 (s), 119.8 (d), 120.0 (d), 121.5 (d), 124.6 (s), 125.1 (d), 127.1 (d), 130.3 (d), 136.6 (s), 142.7 (d), 147.3 (s), 150.5 (s), 160.8 (s). Anal. Calcd for

C₁₈H₁₂N₄S: C, 68.33; H, 3.82; N, 17.71. Found: C, 68.06; H, 4.07; N, 17.45.

3-[4-(1*H*-Indol-3-yl)-1,3-thiazol-2-yl]-1-methyl-1*H*-pyrrolo[2,3-*b*]pyridine (48d)

Conditions: reflux for 1.5 h. Yellow solid; yield: 98%; mp: 276-277 °C; IR 3500 (NH) cm⁻¹; ¹H NMR (200 MHz, DMSO-*d*₆) δ: 3.95 (s, 3H, CH₃), 7.14-7.25 (m, 2H, H-5'', H-6''), 7.41 (dd, 1H, *J* = 5.0, 7.7 Hz, H-5'), 7.50 (dd, 1H, *J* = 2.1, 7.4 Hz, H-7''), 7.69 (s, 1H, H-2''), 8.05 (d, 1H, *J* = 5.0 Hz, H-6'), 8.16-8.21 (m, 1H, H-4''), 8.45-8.48 (m, 2H, H-5, H-2'), 8.78 (dd, 1H, *J* = 2.0, 7.7 Hz, H-4'), 11.49 (s, 1H, NH); ¹³C NMR (50 MHz, DMSO-*d*₆) δ: 31.6 (q), 106.8 (d), 108.4 (s), 110.7 (s), 111.9 (d), 117.3 (d), 119.8 (d), 119.9 (d), 121.6 (d), 124.6 (s), 125.1 (d), 125.9 (s), 130.3 (d), 130.8 (d), 135.7 (s), 136.6 (s), 142.6 (d), 150.3 (s), 160.6 (s). Anal. Calcd for C₁₉H₁₄N₄S: C, 69.07; H, 4.27; N, 16.96. Found: C, 69.31; H, 4.50; N, 16.70.

Synthesis of 5-substituted 1- methyl-1*H*-indoles (73b-d)

To a cold solution of indoles **72b-d** (5 mmol) in anhydrous toluene (50 mL), potassium *t*-butoxide (0.76 g, 6.8 mmol) and TDA-1 (1 or 2 drops) were added. The reaction mixture was stirred at room temperature for 1–24 h, and then methyl iodide (0.31 mL, 5 mmol) was added. Methylation was complete after 0.5–1 h. The solvent was evaporated under reduced pressure. The residue, treated with water, was filtered off and air dried or extracted with DCM, dried (Na₂SO₄), and evaporated to afford the pure methyl derivatives **73b-d**.

5-Methoxy-1-methyl-1*H*-indole (73b) [27]

Conditions: room temperature for 1 h, then room temperature for 0.5 h. Workup: filtration. White solid; yield: 97%; mp: 84 °C; ¹H NMR (200 MHz, CDCl₃) δ: 3.67 (3H, s, CH₃), 3.81 (3H, s, CH₃), 6.38 (1H, d, *J* = 2.9 Hz, H-3), 6.87 (1H, dd, *J* = 2.9, 8.8 Hz, H-6), 6.96 (1H, d, *J* = 2.9 Hz, H-4), 7.07 (1H, d, *J* = 2.9 Hz, H-2), 7.17 (1H, d, *J* = 8.8 Hz, H-7); ¹³C NMR (50 MHz, CDCl₃) δ: 32.8 (q), 55.8 (q), 100.3 (d), 102.4 (d), 109.8 (d), 111.8 (d), 128.7 (s), 129.2 (d), 132.1 (s), 153.9 (s). Anal. Calcd for C₁₀H₁₁NO: C, 74.51; H, 6.88; N, 8.69. Found: C, 74.76; H, 6.84; N, 8.43.

5-Bromo-1-methyl-1*H*-indole (73c) [27]

Conditions: room temperature for 24 h, then room temperature for 1 h. Workup: extraction. Oil; yield: 96%; ¹H NMR (200 MHz, CDCl₃) δ: 3.47 (3H s, CH₃), 6.29 (1H, d, *J* = 3.1 Hz, H-3), 6.84 (1H, d, *J* = 3.1 Hz, H-2), 6.94 (1H, d, *J* = 8.5 Hz, H-7), 7.17 (1H, dd, *J* = 1.7, 8.5 Hz, H-6), 7.65 (1H, d, *J* = 1.7 Hz, H-4); ¹³C NMR (50 MHz, CDCl₃) δ: 32.6 (q), 100.2 (d), 110.5 (d), 121.2 (s), 122.9 (d), 123.9 (d), 127.6 (s), 129.8 (d), 135.1 (s). Anal. Calcd for C₉H₈BrN: C, 51.46; H, 3.84; N, 6.67. Found: C, 51.62; H, 3.78; N, 6.89.

5-Fluoro-1-methyl-1*H*-indole (73d) [31]

Conditions: room temperature for 5 h and then room temperature for 1 h. Workup: extraction. Yellow solid; yield 98%; mp: 55-56 °C. ¹H NMR (200 MHz, CDCl₃) δ: 3.72 (s, 3H, CH₃), 6.41 (d, 1H, *J* = 3.2 Hz, H-3), 6.89-7.05 (m, 2H, H-4 and H-6), 7.15-7.28 (m, 2H, H-2 and H-7); ¹³C NMR (50 MHz, CDCl₃) δ: 33.0 (q), 100.7 (d, *J*_{C3-F} = 4.9 Hz), 105.4 (d, *J*_{C7-F} = 5.6 Hz), 109.6 (d, *J*_{C4-F} = 23.3 Hz), 109.9 (d, *J*_{C6-F} = 10.8 Hz), 130.3 (d), 130.4 (2xs), 157.8 (d, *J*_{C5-F} = 233.0 Hz). Anal. Calcd for C₉H₈FN: C, 72.47; H, 5.41; N, 9.39. Found: C, 72.82; H, 5.21; N, 9.12.

Synthesis of 5-substituted *tert*-butyl 1*H*-indole-1-carboxylates (74a-d) [31]

Di-*tert*-butyl dicarbonate (8.73 g, 40 mmol) and triethylamine (3.3 mL, 23.7 mmol) were added to a solution of appropriate indoles **72a-d** (20 mmol) in tetrahydrofuran (10 mL). The reaction mixture was heated under reflux for 24-48 h. After cooling, the solvent was evaporated under reduced pressure, and the residue (derivatives **74a**, **74b**, **74d**) was purified by column chromatography using DCM or DCM/petroleum ether (9/1) as eluent or recrystallized from ethanol (derivative **74c**).

tert-Butyl 1*H*-indole-1-carboxylate (74a)

Conditions: 24 h at reflux. Column chromatography: DCM. Oil; yield: 93%; IR 1732 (CO) cm⁻¹; ¹H NMR (200 MHz, CDCl₃) δ: 1.66 (s, 9H, 3xCH₃), 6.55 (d, 1H, *J* = 3.7 Hz, H-3), 7.17-7.34 (m, 2H, H-5 and H-6), 7.53-7.59 (m, 2H, H-2 and H-7), 8.15 (d, 1H, *J* = 7.8 Hz, H-4); ¹³C NMR (50 MHz, CDCl₃) δ: 28.1 (3xq), 83.5 (s), 107.2 (d), 115.1 (d), 120.9 (d), 122.6 (d), 124.1 (d), 125.8 (d), 130.5 (s), 135.1 (s), 149.7 (s). Anal. Calcd for C₁₃H₁₅NO₂: C, 71.87; H, 6.96; N, 6.45. Found: C, 71.61; H, 7.32; N, 6.07.

tert-Butyl 5-methoxy-1*H*-indole-1-carboxylate (74b)

Conditions: 48 h at reflux. Column chromatography: DCM/petroleum ether (9/1). Brown solid; yield: 90%; mp: 76 °C; IR 1730 (CO) cm⁻¹; ¹H NMR (200 MHz, DMSO-*d*₆) δ: 1.66 (s, 9H, 3xCH₃), 3.79 (s, 3H, CH₃), 6.64 (d, 1H, *J* = 3.6 Hz, H-3), 6.93 (d, 1H, *J* = 9.0 Hz, H-6), 7.14 (s, 1H, H-4), 7.63 (d, 1H, *J* = 3.6 Hz, H-2) 7.93 (d, 1H, *J* = 9.0 Hz, H-7); ¹³C NMR (50 MHz, DMSO-*d*₆) δ: 27.6 (3xq), 55.2 (q), 83.5 (s), 103.5 (d), 107.4 (d), 112.9 (d), 115.3 (d), 126.5 (d), 129.1 (s), 131.0 (s), 149.0 (s), 155.4 (s). Anal. Calcd for C₁₄H₁₇NO₃: C, 68.00; H, 6.93; N, 5.66. Found: C, 67.64; H, 6.66; N, 5.87.

***tert*-Butyl 5-bromo-1*H*-indole-1-carboxylate (74c)**

Conditions: 24 h at reflux. Oil; yield: 100%; IR 1732 (CO) cm^{-1} ; ^1H NMR (200 MHz, DMSO-*d*6) δ : 1.63 (s, 9H, 3xCH₃), 6.70 (d, 1H, $J = 3.7$ Hz, H-3), 7.47 (dd, 1H, $J = 2.0, 8.8$ Hz, H-6), 7.72 (d, 1H, $J = 3.7$ Hz, H-2), 7.85 (d, 1H, $J = 2.0$ Hz, H-4), 8.00 (d, 1H, $J = 8.8$ Hz, H-7); ^{13}C NMR (50 MHz, DMSO-*d*6) δ : 27.6 (3xq), 84.2 (s), 106.7 (d), 115.2 (s), 116.4 (d), 123.5 (d), 126.7 (d), 127.5 (d), 132.1 (s), 133.3 (s), 148.7 (s). Anal.Calcd for C₁₃H₁₄BrNO₂: C, 52.72; H, 4.76; N, 4.73. Found: C, 53.03; H, 5.03; N, 5.08.

***tert*-Butyl 5-fluoro-1*H*-indole-1-carboxylate (74d)**

Conditions: 48 h at reflux. Oil; yield: 100%; IR 1738 (CO) cm^{-1} ; ^1H NMR (200 MHz, CDCl₃) δ : 1.65 (s, 9H, 3xCH₃), 6.49 (d, 1H, $J = 3.5$ Hz, H-3), 7.01 (td, 1H, $J = 2.7, 9.0, 11.5$ Hz, H-6), 7.18 (dd, 1H, $J = 2.4, 8.8$ Hz, H-4), 7.60 (d, 1H, $J = 3.5$ Hz, H-2), 8.08 (dd, 1H, $J = 4.5, 8.6$ Hz, H-7); ^{13}C NMR (50 MHz, CDCl₃) δ : 28.1 (qx3), 83.8 (s), 106.2 (d, $J_{\text{C4-F}} = 23.6$ Hz), 106.9 (d, $J_{\text{C3-F}} = 4.2$ Hz), 111.8 (d, $J_{\text{C6-F}} = 25.0$ Hz), 116.0 (d, $J_{\text{C7-F}} = 9.2$ Hz), 127.3 (d+s), 131.0 (s), 149.4 (s), 159.1 (s, $J_{\text{C5-F}} = 238.6$ Hz). Anal.Calcd for C₁₃H₁₄FNO₂: C, 66.37; H, 6.00; N, 5.95. Found: C, 66.14; H, 6.19; N, 5.71.

Synthesis of 5-substituted 5-fluoro-1*H*-indole-3-carboxamide, 1-methyl-1*H*-indole-3-carboxamides, 5-substituted-*tert*-butyl 3-carbamoyl-1*H*-indole-1-carboxylates (75d, 76a-d and 77a-c) [30, 31]

To a solution of the appropriate indoles **72d** (0.80 g, 5.9 mmol), **73a-d** or **74a-c** (16 mmol) in anhydrous acetonitrile (20 mL) were added dropwise at 0 °C CSI (0.8 mL, 9.1 mmol for compound **72d** or 1.4 mL, 16 mmol for compounds **73a-d** and **74a-c**). The reaction mixture was warmed to room temperature and stirred for 0.5-2 h (for compounds **73a-d** and **74a-c**) or at reflux for 15 min. (for compound **75d**). A solution of acetone (16 mL) and water (2 mL) was added and the solution was basified using 10% aqueous solution of KOH. The mixture was extracted with ethyl acetate, dried (Na₂SO₄) and the solvent evaporated under reduced pressure. The residue was purified by column chromatography using ethyl acetate (for compounds **75d** and **76a-d**) or DCM/ethyl acetate (1/1) (for compounds **77a-c**) as eluent.

5-Fluoro-1*H*-indole-3-carboxamide (75d)

Conditions: 15 min after CSI addition. at reflux. White solid; yield: 91%; mp: 93 °C. Analytical and spectroscopic data are previously reported [47].

1-Methyl-1*H*-indole-3-carboxamide (76a)

Conditions: 1 h at room temperature after CSI addition. White solid; yield: 50%; mp: 185-186 °C; IR 1603 (CO), 3178, 3392 (NH₂) cm⁻¹; ¹H NMR (200 MHz, DMSO-*d*₆) δ: 3.81 (s, 3H, CH₃), 6.92 (bs, 2H, NH₂), 7.10-7.25 (m, 2H, H-5, H-6), 7.47 (d, 1H, *J* = 7.9 Hz, H-7), 7.99 (s, 1H, H-2), 8.17 (d, 1H, *J* = 7.9 Hz, H-4); ¹³C NMR (50 MHz, DMSO-*d*₆) δ: 32.9 (q), 109.5 (s), 110.1 (d), 120.6 (d), 121.2 (d), 121.8 (d), 126.6 (s), 132.3 (d), 136.8 (s), 166.2 (s). Anal. Calcd for C₁₀H₁₀N₂O: C, 68.95; H, 5.79; N, 16.08. Found: C, 68.74; H, 6.05; N, 15.99.

5-Methoxy-1-methyl-1*H*-indole-3-carboxamide (76b)

Conditions: 1 h rt after CSI addition. White solid; yield: 55%; mp: 169-170°C; IR 1605 (CO), 3182, 3373 (NH₂) cm⁻¹; ¹H NMR (200 MHz, DMSO-*d*₆) δ: 3.77 (s, 3H, CH₃), 3.78 (s, 3H, CH₃), 6.84 (d, 1H, *J* = 8.9 Hz, H-6), 7.10 (bs, 2H, NH₂), 7.37 (d, 1H, *J* = 8.9 Hz, H-7), 7.67 (s, 1H, H-4), 7.94 (s, 1H, H-2); ¹³C NMR (50 MHz, DMSO-*d*₆) δ: 33.0 (q), 55.2 (q), 102.7 (d), 109.0 (s), 110.9 (d), 112.0 (d), 127.2 (s), 131.9 (s), 132.5 (d), 154.6 (s), 166.3 (s). Anal. Calcd for C₁₁H₁₂N₂O₂: C, 64.69; H, 5.92; N, 13.72. Found: C, 64.39; H, 5.72; N, 13.45.

5-Bromo-1-methyl-1*H*-indole-3-carboxamide (76c)

Conditions: 0.5 h at room temperature after CSI addition. White solid; yield: 60%; mp: 235°C; IR 1608 (CO), 3172, 3373 (NH₂); ¹H NMR (200 MHz, DMSO-*d*₆) δ: 3.83 (s, 3H, CH₃), 7.00 (bs, 2H, NH₂), 7.34 (d, 1H, *J* = 8.4 Hz, H-6), 7.49 (d, 1H, *J* = 8.4 Hz, H-7), 8.06 (s, 1H, H-4), 8.35 (s, 1H, H-2); ¹³C NMR (50 MHz, DMSO-*d*₆) δ: 33.2 (q), 109.1 (s), 112.4 (d), 113.6 (s), 123.4 (d), 124.4 (d), 128.3 (s), 133.5 (d), 135.5 (s), 165.7 (s). Anal. Calcd for C₁₀H₉BrN₂O: C, 47.46; H, 3.58; N, 11.07. Found: C, 47.17; H, 3.52; N, 11.34.

5-Fluoro-1-methyl-1*H*-indole-3-carboxamide (76d)

Conditions: 1 h rt after CSI addition. White solid; yield: 40%; mp: 174-175 °C; IR 1626 (CO), 3178, 3369 (NH₂); ¹H NMR (200 MHz, DMSO-*d*₆) δ: 3.82 (s, 3H, CH₃), 6.88 (bs, 2H, NH₂), 7.06 (td, 1H, *J* = 10.3, 8.9, 2.5 Hz, H-6), 7.51 (dd, 1H, *J* = 8.9, 4.6 Hz, H-7), 7.84 (dd, 1H, *J* = 10.3, 2.5 Hz, H-4) 8.05 (s, 1H, H-2); ¹³C NMR (50 MHz, DMSO-*d*₆) δ: 33.3 (q), 105.8 (d, *J*_{C4-F} = 24.5 Hz), 110.0 (d, *J*_{C6-F} = 26.5 Hz), 111.5 (d, *J*_{C7-F} = 10.0 Hz), 109.4 (s), 127.2 (s), 133.5 (s), 133.9 (d), 158.0 (d, *J*_{C5-F} = 234 Hz), 165.8 (s). Anal. Calcd for C₁₀H₉FN₂O: C, 62.49; H, 4.72; N, 14.58. Found: C, 62.20; H, 4.48; N, 14.32.

***tert*-Butyl 3-carbamoyl-1*H*-indole-1-carboxylate (77a)**

Conditions: 1 h at reflux after CSI addition. White solid; yield: 40%; mp: 163-164 °C. Analytical and spectroscopic data are previously reported [48].

***tert*-Butyl 3-carbamoyl-5-methoxy-1*H*-indole-1-carboxylate (77b)**

Conditions: 1 h after CSI addition. White solid; yield: 48%; mp: 168-169°C; IR 1660, 1728 (CO), 3215, 3343 (NH₂); ¹H NMR (200 MHz, DMSO-*d*₆) δ: 1.65 (s, 9H, 3xCH₃), 3.81 (s, 3H, CH₃), 6.98 (dd, 1H, *J* = 8.9, 2.0 Hz, H-6), 7.20 (s, 1H, NH), 7.77 (d, 1H, *J* = 2.0 Hz, H-4), 7.89 (s, 1H, NH), 7.96 (d, 1H, *J* = 8.9 Hz, H-7), 8.44 (s, 1H, H-2); ¹³C NMR (50 MHz, DMSO-*d*₆) δ: 27.6 (3xq), 55.2 (q), 84.5 (s), 104.1 (d), 113.7 (d), 114.7 (s), 115.3 (d), 128.8 (d), 128.9 (s), 129.3 (s), 148.8 (s), 155.9 (s), 165.2 (s). Anal. Calcd for C₁₅H₁₈N₂O₄: C, 62.06; H, 6.25; N, 9.65. Found: C, 62.35; H, 6.19; N, 9.99.

***tert*-Butyl 5-bromo-3-carbamoyl-1*H*-indole-1-carboxylate (77c)**

Conditions: 2 h after CSI addition. White solid; yield: 45%; mp: 170-171°C; IR 1662, 1720 (CO), 3233, 3352 (NH₂) cm⁻¹; ¹H NMR (200 MHz, DMSO-*d*₆) δ: 1.65 (s, 9H, 3xCH₃), 7.29 (s, 1H, NH), 7.52 (dd, 1H, *J* = 8.8, 1.9 Hz, H-6), 7.96 (s, 1H, NH), 8.02 (d, 1H, *J* = 8.8 Hz, H-7), 8.41 (d, 1H, *J* = 1.9 Hz, H-4), 8.53 (s, 1H, H-2); ¹³C NMR (50 MHz, DMSO-*d*₆) δ: 27.6 (3xq), 85.2 (s), 114.0 (s), 116.1 (s), 116.6 (d), 124.2 (d), 127.3 (d), 129.6 (d), 130.2 (s), 133.6 (s), 146.6 (s), 148.4 (s). Anal. Calcd for C₁₄H₁₅BrN₂O₃: C, 49.57; H, 4.46; N, 8.26. Found: C, 49.34; H, 4.41; N, 7.99.

Synthesis of 5-substituted-5-fluoro-1*H*-indole-3-carbothioamide, 1-methyl-1*H*-indole-3-carbothioamides and 5-substituted-*tert*butyl 3-carbamothioyl-1*H*-indole-1-carboxylates (78d, 79a-d and 80a-c). [31]

To a solution of appropriate derivatives **75d** (0.17 g, 0.95 mmol) or **76a-d** and **77a-c** (4 mmol) in anhydrous toluene (20 mL) Lawesson's reagent (0.38 g, 0.96 mmol for compound **75d** or 0.8 g, 2 mmol for compounds **76a-d** and **77a-c**) was added. The mixture was heated at reflux under nitrogen atmosphere for 0.5-24 h. After cooling the solvent was evaporated under reduced pressure and the residue was purified by column chromatography using ethyl acetate (for compound **78d**), DCM/ethyl acetate (98/2) (for compounds **79a-d**) or DCM (for compounds **80a-c**) as eluent.

5-Fluoro-1*H*-indole-3-carbothioamide (78d)

Conditions: 24 h at reflux. Orange solid; yield: 90%; mp: 175-176°C; IR 1626 (CS) cm⁻¹; ¹H NMR (200 MHz, DMSO-*d*₆) δ: 7.03 (td, 1H, *J* = 9.0, 8.7, 2.4 Hz, H-6), 7.60 (dd, 1H, *J* = 8.7, 4.9

Hz, H-7), 8.19 (d, 1H, $J = 2.8$ Hz, H-2), 8.47 (dd, 1H, $J = 9.0, 2.4$ Hz, H-4), 8.89 (s, 1H, SH), 9.00 (s, 1H, NH); ^{13}C NMR (50 MHz, DMSO- d_6) δ : 106.8 (d, $J_{\text{C4-F}} = 25.7$ Hz), 110.3 (d, $J_{\text{C6-F}} = 26.5$ Hz), 113.1 (d, $J_{\text{C7-F}} = 9.6$ Hz, H-7), 116.0 (d, $J_{\text{C7a-F}} = 4.6$ Hz), 126.8 (d, $J_{\text{C3a-F}} = 11.1$ Hz), 129.4 (d), 133.4 (s), 157.9 (d, $J_{\text{C5-F}} = 232.6$ Hz), 193.2 (s). Anal. Calcd for $\text{C}_9\text{H}_7\text{FN}_2\text{S}$: C, 55.65; H, 3.63; N, 14.42. Found: C, 55.90; H, 3.40; N, 14.13.

1-Methyl-1H-indole-3-carbothioamide (79a)

Conditions: 1 h at reflux. Orange solide; yield: 79%; mp: 126-127 °C. Analytical and spectroscopic data are previously reported [49].

5-Methoxy-1-methyl-1H-indole-3-carbothioamide (79b)

Conditions: 1 h at reflux. Orange solid; yield: 95%; mp: 176-177°C; IR 1626 (CO), 3354, 3273 (NH_2) cm^{-1} ; ^1H NMR (200 MHz, DMSO- d_6) δ : 3.79 (s, 6H, CH_3), 6.87 (dd, 1H, $J = 8.9, 1.8$ Hz, H-6), 7.39 (d, 1H, $J = 8.9$ Hz, H-7), 8.05 (s, 1H, H-2), 8.17 (d, 1H, $J = 1.8$ Hz, H-4), 8.72 (s, 1H, SH), 8.90 (s, 1H, NH); ^{13}C NMR (50 MHz, DMSO- d_6) δ : 33.2 (q), 55.3 (q), 103.9 (d), 111.2 (d), 111.8 (d), 114.9 (s), 126.7 (s), 132.4 (s), 132.8 (d), 155.0 (s), 192.9 (s). Anal. Calcd for $\text{C}_{11}\text{H}_{12}\text{N}_2\text{OS}$: C, 59.97; H, 5.49; N, 12.72. Found: 59.69; H, 5.28; N, 13.10.

5-Bromo-1-methyl-1H-indole-3-carbothioamide (79c)

Conditions: 1 h at reflux. Orange solid; yield: 93%; mp: 206-207 °C; IR 1628 (CO), 3276, 3157 (NH_2) cm^{-1} ; ^1H NMR (200 MHz, DMSO- d_6) δ : 3.83 (s, 3H, CH_3), 7.37 (dd, 1H, $J = 8.7, 1.8$ Hz, H-6), 7.50 (d, 1H, $J = 8.7$ Hz, H-7), 8.12 (s, 1H, H-2), 8.86 (d, 1H, $J = 1.8$ Hz, H-4), 8.90 (s, 1H, SH), 9.06 (s, 1H, NH); ^{13}C NMR (50 MHz, DMSO- d_6) δ : 33.3 (q), 112.6 (d), 114.2 (s), 114.6 (s), 124.1 (d), 124.7 (d), 128.0 (s), 133.0 (d), 136.1 (s), 192.5 (s). Anal. Calcd for $\text{C}_{10}\text{H}_9\text{BrN}_2\text{S}$: C, 44.62; H, 3.37; N, 10.41. Found: C, 44.87; H, 3.30; N, 10.34.

5-Fluoro-1-methyl-1H-indole-3-carbothioamide (79d)

Conditions: 0.5 h at reflux. Orange solid; yield: 93%; mp: 159-160°C; IR 1626 (CS), 3375, 3489 (NH_2) cm^{-1} ; ^1H NMR (200 MHz, DMSO- d_6) δ : 3.84 (s, 3H, CH_3), 7.11 (td, 1H, $J = 11.0, 9.0, 2.6$ Hz, H-6), 7.60 (dd, 1H, $J = 9.0, 4.6$ Hz, H-7), 8.16 (s, 1H, H-2), 8.43 (dd, 1H, $J = 11.0, 2.6$ Hz, H-4), 8.86 (s, 1H, SH), 9.04 (s, 1H, NH); ^{13}C NMR (50 MHz, DMSO- d_6) δ : 33.3 (q), 106.8 (d, $J_{\text{C4-F}} = 26.0$ Hz), 110.3 (d, $J_{\text{C6-F}} = 26.0$ Hz), 111.8 (d, $J_{\text{C7-F}} = 10.0$ Hz, H-7), 115.0 (d, $J_{\text{C7a-F}} = 4.8$ Hz), 126.8 (d, $J_{\text{C3a-F}} = 11.0$ Hz), 133.6 (d), 134.0 (s), 158.21 (d, $J_{\text{C5-F}} = 233.1$ Hz), 192.6 (s). Anal. Calcd for $\text{C}_{10}\text{H}_9\text{FN}_2\text{S}$: C, 57.67; H, 4.36; N, 13.45. Found: C, 57.29; H, 4.28; N, 13.22.

***tert*-Butyl 3-carbamothioyl-1*H*-indole-1-carboxylate (80a)**

Conditions: 1 h at reflux. Orange solid; yield: 40%; mp: 98-99 °C. Analytical and spectroscopic data are reported elsewhere. [48]

***tert*-Butyl 3-carbamothioyl-5-methoxy-1*H*-indole-1-carboxylate (80b)**

Conditions: 1 h at reflux. Orange solid; yield: 98%; mp: 153-154°C; IR 1597 (CO), 1738 (CS), 3415, 3365 (NH₂); ¹H NMR (200 MHz, DMSO-*d*₆) δ: 1.65 (s, 9H, 3xCH₃), 3.80 (s, 3H, CH₃), 7.00 (dd, 1H, *J* = 9.1, 2.6, Hz, H-6), 7.99 (d, 1H, *J* = 9.1 Hz, H-7), 8.21 (d, 1H, *J* = 2.6 Hz, H-4), 8.32 (s, 1H, H-2), 9.34 (s, 1H, SH), 9.52 (s, 1H, NH); ¹³C NMR (50 MHz, DMSO-*d*₆) δ: 27.6 (3xq), 55.3 (q), 84.8 (s), 105.1 (d), 113.5 (d), 115.3 (d), 119.8 (s), 126.8 (d), 128.8 (s), 129.6 (s), 148.7 (s), 155.7 (s), 192.8 (s). Anal. Calcd for C₁₅H₁₈N₂O₃S: C, 58.80; H, 5.92; N, 9.14. Found: C, 58.51; H, 5.86; N, 9.44.

***tert*-Butyl 5-bromo-3-carbamothioyl-1*H*-indole-1-carboxylate (80c)**

Conditions: 1 h at reflux. Orange solid; yield: 96%; mp: 150-151°C; IR 1633 (CO), 1720 (CS), 3380, 3284 (NH₂) cm⁻¹; ¹H NMR (200 MHz, DMSO-*d*₆) δ: 1.66 (s, 9H, 3xCH₃), 7.54 (dd, 1H, *J* = 8.8, 2.0 Hz, H-6), 8.05 (d, 1H, *J* = 8.8 Hz, H-7), 8.42 (s, 1H, H-2), 8.90 (d, 1H, *J* = 2.0 Hz, H-4), 9.44 (s, 1H, SH), 9.60 (s, 1H, NH); ¹³C NMR (50 MHz, DMSO-*d*₆) δ: 27.5 (3xq), 85.4 (s), 116.1 (s), 116.5 (d), 118.9 (s), 124.9 (d), 127.3 (d), 127.4 (d), 129.8 (s), 134.0 (s), 148.4 (s), 192.1 (s). Anal. Calcd for C₁₄H₁₅BrN₂O₂S: C, 47.33; H, 4.26; N, 7.89. Found: C, 47.12; H, 4.24; N, 8.27.

Synthesis of 7-chloro-1*H*-pyrrolo[2,3-*c*]pyridine (83)

Chloro-3-nitropyridine 4 (0.3 g, 1.89 mmol) was dissolved in 13 mL of dry THF under nitrogen atmosphere and cooled to -78 °C. After dropwise addition of vinylmagnesium bromide solution (1 M, 6.1 mL) the mixture was stirred for 7 h, quenched with 20% NH₄Cl solution, extracted with ethyl acetate, dried over Na₂SO₄ and concentrated in vacuo. Crude product was purified by column chromatography using DCM/ethyl acetate (98/2) as eluent. Brown solid; yield: 33%; mp: 188-190 °C. Analytical and spectroscopic data are reported elsewhere [37].

Synthesis of 7-chloro-1-methyl-1*H*-pyrrolo[2,3-*c*]pyridine (84)

To a cold solution of 6-azaindole **83** (0.12 g, 0.8 mmol) in anhydrous toluene (4 mL), potassium *t*-butoxide (0.12 g, 1.1 mmol) and TDA-1 (1 or 2 drops) were added at 0 °C. The reaction mixture was stirred at room temperature for 5 h and then methyl iodide (0.8 mmol, 0.05 mL) was added at 0 °C. TLC analysis (DCM/ethyl acetate 9/1) revealed that methylation was complete after 2 h. The

solvent was evaporated under reduced pressure. The residue was treated with water, extracted with DCM, dried (Na_2SO_4), evaporated and purified by column chromatography using DCM/ethyl acetate (95/5) as eluent. White solid; yield: 70%; mp: 60-61 °C; ^1H NMR (200 MHz, CDCl_3) δ : 4.16 (s, 3H, CH_3), 6.49 (d, 1H, $J = 3.1$ Hz, H-3), 7.16 (d, 1H, $J = 3.1$ Hz, H-2), 7.41 (d, 1H, $J = 5.4$ Hz, H-4), 7.95 (d, 1H, $J = 5.4$ Hz, H-5); ^{13}C NMR (50 MHz, CDCl_3) δ : 36.7 (q), 101.0 (d), 115.2 (d), 129.2 (s), 134.1 (s), 134.7 (d), 136.5 (s), 137.5 (d). Anal. Calcd for: $\text{C}_8\text{H}_7\text{ClN}_2$: C, 57.67; H, 4.23; N, 16.81. Found: C, 57.90; H, 3.97; N, 16.63.

Synthesis of 1-(7-chloro-1H-pyrrolo[2,3-c]pyridin-3-yl)ethanones (85,86)

To a solution of appropriate 6-azaindoles **83**, **84** (2.5 mmol) in 10 mL of anhydrous DCM, anhydrous aluminium chloride (1.2 g, 8.8 mmol) was slowly added. The reaction mixture was heated under reflux and bromoacetyl bromide (2.5 mmol, 0.2 mL) in 2 mL of anhydrous DCM was added drop wise. The resulting solution was allowed to stir under reflux for 40 min. After cooling, water and ice were slowly added and the obtained precipitate (for derivative **85**) was filtered off or the oil residue (for derivative **86**) was extracted with DCM and purified by column chromatography using DCM/ethyl acetate (9/1) as eluent.

2-Bromo-1-(7-chloro-1H-pyrrolo[2,3-c]pyridin-3-yl)ethanone (85)

White solid; yield: 88%; mp: 324-325 °C; 1676 (CO), 3557 (NH) cm^{-1} ; ^1H NMR (200 MHz, $\text{DMSO}-d_6$) δ : 4.76 (s, 2H, CH_2), 8.05 (d, 1H, $J = 5.2$ Hz, H-4), 8.15 (d, 1H, $J = 5.2$ Hz, H-5), 8.74 (d, 1H, $J = 3.0$ Hz, H-2), 13.03 (bs, 1H, NH); ^{13}C NMR (50 MHz, $\text{DMSO}-d_6$) δ : 33.8 (t), 114.2 (s), 115.6 (d), 130.2 (s), 132.7 (s), 134.3 (s), 138.5 (d), 140.6 (d), 186.6 (s). Anal. Calcd for: $\text{C}_9\text{H}_6\text{BrClN}_2\text{O}$: C, 39.52; H, 2.21; N, 10.24. Found: C, 39.28; H, 2.36; N, 10.13.

2-Bromo-1-(7-chloro-1-methyl-1H-pyrrolo[2,3-c]pyridin-3-yl)ethanone (86)

White solid; yield: 98%; mp: 249-250 °C; IR 1647 (CO) cm^{-1} ; ^1H NMR (200 MHz, $\text{DMSO}-d_6$) δ : 4.18 (s, 3H, CH_3), 4.90 (s, 2H, CH_2), 8.07 (d, 1H, $J = 5.3$ Hz, H-4), 8.12 (d, 1H, $J = 5.3$ Hz, H-5), 8.72 (s, 1H, H-2); ^{13}C NMR (50 MHz, $\text{DMSO}-d_6$) δ : 33.3 (t), 37.4 (q), 111.8 (s), 115.7 (d), 129.6 (s), 133.9 (s), 134.3 (s), 140.7 (d), 143.2 (d), 185.9 (s). Anal. Calcd for: $\text{C}_{10}\text{H}_8\text{BrClN}_2\text{O}$: C, 41.77; H, 2.80; N, 9.74. Found: C, 41.51; H, 3.07; N, 9.56.

Synthesis of indolyl-thiazolyl-pyrrolo[2,3-*c*]pyridines (49a-j), (50a-f)

A suspension of the appropriate indole-3-carbothioamides **78d**, **79a-d**, **80a-c** (5 mmol) and proper 3-bromoacetyl-pyrrolo[2,3-*c*] pyridines **85,86** (5 mmol) in anhydrous ethanol (20 mL) was heated under reflux for 1-3 h. The precipitate, obtained after cooling, was filtered off, dried and crystallized with ethanol to afford derivatives **49a-j** and **50a-f**.

7-Chloro-3-[2-(1-methyl-1*H*-indol-3-yl)-1,3-thiazol-4-yl]-1*H*-pyrrolo[2,3-*c*]pyridine (49a)

Conditions: reflux for 1 h. Yellow solid; yield: 98%; mp: 326-327 °C; IR 3393 (NH) cm⁻¹; ¹H NMR (200 MHz, DMSO-*d*₆) δ: 3.93 (s, 3H, CH₃), 7.29-7.35 (m, 2H, H-5', H-6'), 7.56-7.61 (m, 1H, H-7'), 7.85 (s, 1H, H-2'), 8.12 (d, 1H, *J* = 5.6 Hz, H-4''), 8.26 (s, 1H, H-5), 8.28-8.31 (m, 1H, H-4'), 8.33 (d, 1H, *J* = 5.6 Hz, H-5''), 8.40 (d, 1H, *J* = 2.7 Hz, H-2''), 12.62 (bs, 1H, NH); ¹³C NMR (50 MHz, DMSO-*d*₆) δ: 32.9 (q), 108.3 (d), 109.2 (s), 110.7 (d), 112.4 (s), 115.3 (d), 120.2 (d), 121.1 (d), 122.5 (d), 124.5 (s), 129.8 (s), 130.5 (d), 130.8 (d), 131.8 (s), 133.4 (s), 136.7 (d), 137.0 (s), 148.1 (s), 162.2 (s). Anal. Calcd for: C₁₉H₁₃ClN₄S: C, 62.55; H, 3.59; N, 15.36. Found: C, 62.28; H, 3.34; N, 15.53.

7-Chloro-3-[2-(5-methoxy-1-methyl-1*H*-indol-3-yl)-1,3-thiazol-4-yl]-1*H*-pyrrolo[2,3-*c*]pyridine (49b)

Conditions: reflux for 1 h. Yellow solid; yield: 65%; mp: 216-217 °C; IR 3396 (NH) cm⁻¹; ¹H NMR (200 MHz, DMSO-*d*₆) δ: 3.87 (s, 3H, CH₃), 3.91 (s, 3H, OCH₃), 6.95 (dd, 1H, *J* = 2.4, 8.9 Hz, H-6'), 7.49 (d, 1H, *J* = 8.9 Hz, H-7'), 7.79 (s, 1H, H-2'), 7.90 (d, 1H, *J* = 2.4 Hz, H-4'), 8.05 (d, 1H, *J* = 5.5 Hz, H-4''), 8.17 (s, 1H, H-5), 8.32 (d, 1H, *J* = 2.7 Hz, H-2''), 8.37 (d, 1H, *J* = 5.5 Hz, H-5''), 12.46 (bs, 1H, NH); ¹³C NMR (50 MHz, DMSO-*d*₆) δ: 33.0 (q), 55.1 (q), 96.3 (s), 101.8 (d), 107.7 (d), 108.6 (s), 110.1 (s), 111.6 (d), 112.6 (d), 115.4 (d), 124.8 (s), 129.9 (d), 131.0 (d), 132.1 (s), 132.8 (s), 134.2 (s), 136.8 (d), 146.6 (s), 155.1 (s), 162.8 (s). Anal. Calcd for: C₂₀H₁₅ClN₄OS: C, 60.83; H, 3.83; N, 14.19. Found: C, 60.62; H, 3.99; N, 13.99.

3-[2-(5-Bromo-1-methyl-1*H*-indol-3-yl)-1,3-thiazol-4-yl]-7-chloro-1*H*-pyrrolo[2,3-*c*]pyridine (49c)

Conditions: reflux for 1 h. Yellow solid; yield: 93%; mp: 374-375 °C; IR 3410 (NH) cm⁻¹; ¹H NMR (200 MHz, DMSO-*d*₆) δ: 3.89 (s, 3H, CH₃), 7.42 (dd, 1H, *J* = 1.8, 8.7 Hz, H-6'), 7.57 (d, 1H, *J* = 8.7 Hz, H-7'), 7.84 (s, 1H, H-2'), 8.09 (d, 1H, *J* = 5.6 Hz, H-4''), 8.28 (s, 1H, H-5), 8.30 (d, 1H, *J* = 5.6 Hz, H-5''), 8.34 (d, 1H, *J* = 2.8 Hz, H-2''), 8.49 (d, 1H, *J* = 1.8 Hz, H-4'), 12.56 (bs, 1H, NH); ¹³C NMR (50 MHz, DMSO-*d*₆) δ: 33.1 (q), 108.4 (d), 108.9 (s), 112.5 (s), 112.8 (d), 113.8 (s), 115.2 (d), 122.7 (d), 124.9 (d), 126.1 (s), 129.8 (s), 130.1 (d), 131.7 (s), 131.9 (d), 133.5 (s), 135.8

(s), 136.7 (d), 148.5 (s), 161.5 (s). Anal. Calcd for: C₁₉H₁₂BrClN₄S: C, 51.43; H, 2.73; N, 12.63. Found: C, 51.17; H, 2.62; N, 12.88.

7-Chloro-3-[2-(5-fluoro-1-methyl-1*H*-indol-3-yl)-1,3-thiazol-4-yl]-1*H*-pyrrolo[2,3-*c*]pyridine (49d)

Conditions: reflux for 1 h. Yellow solid; yield: 97%; mp: 337-338 °C; IR 3509 (NH) cm⁻¹; ¹H NMR (200 MHz, DMSO-*d*₆) δ: 3.91 (s, 3H, CH₃), 7.18 (td, 1H, *J* = 2.5, 9.2, 11.7 Hz, H-6'), 7.61 (dd, 1H, *J* = 4.5, 9.2 Hz, H-7'), 7.82 (s, 1H, H-2'), 8.02 (dd, 1H, *J* = 2.5, 11.7 Hz, H-4'), 8.09 (d, 1H, *J* = 5.6 Hz, H-4''), 8.25 (d, 1H, *J* = 5.6 Hz, H-5''), 8.30 (s, 1H, H-5), 8.34 (d, 1H, *J* = 2.8 Hz, H-2''), 12.50 (bs, 1H, NH). Anal. Calcd for: C₁₉H₁₂ClFN₄S: C, 59.61; H, 3.16; N, 14.63. Found: C, 59.34; H, 3.21; N, 14.47.

7-Chloro-1-methyl-3-[2-(1-methyl-1*H*-indol-3-yl)-1,3-thiazol-4-yl]-1*H*-pyrrolo[2,3-*c*]pyridine (49e)

Conditions: reflux for 1 h. Yellow solid; yield: 96%; mp: 265-266 °C; ¹H NMR (200 MHz, DMSO-*d*₆) δ: 3.91 (s, 3H, CH₃), 4.24 (s, 3H, CH₃), 7.27 (m, 2H, H-5', H-6'), 7.57-7.61 (m, 1H, H-7'), 7.75 (s, 1H, H-2'), 8.06 (d, 1H, *J* = 5.5 Hz, H-4''), 8.22 (s, 1H, H-2''), 8.25 (d, 1H, *J* = 5.5 Hz, H-5''), 8.33 (s, 1H, H-5), 8.35-8.38 (m, 1H, H-4'). Anal. Calcd for: C₂₀H₁₅ClN₄S: C, 63.40; H, 3.99; N, 14.79. Found: C, 63.14; H, 3.75; N, 14.59.

7-Chloro-3-[2-(5-methoxy-1-methyl-1*H*-indol-3-yl)-1,3-thiazol-4-yl]-1-methyl-1*H*-pyrrolo[2,3-*c*]pyridine (49f)

Conditions: reflux for 1 h. Yellow solid; yield: 79%; mp: 232-233 °C; ¹H NMR (200 MHz, DMSO-*d*₆) δ: 3.87 (s, 3H, CH₃), 3.90 (s, 3H, OCH₃), 4.22 (s, 3H, CH₃), 6.94 (d, 1H, *J* = 8.8 Hz, H-6'), 7.48 (d, 1H, *J* = 8.8 Hz, H-7'), 7.69 (s, 1H, H-2'), 7.87 (m, 1H, H-4'), 8.02 (d, 1H, *J* = 5.4 Hz, H-4''), 8.15 (s, 1H, H-2''), 8.28 (s, 1H, H-5), 8.35 (d, 1H, *J* = 5.4 Hz, H-5''). Anal. Calcd for: C₂₁H₁₇ClN₄OS: C, 61.68; H, 4.19; N, 13.70. Found: C, 61.42; H, 4.08; N, 13.47.

3-[2-(5-Bromo-1-methyl-1*H*-indol-3-yl)-1,3-thiazol-4-yl]-7-chloro-1-methyl-1*H*-pyrrolo[2,3-*c*]pyridine (49g)

Conditions: reflux for 2 h. Yellow solid; yield: 98%; mp: 249-250 °C; ¹H NMR (200 MHz, DMSO-*d*₆) δ: 3.90 (s, 3H, CH₃), 4.23 (s, 3H, CH₃), 7.44 (dd, 1H, *J* = 1.9, 8.7 Hz, H-6'), 7.58 (d, 1H, *J* = 8.7 Hz, H-7'), 7.74 (s, 1H, H-2'), 8.04 (d, 1H, *J* = 5.5 Hz, H-4''), 8.24-8.28 (m, 3H, H-2'', H-5, H-5''), 8.48 (d, 1H, *J* = 1.9 Hz, H-4'); ¹³C NMR (50 MHz, DMSO-*d*₆) δ: 33.1 (q), 36.0 (q), 108.4 (d), 109.0 (s), 110.4 (s), 112.8 (d), 113.8 (s), 115.3 (d), 122.8 (d), 124.9 (d), 126.0 (s), 128.8 (s), 131.9 (d), 133.0 (s), 133.3 (s), 135.3 (d), 135.8 (s), 137.0 (d), 148.1 (s), 161.5 (s). Anal. Calcd for:

C₂₀H₁₄BrClN₄S: C, 52.47; H, 3.08; N, 12.24. Found: C, 52.23; H, 2.94; N, 12.11.

7-Chloro-3-[2-(5-fluoro-1-methyl-1*H*-indol-3-yl)-1,3-thiazol-4-yl]-1-methyl-1*H*-pyrrolo[2,3-*c*]pyridine (49h)

Conditions: reflux for 1 h. Yellow solid; yield: 95%; mp: 284-285 °C; ¹H NMR (200 MHz, DMSO-*d*₆) δ: 3.91 (s, 3H, CH₃), 4.24 (s, 3H, CH₃), 7.18 (td, 1H, *J* = 2.5, 9.3, 11.7 Hz, H-6'), 7.61 (dd, 1H, *J* = 4.4, 9.3 Hz, H-7'), 7.75 (s, 1H, H-2'), 8.02-8.07 (m, 2H, H-4', H-4''), 8.22 (d, 1H, *J* = 5.6 Hz, H-5''), 8.28 (s, 1H, H-2''), 8.35 (s, 1H, H-5). Anal. Calcd for: C₂₀H₁₄ClFN₄S: C, 60.53; H, 3.56; N, 14.12. Found: C, 60.29; H, 3.30; N, 14.27.

7-Chloro-3-[2-(5-fluoro-1*H*-indol-3-yl)-1,3-thiazol-4-yl]-1-methyl-1*H*-pyrrolo[2,3-*c*]pyridine (49i)

Conditions: reflux for 3 h. Yellow solid; yield: 82%; mp: 284 -285 °C; IR 3399 (NH) cm⁻¹; ¹H NMR (200 MHz, DMSO-*d*₆) δ: 4.25 (s, 3H, CH₃), 7.11 (td, 1H, *J* = 2.5, 9.2, 11.7 Hz, H-6'), 7.53 (dd, 1H, *J* = 4.6, 9.2 Hz, H-7'), 7.75 (s, 1H, H-2''), 8.02 (d, 1H, *J* = 2.5 Hz, H-4'), 8.06 (d, 1H, *J* = 5.5 Hz, H-4''), 8.22 (d, 1H, *J* = 5.5 Hz, H-5''), 8.25 (d, 1H, *J* = 2.9 Hz, H-2'), 8.35 (s, 1H, H-5), 11.93 (bs, 1H, NH); ¹³C NMR (50 MHz, DMSO-*d*₆) δ: 36.6 (q), 105.2 (d, *J*_{C4'-F} = 24.3 Hz), 108.2 (d), 110.5 (s), 110.7 (d, *J*_{C6'-F} = 26.0 Hz), 113.4 (d, *J*_{C7'-F} = 9.6 Hz), 115.1 (s), 115.2 (d), 124.5 (s, *J*_{C3a-F} = 10.8 Hz), 128.7 (d), 128.9 (s), 132.9 (s), 133.2 (s), 133.4 (s), 135.8 (d), 137.0 (d), 137.5 (s), 148.1 (s), 159.7 (s, *J*_{C5'-F} = 254 Hz). Anal. Calcd for: C₁₉H₁₂ClFN₄S: C, 59.61; H, 3.16; N, 14.63. Found: C, 59.37; H, 2.90; N, 14.83.

7-Chloro-3-[2-(5-fluoro-1*H*-indol-3-yl)-1,3-thiazol-4-yl]-1*H*-pyrrolo[2,3-*c*]pyridine (49j)

Conditions: reflux for 2 h. Yellow solid; yield 66%; mp: 281-282 °C; IR 3418, 3557 (NH) cm⁻¹; ¹H NMR (200 MHz, DMSO-*d*₆) δ: 7.12 (td, 1H, *J* = 2.5, 9.2, 11.7 Hz, H-6'), 7.53 (dd, 1H, *J* = 4.6, 9.2 Hz, H-7'), 7.83 (s, 1H, H-2'), 8.00 (dd, 1H, *J* = 2.5, 11.7 Hz, H-4'), 8.08 (d, 1H, *J* = 5.6 Hz, H-4''), 8.24-8.29 (m, 2H, H-5, H5''), 8.32 (d, 1H, *J* = 2.8 Hz, H-2''), 11.95 (bs, 1H, NH), 12.45 (bs, 1H, NH). Anal. Calcd for: C₁₈H₁₀ClFN₄S: C, 58.62; H, 2.73; N, 15.19. Found: C, 58.51; H, 2.47; N, 14.94.

***tert*-Butyl 3-[4-(7-chloro-1*H*-pyrrolo[2,3-*c*]pyridin-3-yl)-1,3-thiazol-2-yl]-1*H*-indole-1-carboxylate (50a)**

Conditions: reflux for 2 h. Yellow solid; yield: 84%, mp: 225-226 °C; IR 3417 (NH), 1736 (CO) cm⁻¹; ¹H NMR (200 MHz, DMSO-*d*₆) δ: 1.69 (s, 9H, 3xCH₃), 7.44-7.53 (m, 2H, H-5', H-6'), 8.02 (s, 1H, H-2'), 8.09 (d, 1H, *J* = 5.5 Hz, H-4''), 8.16-8.21 (m, 1H, H-7'), 8.23 (d, 1H, *J* = 5.5 Hz, H-5''), 8.35-8.36 (m, 2H, H-2'', H-5), 8.47-8.51 (m, 1H, H-4'), 12.48 (bs, 1H, NH); ¹³C NMR (50

MHz, DMSO-*d*₆) δ: 27.6 (3xq), 84.9 (s), 110.4 (d), 112.2 (s), 114.9 (s), 115.0 (d), 121.3 (d), 123.8 (d), 123.9 (d), 125.4 (d), 125.6 (d), 126.6 (s), 129.8 (s), 129.9 (d), 131.4 (s), 133.8 (s), 135.0 (s), 137.5 (d), 148.6 (s), 149.3 (s), 159.9 (s). Anal. Calcd for: C₂₃H₁₉ClN₄O₂S: C, 61.26; H, 4.25; N, 12.42. Found: C, 61.02; H, 4.06; N, 12.13.

***tert*-Butyl 3-[4-(7-chloro-1*H*-pyrrolo[2,3-*c*]pyridin-3-yl)-1,3-thiazol-2-yl]-5-methoxy-1*H*-indole-1-carboxylate (50b)**

Conditions: reflux for 1 h. Yellow solid; yield: 77%; mp: 312-313 °C; IR 3418 (NH), 1650 (CO) cm⁻¹; ¹H NMR (200 MHz, DMSO-*d*₆) δ: 1.68 (s, 9H, 3xCH₃), 3.92 (s, 3H, OCH₃), 7.09 (dd, 1H, *J* = 2.4, 9.1 Hz, H-6'), 7.99-8.07 (m, 4H, ArH), 8.30-8.35 (m, 3H, ArH), 12.47 (bs, 1H, NH); ¹³C NMR (50 MHz, DMSO-*d*₆) δ: 27.6 (3xq), 55.1 (q), 84.7 (s), 103.2 (d), 110.2 (d), 112.2 (s), 114.5 (d), 114.8 (s), 115.2 (d), 115.8 (d), 125.9 (d), 127.5 (s), 129.5 (s), 130.0 (d), 131.6 (s), 133.7 (s), 136.9 (d), 137.2 (s), 148.5 (s), 149.2 (s), 156.1 (s), 160.2 (s). Anal. Calcd for: C₂₄H₂₁ClN₄O₃S: C, 59.93; H, 4.40; N, 11.65. Found: C, 59.66; H, 4.61; N, 11.50.

***tert*-Butyl 5-bromo-3-[4-(7-chloro-1*H*-pyrrolo[2,3-*c*]pyridin-3-yl)-1,3-thiazol-2-yl]-1*H*-indole-1-carboxylate (50c)**

Conditions: reflux for 3 h. Yellow solid; yield 77%, mp: 241-242 °C; IR 3559 (NH), 1748 (CO) cm⁻¹; ¹H NMR (200 MHz, DMSO-*d*₆) δ: 1.67 (s, 9H, 3xCH₃), 7.60 (d, 1H, *J* = 8.6 Hz, H-6'), 7.98 (s, 1H, H-2'), 8.04-8.07 (m, 2H, H-2'', H-7'), 8.19 (d, 1H, *J* = 5.3 Hz, H-4''), 8.29-8.33 (m, 2H, H-4', H-5''), 8.65 (s, 1H, H-5), 12.45 (bs, 1H, NH); ¹³C NMR (50 MHz, DMSO-*d*₆) δ: 27.6 (3xq), 85.3 (s), 110.5 (d), 112.0 (s), 114.1 (s), 114.9 (d), 116.8 (d), 123.8 (d), 126.8 (d), 127.9 (d), 128.4 (s), 129.5 (d), 129.8 (s), 129.9 (s), 131.4 (s), 133.8 (s), 134.0 (s), 137.4 (d), 148.3 (s), 149.3 (s), 159.4 (s). Anal. Calcd for: C₂₃H₁₈BrClN₄O₂S: C, 52.14; H, 3.42; N, 10.57. Found: C, 52.03; H, 3.55; N, 10.32.

***tert*-Butyl 3-[4-(7-chloro-1-methyl-1*H*-pyrrolo[2,3-*c*]pyridin-3-yl)-1,3-thiazol-2-yl]-1*H*-indole-1-carboxylate (50d)**

Conditions: reflux for 2 h. Yellow solid; yield: 91%; mp: 279-280 °C; IR 1736 (CO) cm⁻¹; ¹H NMR (200 MHz, DMSO-*d*₆) δ: 1.69 (s, 9H, 3xCH₃), 4.24 (s, 3H, CH₃), 7.44-7.54 (m, 2H, H-5', H-6'), 7.96 (s, 1H, H-2'), 8.07 (d, 1H, *J* = 5.5 Hz, H-4''), 8.16-8.20 (m, 1H, H-7'), 8.20 (d, 1H, *J* = 5.5 Hz, H-5''), 8.34 (s, 1H, H-2''), 8.37 (s, 1H, H-5), 8.48-8.52 (m, 1H, H-4'); ¹³C NMR (50 MHz, DMSO-*d*₆) δ: 27.6 (3xq), 36.6 (q), 84.9 (s), 110.2 (s), 110.4 (d), 114.9 (s), 115.0 (d), 115.1 (d), 121.4 (d), 123.8 (d), 125.5 (d), 125.6 (d), 126.6 (s), 128.9 (s), 132.8 (s), 133.3 (s), 135.0 (s), 135.7 (d), 137.4 (d), 148.6 (s), 149.6 (s), 159.9 (s). Anal. Calcd for: C₂₄H₂₁ClN₄O₂S: C, 62.00; H, 4.55; N,

12.05. Found: C, 61.73; H, 4.41; N, 11.94.

***tert*-Butyl 3-[4-(7-chloro-1-methyl-1*H*-pyrrolo[2,3-*c*]pyridin-3-yl)-1,3-thiazol-2-yl]-5-methoxy-1*H*-indole-1-carboxylate (50e)**

Conditions: reflux for 1 h. Yellow solid; yield: 92%; mp: 212-213 °C; IR 1723 (CO) cm⁻¹; ¹H NMR (200 MHz, DMSO-*d*₆) δ: 1.68 (s, 9H, 3xCH₃), 3.91 (s, 3H, OCH₃), 4.21 (s, 3H, CH₃), 7.08 (d, 1H, *J* = 9.0 Hz, H-6'), 7.89-8.06 (m, 4H, ArH), 8.27-8.29 (m, 3H, ArH). Anal. Calcd for: C₂₅H₂₃ClN₄O₃S: C, 60.66; H, 4.68; N, 11.32. Found: C, 60.45; H, 4.89; N, 11.56.

***tert*-Butyl 5-bromo-3-[4-(7-chloro-1-methyl-1*H*-pyrrolo[2,3-*c*]pyridin-3-yl)-1,3-thiazol-2-yl]-1*H*-indole-1-carboxylate (50f)**

Conditions: reflux for 3 h. Yellow solid; yield: 91%; mp: 257-258 °C; IR 1727 (CO) cm⁻¹; ¹H NMR (200 MHz, DMSO-*d*₆) δ: 1.69 (s, 9H, 3xCH₃), 4.22 (s, 3H, CH₃), 7.63 (dd, 1H, *J* = 1.9, 8.9 Hz, H-6'), 7.91 (s, 1H, H-2'), 8.03 (d, 1H, *J* = 5.5 Hz, H-4''), 8.09 (d, 1H, *J* = 8.9 Hz, H-7'), 8.18 (d, 1H, *J* = 5.5 Hz, H-5''), 8.27 (s, 1H, H-2''), 8.35 (s, 1H, H-5), 8.61 (d, 1H, *J* = 1.9 Hz, H-4'). Anal. Calcd for: C₂₄H₂₀BrClN₄O₂S: C, 53.00; H, 3.71; N, 10.30. Found: C, 53.27; H, 3.97; N, 10.16.

Synthesis of indolyl-thiazolyl-pyrrolo[2,3-*c*]pyridines (51a-f)

To a suspension of appropriate derivatives **50a-f** (0.78 mmol) in DCM (10 mL) trifluoroacetic acid (1.1 mL) was added. The reaction was heated at reflux for 24 h. The mixture was neutralized with saturated aqueous sodium hydrogen carbonate solution. The solvent was dried (Na₂SO₄), evaporated under reduced pressure and the residue recrystallized with ethanol to afford derivatives **51a-f**.

7-Chloro-3-[2-(1*H*-indol-3-yl)-1,3-thiazol-4-yl]-1*H*-pyrrolo[2,3-*c*]pyridine (51a)

Green solid; yield: 93%; mp: 271-272 °C; IR 3556, 3394 (NH) cm⁻¹; ¹H NMR (200 MHz, DMSO-*d*₆) δ: 7.21-7.31 (m, 2H, H-5', H-6'), 7.48-7.55 (m, 1H, H-7'), 7.81 (s, 1H, H-2'), 8.08 (d, 1H, *J* = 5.5 Hz, H-4''), 8.20 (d, 1H, *J* = 2.8 Hz, H-2''), 8.27-8.35 (m, 3H, H-5, H-4', H-5''), 11.82 (bs, 1H, NH), 12.41 (bs, 1H, NH); ¹³C NMR (50 MHz, DMSO-*d*₆) δ: 108.0 (d), 110.4 (s), 112.2 (d), 112.5 (s), 115.3 (d), 120.2 (d), 120.8 (d), 122.4 (d), 124.2 (s), 126.8 (d), 129.4 (d), 129.8 (s), 131.4 (s), 133.9 (s), 136.6 (s), 137.5 (d), 148.6 (s), 162.5 (s). Anal. Calcd for: C₁₈H₁₁ClN₄S: C, 61.62; H, 3.16; N, 15.97. Found: C, 61.47; H, 3.40; N, 15.82.

7-Chloro-3-[2-(5-methoxy-1H-indol-3-yl)-1,3-thiazol-4-yl]-1H-pyrrolo[2,3-c]pyridine (51b)

Yellow solid; yield: 62%; mp: 223-224 °C; IR 3555, 3379 (NH) cm^{-1} ; ^1H NMR (200 MHz, DMSO- d_6) δ : 3.90 (s, 3H, OCH₃), 6.89 (dd, 1H, $J = 2.5, 8.8$ Hz, H-6'), 7.42 (d, 1H, $J = 8.8$ Hz, H-7'), 7.80 (s, 1H, H-5), 7.89 (d, 1H, $J = 2.5$ Hz, H-4'), 8.07 (d, 1H, $J = 5.6$ Hz, H-4''), 8.15 (d, $J = 2.9$ Hz, H-2'), 8.35 (d, 1H, $J = 2.8$ Hz, H-2''), 8.39 (d, 1H, $J = 5.6$ Hz, H-5''), 11.72 (bs, 1H, NH), 12.51 (bs, 1H, NH); ^{13}C NMR (50 MHz, DMSO- d_6) δ : 55.1 (q), 101.6 (d), 107.7 (d), 110.1 (s), 112.4 (s), 112.7 (d), 113.0 (d), 115.4 (d), 124.7 (s), 127.2 (d), 129.6 (d), 129.8 (s), 131.5 (s), 131.7 (s), 133.7 (s), 137.0 (d), 148.3 (s), 154.7 (s), 162.9 (s). Anal. Calcd for: C₁₉H₁₃ClN₄OS: C, 59.92; H, 3.44; N, 14.71. Found: C, 59.68; H, 3.33; N, 14.56.

3-[2-(5-Bromo-1H-indol-3-yl)-1,3-thiazol-4-yl]-7-chloro-1H-pyrrolo[2,3-c]pyridine (51c)

Yellow solid; yield: 98%; mp: 265-266 °C; IR 3395, 3124 (NH) cm^{-1} ; ^1H NMR (200 MHz, DMSO- d_6) δ : 7.37 (dd, 1H, $J = 1.9, 8.6$ Hz, H-6'), 7.51 (d, 1H, $J = 8.6$ Hz, H-7'), 7.84 (s, 1H, H-2''), 8.08 (d, 1H, $J = 5.6$ Hz, H-4''), 8.24-8.28 (m, 2H, H-5, H-5''), 8.32 (d, 1H, $J = 2.9$ Hz, H-2'), 8.53 (d, 1H, $J = 1.9$ Hz, H-4'), 12.02 (bs, 1H, NH), 12.48 (bs, 1H, NH); ^{13}C NMR (50 MHz, DMSO- d_6) δ : 108.3 (d), 110.0 (s), 112.5 (s), 113.4 (s), 114.3 (d), 115.2 (d), 112.6 (d), 124.9 (d), 126.0 (s), 128.2 (d), 129.6 (d), 129.8 (s), 131.6 (s), 133.8 (s), 135.3 (s), 137.1 (d), 148.6 (s), 161.9 (s). Anal. Calcd for: C₁₈H₁₀BrClN₄S: C, 50.31; H, 2.35; N, 13.04. Found: C, 50.55; H, 2.09; N, 12.88.

7-Chloro-3-[2-(1H-indol-3-yl)-1,3-thiazol-4-yl]-1-methyl-1H-pyrrolo[2,3-c]pyridine (51d)

Green solid; yield: 75%; mp: 210-211 °C; IR 3397 (NH) cm^{-1} ; ^1H NMR (200 MHz, DMSO- d_6) δ : 4.25 (s, 3H, CH₃), 7.22-7.30 (m, 2H, H-6', H-5'), 7.48-7.54 (m, 1H, H-7'), 7.75 (s, 1H, H-2''), 8.06 (d, 1H, $J = 5.5$ Hz, H-4''), 8.18 (d, 1H, $J = 2.8$ Hz, H-2'), 8.26 (d, 1H, $J = 5.5$ Hz, H-5''), 8.33 (s, 1H, H-5), 8.36-8.39 (m, 1H, H-4'), 11.82 (bs, 1H, NH); ^{13}C NMR (50 MHz, DMSO- d_6) δ : 36.6 (q), 108.0 (d), 110.4 (s), 110.6 (s), 112.2 (d), 115.3 (d), 120.3 (d), 120.8 (d), 122.4 (d), 124.2 (s), 126.7 (d), 128.9 (s), 132.9 (s), 133.4 (s), 136.6 (s), 135.2 (d), 137.6 (d), 148.0 (s), 162.5 (s). Anal. Calcd for: C₁₉H₁₃ClN₄S: C, 62.55; H, 3.59; N, 15.36. Found: C, 62.31; H, 3.45; N, 15.21.

7-Chloro-3-[2-(5-methoxy-1H-indol-3-yl)-1,3-thiazol-4-yl]-1-methyl-1H-pyrrolo[2,3-c]pyridine (51e)

Orange solid; yield: 73%; mp: 184-185 °C; IR 3383 (NH) cm^{-1} ; ^1H NMR (200 MHz, DMSO- d_6) δ : 3.89 (s, 3H, OCH₃), 4.22 (s, 3H, CH₃), 6.88 (dd, 1H, $J = 2.5, 8.8$ Hz, H-6'), 7.41 (d, 1H, $J = 8.8$ Hz, H-7'), 7.69 (s, 1H, H-2''), 7.87 (d, 1H, $J = 2.4$ Hz, H-4'), 8.02 (d, 1H, $J = 5.5$ Hz, H-4''), 8.11 (d, 1H, $J = 2.9$ Hz, H-2'), 8.28 (s, 1H, H-5), 8.36 (d, 1H, $J = 5.5$ Hz, H-5''), 11.67 (bs, 1H,

NH); ^{13}C NMR (50 MHz, DMSO- d_6) δ : 36.6 (q), 55.1 (q), 101.7 (d), 107.6 (d), 110.2 (s), 110.5 (s), 112.6 (d), 113.0 (d), 115.5 (d), 124.7 (s), 127.1 (d), 128.9 (s), 131.5 (s), 133.1 (s), 133.4 (s), 134.9 (d), 137.3 (d), 148.0 (s), 154.6 (s), 162.8 (s). Anal. Calcd for: $\text{C}_{20}\text{H}_{15}\text{ClN}_4\text{OS}$: C, 60.83; H, 3.83; N, 14.19. Found: C, 60.59; H, 3.72; N, 13.94.

3-[2-(5-Bromo-1*H*-indol-3-yl)-1,3-thiazol-4-yl]-7-chloro-1-methyl-1*H*-pyrrolo[2,3-*c*]pyridine (51f)

Green solid; yield: 99%; mp: 273-274 °C; IR 3378 (NH) cm^{-1} ; ^1H NMR (200 MHz, DMSO- d_6) δ : 4.24 (s, 3H, CH_3), 7.37 (dd, 1H, $J = 1.9, 8.6$ Hz, H-6'), 7.50 (d, 1H, $J = 8.6$ Hz, H-7'), 7.75 (s, 1H, H-2''), 8.04 (d, 1H, $J = 5.5$ Hz, H-4''), 8.24-8.29 (m, 3H, H-2', H-5, H-5''), 8.50 (d, 1H, $J = 1.8$ Hz, H-4'), 12.02 (bs, 1H, NH); ^{13}C NMR (50 MHz, DMSO- d_6) δ : 36.6 (q), 108.4 (d), 110.0 (s), 110.5 (s), 113.4 (s), 114.3 (d), 115.3 (d), 117.8 (s), 122.5 (d), 125.0 (d), 125.9 (s), 128.2 (d), 128.9 (s), 133.1 (s), 133.3 (s), 135.2 (d), 137.2 (d), 148.1 (s), 162.0 (s). Anal. Calcd for: $\text{C}_{19}\text{H}_{12}\text{BrClN}_4\text{S}$: C, 51.43; H, 2.73; N, 12.63. Found: C, 51.19; H, 2.60; N, 12.47.

BIOLOGY

Drugs Preparation

To obtain stock solutions of compounds **45a-l**, **46a-d**, **47a-d**, **48a-d** and **49a-j**, **50a-f**, **51a-f**, each compound was initially dissolved in DMSO in order to obtain 50mM solution, stored at +4°C, and diluted in complete culture medium immediately before use at the appropriate concentration.

Human Tumour Cell Lines.

Human diffuse malignant peritoneal mesothelioma (DMPM) cell lines (STO and MesoII) were established from surgical specimens of patients who underwent surgery at Fondazione IRCCS Istituto Nazionale dei Tumori of Milan, as previously described [32].

Human Tumour Cell Lines Growth Conditions

Cells were maintained in the logarithmic growth phase as a monolayer in DMEM F12 supplemented with 10% heat-inactivated fetal bovine serum in a humidified incubator at 37°C with a supply of 5% CO_2 /95% air atmosphere. Cell lines were tested fortnightly for the absence of Mycoplasma and periodically monitored for DNA profile of short tandem repeats analysis by the AmpFISTR Identifier PCR amplification kit (Applied Biosystems).

Evaluation of the Antiproliferative Potential of Nortopsentin Derivatives

After harvesting in the logarithmic growth phase, 4×10^3 cells were plated in 96-well flat-bottomed microtiter plates (EuroClone) for 24 hours and then treated with varying concentrations of different derivatives (0.01-50 μM) for 72 hours. Control cells received vehicle alone (0.1% DMSO). All studies were performed in eight replicates and repeated at least three times independently.

At the end of drug exposure, the antiproliferative potential was determined by the CellTiter 96® AQueous One Solution Cell Proliferation Assay (MTS; Promega), according to the manufacturer's protocols. Briefly, 20 μl of CellTiter 96® AQueous One Solution Reagent were added into each well of the 96-well assay plates containing the samples in 100 μl of culture medium. The plates were then incubated at 37°C for 3 hours in a humidified, 5% CO_2 atmosphere. Optical density was read at 490 nm on a microplate reader (POLARstar OPTIMA, BMG Labtech GmbH) and the results were expressed as a percentage, relative to DMSO-treated cells.

Dose-response curves were created and IC_{50} values (i.e., concentrations able to inhibit cell growth by 50%) were determined graphically from the curve for each compound obtained after 72 hour exposure of cells to Nortopsentin derivatives.

Viability assay *in vitro*

Nortopsentin analogues, prepared as described above, were dissolved in dimethyl sulfoxide (DMSO) (all reagents and chemicals were from Sigma Chemical Co (St. Louis, MO), unless indicated) and then diluted in culture medium to have a DMSO concentration not exceeding 0.1%. HCT-116 and Caco-2 cell lines were purchased from American Type Culture Collection, Rockville, MD, USA and DMEM supplemented with 10% fetal, 10% fetal bovine serum (FBS), penicillin (100 U/mL), streptomycin (100 $\mu\text{g}/\text{mL}$) and gentamicin (5 $\mu\text{g}/\text{mL}$). Cells were maintained in log phase by seeding twice a week at a density of 3×10^8 cells/L in humidified 5% CO_2 atmosphere, at 37 °C. In all experiments, HCT-116 cells were made quiescent through overnight incubation before treatment with tested compounds or vehicle alone (control cells), while Caco-2 cells were treated 15 days after confluence, at which time the cells are differentiated in normal intestinal-like cells [50].

No differences were found between cells treated with DMSO 0.1% and untreated cells in terms of cell number and viability. Cytotoxic activity of the nortopsentin derivatives **45k** and **51c** was determined by the colorimetric assay based on the reduction of 3-(4,5-dimethyl-2-thiazolyl)bromide-2,5-diphenyl-2H-tetrazolium (MTT) to purple formazan by mitochondrial dehydrogenases. Briefly, HCT-116 and Caco-2 lines cells were seeded at 2×10^4 cells/well in 96-well plates containing 200 μL RPMI. When appropriated, monolayer cultures were treated for 24 h with various concentrations (5-100 μM) of the drugs. Then cells were washed with fresh medium and 50 μL FBS-free medium containing 5 mg/mL MTT added. Cells were incubated 2 h at 37 °C,

then medium was discarded by centrifugation, formazan blue formed in the cells dissolved in DMSO, and absorbance measured at 570 nm in a microplate reader (Bio-RAD, Hercules, CA). Formazan of control cells was taken as 100% viability. GI₅₀ was calculated by the curve of percent viability versus concentration. Each experiment was repeated at least three times in triplicate.

Cell cycle analysis

Cell cycle stage was analyzed by flow cytometry. HCT-116 cells (5.0×10^4 cells/cm²) were seeded in triplicate in 24-wells culture plates. After an overnight incubation, the cells were washed with fresh medium and incubated with compounds **45k** and **51c** in RPMI for 24 h. Then cells were harvested by trypsinization. Aliquots of 1×10^6 cells were washed with PBS and incubated in the dark in a PBS solution containing 20 µg/ml propidium iodide (PI) and 200µg/ml RNase, for 30 min, at room temperature. Then samples of at least 1.0×10^4 cells were subjected to fluorescence-activated cell sorting (FACS) analysis by Epics XL™ flow cytometer using Expo32 software (Beckman Coulter, Fullerton, CA).

Measurement of phosphatidylserine (PS) exposure

The apoptosis-induced PS externalization to the cell surface was measured by flow cytometry by double staining with Annexin V-Fluorescein isothiocyanate (Annexin V-FITC)/propidium iodide (PI). Annexin V binding to phosphatidylserine is used to identify the earliest stage of apoptosis. PI, which does not enter cells with intact membranes, is used to distinguish between early apoptotic cells (Annexin V-FITC positive and PI negative), late apoptotic cells (Annexin V-FITC/PI-double positive) or necrotic cells (annexin V-FITC negative and PI positive). After 24 h treatment, HCT-116 cells were harvested by trypsinization and adjusted at 1.0×10^6 cells/mL with combining buffer according to the manufacturer instructions (eBioscience, San Diego, CA). One hundred µL of cell suspensions were added to a new tube, and incubated with Annexin V-FITC and PI solution at room temperature in the dark for 15 min. Then samples of at least 1.0×10^4 cells were subjected to FACS analysis using appropriate 2-bidimensional gating method.

Measurement of mitochondrial transmembrane potential

Changes of mitochondrial transmembrane potential ($\Delta\psi_m$) were assessed by flow cytofluorometry, using the cationic lipophilic dye 3,3'-dihexyloxacarbocyanine iodide(3) (DiOC6) (Molecular Probes, Inc.) which accumulates in the mitochondrial matrix. Changes in mitochondrial membrane potential are indicated by a reduction in the DiOC6-induced fluorescence intensity. After 24 h treatment, HCT116 cells were incubated with DiOC6 at a 40 nmol/L final concentration, for 15 min

at 37 °C. After centrifugation, cells were washed with PBS and suspended in 500 µL PBS. Fluorescent intensities were analysed in at least 1×10^4 cells for each sample.

Morphology

To analyse cell morphology, cells were fixed with methanol for 10 min and then stained with Giemsa (10% in PBS) for 15 min followed by washing with distilled water. Cell images were captured using Zeiss, AxioCam, AxioSkop microscope, (West Germany) with 40x lenses.

Quantification of acidic vesicular organelles (AVO) by acridine orange (AO) staining

AO is a fluorescent molecule used either to identify apoptotic cell death or autophagy. It can interact with DNA emitting green fluorescence or accumulate in acidic organelles where it is protonated forming aggregates that emit bright red fluorescence [41]. Briefly, cells were stained with AO solution (5 µg/mL) for 15 min. Then they were washed, re-suspended in PBS and subjected to FACS analysis. The green (510-530 nm, FL-1) and red (650 nm, FL-3) fluorescence of AO with blue (488 nm) excitation, was determined over 10,000 events.

Statistics

Results are given as means and their standard deviations. Three independent observations were carried out for each experiment, replicated three times. Statistical comparisons were made using a one-way ANOVA, followed by Bonferroni's test. $P < 0.05$ was considered statistically significant.

REFERENCES

1. L. Annunziato, G. Di Renzo, *Trattato di Farmacologia*, Idelson-Gnocchi edition, **2010**, pp 1468-1514.
2. C.A. Shih, S.P. Ho, F.W. Tsay, K.H. Lai, P.I. Hsu, *J. Med. Sci.*, **2013**, *29*, 642-645.
3. L.V. Monteiro de Assis, J. Locatelli, M.C. Isoldi, *Biochim. Biophys. Acta*, **2014**, *1845*, 232-247.
4. B. Price, A. Ware, *Crit. Rev. Toxicol.*, **2009**, *39*, 576-588.
5. M. Deraco, D. Bartlett, S. Kusamura, D. Baratti, *J. Surgical Oncology*, **2008**, *98*, 268-272.
6. F. Mohamed, P.H. Sugarbaker, *Curr. Treat. Options Oncol.*, **2002**, *3*, 375-86.
7. D. Baratti, S. Kusamura, A.D. Cabras, R. Bertulli, I. Hutanu, M. Deraco, *Eur. J. Cancer*, **2010**, *46*, 2837-2848.
8. A.L. Feldman, S.K. Libutti, J.F. Pingpank, D.L. Bartlett, T.H. Beresnev, S.M. Mavroukakis, S.M. Steinberg, D.J. Liewehr, D.E. Kleiner, H.R. Alexander, *J. Clin. Oncol.*, **2003**, *21*, 4560-4567.
9. K. Turner, S. Varghese, H.R. Alexander, *J. Natl. Compr. Canc. Netw.*, **2012**, *10*, 49-57.
10. G.R. Simon, C.F. Verschraegen, P.A. Jänne, C.J. Langer, A. Dowlati, S.M. Gadgeel, K. Kelly, G.P. Kalemkerian, A.M. Traynor, G. Peng, J. Gill, C.K. Obasaju, H.L. Kindler, *J. Clin. Oncol.*, **2008**, *26*, 3567-72.
11. G. Carteni, C. Manegold, G. Martin Garcia, S. Siena, C.C. Zielinski, D. Amadorif, Y. Liug, J. Blatter, C. Visseren-Grul, R. Stahel, *Lung Cancer*, **2009**, *64*, 211-218.
12. R. Tohme, N. Darwiche, H. Gali-Muhtasib, *Molecules*, **2011**, *16*, 9665-9696.
13. T.F. Molinski, D.S. Dalisay, S.L. Lievens, J.P. Saludes, *Nat. Rev. Drug Discov.* **2009**, *8*, 69-85.
14. K. Oh, W. Mar, S. Kim, J.Y. Kim, T.H. Lee, J.G. Kim, D. Shin, C. J. Sim, J. Shin, *Biol. Pharm. Bull.*, **2006**, *29*, 570-573.
15. D. Kumar, D.S. Rawat, *Research Sighpost*, **2011**, 213-268.
16. G.R. Pettit, J. McNulty, D.L. Herald, D.L. Doubek, J.C. Chapuis, J.M. Schmidt, L.P. Tackett, M.R. Boyd, *J. Nat. Prod.*, **1997**, *60*, 180-183.
17. A. Fontana, P. Cavaliere, S. Wahidulla, C.G. Naikb, G. Cimino, *Tetrahedron*, **2000**, *56*, 7305-7308.
18. W.D. Inman, W.M. Bray, N.C. Gassner, R.S. Lokey, K. Tenney, Y. Yongchun Shen, K. TenDyke, T. Suh, P. Crews, *J. Nat. Prod.*, **2010**, *73*, 255-257.
19. S. Shimizu, Y. Yamamoto, L. Inagaki, S. Koshimura, *Gann*, **1982**, *73*, 642-648.

20. A. Kaji, R. Saito, M. Nomura, K. Miyamoto, N. Kiriya, *Biol. Pharm. Bull.*, **1998**, *21*, 945-949.
21. M. Oikawa, M. Ikoma, M. Sasaki, *Eur. J. Org. Chem.*, **2011**, *2011*, 4654-4666.
22. S. Sakemi, H.H. Sun, *J. Org. Chem.*, **1991**, *56*, 4307-4308.
23. X.H.Gu, X.Z. Wan, B. Jiang, *Bioorg. Med. Chem. Lett.*, **1999**, *9*, 569-572.
24. B. Jiang, X.H.Gu, *Bioorg. Med. Chem.*, **2000**, *8*, 363-371.
25. P. Diana, A. Carbone, P. Barraja, A. Montalbano, A. Martorana, G. Dattolo, O. Gia, L. Dalla Via, G. Cirrincione, *Bioorg. Med. Chem. Lett.*, **2007**, *17*, 2342-2346.
26. P. Diana, A. Carbone, P. Barraja, A. Martorana, O. Gia, L. Dalla Via, G. Cirrincione, *Bioorg. Med. Chem. Lett.*, **2007**, *17*, 6134-6137.
27. P. Diana, A. Carbone, P. Barraja, G. Kelter, H.H. Fiebig, G. Cirrincione, *Bioorg. Med. Chem.*, **2010**, *18*, 4524-4529.
28. A. Carbone, B. Parrino, V. Spanò, P. Barraja, G. Cirrincione, P. Diana, A. Majer, G. Kelter, H.H. Fiebig, *Marine Drugs*, **2013**, *11*, 643-654.
29. P. Diana, A. Carbone, P. Barraja, A. Montalbano, B. Parrino, A. Lopergolo, M. Pennati, N. Zaffaroni, G. Cirrincione, *Chem. Med. Chem.*, **2011**, *6*, 1300-1309.
30. A. Carbone, M. Pennati, P. Barraja, A. Montalbano, B. Parrino, V. Spanò, A. Lopergolo, S. Sbarra, V. Doldi, N. Zaffaroni, G. Cirrincione, P. Diana, *Curr. Med. Chem.*, **2014**, *21*, 1654-166.
31. A. Carbone, M. Pennati, B. Parrino, A. Lopergolo, P. Barraja, A. Montalbano, V. Spanò, S. Sbarra, V. Doldi, M. De Cesare, G. Cirrincione, P. Diana, N. Zaffaroni, *J. Med. Chem.*, **2013**, *56*, 7060-7072.
32. N. Zaffaroni, A. Costa, M. Pennati, C. De Marco, E. Affini, M. Madeo, R. Erdas, A. Cabras, S. Kusamura, D. Baratti, M. Deraco, M.G. Daidone, *Cell Oncology*, **2007**, *29*, 453-466.
33. M. Pennati, M. Folini, N. Zaffaroni, *Expert Opin. Ther. Targets*, **2008**, *12*, 463-476.
34. D.S. O' Connor, N.R. Wall, A.C. Porter, D.C. Altieri, *Cancer Cell*, **2002**, *2*, 43-54.
35. J. Green, A. Miller, J.M. Jimenez, C. Marhefka, J. Crao, J. Court, U. Bandarage, H. Gao, S. Nanthakumar, US Patent, **2009**, 7,514,448 B2; Chemical abst., 2009, 150, 398519.
36. J. Green, A. Miller, J.M. Jimenez, C. Marhefka, J. Crao, J. Court, U. Bandarage, H. Gao, S. Nanthakumar, **2005**, WO2005/103050; Chemical abst., 2005, 143, 440389.
37. C. Ganser, E. Lauermann, A. Maderer, T. Stauder, J.P. Kramb, S. Plutizki, T. Kindler, M. Moehler, G. Dannhardt, *J. Med. Chem.*, **2012**, *55*, 9531-9540.
38. G. Bartoli, G. Palmieri, M. Bosco, R. Dalpozzo, *Tetrahedron Letters*, **1989**, *30*, 2129-2132.
39. J. Van Meerloo, G.J. Kaspers, J. Cloos, *Methods Mol. Biol.*, **2011**, *731*, 237-245.

40. T.L. Riss, R.A. Moravec, A.L. Niles, H.A. Benink, T.J. Worzella, L. Minor, "Cell viability assays," in *Assay Guidance Manual*, Eli Lilly & Company and the National Center for Advancing Translational Sciences, Bethesda, Md, USA, **2004-2013**.
41. S. Paglin, T. Hollister, T. Delohery, N. Hackett, M. McMahill, E. Sphicas, D. Domingo, J. Yahalom, *Cancer Res.*, **2001**, *61*, 439-444.
42. L.M. Schwartz, S.W. Smith, M.E.E. Jones, B.A. Osbourne, *Proc. Natl. Acad. Sci. USA*, **1993**, *90*, 980-984.
43. Z. Zakeri, W. Bursch, M. Tenniswood, R.A. Lockshin, *Cell Death Differ.*, **1995**, *2*, 87-96.
44. E. Finkel, *Science*, **1999**, *286*, 2256-2258.
45. E. Tasdemir, M.C. Tajeddine, I. Vitale, A. Criollo, J.M. Vicencio, J.A. Hickman, O. Geneste, G. Kroemer, *Cell Cycle* **2007**, *6*, 2263-2267.
46. G.C.G. Pais, X. Zhang, C. Marchand, N. Neamati, K. Cowansage, E.S. Svarovskaia, V.K. Pathak, Yun Tang, M. Nicklaus, Y. Pommier, T.R. Burke, *J. Med.Chem.*, **2002**, *45*, 3184-3194.
47. M. Soledade, C. Pedras, J. Liu, *Org. Biomol. Chem.*, **2004**, *2*, 1070-1076.
48. C.J. Moody, J.R.A. Roffey, *Arkivoc*, **2000**, *1*, 393-401.
49. C.J. Moody, J.R.A. Roffey, M.A. Stephens, I.J. Stratford, *Anti-Cancer Drugs*, **1997**, *8*, 489-499.
50. D. Sun, H. Lennernas, L.S. Welage, J.L. Barnett, C.P. Landowski, D. Foster, D. Fleisher, K.D. Lee, G.L. Amidon, *Pharm. Res.*, **2002**, *19*, 1400-1416.

SYNTHESIS OF NAPHTHALENE DIIMIDE DERIVATIVES AS G-QUADRUPLEX LIGANDS

(UCL, SCHOOL OF PHARMACY)

INTRODUCTION

During the second year of my PhD, I spent 7 months at the University College of London, School of Pharmacy, Biomolecular Structure Group (BMSG), under the supervision of Professor Stephen Neidle, where I carried out a project based on the synthesis of naphthalene diimides, potential ligand of G-quadruplex DNA.

The DNA, the center of genetic information in the cell, is one of the most important targets of several anticancer drugs. Drugs that interact with this receptor are generally very toxic to normal cells, so a perfect chemotherapeutic DNA - interactive, should be a non-peptide molecule that can diffuse through the membrane without being degraded and that have as target a specific sequence of appropriate size of nitrogenous bases. The development of alkylating agents that react covalently with the nitrogenous bases of the DNA, as antitumor agents is strongly dependent on the discovery and development of the double-stranded DNA and its associated processes. Unluckily, numerous of these drugs are highly cytotoxic and non-selective. For this reason, significant efforts have been directed toward the discovery of new agents with improved selectivity and reduced cytotoxicity [1].

In addition to the typical right-handed double helix proposed by Watson and Crick, DNA can assume other biologically significant structures, such as the G-quadruplex structure. The G-quadruplex sequences are noncanonical secondary structures, rich in guanine d(TTAGGG), present in different regions of the eukaryotic genome, such as telomeres or the regulatory regions of many genes. These structures play important roles in the regulation of many biological events in the body and in recent decades have become valid targets for the development of new anticancer drugs.

The nucleic acid sequences show a high propensity to self-association in planar quartets (G-quartets) to form four filaments structures called G-quadruplex (or G-tetrads or G4-DNA), reported for the first time by Davis and co. in 1962 [1, 2].

G-quadruplex structures are formed when four guanine are distributed in a planar arrangement through Hoogsteen hydrogen bondings and the structure is stabilized by the presence of a monovalent cation (usually K^+ or Na^+), which is at the center of the tetrad and it is coordinated with the lone pairs of the O_6 of each guanine. Four hydrogen bonds are formed for each pair of guanines through N_1 , N_2 , N_7 and O_6 atoms (Fig.1).

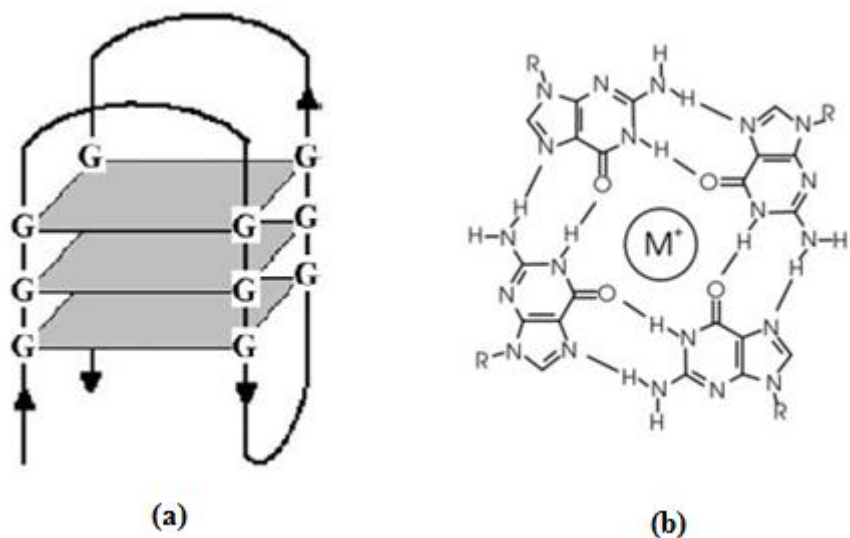


Figure 1. A possible G-quadruplex monomeric structure (a) and the hydrogen-bonding arrangement in the G-quartet (b).

The space between the G-tetrads can coordinate cations of these dimensions because the two planes of the tetrads are coated by eight oxygen atoms of the carbonyl groups (with a strong negative electrostatic potential) which create a central channel with a negative charge inside of the stack of G-tetrad (Fig.2) [1, 3, 4].

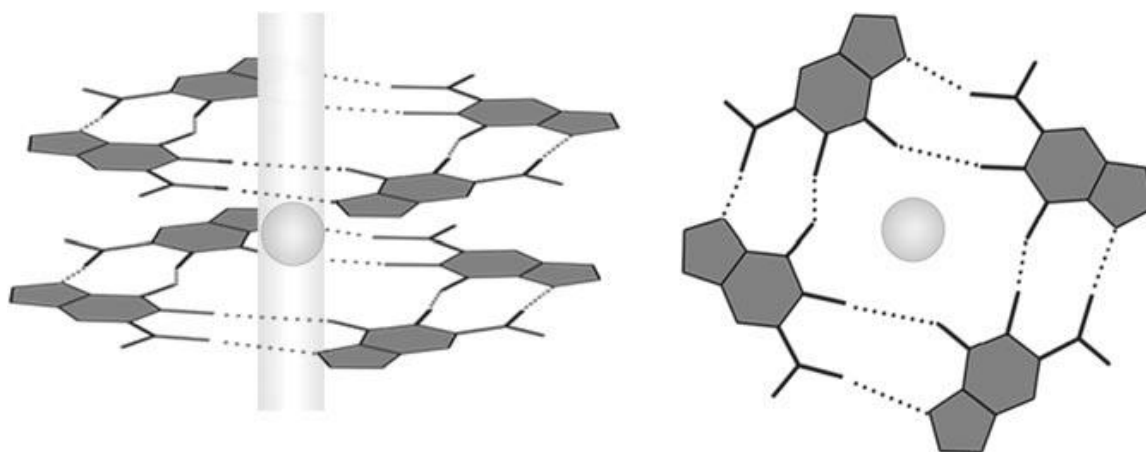


Figure 2. G-quadruplex ion channel.

The G-quadruplex crystal structure shows that the quartet can be considered as a square aromatic surface, whose dimensions are much larger than the base pairs of Watson-Crick (Fig.3), and this difference is the base for the design of new G-quadruplex-specific ligands [1, 5].

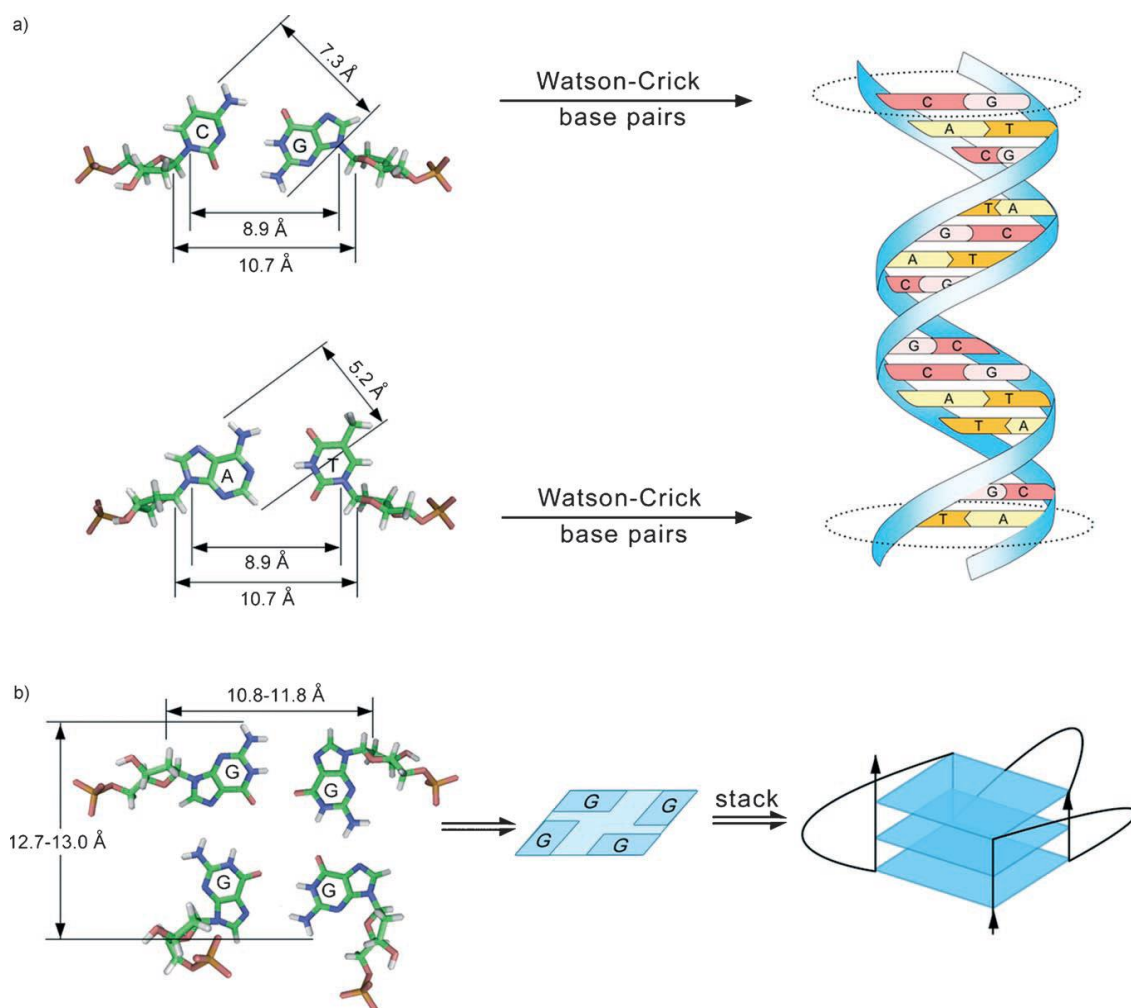


Figure 3. Comparison of the dimensions of duplex and G-quadruplex DNA structures. a) The double helix and its base pair surface. b) The quadruplex structure and the G-quartet surface.

In general, structural polymorphism arises mostly from the nature of the loop, such as variations of strand stoichiometry, strand polarity, glycosidic torsion angle, and the location of the loops that link the guanine strands. Meanwhile, the solution environment, such as the presence of metal ions, ligands, or molecular crowding conditions, may influence the topology of quadruplex. G-quadruplex structures are made up of one, two, or four DNA strands, which can run parallel or antiparallel, and the DNA sections which are involved in the quadruplex, form loops. Loops can be diagonal, lateral or propeller (or chain-reversal) depending on the number of G-quartets comprising the stem of a quadruplex and on loop length (Fig. 4) [6].

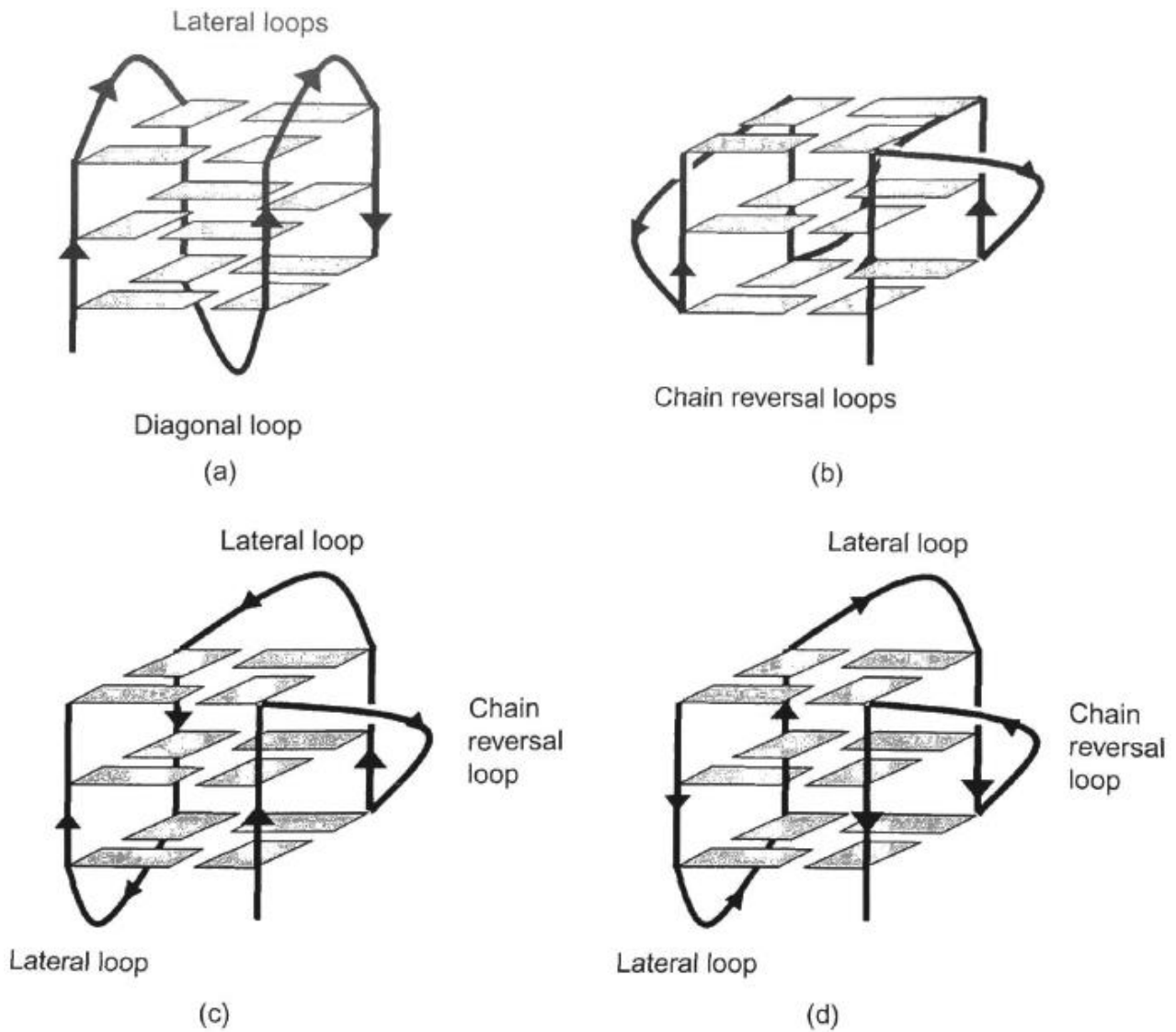


Figure 4. The major experimentally observed topologies for human telomeric DNA quadruplex sequences.

G-quadruplexes can be folded from a single G-rich sequence intramolecularly or by the intermolecular association of two (dimeric) or four (tetrameric) separate strands [1]. The heterogeneity of the G-quadruplex sequences also depends on the conformation of the guanine (*syn* or *anti*) [4, 7, 8].

G-Quadruplex sequences are present in specific regions of the genome with key biological contexts. These include:

- the ends of telomeric DNA [4],
- promoter regions of several oncogenes and in a number of genes involved in cellular proliferation. Examples reported are *c-myc* [4], *c-kit* [9], *K-ras* [10], RET oncogenes [11],

androgen receptor [12] and HSP90 genes [13], the platelet-derived growth factor (PDGF) [14] and vascular endothelial growth factor (VEGF) [15],

- 5'-untranslated RNA sequences [16]. Examples of genes containing such sequences include the estrogen receptor [17], the MT3 matrix metalloprotease gene [18], and the Bcl2 gene [19].

The therapeutic concept developed is that the stabilization of quadruplex sequences with a small molecule can cause inhibition of transcription (in the case of the quadruplex promotor) or translation (5'quadruplex-UTR) of the gene involved, and that this could, therefore, confer a therapeutic advantage if the gene is critically involved in the maintenance of the malignant phenotype or metastatic disease [20].

DNA G-quadruplex as target for a therapeutic strategy was initially developed for telomeric DNA and the inhibition of telomerase enzyme.

Telomeric DNA is non-coding DNA sequence present at the ends of the chromosomes of eukaryotic cells, which is essential for the preservation of genome stability [1].

The role of the telomeric DNA-protein complex is to protect the ends of chromosomes from degradation and unwanted chromosomal fusions [20, 21, 22].

Telomers are specialized complexes consisting of a repetitive sequence in double-stranded length of about 10-15 Kb and ending with a single strand of 200 nucleotides at the 3' rich in guanine which protrudes beyond the double-stranded region [4].

The single-stranded DNA can be recognized as damage so it is not usually exposed to the cell environment, but it is folded on the double-stranded region leading to the formation of a large telomeric loop, called T-loop. The 3'end of the strand invades the adjacent duplex DNA, forming a region of single-stranded DNA called D-loop. The loops are associated with a large number of proteins, called shelterins, which help the stabilization of the secondary structure of the T-loop.

These proteins include the complex of telomere repeat binding factor 1 and 2 (TRF1 and TRF2) that binds to double-stranded telomeric DNA; the protection protein of telomeres 1 (POT1) that binds the single-stranded 3' rich in guanine. There are three other proteins (TIN2, TPP1 and RAP1) which protect the integrity of telomeres and help in the development of T and D-loop (Fig. 5) [4, 21]. The role of the shelterin complex is to regulate telomeric DNA responses to potentially lethal damage events and the length of telomeric DNA.

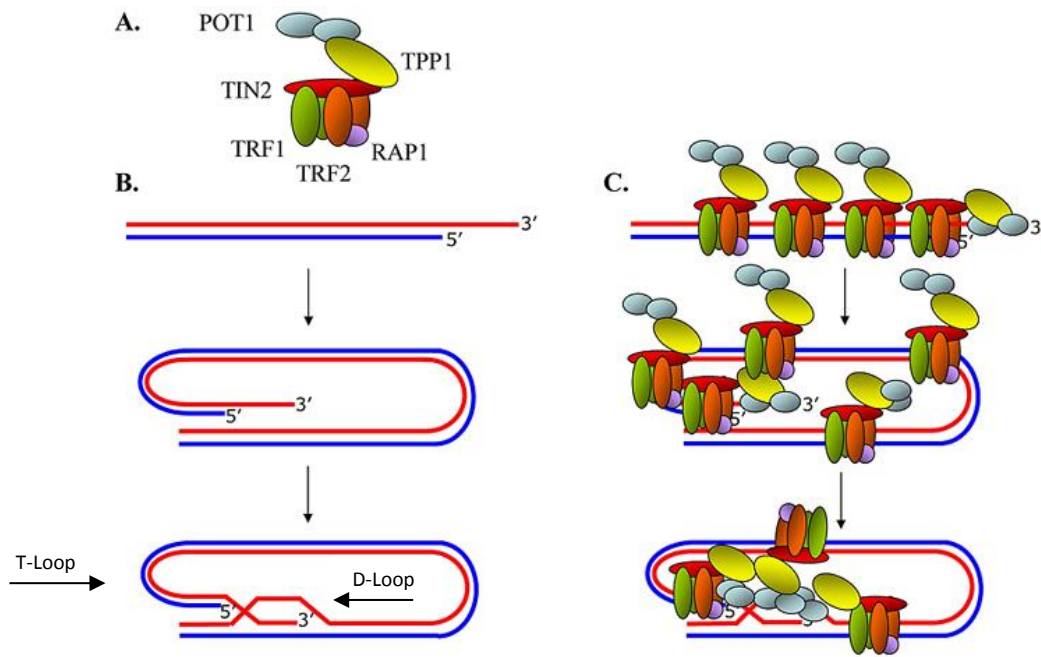


Figure 5. (a) View of the shelterin complex, (b) T and D-loops structures, (c) Schematic representation of the associated proteins and their mutual interactions.

Due to the inability of the DNA polymerase replication system to replicate the whole length of the ends of telomeric DNA in somatic cells, in the absence of any compensating mechanism, telomeric DNA in normal cells is progressively reduced to 50-100 nucleotides during each round of cellular replication. When telomeres become critically short, they reach a critical point, called the “Hayflick limit” and cells go into a state of senescence with a consequent up regulation of proteins p21(WAF) and p16^{INK4a}, increased phosphorylation of the proteins *p53* and *pRB* (retinoblastoma), and subsequent cellular apoptosis (Fig. 6) [1, 6, 20, 23, 24].

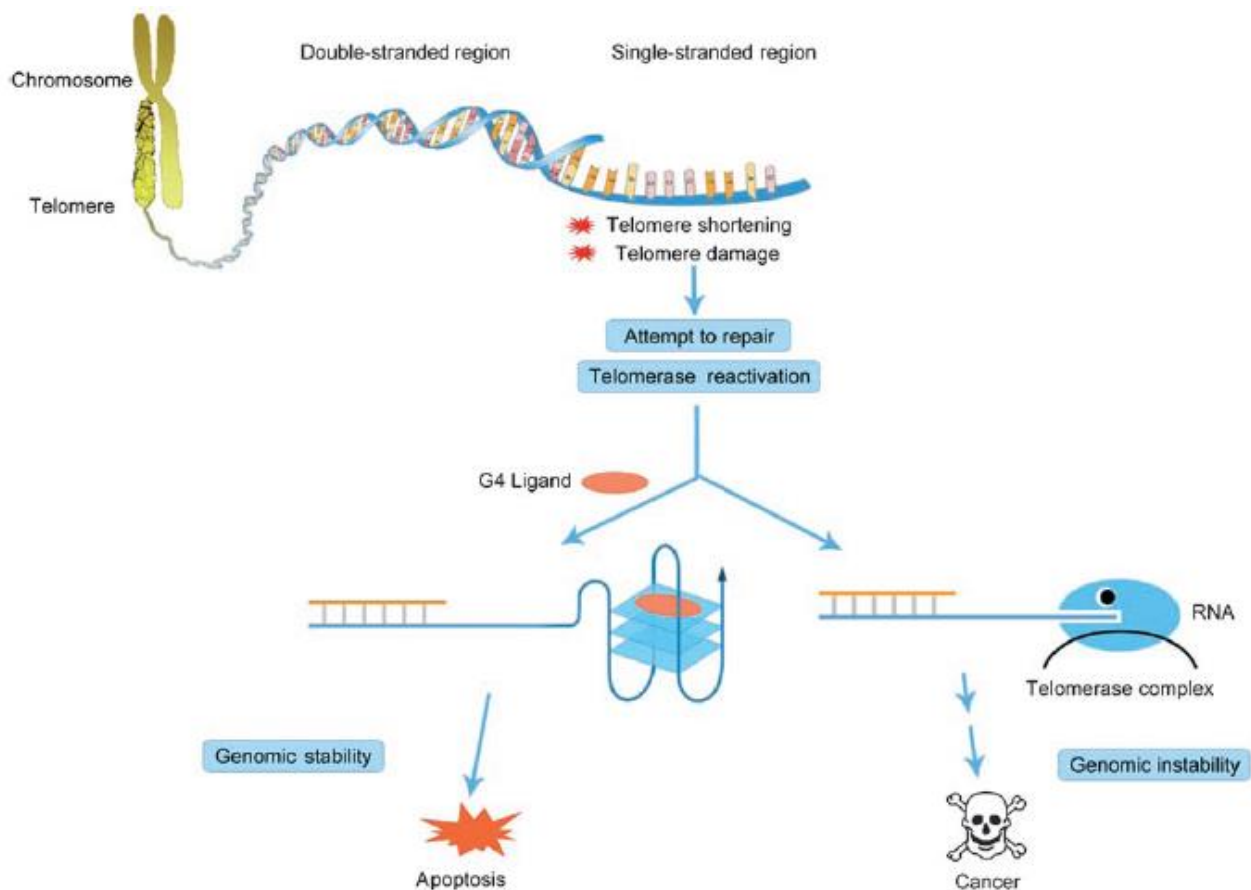


Figure 6. Structures and biological roles of telomers.

In tumor cells, the telomeres are maintained at a constant length by the activation of the enzyme telomerase (enzyme-dependent RNA or reverse transcriptase) (Fig. 6) that compensates for the shortening, adding the sequence TTAGGG at the end of telomeric DNA, resulting in a stabilization of the genomic DNA and inducing uncontrolled cell proliferation. This enzyme reverses the behavior of telomeric DNA in somatic cells, causing cellular immortality. This is the reason why the activity of telomerase is closely related to the proliferation of some types of tumor cells [25].

The enzyme telomerase is not significantly expressed in normal somatic cells, suggesting the existence of a large therapeutic window for inhibitors of telomerase.

Telomerase enzyme complex is a reverse transcriptase formed by two principal subunits, a catalytic domain (hTERT) and an RNA domain (hTR), containing a single stranded RNA template, scaffold for DNA retrosynthesis. The catalytic subunit adds deoxynucleotide triphosphates to the 3' single stranded telomeric overhang (Fig. 7) [6].

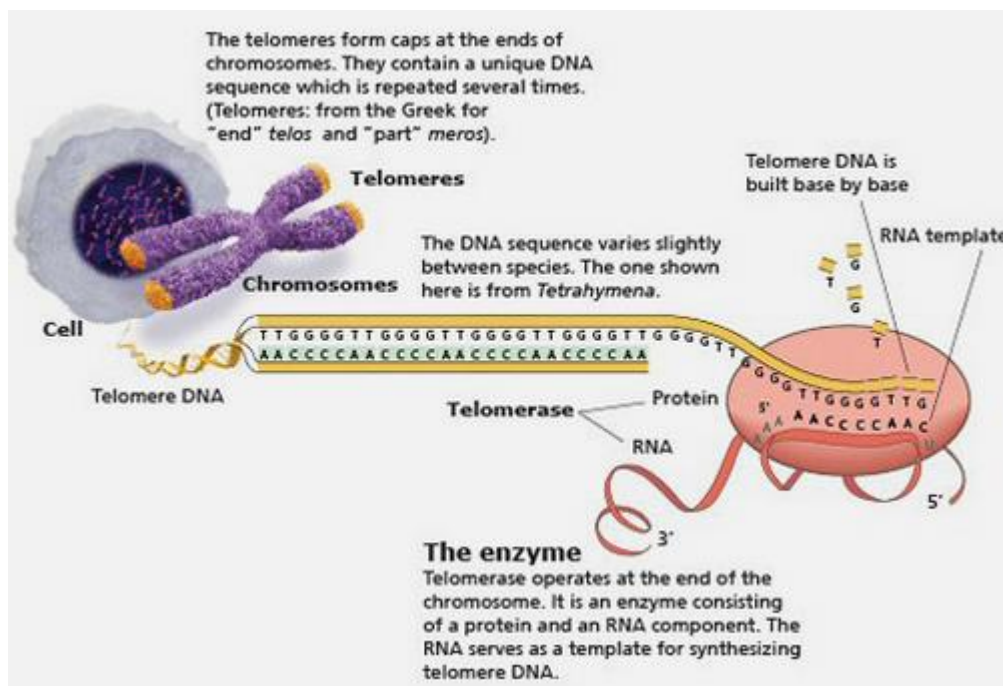


Figure 7. Telomerase complex.

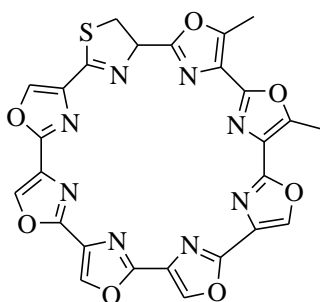
The relation between tumor and telomerase enzyme was proved by a great number of studies on cancer cell lines concluding that approximately 80-85% of human cancers express significant levels of active form of telomerase. So telomerase has been identified as one of the essential factors required in order to transform a normal cell in an immortalized one [6] and the inhibition of this enzyme has gained significant consideration for new, more selective and less toxic anticancer strategies [26].

The therapeutic potential of the G-quadruplex sequences has led to an increase in the number of studies in which ligand molecules have been used as stabilizers of the G-quadruplex DNA. Several compounds that interact with G-quadruplex have been described in the literature [4].

The key characteristics common to these ligands include aromatic flat wide surface suitable for π - π stacking interactions with the terminal of a G-quadruplex DNA, the presence of cationic charges and basic groups (often amino groups which can be protonated at physiological pH) and chains hydrophilic side which interact with the grooves of the DNA.

These compounds are chemically different, some of these derive from natural sources, such as telomestatin, while others have synthetic origin, such as phenanthrolines, triazines, acridines as BRACO 19, perylene diimides, anthraquinones, cationic porphyrins, fluoroquinolones, carbazole derivatives and naphthalene dimiides (ND).

Telomestatin **1** is a macrocyclic compound containing a pentaoxazole ring system and a thiazoline ring isolated from *Streptomyces anulatus*. It showed exceptional quadruplex-binding and telomerase inhibitory activity [27]. Telomestatin **1** induced the formation of *basket type* G-quadruplex structures in the telomeric region, damaged the telomeric replication and inhibited the growth of cancer cells [28]. Studies shown that telomestatin, like synthetic compounds as BRACO19 **8**, acted not only by the inhibition of the catalytic activity of telomerase, but also by the uncapping of the 3' strand of telomeres [4, 29].

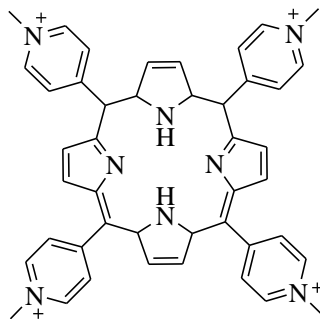


Telomestatin

1

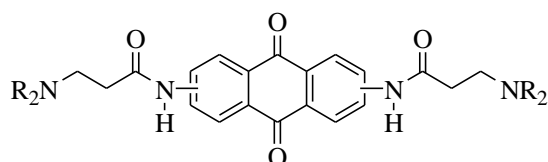
Porphyrins are considered to be ideal ligands of the G-quadruplex due to their extended conjugation that allows an optimal level of tetrads stacking.

The porphyrin compound TMPyP4 (tetra-(*N*-methyl-4-pyridyl)porphyrin) **2** is a G-quadruplex ligand that has been used in a large number of studies. It has been reported to show anti-cancer activity in MX-1 mammary tumors and PC-3 human prostate carcinomas. Data *in vitro* and *in vivo* showed that TMPyP4 **2** binded tightly to the quadruplexes and reduced *c-myc* expression in cell-free system and in cells. However, this compound is able to bind equally well to many other quadruplexes such as human telomeric ones and the double DNA [30].



TMPyP4

2



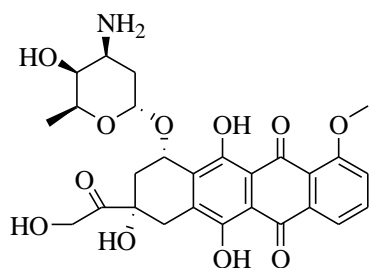
Amido-anthraquinones

5

The key features, including the anthraquinone core and the side chains terminating with cationic end-group are important for the interaction with the G-quadruplex DNA and inhibition of telomerase. From the telomerase inhibitor data it was possible to deduce a set of structural characteristics important for the activity [35]:

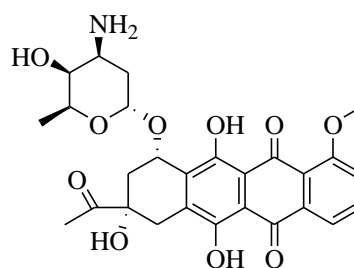
- Two side-chains;
- The best side-chain length is $-(\text{CH}_2)_{2-3}-$;
- The amido group;
- Piperidine or pyrrolidine cationic end-group;
- The cationic group.

Examples of known anthraquinones include the anti-tumor agent doxorubicin (Adriamycin) **6**, and the antitumor antibiotic daunorubicin **7**.



6

Doxorubicin (Adriamycin)



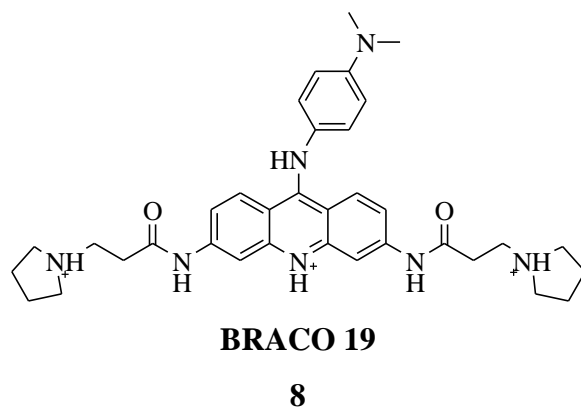
7

Daunorubicin

The acridine derivative BRACO 19 **8**, similarly to the telomestatine, causes a rapid senescence at the level of the tumor cells and activates the same response that occurs following the double-strand break of the DNA. This involves, in particular, the activation of the ATM pathway, the kinase $p16^{\text{INK4a}}$ and the pro-apoptotic protein $p53$. This response is a consequence of the displacement of proteins bounding to single-stranded 3'telomeric sequence, in particular hPOT1.

Protein hPOT1 interacts with the telomeric protein TPP1, helping the elongation of the telomere by telomerase. The displacement of this protein therefore results in an alteration of the function of telomerase [36]. *In vivo* activity against a human tumor xenograft was also found, where the

cytotoxic agent taxol was used to produce tumor regression and BRACO-19 **8**, given after debulking, was able to suppress tumor regrowth [38].



A number of recent studies have employed the naphthalene diimide (ND) core system as a quadruplex-binding motif, due to its combination of chemical accessibility and extended planar surfaces suggestive of favorable quadruplex-binding. Most of these published studies have focused on mono-di- or trisubstituted compounds. Some tri- and tetra-substituted naphthalene diimides (Fig. 8) showed exceptional ligand properties for G-quadruplex DNA with stabilizing value for G-quadruplex DNA, in classical and competition FRET assays, twice higher than those obtained with acridine compound BRACO19 **8**, and significantly greater than effects produced by TMPyP4 **2** and telomestatine **1**. These compounds were able to inhibit the telomerase activity in the TRAP assay, they showed antiproliferative activity against MCF7 and A549 cell lines, and they were localized in the nucleolus of MCF7 cells [38].

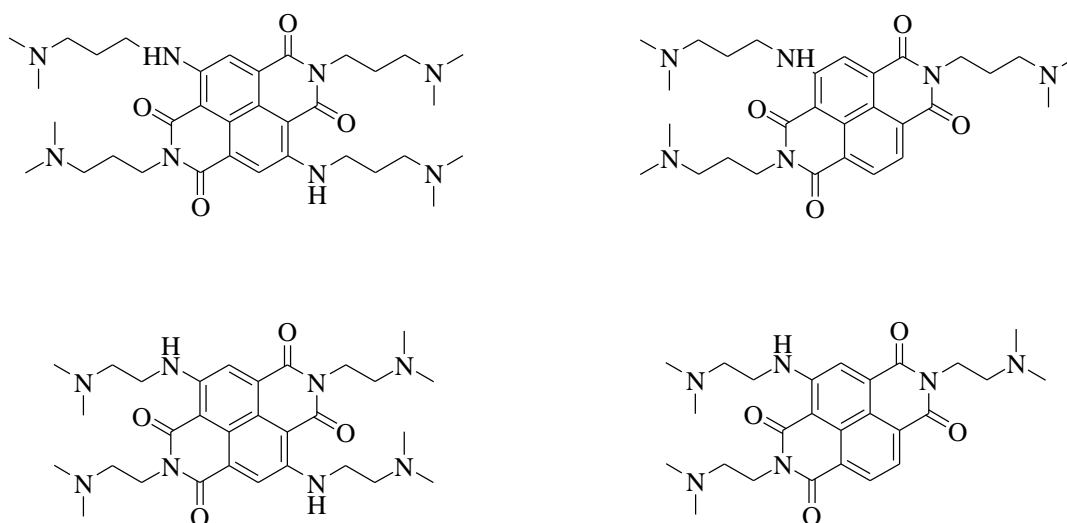


Figure 8. Some tri- and tetra-substituted naphthalene diimides.

Then, a series of tetrasubstituted naphthalene diimide compounds, in particular with *N*-methylpiperazine end groups, were synthesized (Fig. 9). They showed high affinity and selectivity for telomeric G-quadruplex DNA F21T (Δt_m values from 23.8 to 28.3 °C) and low affinity for duplex DNA T-loop sequence (Δt_m values from 0.1 to 1.3 °C). These compounds presented extraordinary activity in a panel of cancer cell lines, including the pancreatic cell lines MIA Paca-2, PANC-1 and HPAC, with IC_{50} values of 0.1-0.2 μM . They were significantly less toxic to the normal human fibroblast cell line WI38 than to the panel of cancer cell examined [39].

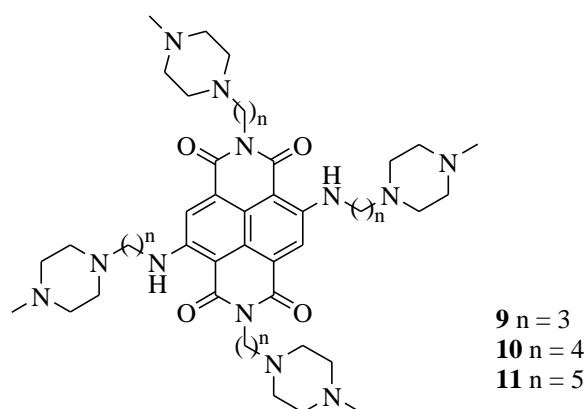
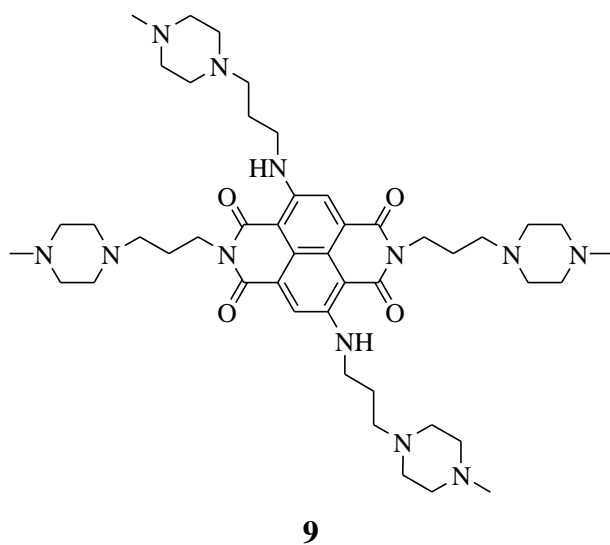


Figure 9. Naphthalene diimides with *N*-methyl piperazine end-group.

In particular, a pancreatic cancer xenograft model of one of these compounds (**9**) revealed a significant antitumoral activity. After an intraperitoneal (ip) administration, 50% reduction in tumor volume and high inhibition of telomerase activity (in MCF7 breast carcinoma) it was observed [40].

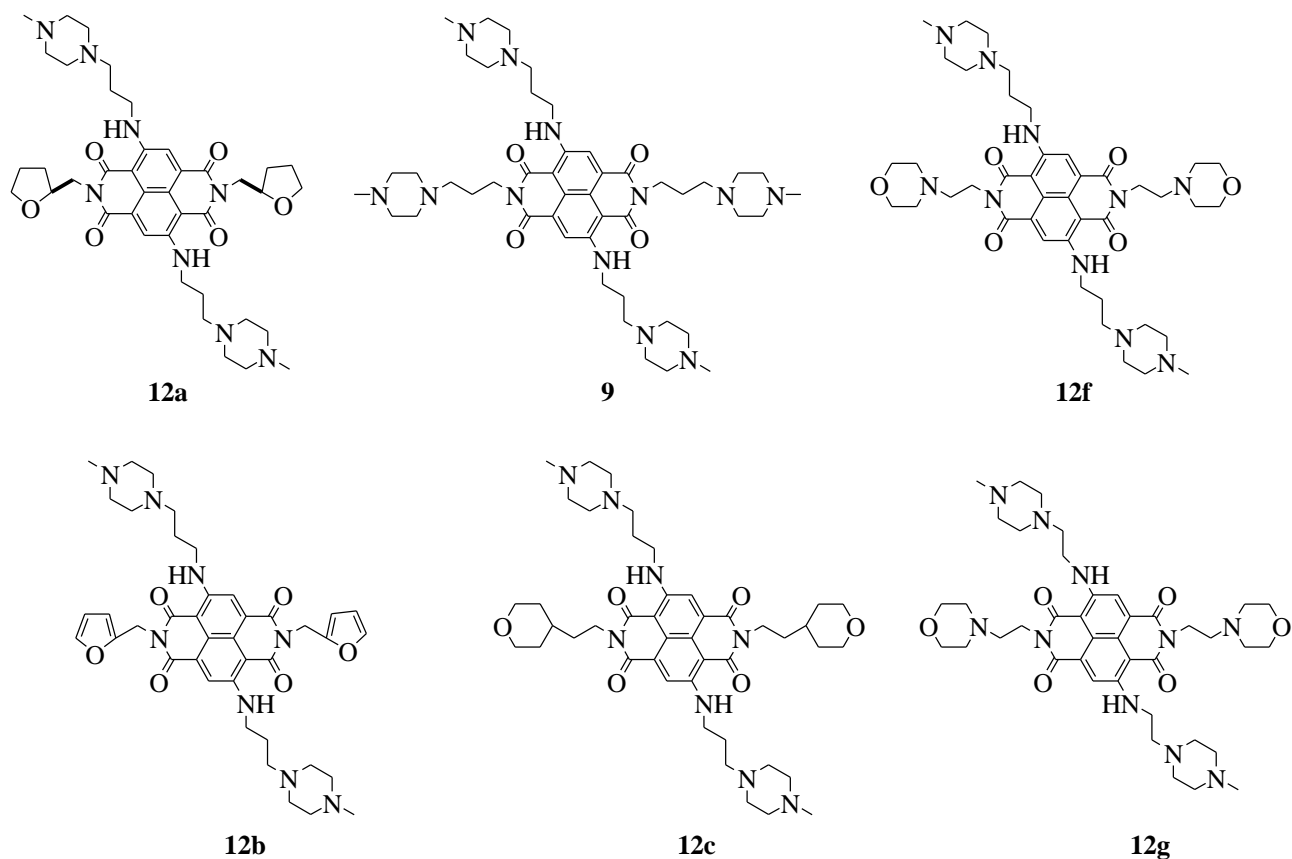


In the cocrystal structures [41] was observed that the charged nitrogen atom of the *N*-methyl piperazine ring of compound **9** is in proximity to a phosphate oxygen group through hydrogen bonds. The *N*-methyl piperazine ring next to the side chain indirectly interacts with a phosphate group, through a network of water molecules in the groove.

The four positive charges of this compound have been modulated through the replacement of the two *N*-methyl piperazine groups with weaker *N*-basic groups, with the purpose to increase the pharmacological properties of the series of naphthalene diimides without compromising the interaction with the G-quadruplex DNA. It has been suggested that a slight decrease of the cationic nature of the naphthalene diimides could increase the cellular uptake and the potential distribution in the tumor, while maintaining the affinity for DNA G-quadruplex [42].

In particular, two morpholine groups were introduced, which not only reduce the overall molecular weight of the molecule but they are less basic groups relative to the *N*-methyl piperazine protonated ring, with a pK value of 8.5 compared to that for the latter of 9.2.

The series was further explored with ND compounds having a diversity of noncharged end-groups as methoxy groups, furan, tetrahydrofuran or tetrahydropyran **12a-h** (Fig. 10) [42].



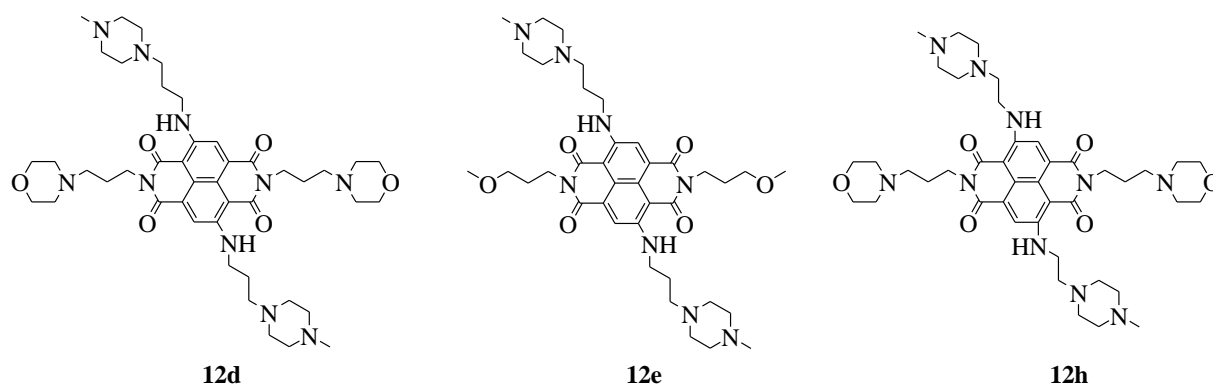


Figure 10. Molecular structure of tetrasubstituted naphthalene diimides.

High-throughput fluorescence resonance energy transfer (FRET) is a melting technique used to evaluate the ability of these compounds to stabilize a human telomeric quadruplex sequence.

In table 1 the ΔT_m values ($^{\circ}\text{C}$) for a duplex DNA, a human telomeric quadruplex sequence and two HSP90 quadruplex sequences are reported. With the exception of tetra-*N*-methyl-piperazine compound **9** [39], only derivatives with morpholine rings revealed significant stabilization of G-quadruplex DNA, and also some binding to the duplex DNA sequence. The dimethoxy compound **12e** exhibited a very slight interaction with the telomeric quadruplex but a greater stabilizing effect on HSP90 promoter sequences, with ΔT_m values of 23.8 and 29.0 $^{\circ}\text{C}$. Compounds with furan, pyranose and acyclic ether rings (**12b,c,e**) did not show any effect on telomeric quadruplex or duplex stability. All the morpholine compounds determined high ΔT_m values in the telomeric quadruplex, with values comparable to that reported for compound **9**. Nevertheless, compounds **12f** and **12g**, in which the linker to the morpholine group is $n = 2-(\text{CH}_2)_n$, exhibited higher selectivity for quadruplex DNA over duplex DNA compared to compounds with $n = 3$ (Tab. 1).

Table 1. ΔT_m Values ($^{\circ}\text{C}$) for a Duplex DNA (T-loop), a Human Telomeric Quadruplex Sequence (htel), and Two HSP90 Quadruplex Sequences at a 1 μM Ligand Concentration (with 60 mM K^+ at pH 7.4)^a

| Compd | T-loop | Htel | HSP90A | HSP90B |
|------------|--------|------|--------|--------|
| 9 | 1.3 | 28.3 | 36.3 | 32.0 |
| 12a | 0.2 | 22.7 | 27.1 | 21.0 |
| 12b | 0.3 | 0.2 | 0.9 | 1.1 |
| 12c | 0.2 | 0.1 | 0.7 | 0.8 |
| 12d | 4.9 | 26.6 | 33.1 | 28.6 |
| 12e | 0.0 | 0.5 | 29.0 | 23.8 |
| 12f | 0.8 | 27.0 | 33.9 | 29.1 |
| 12g | 1.7 | 24.7 | 30.6 | 27.6 |
| 12h | 8.1 | 27.8 | 31.9 | 31.1 |

^aESDs are ± 0.1 $^{\circ}\text{C}$, estimated from multiple readings.

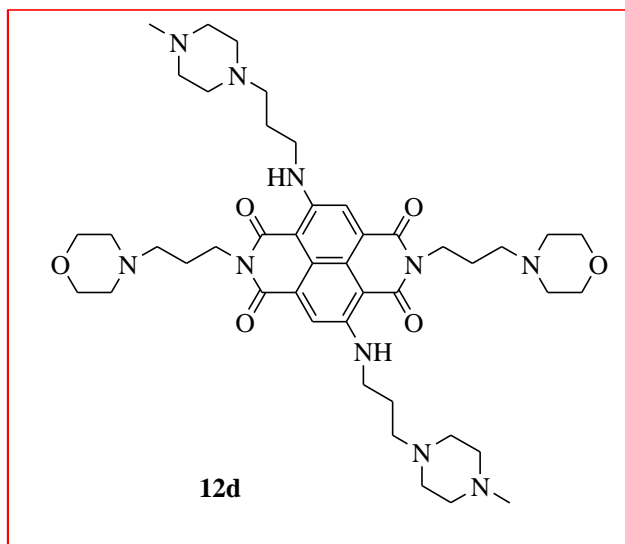
The SRB (Sulforodamine) assay was used to assign the antiproliferative activity of naphthalene diimide derivatives (Tab. 2). After 96 hours exposure to 2-fold serial dilutions of each compound in a panel of cancer cell lines together with a normal fibroblast line, it was observed that compound **12a** resulted devoid of significant antiproliferative activity in all the cancer cell lines, with the exception of MIA PaCa-2 and A549 lines, even though compounds **12b**, **12c**, **12e** showed IC₅₀ values in the range of 1-8 μ M. In particular, compound **12c** revealed up to 10-fold selectivity for the renal carcinoma cell line 786-0. Instead, the morpholine compound **12d** and **12h**, with a n = 3-(CH₂)_n-linkers to the morpholine group, exhibited a potent activity in the MIA PaCa-2 pancreatic carcinoma and A549 lung adenocarcinoma cell lines, showing IC₅₀ values between 10-20 nM.

Table 2. Growth Inhibition data for Compounds **12a-h** and **9** using a panel of cancer cell lines and a normal human fibroblast line (WI-38), Measured by the SRB Assay for 96 h exposure and expressed as IC₅₀ Values in μ M.

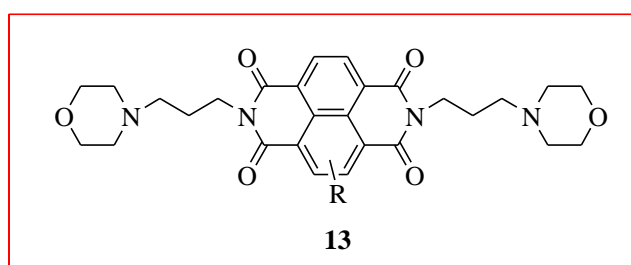
| Compd | A549 | RCC4 | MIA-PaCa-2 | 786-0 | MCF-7 | WI-38 |
|-----------------------|-------------------|------------------|-----------------|-----------------|------------------|------------------|
| 12^o | 5.57 \pm 0.31 | >10 | 5.65 \pm 0.14 | >10 | >10 | >10 |
| 12b | 2.41 \pm 0.01 | 3.11 \pm 0.06 | 2.83 \pm 0.01 | 1.10 \pm 0.03 | 2.61 \pm 0.06 | 6.84 \pm 0.05 |
| 12c | 2.92 \pm 0.01 | 8.38 \pm 0.50 | 2.50 \pm 0.01 | 1.20 \pm 0.03 | 3.12 \pm 0.13 | 12.65 \pm 0.11 |
| 12d | <0.01 \pm 0.005 | 0.56 \pm 0.05 | 0.01 \pm 0.01 | 0.32 \pm 0.01 | 0.07 \pm 0.007 | 0.23 \pm 0.01 |
| 12e | 2.54 \pm 0.01 | 10.51 \pm 0.14 | 2.79 \pm 0.09 | 7.17 \pm 0.41 | 5.62 \pm 0.15 | 3.32 \pm 0.50 |
| 12f | 1.55 \pm 0.02 | 1.75 \pm 0.18 | 0.04 \pm 0.01 | 0.63 \pm 0.06 | 0.17 \pm 0.01 | 0.61 \pm 0.02 |
| 12g | 4.93 \pm 0.05 | 5.10 \pm 0.70 | n/a | 1.48 \pm 0.17 | 0.18 \pm 0.03 | 1.17 \pm 0.11 |
| 12h | <0.01 \pm 0.006 | 0.28 \pm 0.06 | 0.01 \pm 0.01 | n/a | 0.03 \pm 0.01 | 2.46 \pm 0.02 |
| 9 | 0.11 \pm 0.02 | n/a | 0.11 \pm 0.02 | n/a | 0.17 \pm 0.03 | 9.0 \pm 3.2 |

The panel of cancer carcinoma cell lines used includes: A549 (lung), RCC4, and 786-0 (renal), MIA PaCa-2 (pancreatic), and MCF-7 (breast).

Considering the interesting results shown, during the 7 months at the Biomolecular Structure Group (BMSG), I initially synthesized again compound **12d** (100 mg), already published by this research group [42], in order to obtain a higher quantity sufficient for more biophysical studies (FRET) using other human G-quadruplex sequences, biological studies (SRB assay) in other cancer cell lines and mouse xenograft studies, in MIA PaCa-2 cells that were explanted into the mouse flank. However resulted related to mouse xenograft studies cannot be shown for publication reasons.



Then I was involved in a project related to the design, the synthesis and the evaluation of the antitumor activity of a series of new trisubstituted naphthalene diimide derivatives (**13**), obtained with a different panel of amines. The differences in the amines have provided diversity in the library, enabling the exploration of the effects of differing end groups and side-chain lengths.

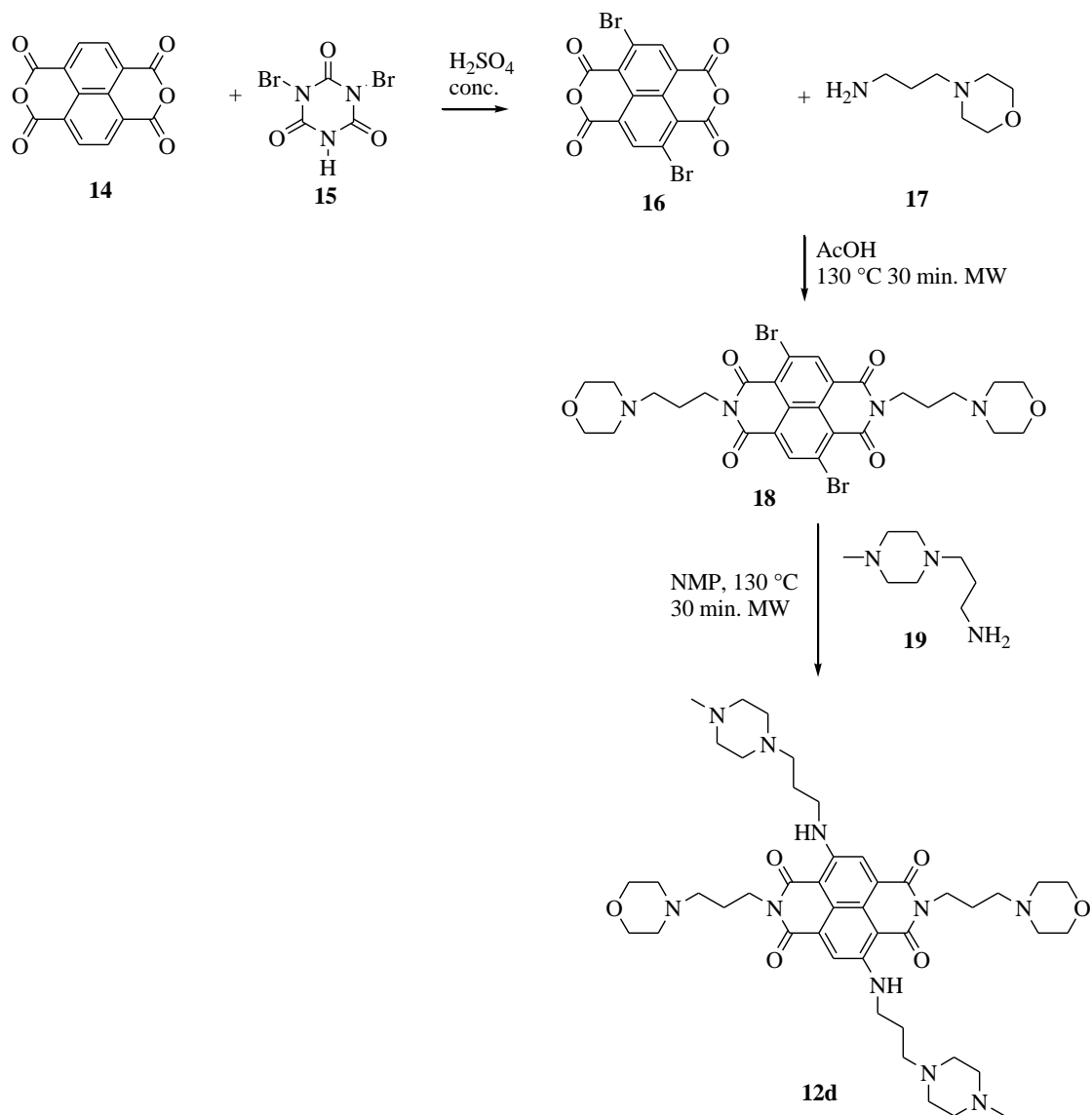


RESULTS AND DISCUSSION: CHEMISTRY

The synthetic pathway for the synthesis of compound **12d** involves three steps (Scheme 1) [42]. Commercial isochromeno-[6,5,4,*def*]-isochromene-1,3,6,8-tetraone **14**, dissolved in fuming sulphuric acid, was brominated using dibromoisocyanuric acid **15** in hot sulphuric acid solution (40 °C). The yellow solid obtained **16** was used without purification for the next step [43]. In the second step, the dibrominated naphthalene anhydride **16** and 3-morpholino propylamine **17** were solubilized in acetic acid and heated at 130 °C for 30 minutes under microwave waves. The obtained semisolid was purified using reverse phase HPLC and compound **18** was isolated in 32% of yield. Then compound **18** was subjected to amination in order to introduce two more amino groups and to obtain tetra-substitute derivative **12d**.

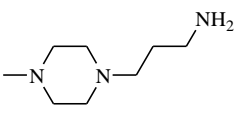
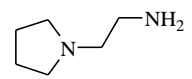
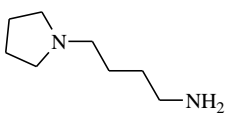
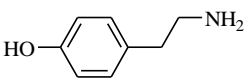
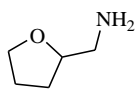
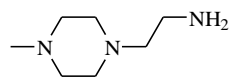
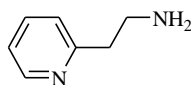
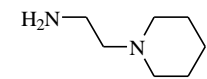
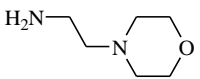
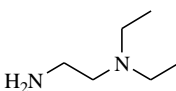
Di-brominated compound **18** and *N*-methylpiperazine propylamine **19** were solubilized in NMP (*N*-methyl-2-pyrrolidinone) and the reaction mixture was heated at 130 °C for 30 minutes under microwave irradiation. After purification with reverse phase HPLC, it was possible to isolate tetra-substituted ND **12d** in 18% of yield.

Scheme 1. Synthetic route to prepare the tetra-substituted naphthalene diimide derivative **10d**.



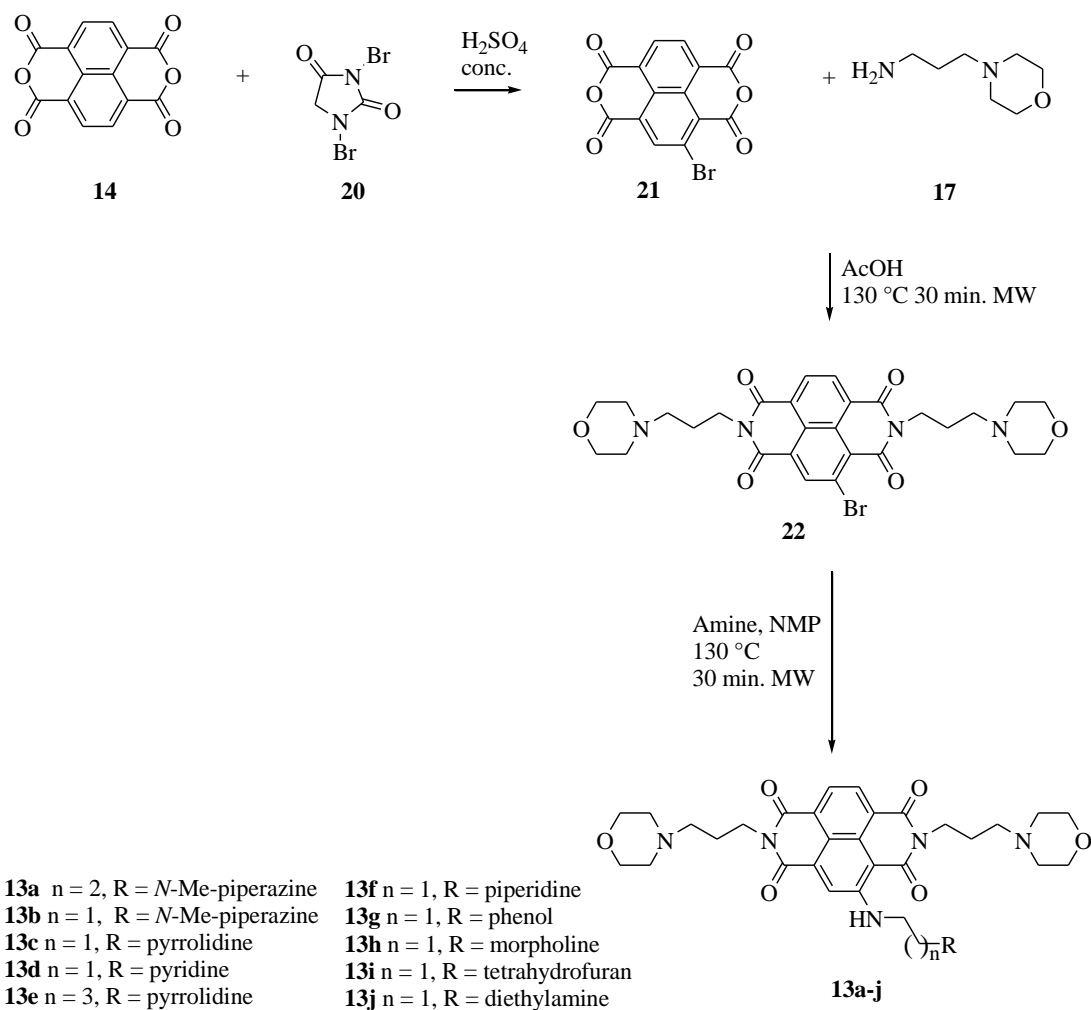
Tri-substituted naphthalene diimides **13a-j** were obtained from the monobromo precursor **22**, using commercially available amines **19**, **23-31** (Tab. 3).

Table 3. Amines **19**, **23-31**.

| Amine | Amine | Amine | Amine | Amine |
|--|--|--|---|--|
| 19  | 24  | 26  | 28  | 30  |
| 23  | 25  | 27  | 29  | 31  |

A representative 3 steps synthesis is outlined in scheme 2.

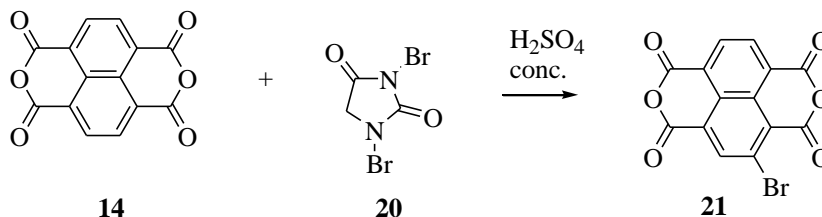
Scheme 2. Synthetic route to prepare the tri-substituted naphthalene diimide derivatives **13a-j**.



The first step involved the synthesis of the mono-brominated derivative **21**. Isochromeno[6,5,4,def]-isochromene-1,3,6,8-tetraone **14** was treated with dibromo hydantoin (DBH) **20** in

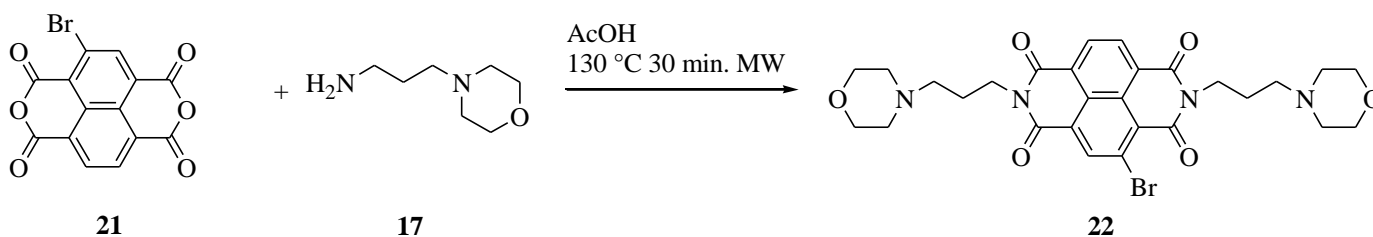
sulfuric acid at room temperature for 24 h. After crystallization with *N,N*-dimethylformamide the desired compound **21** was obtained in good yield (83%) [44] (Scheme 3).

Scheme 3.



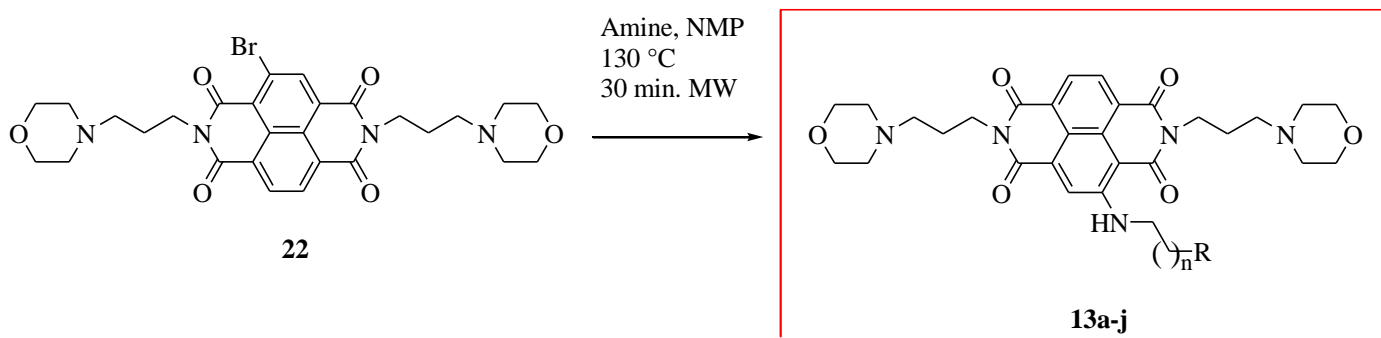
The monobromo precursor **21** was subjected to amination using 3-morpholino-propylamine **17** in acetic acid under microwave irradiation. Derivative **22** was isolated in low yield (20%) (Scheme 4).

Scheme 4.



The final step involved a secondary amination of the mono-brominated derivative **22** with several amines **19**, **23-31** to obtain different tri-substituted naphthalene diimides **13a-j** from low to good yields (8-60%) (Scheme 5).

Scheme 5.



- | | |
|---|---------------------------------------|
| 13a n = 2, R = <i>N</i> -Me-piperazine | 13f n = 1, R = piperidine |
| 13b n = 1, R = <i>N</i> -Me-piperazine | 13g n = 1, R = phenol |
| 13c n = 1, R = pyrrolidine | 13h n = 1, R = morpholine |
| 13d n = 1, R = pyridine | 13i n = 1, R = tetrahydrofuran |
| 13e n = 3, R = pyrrolidine | 13j n = 1, R = diethylamine |

RESULTS AND DISCUSSIONS: BIOLOGY

The ability of tetra-substituted compound **12d** and tri-substitute compounds **13a-j** to stabilize human telomeric quadruplex was assessed by FRET (Fluorescence Resonance Energy Transfer) assay modified to be used as a high-throughput screen in a 96-well format. This technique evaluate the distance-dependent interaction between the electronic excited states of two molecules in which excitation was transferred from a donor molecule to an acceptor molecule through non-radiative dipole–dipole coupling, resulting in the return of the donor to its ground state causing a fluorescent emission (Fig. 11) [45].

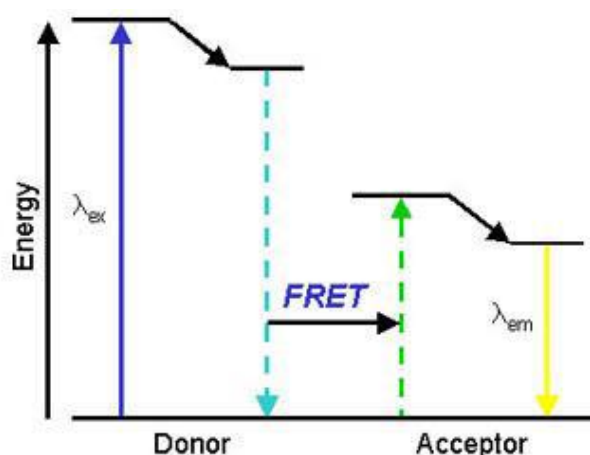


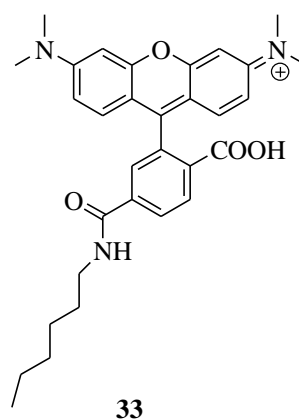
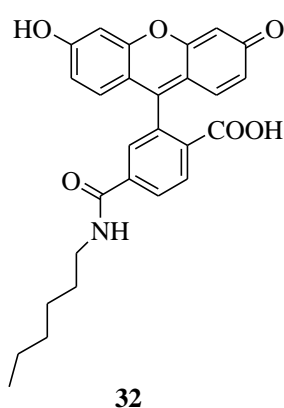
Figure 11. Schematic representation of FRET technique.

The FRET *efficiency* (E) is the quantum yield of the energy transfer transition and it was described in the empirical Förster equation. The efficiency depends on the distance between the donor and the acceptor (r) (typically in the range of 10–100 Å), with an inverse 6th power law due to the dipole-dipole coupling mechanism:

$$E = \frac{1}{1 + (r/R_0)^6}$$

R_0 is the Förster distance of this pair of donor and acceptor, i.e. the distance at which the energy transfer efficiency is 50%.

DNA can be synthesized with its 3' and 5' ends tagged with fluorescent dyes, at the 5' end 6-carboxyfluorescein (FAM) **32** as the donor, and tetramethyl-6-carboxyrhodamine (TAM) **33** at the 3' end as the acceptor, using 6 carbon linkers.



When nucleotides are folded in the G-quadruplex structure, the fluorophores are closer in space and the FRET efficiency is high. Using this property, by increasing the temperature while measuring the fluorescence intensity, melting experiments could be done on DNA and the melting temperature of the labelled oligonucleotides could be monitored to screen the G-quadruplex stabilising ability of small molecules [46]. The experiment was performed with different sequences of labelled DNA, including G-quadruplex DNA sequences (F21T, Hsp90A, Hsp90B, Kras21, Kras32, Bcl-2) and the duplex DNA sequence (T-Loop). The FRET probe sequences were diluted from stock to the correct concentration (400 nM) in a 60 mM potassium cacodylate buffer (pH 7.4) and then annealed by heating to 85 °C for 10 min, followed by cooling to room temperature in the heating block (3-3.5 h). The ΔT_m values obtained for all the derivatives (at 1 μ M concentration) were reported in the table 4.

Table 4. ΔT_m values (°C) for FRET analyses of compounds **13a-j** at 1 μ M concentrations with a series of G-rich sequences: hTel (F21T), Hsp90A, Hsp90B (Heat Shock Protein 90), Tloop (duplex DNA). Esds are from triplicate measurements and average 0.3 °C. Compound **12d** is the dimorpholino-di-N-methyl-piperazine naphthalene diimide derivative highlighted in Micco et al J. Med. Chem., 2013 [42].

| Compd | ΔT_m values (°C) | | | | | | |
|------------|--------------------------|--------|--------|--------|--------|-------|-------|
| | F21T | Hsp90A | Hsp90B | Kras21 | Kras32 | Bcl-2 | Tloop |
| 13a | 14.3 | 19.8 | 16.5 | 9.8 | 6.1 | 15.8 | 0.8 |
| 13b | 12.3 | 18.1 | 15.0 | 11.0 | 6.1 | 15.1 | 0.4 |
| 13c | 11.8 | 15.7 | 12.7 | 11.0 | 9.6 | 13.3 | 0.6 |
| 13d | <2 | 2.5 | <2 | 3.0 | 1.5 | 2.8 | 0 |
| 13e | 15.9 | 20.6 | 16.9 | 11.7 | 6.6 | 16.1 | 0.2 |
| 13f | 9.8 | 9.1 | 8.7 | 4.8 | 2.2 | 5.9 | 0.6 |
| 13g | 6.0 | 11.0 | 9.4 | 2.4 | 1.5 | 5.8 | 1.5 |
| 13h | 1.4 | 3.9 | 6.8 | 3.4 | 1.2 | 4.2 | 0 |
| 13i | <2 | 2.7 | 4.5 | 0.7 | 0.2 | 2.4 | 0 |
| 13j | 9 | 15.7 | 13.8 | 6.1 | 3.0 | 10.0 | 0.1 |
| 12d | 26.6 | 33.1 | 28.6 | 22.5 | 19.8 | 26.4 | 4.9 |

Table 4 shows that all the compounds exhibited significant telomeric quadruplex stabilization and a general preference for G-quadruplex DNA over duplex DNA. The best results were obtained with compounds **12d**, **13a** and **13e**. In particular, the tetra-substituted derivative **12d** exhibited the best telomeric quadruplex stabilization with ΔT_m values equal to 26.6 °C for F21T, 33.1 °C and 28.6 °C for Hsp90A and B, 22.5 °C for Kras21, 19.8 °C for Kras32, 26.4 °C for Bcl-2, as well as some binding to the duplex DNA sequence, with ΔT_m values equal to 4.9 °C.

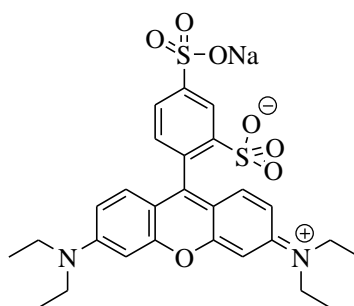
Tri-substituted naphthalene diimide **13a**, containing a *N*-methylpiperazine ring, showed good ΔT_m values for quadruplex DNA sequences (14.3 °C for F21T, 19.8 °C and 16.5 °C for Hsp90A and B, 9.8 °C for Kras21, 6.1 °C for Kras32, 15.8 °C for Bcl-2), and a low ΔT_m value for duplex DNA (0.8 °C).

Tri-substituted naphthalene diimide **13e**, containing a pyrrolidine ring, showed instead good ΔT_m values for quadruplex DNA sequences (15.9 °C for F21T, 20.6 °C and 16.9 °C for Hsp90A and B, 11.7 °C for Kras21, 6.6 °C for Kras32, 16.1 °C for Bcl-2), and a small ΔT_m value for duplex DNA (0.2 °C).

In general for all tri-substituted compounds the stabilization of the duplex DNA sequence (T-Loop) was not significant at the biologically relevant concentrations employed (1 μ M).

The antiproliferative activity of all compounds was assessed using the SRB (sulforhodamine) assay, against a panel of cancer and non-cancer cell lines (referred to as normal fibroblast cell line, WI38). The cancer-derived cell lines studied were A549 (human lung adenocarcinoma), MCF7 (human breast adenocarcinoma), Mia PaCa-2 and Panc1 (pancreatic cancer) and ALT (Alternative Lengthening of Telomeres). The experiment was based on a 96 hours exposure to 2-fold serial dilutions of each compound in order to evaluate the IC_{50} value of each of them.

The assay used is the sulforhodamine B colorimetric assay (SRB). It is based on the ability of the purple dye SRB **34** to interact with the basic amino acid residues of cellular proteins. This molecule is UV active and the quantification of the dye bound to the cells at 540 nm is an indirect measure of the amount of viable cells.



34

Cells were seeded in a 96-well plate and incubated for 24 hours, and then with different concentrations of ligand for 96 hours. The supernatant was removed and the remaining cells were fixed with trichloroacetic acid and stained with sulforhodamine B.

The results obtained were adjusted by the negative control (cells without ligand and without SRB) and normalized by the positive control (cells only with SRB) to obtain the rate of viable cells. The IC₅₀ values were calculated as the concentration responsible for a 50% decrease of cell viability.

The results obtained are shown in table 5.

Table 5. Short-term 96 h IC₅₀ values (in μM) for compounds **13a-j** and **12d** in a cancer cell line panel, comprising MCF7 (breast), A549 (lung cancer), Mia-PaCa2/Panc1 (pancreatic cancer), ALT (Alternative Lengthening of Telomeres) and WI38 (lung fibroblast) cell lines. Esds average 0.25 μM . Compound **12d** is the di-morpholino-di-*N*-methyl-piperazine naphthalene diimide derivative highlighted in Micco et al J Med Chem, 2013 [42].

| Compd | IC ₅₀ (μM) | | | | | |
|------------|------------------------------------|-------|----------|-------|--------|-------|
| | A549 | MCF7 | MiaPaCa2 | Panc1 | ALT | WI38 |
| 13a | 0.067 | 0.357 | 0.059 | 0.045 | 0.224 | 1.83 |
| 13b | 0.086 | 0.316 | 0.048 | 0.046 | 0.085 | 1.49 |
| 13c | 0.024 | 0.159 | 0.012 | 0.022 | 0.093 | 1.19 |
| 13d | 0.130 | 1.070 | 0.220 | 0.340 | 1.29 | 2.24 |
| 13e | 0.026 | 0.222 | 0.036 | 0.033 | 0.089 | 1.22 |
| 13f | 0.198 | 1.110 | 0.108 | 0.084 | 0.535 | 5.33 |
| 13g | 2.18 | >25 | 0.206 | 0.220 | 10.874 | 17.65 |
| 13h | 0.146 | 1.03 | 0.139 | 0.808 | 0.71 | 1.88 |
| 13i | 0.825 | 3.33 | 1.085 | 0.909 | 2.67 | 5.53 |
| 13j | 0.092 | 1.538 | 0.059 | 0.163 | 0.451 | 1.65 |
| 12d | 0.019 | 0.070 | 0.011 | 0.003 | 0.063 | 0.230 |

As shown in the table 5, with the exception of compound **13g** that did not show a significant antiproliferative activity in all cell lines, all other compounds were found to be cytotoxic for almost all the tumor cell lines, with the IC₅₀ values in the micro-, submicro- and nano molar range.

In particular, the most active compounds were found to be the tetra-substituted **12d** and the tri-substituted compounds **13b**, **13c** and **13e**.

The tetrasubstituted **12d** with $n = 3-(\text{CH}_2)_n$ -linkers to the morpholine group, showed particularly potent activity in the MIA PaCa-2 pancreatic carcinoma (0.011 μM), A549 lung adenocarcinoma (0.019 μM) and panc-1 pancreatic cell lines (0.003 μM).

Compound **13c** with $n = 1$ -(CH₂)_n-linkers to the pyrrolidine ring, showed a particular selectivity against MIA PaCa-2 cell lines (0.012 μM) and compound **13e** with $n = 3$ -(CH₂)_n-linkers to the pyrrolidine ring, exhibited selectivity against A549 cells (0.026 μM).

The small library of tri-substituted naphthalene diimides reported here shows a wide range of antiproliferative activity in this particular panel of cancer cell lines.

In conclusion, tri-substituted derivatives **13a-j** and the tetra-substituted derivative **12d** have good G-quadruplex stabilization ability and a low duplex DNA affinity. They inhibit cancer cell growth at low micro molar/high nano molar levels, suggesting that these correlated compounds may have potential as drug-like quadruplex targeting agents.

EXPERIMENTAL DATA

General Methods

All reagents, solvents and chemicals were purchased from Sigma-Aldrich UK, Alfa Aesar, Lancaster Synthesis, Flurochem, TCI and Fluka. Column chromatography was performed using BDH silica gel (BDH 153325P). Preparative HPLC was carried out with a Gilson apparatus combining a 322 pump and UV/VIS-155 detector with detection 280nm, using a C-18 5 μ (100 mm x 20 mm) column (201022272) (W), YWC, Japan at a flow of 20 mL/min. Water and methanol 0.1% formic acid were used as HPLC solvents. NMR spectra were recorded at 400 or 500 MHz (^1H NMR and ^{13}C) on a Bruker spectrometer in CDCl_3 (with 0.05% TMS Cambridge Isotope Laboratories USA), DMSO-d_6 or D_2O . NMR multiplicity abbreviations are s (singlet), bs (broad singlet), d (doublet), t (triplet) and m (multiplet). Coupling constants J are given in hertz (Hz). FRET biophysical testing was done using different DNA sequences: F21T, Hsp90A, Hsp90B, T-loop, KRas21, KRas32. The DNA sequences were purchased from Eurofins, MWG Synthesis, GmbH Germany.

CHEMISTRY

Synthesis of 4,9-dibromoisochromeno[6,5,4-*def*]isochromene-1,3,6,8-tetrone (16) [43]

In a round bottom flask to a solution of dibromoisocyanuric acid **15** (2.14 g, 7.46 mmol) dissolved in concentrated sulphuric acid (40 mL) a solution of isochromeno [6,5,4-*def*]isochromene-1,3,6,8-tetraone **14** (2 g, 7.46 mmol) dissolved in fuming sulphuric acid (80 mL) was added dropwise, over a period of 4 hours at 40 °C. The reaction mixture was stirred further for 1 h at 40 °C. After cooling at room temperature, the reaction mixture was poured onto ice affording a yellow precipitate. The precipitate was filtered using a sinter funnel under vacuum. The yellow product obtained was dried under vacuum and used without purification for the next step.

4,9-dibromo-2,7-bis[3-(morpholin-4-yl)propyl]benzo[*lmn*][3,8]phenanthroline-1,3,6,8(2*H*,7*H*)-tetrone (18) [47]

In a microwave reaction vessel compound **16** (0.13 g, 0.31 mmol) and 3-morpholino-propylamine **17** (0.93 mmol, 0.14 mL) were suspended in acetic acid (5 mL) and refluxed for 30 minutes at 130 °C under microwave irradiation. This reaction was also carried out in a round bottom flask and it was stirred at 130 °C for 5 h. After cooling at room temperature, the solution was concentrated in vacuum and purified using reverse phase HPLC. Compound **18** was obtained as a red semi-solid (32% yield). ^1H NMR (400 MHz, D_2O) δ : 2.27-2.24 (m, 4H, ArH), 3.31-3.29 (m, 4H, ArH), 3.40-3.44 (m, 4H, ArH), 3.63-3.66 (m, 4H, ArH), 3.89-3.95 (m, 4H, ArH), 4.18-4.25 (m, 8H, ArH), 8.30

(s, 1H, ArH), 8.75 (s, 1H, ArH); ^{13}C NMR (100 MHz, D_2O) δ : 21.7 (t), 38.5 (t), 51.7 (t), 54.7 (t), 63.7 (t), 123.4 (d), 124.5 (s), 126.7 (d), 128.2 (s), 138.5 (s), 161.5 (s).

Synthesis of 4,9-bis{[3-(4-methylpiperazin-1-yl)propyl]amino}-2,7-bis[3-(morpholin-4-yl)propyl]benzo[*lmn*][3,8]phenanthroline-1,3,6,8(2*H*,7*H*)-tetrone (12d) [42]

Compound **18** (0.2 g, 0.295 mmol), 1 (3-aminopropyl)-4-methyl-piperazine (1.18 mmol, 0.20 mL) **19** and NMP (2 mL) were suspended in a microwave reaction vessel. After bubbling nitrogen through the solution, the tube was capped and heated at 130 °C for 30 minutes under microwave irradiation. After cooling at room temperature, the solvent was concentrated in vacuo and the crude mixture was purified by preparative HPLC. Compound **12d** was obtained as blue oil (12% yield). ^1H NMR (400 MHz, CDCl_3) δ : 1.99-1.88 (m, 8H, 4x CH_2), 2.30 (s, 6H, 2x CH_3), 2.53-2.44 (m, 30H, 15x CH_2), 3.57 (q, 4H, $J = 6.8$ Hz, 2x CH_2), 3.61 (t, 8H, $J = 4.4$ Hz, 4x CH_2), 4.24 (t, 4H, $J = 6.8$ Hz, 2x CH_2), 8.12 (s, 2H, ArH), 9.38 (t, 2H, $J = 5.4$ Hz, 2xNH); ^{13}C NMR (100 MHz, CDCl_3) δ : 23.6 (q), 25.6 (t), 37.8 (t), 40.3 (t), 44.5 (t), 51.7 (t), 52.5 (t), 53.6 (t), 54.6 (t), 55.5 (t), 65.9 (t), 100.9 (s), 117.3 (d), 120.1 (s), 124.8 (d), 148.1(s), 162.1(s), 165.1 (s).

Synthesis of 4-bromoisochromeno[6,5,4-*def*]isochromene-1,3,6,8-tetrone (21) [44]

In a single-necked round bottom flask isochromeno [6,5,4-*def*]isochromene-1,3,6,8-tetraone **14** (0.8 g, 2.98 mmol) was solubilized in concentrated sulphuric acid (6 mL) at room temperature. Dibromo hydantoin **20** (0.47 g, 1.64 mmol, 0.55 equ.) was added in portions over a period of 2 h and the reaction mixture was stirred at room temperature for 24 h. The reaction mixture was poured into ice affording a yellow precipitate. The solid was filtered and recrystallized from DMF to obtain the pure product as light yellow solid (83% of yield). Analytical and spectroscopic data are reported elsewhere [35].

Synthesis of 4-bromo-2,7-bis[3-(morpholin-4-yl)propyl]benzo[*lmn*][3,8]phenanthroline-1,3,6,8(2*H*,7*H*)-tetrone (22) [47]

In a microwave reaction vessel **21** (0.13 mg, 0.31 mmol) and 3-morpholino-propylamine **17** (3 eq., 0.93 mmol, 0.136 ml) were suspended in acetic acid (4.5 mL) and refluxed for 30 minutes at 125 °C under microwave irradiation. After cooling at room temperature, the solution was concentrated and purified using reverse phase HPLC. Compound **22** was obtained as a red solid (20% yield).

^1H NMR (400 MHz, CDCl_3) δ : 2.10 (q, 4H, $J = 7.3$ Hz, 2x CH_2), 2.83-2.77 (m, 12H, 6x CH_2), 3.76-3.73 (m, 8H, 4x CH_2), 4.28 (q, 4H, $J = 7.2$ Hz, 2x CH_2), 8.75 (d, 1H, $J = 7.6$ Hz, ArH), 8.80 (d, 1H, $J = 7.6$ Hz, ArH), 8.91 (s, 1H, ArH); ^{13}C NMR (100 MHz, CDCl_3) δ : 23.3 (t), 23.4 (t), 38.8 (t), 39.1

(t), 52.5 (t), 55.5 (t), 55.6 (t), 65.3 (t), 65.4 (t), 123.9 (d), 125.7 (s), 125.9 (d), 126.0 (d), 126.8 (s), 128.7 (s), 128.8 (s), 130.7 (s), 131.7 (s), 138.4 (s), 161.2 (s), 161.9 (s), 162.0 (s), 162.6 (s).

General procedure

Synthesis of 4-[[3-(4-methylpiperazin-1-yl)propyl]amino]-2,7-bis[3-(morpholin-4-yl)propyl]benzo[*lmn*][3,8]phenanthroline-1,3,6,8(2*H*,7*H*)-tetrone (13a)

Compound **22** (0.15 g, 0.25 mmol), 1(3-aminopropyl)-4-methyl-piperazine **19** (0.085 mL, 0.5 mmol) and NMP (*N*-methyl-2-pyrrolidinone) (2 mL) were suspended in a microwave reaction vessel. After bubbling nitrogen through the solution, the tube was capped and heated at 130 °C for 25 minutes under microwave irradiation. After cooling at room temperature, the solvent was concentrated and the crude mixture was purified by reverse phase HPLC. Compound **13a** was obtained as red oil (31% yield). ¹H NMR (400 MHz, CDCl₃) δ: 2.09-1.98 (m, 6H, 3xCH₂), 2.80-2.62 (m, 21H, 9xCH₂, 1xCH₃), 3.17 (bs, 4H, 2xCH₂), 3.69 (t, 6H, *J* = 5.0 Hz, 3xCH₂), 3.749 (t, 4H, *J* = 4.5 Hz, 2xCH₂), 4.23 (q, 4H, *J* = 6.73 Hz, 2xCH₂), 8.23 (s, 1H, ArH), 8.31 (d, 1H, *J* = 7.8 Hz, ArH), 8.61 (d, 1H, *J* = 7.8 Hz, ArH), 10.16 (t, 1H, *J* = 5.7 Hz, NH); ¹³C MNR (100 MHz, CDCl₃) δ: 23.61 (q), 23.67 (t), 26.2 (t), 38.2 (t), 38.8 (t), 41.2 (t), 43.3 (t), 50.2 (t), 52.5 (t), 52.7 (t), 53.0 (t), 54.5 (t), 55.7 (t), 65.5 (t), 65.7 (t), 99.9 (s), 119.4 (d), 119.7 (d), 123.4 (d), 124.6 (s), 126.1 (s), 127.9 (s), 129.5 (s), 131.4 (s), 152.3 (s), 163.0 (s), 163.1 (s), 163.3 (s), 166.0 (s).

Synthesis of 4-[[2-(4-methylpiperazin-1-yl)ethyl]amino]-2,7-bis[3-(morpholin-4-yl)propyl]benzo[*lmn*][3,8]phenanthroline-1,3,6,8(2*H*,7*H*)-tetrone (13b)

Compound **22** (0.073 g, 0.12 mmol), 2-(4-methyl-piperazin-1-yl) ethylamine **23** (0.036 mL, 0.24 mmol) and NMP (2 mL) were reacted according to General Procedure. Compound **13b** was obtained as a red oil (12% yield). ¹H NMR (400 MHz, CDCl₃) δ: 2.06-1.94 (m, 4H, 2xCH₂), 2.53 (bs, 4H, 2xCH₂), 2.58-2.68 (m, 11H, 4xCH₂ and 1xCH₃), 2.85-2.89 (m, 6H, 2xCH₂), 3.05 (bs, 4H, 2xCH₂), 3.61-3.63 (t, 4H, *J* = 4.4 Hz, 2xCH₂), 3.66-3.72 (m, 6H, 3xCH₂), 4.26 (q, 4H, *J* = 8.2 Hz, 2xCH₂), 8.21 (s, 1H, ArH), 8.34 (d, 1H, *J* = 7.8 Hz, ArH), 8.64 (d, 1H, *J* = 7.8 Hz, ArH), 10.79 (t, 1H, *J* = 4.9 Hz, NH); ¹³C NMR (100 MHz, CDCl₃) δ: 24.0 (q), 38.3 (t), 39.1 (t), 40.2 (t), 43.7 (t), 50.4 (t), 52.9 (t), 53.1 (t), 53.6 (t), 55.8 (t), 56.0 (t), 56.1 (t), 66.1 (t), 66.4 (t), 100.3 (s), 119.5 (d), 120.0 (d), 123.6 (s), 124.7 (d), 126.3 (s), 128.0 (s), 129.5 (s), 131.4 (s), 152.1 (s), 163.0 (s), 163.1 (s), 163.4 (s), 165.9 (s).

Synthesis of 2,7-bis[3-(morpholin-4-yl)propyl]-4-[[2-(pyrrolidin-1-yl)ethyl]amino]benzo[*lmn*][3,8]phenanthroline-1,3,6,8(2*H*,7*H*)-tetrone (13c)

Compound **22** (0.15 g, 0.25 mmol), 1-(2-aminoethyl)pyrrolidine **24** (0.063 mL, 0.5 mmol) and NMP (2 mL) were reacted according to General Procedure. The crude mixture was purified by column chromatography (DCM/MeOH/NH₃). Compound **13c** was obtained as red oil (16% yield).

¹H NMR (400 MHz, CDCl₃) δ: 2.04 (m, 8H, 4xCH₂), 2.68-2.78 (m, 12H, 6xCH₂), 3.19 (t, 4H, *J* = 6.3 Hz, 2xCH₂), 3.32 (t, 2H, *J* = 6.6 Hz, 1xCH₂), 3.71 (t, 4H, *J* = 4.6 Hz, 2xCH₂), 3.76 (t, 4H, *J* = 4.6 Hz, 2xCH₂), 4.01 (q, 2H, *J* = 6.5 Hz, 1xCH₂), 4.22 (t, 4H, *J* = 6.8 Hz, 2xCH₂), 8.14 (s, 1H, ArH), 8.29 (d, 2H, *J* = 4.1 Hz, ArH), 8.56 (d, 1H, *J* = 7.8 Hz, ArH), 10.17 (t, 1H, *J* = 5.7 Hz, NH); ¹³C NMR (100 MHz, CDCl₃) δ: 23.3 (t), 23.6 (t), 23.7 (t), 38.2 (t), 38.8 (t), 40.0 (t), 52.6 (t), 52.7 (t), 53.9 (t), 54 (t), 55.7 (t), 55.2 (t), 65.5 (t), 65.8 (t), 100.7 (s), 119.1 (d), 119.4 (d), 123.5 (s), 124.9 (s), 126.1 (d), 128.0 (s), 129.2 (s), 131.4 (s), 151.8 (s), 162.7 (s), 162.8 (s), 163.2 (s), 165.9 (s).

Synthesis of 2,7-bis[3-(morpholin-4-yl)propyl]-4-[[2-(pyridin-2-yl)ethyl]amino]benzo[*lmn*][3,8]phenanthroline-1,3,6,8(2*H*,7*H*)-tetrone (13d)

Compound **22** (0.15 g, 0.25 mmol), 2-(2-pyridyl)ethyl amine **25** (0.06 mL, 0.5 mmol) and NMP (2 mL) were reacted according to General Procedure. Compound **13d** was obtained as a red oil (8% yield). ¹H NMR (400 MHz, CDCl₃) δ: 1.90-1.96 (m, 4H, 2xCH₂), 2.49-2.58 (m, 12H, 6xCH₂), 3.22 (t, 2H, *J* = 7.2 Hz, 1xCH₂), 3.57 (t, 4H, *J* = 4.8 Hz, 2xCH₂), 3.61 (t, 4H, *J* = 4.4 Hz, 2xCH₂), 3.99 (q, 2H, *J* = 6.8 Hz, 1xCH₂), 4.16-4.20 (m, 4H, 2xCH₂), 7.11-7.13 (m, 1H, ArH), 7.14 (s, 1H, ArH), 7.56-7.61 (m, 1H, ArH), 8.20 (s, 1H, ArH), 8.26 (d, 1H, *J* = 7.82 Hz, ArH), 8.56 (m, 2H, ArH), 10.21 (t, 1H, *J* = 4.9 Hz, NH); ¹³C NMR (100 MHz, CDCl₃) δ: 23.2 (t), 24.2 (t), 37.6 (t), 37.7 (t), 38.5 (t), 39.2 (t), 42.8 (t), 53.2 (t), 53.3 (t), 56.2 (t), 66.4 (t), 66.5 (t), 100.1 (s), 119.8 (d), 121.9 (d), 123.5 (s), 123.6 (d), 124.5 (s), 126.2 (d), 128.0 (d), 129.5 (d), 131.3 (s), 136.8 (d), 149.7 (s), 152.3 (s), 157.8 (s), 163.0 (s), 163.1 (s), 163.4 (s), 166.1 (s).

Synthesis of 2,7-bis[3-(morpholin-4-yl)propyl]-4-[[4-(pyrrolidin-1-yl)butyl]amino]benzo[*lmn*][3,8]phenanthroline-1,3,6,8(2*H*,7*H*)-tetrone (13e)

Compound **22** (0.10 g, 0.17 mmol), 4-(1-pyrrolidinyl)-1-butylamine **26** (0.051 mL, 0.33 mmol) and NMP (2 mL) were reacted according to General Procedure. Compound **13e** was obtained as a red oil (15% yield). ¹H NMR (400 MHz, CDCl₃) δ: 1.75-1.84 (m, 12H, 6xCH₂), 2.32 (d, 8H, *J* = 4.0 Hz, 4xCH₂), 2.38-2.42 (m, 4H, 2xCH₂), 2.54 (d, 6H, *J* = 6.8 Hz, 3xCH₂), 3.44-3.52 (m, 10, 5xCH₂), 4.18 (bs, 4H, 2xCH₂), 8.09 (s, 1H, ArH), 8.23 (d, 1H, *J* = 7.8 Hz, ArH), 8.54 (d, 1H, *J* = 7.8 Hz, ArH), 10.03 (t, 1H, *J* = 5.36 Hz, NH); ¹³C NMR (100 MHz, CDCl₃) δ: 23.2 (t), 23.4 (t), 23.7 (t),

23.8 (t), 26.7 (t), 38.3(t), 38.9 (t), 42.4 (t), 52.7(t), 52.8 (t), 53.3 (t), 54.7 (t), 55.8 (t), 55.9 (t), 65.7 (t), 66.0 (t), 100.2 (s), 119.50 (d), 119.6 (d), 123.6 (s), 124.7 (d), 126.3 (s), 128.1 (s), 129.5 (s), 131.5 (s), 152.3 (s), 162.9 (s), 163.1 (s), 163.4 (s), 166.2 (s).

Synthesis of 2,7-bis[3-(morpholin-4-yl)propyl]-4-[[2-(piperidin-1-yl)ethyl]amino]benzo[*lmn*][3,8]phenanthroline-1,3,6,8(2*H*,7*H*)-tetrone (13f)

Compound **22** (0.10 g, 0.17 mmol), 1-(2-aminoethyl)piperidine **27** (0.05 mL, 0.33 mmol) and NMP (2 mL) were reacted according to General Procedure. Compound **13f** was obtained as a red oil (12% yield). ¹H NMR (400 MHz, CDCl₃) δ: 1.52-1.55 (m, 2H, CH₂), 1.69-1.75 (m, 4H, 2xCH₂), 1.93-2.02 (m, 4H, 2xCH₂), 2.51-2.62 (m, 12H, 6xCH₂), 2.68 (bs, 4H, 2xCH₂), 2.87 (t, 2H, *J* = 6.5 Hz, 1xCH₂), 3.61 (t, 4H, *J* = 4.5 Hz, 2xCH₂), 3.67 (t, 4H, *J* = 4.5 Hz, 2xCH₂), 3.78 (q, 2H, *J* = 6.2 Hz, CH₂), 4.25 (q, 4H, *J* = 8.6 Hz, 2xCH₂), 8.18 (s, 1H, ArH), 8.30 (d, 1H, *J* = 7.8 Hz, ArH), 8.61 (d, 1H, d, *J* = 7.8 Hz, ArH), 10.24 (t, 1H, t, *J* = 5.0 Hz, NH); ¹³C NMR (100MHz, CDCl₃) δ: 23.8 (t), 24.2 (t), 25.2 (t), 38.5 (t), 39.1 (t), 39.9 (t), 40.0 (t), 53.1 (t), 53.2 (t), 54.3 (t), 56.2 (t), 56.8 (t), 66.4 (t), 66.5 (t), 100.3 (s), 119.5 (d), 119.8 (s), 123.6 (d), 124.5 (d), 126.2 (s), 128.0 (s), 129.5 (s), 131.3 (s), 152.0 (s), 162.9 (s), 163.1 (s), 163.4 (s), 165.9 (s).

Synthesis of 4-[[2-(4-hydroxyphenyl)ethyl]amino]-2,7-bis[3-(morpholin-4-yl)propyl]benzo[*lmn*][3,8]phenanthroline-1,3,6,8(2*H*,7*H*)-tetrone [13g]

Compound **22** (0.14 g, 0.23 mmol), tyramine-hydrochloride **28** (0.08 g, 0.46 mmol), NMP (2 mL) and triethylamine (0.46 mmol, 0.065 mL) were suspended in a microwave reaction vessel. After bubbling nitrogen through the solution, the tube was capped and heated at 130 °C for 25 minutes under microwave irradiation. After cooling at room temperature, the solvent was concentrated in vacuo and the crude mixture was purified by column chromatography on a silica gel (DCM, MeOH, NH₃). Compound **13g** was obtained as red oil (23% yield). ¹H NMR (400 MHz, DMSO-*d*₆) δ: 1.75-1.82 (m, 4H, 2xCH₂), 2.31-2.44 (m, 12H, 6xCH₂), 2.90 (t, 2H, *J* = 6.7 Hz, CH₂), 3.41-3.44 (m, 8H, 4xCH₂), 3.70 (d, 2H, *J* = 5.8, 1xCH₂), 4.02 (bs, 4H, 2xCH₂), 6.71-6.73 (m, 2H, ArH), 7.14-7.16 (m, 2H, ArH), 7.84 (s, 1H, ArH), 8.02 (d, 1H, *J* = 7.7 Hz, ArH), 8.31 (d, 1H, d, *J* = 7.7 Hz, ArH), 9.86 (s, 1H, OH); ¹³C NMR (100 MHz, CDCl₃) δ: 24.3 (t), 24.6 (t), 29.7 (t), 35.2 (t), 38.4 (t), 44.9 (t), 53.4 (t), 53.5 (t), 56.2 (t), 56.4 (t), 66.6 (t), 66.8 (t), 116.0 (d), 116.1 (d), 119.5 (s), 120.2 (s), 124.6 (d), 126.2 (s), 130.2 (d), 131.3 (d), 145.4 (s), 152.8 (s), 155.3 (s), 163.0 (s), 163.2 (s), 163.5 (s), 165.7 (s).

Synthesis of 4-{{2-(morpholin-4-yl)ethyl}amino}-2,7-bis[3-(morpholin-4-yl)propyl]benzo[*lmn*][3,8]phenanthroline-1,3,6,8(2*H*,7*H*)-tetrone [13h]

Compound **22** (0.06 g, 0.1 mmol), 4-(2-aminoethyl) morpholine **29** (0.03 mL, 0.2 mmol), NMP (1 mL) were reacted according to General Procedure. The crude mixture was purified by column chromatography (DCM/MeOH). Compound **13h** was obtained as red oil (23% yield). ¹H NMR (500 MHz, CDCl₃) δ: 1.89-1.98 (m, 4H, 2xCH₂), 2.41-2.45 (m, 8H, 4xCH₂), 2.51 (q, 4H, *J* = 6.9 Hz, 2xCH₂), 2.59 (t, 4H, *J* = 4.5 Hz, 2xCH₂), 2.80 (t, 2H, *J* = 6.2 Hz, 1xCH₂), 3.56 (t, 4H, *J* = 4.5 Hz, 2xCH₂), 3.62 (t, 4H, *J* = 4.5 Hz, 2xCH₂), 3.68 (q, 2H, *J* = 5.9 Hz, 1xCH₂), 3.78 (t, 4H, *J* = 4.5 Hz, 2xCH₂), 4.24-4.30 (m, 4H, 2xCH₂), 8.21 (s, 1H, ArH), 8.33 (d, 1H, *J* = 7.8 Hz, ArH), 8.64 (d, 1H, *J* = 7.8 Hz, ArH), 10.34 (t, 1H, *J* = 4.5 Hz, NH); ¹³C NMR (100 MHz, CDCl₃) δ: 24.4 (t), 24.6 (t), 38.7 (t), 39.3 (t), 40.1 (t), 53.5 (t), 53.6 (t), 56.4 (t), 56.5 (t), 56.8 (t), 66.9 (t), 67.0 (t), 67.1 (t), 100.3 (s), 119.4 (d), 120.0 (s), 123.8 (d), 124.5 (d), 126.2 (s), 127.9 (s), 129.5 (s), 131.3 (s), 152.1 (s), 163.1 (s), 163.5 (s), 166.0 (s).

Synthesis of 2,7-bis[3-(morpholin-4-yl)propyl]-4-[(tetrahydrofuran-2-ylmethyl)amino]benzo[*lmn*][3,8]phenanthroline-1,3,6,8(2*H*,7*H*)-tetrone [13i]

Compound **22** (0.06 g, 0.1 mmol), racemic tetrahydrofurfurylamine **30** (0.021 mL, 0.21 mmol), NMP (1 mL) were reacted according to General Procedure. The crude mixture was purified by column chromatography (DCM/MeOH). Compound **13i** was obtained as red oil (17% yield). ¹H NMR (500 MHz, CDCl₃) δ: 1.26-1.77 (m, 4H, 2xCH₂), 1.94-2.18 (m, 8H, 4xCH₂), 2.43-2.51 (m, 10H, 5xCH₂), 3.64-3.56 (m, 8H, 4xCH₂), 3.74-4.0 (m, 2H), 4.25-4.28 (m, 4H, 2xCH₂), 8.27 (s, 1H, ArH), 8.34 (d, 1H, *J* = 7.7 Hz, ArH), 8.65 (d, 1H, *J* = 7.7 Hz, ArH), 10.34 (s, 1H, NH); ¹³C NMR (100 MHz, CDCl₃) δ: 24.4 (t), 24.6 (t), 25.9 (t), 29.2 (t), 38.7 (t), 39.3 (t), 47.3 (t), 53.6 (t), 56.5 (t), 56.6 (t), 66.9 (t), 67.0 (t), 68.6 (t), 100.2 (t), 119.5 (d), 120.0 (d), 123.7 (s), 124.5 (d), 126.2 (s), 127.9 (s), 129.5 (s), 131.2 (s), 152.5 (s), 163.1 (s), 163.2 (s), 163.4 (s), 166.2 (s).

Synthesis of 4-{{2-(diethylamino)ethyl}amino}-2,7-bis[3-(morpholin-4-yl)propyl]benzo[*lmn*][3,8]phenanthroline-1,3,6,8(2*H*,7*H*)-tetrone [13j]

Compound **22** (0.024 g, 0.04 mmol), 2-diethylamino ethylamine **31** (0.08 mmol, 0.011 mL), NMP (1 mL) were reacted according to General Procedure. The crude mixture was purified by column chromatography (DCM/MeOH/NH₃). Compound **13j** was obtained as red oil (60 % of yield). ¹H NMR (500 MHz, CDCl₃) δ: 1.08-1.11 (m, 6H, 2xCH₃), 1.90-2.98 (m, 4H, 2xCH₂), 2.43-2.54 (m, 12H, 6xCH₂), 2.67 (q, 4H, *J* = 6.6 Hz, 2xCH₂), 2.86 (t, 2H, *J* = 6.0 Hz, 1xCH₂), 3.57 (t, 4H, *J* = 4.4 Hz, 2xCH₂), 3.61-3.65 (m, 6H, 3xCH₂), 4.23-4.30 (m, 4H, 2xCH₂), 8.21 (s, 1H, ArH), 8.31 (d, 1H,

$J = 7.8$ Hz, ArH), 8.62 (d, 1H, $J = 7.8$ Hz, ArH), 10.27 (t, 1H, $J = 4.9$ Hz, NH); ^{13}C NMR (100 MHz, CDCl_3) δ : 11.8 (q), 24.4 (t), 24.5 (t), 38.6 (t), 39.3 (t), 47.1 (t), 51.6 (t), 53.5 (t), 53.56 (t), 56.5 (t), 66.9 (t), 100.1 (s), 119.4 (d), 120.2 (d), 123.7 (s), 124.3 (d), 126.2 (s), 127.8 (s), 129.6 (s), 131.2 (s), 152.1 (s), 163.1 (s), 163.2 (s), 163.5 (s), 165.9 (s).

BIOPHYSICAL STUDIES: FRET ASSAY

The ability of the naphthalene diimide compounds to stabilize DNA sequences was investigated using a fluorescence resonance energy transfer (FRET) assay modified to be used as a high-throughput screen in a 96-well format. Several quadruplex sequences were studied (including the human telomeric G-quadruplex DNA sequence 5'-FAM-d(GGG[TTAGGG]₃)-TAMRA-3' and the duplex sequence 5'-FAM-dTATAGCTATA-HEG-TATAGCTATA-TAMRA-3' (HEG linker: [(-CH₂-CH₂-O-)]₆).

The labelled oligonucleotides have attached to them the donor fluorophore FAM: 6-carboxyfluorescein and the acceptor fluorophore TAMRA: 6-carboxytetramethylrhodamine. The FRET probe sequences were diluted from stock to the correct concentration (400 nM) in a 60 mM potassium cacodylate buffer (pH 7.4) and then annealed by heating to 85 °C for 10 min, followed by cooling to room temperature in the heating block. The compound was stored as a 10 mM stock solution in DMSO; final solutions (at 2 × concentration) were prepared using 10 mM HCl in the initial 1:10 dilution, after which 60 mM potassium cacodylate buffer (pH 7.4) was used in all subsequent steps. The maximum HCl concentration in the reaction volume (at a ligand concentration of 20 μM) is thus 200 μM, well within the range of the buffer used. Relevant controls were also performed to check for interference with the assay. 96-Well plates (MJ Research, Waltham, MA) were prepared by aliquoting 50 μl of the annealed DNA into each well, followed by 50 μl of the compound solutions. Measurements were made on a DNA Engine Opticon (MJ Research) with excitation at 450–495 nm and detection at 515–545 nm. Fluorescence readings were taken at intervals of 0.5 °C in the range 30–100 °C, with a constant temperature being maintained for 30 s prior to each reading to ensure a stable value. Final analysis of the data was carried out using a script written in the program Origin 7.0 (OriginLab Corp., Northampton, MA). The advanced curve-fitting function in Origin 7.0 was used for calculation of ΔT_m values. All determinations were performed in triplicate or better. Esds in ΔT_m are ± 0.1 °C.

IN VITRO CELL ASSAY

Cell culture and cytotoxicity testing. Human cancer cell lines and the somatic human cell line WI-38 (lung fibroblast) were purchased from ATCC. Cell lines were maintained in appropriate medium supplemented with 10 % foetal bovine serum (Invitrogen, UK), 2 mM L-glutamine (Invitrogen, Netherlands), and other components as specified by the suppliers. Cell lines were maintained at 37 °C, 5% CO₂ and routinely passaged. Drugs were dissolved in DMSO and filtered through 0.22 µm pore-size filter units before addition to cell line appropriate media. Cellular growth inhibition was measured using the sulforhodamine B (SRB) assay in 96 well plates as described previously [39, 48]. Fifty percent inhibitory concentrations (IC₅₀) were determined by taking the mean absorbance at 540 nm for each drug concentration expressed as a percentage of the absorbance of untreated control wells. For qRT-PCR analysis, Mia PaCa-2 cells were seeded to a density equivalent to that used for IC₅₀ determinations in T75 culture flasks and grown for 24 h in 10 ml DMEM to allow attachment before addition of compounds to the culture medium. Following compound exposure, cells were washed twice in PBS, harvested by trypsinisation, collected by centrifugation (300 g, 5 min, 4°C) and re-suspended in RLT buffer (Qiagen). Samples were homogenised using QIAshredder spin columns and stored at -80 °C prior to RNA extraction. Three biological replicates were performed on separate days.

REFERENCES

1. T. Ou, Y. Lu, J. Tan, Z. Huang, K.Y. Wong, L.Gu, *Chem. Med. Chem.*, **2008**, *3*, 690-713.
2. M. Gellert, M. N. Lipsett, D. R. Davies, *Proc. Natl. Acad. Sci. USA*, **1962**, *48*, 2013-2018.
3. M. Franceschin, A. Alvino, G. Ortaggi, A. Bianco, *Tetrahedron Letters*, **2004**, *45*, 9015-9020.
4. T. Shalaby, G. Fiaschetti, K. Nagasawa, K. Shin-ya, M. Baumgartner, M. Grotzer, *Molecules*, **2013**, *18*, 12500-12537.
5. A. De Cian, E. De Lemos, J.L. Mergny, M.P. Teulade-Fichou, D. Monchaud, *J. Am. Chem. Soc.*, **2007**, *129*, 1856-1857.
6. S. Needle, *Therapeutic Applications of Quadruplex Nucleic Acids*, edited by Elsevier, **2012**, Ch.1.
7. G.N. Parkinson, M.P. Lee, S. Neidle, *Nature*, **2002**, *417*, 876-880.
8. A.T. Phan, Y.S. Modi, D.J. Patel, *J. Am. Chem. Soc.*, **2004**, *126*, 8710-8716.
9. S. Rankin, A.P. Reszka, J. Huppert, M. Zloh, G.N. Parkinson, A.K. Todd, S. Ladame, S. Balasubramanian, S. Neidle, *J. Am. Chem. Soc.*, **2005**, *127*, 10584-10589.
10. S. Cogoi, L.E. Xodo, *Nucleic Acids Res.*, **2006**, *34*, 2536-2549.
11. K. Guo, A. Pourpak, K. Beetz-Rogers, V. Gokhale, D. Sun, L.H. Hurley, *J. Am. Chem. Soc.*, **2007**, *129*, 10220-10228.
12. T. Mitchell, A. Ramos-Montoya, M. Di Antonio, P. Murat, S. Ohnmacht, M. Micco, S. Jurmeister, L. Fryer, S. Balasubramanian, S. Neidle, D.E. Neal, *Biochemistry*, **2013**, *52*, 1429-1436.
13. S.A. Ohnmacht, M. Micco, V. Petrucci, A.K. Todd, A.P. Reszka, M. Gunaratnam, M.A. Carvalho, M. Zloh, S. Neidle, *Bioorg. Med. Chem. Lett.*, **2013**, *22*, 5930-5935.
14. Y. Qin, E.M. Rezler, V. Gokhale, D. Sun, L.H. Hurley, *Nucleic Acids Res.*, **2007**, *35*, 7698-7713.
15. D. Sun, W.J. Liu, K. Guo, J.J. Rusche, S. Ebbinghaus, V. Gokhale, L.H. Hurley, *Mol. Cancer Ther.* **2008**, *7*, 880-889.
16. J.L. Huppert, A. Bugaut, S. Kumari, S. Balasubramanian, *Nucleic Acids Res.*, **2008**, *36*, 6260-6268.
17. K. Derecka, G.D. Balkwill, T.P. Garner, C. Hodgman, A.P. Flint, M.S. Searle, *Biochemistry*, **2010**, *49*, 7625-7633.

18. M.J. Morris, S. Basu, *Biochemistry*, **2009**, *48*, 5313-5319.
19. R. Shahid, A. Bugaut, S. Balasubramanian, *Biochemistry*, **2010**, *49*, 8300-8306.
20. S. Neidle, *Medicinal Chemistry Approaches to Personalized Medicine (Methods and Principles in Medicinal Chemistry)*, edited by K. Lackey and B. Roth, **2013**, Ch. 6.
21. T. De Lange, *Genes & Development*, **2005**, *19*, 2100-2110.
22. J. Nandakumar, T.R. Cech, *Nature Reviews Molecular Cell Biology*, **2013**, *14*, 69-82.
23. G.Z. Li, M.S. Eller, R. Firoozabadi, B.A. Gilchrest, *Proceedings of the National Academy of Sciences of the United States of America*, **2003**, *100*, 527-531.
24. J. Vargas, BC. Feltes, J. de Faria Poloni, G. Lenz, D. Bonatto, *Frontiers in Bioscience*, **2012**, *17*, 2616-2643.
25. N.W. Kim, M.A. Piatyszek, K.R. Prowse, C.B. Harley, M.D. West, P.L. Ho, G.M. Corvillo, W.E. Wright, S.L. Weinrich, J.W. Shay, *Science*, **1994**, *266*, 2011-2015.
26. M. Franceschin, A. Alvino, V. Casagrande, C. Mauriello, E. Pascucci, M. Savino, G. Ortaggi, A. Bianco, *Bioorg. Med. Chem.*, **2007**, *15*, 1848-1858.
27. K. Shin-ya, K. Wierzba, K. Matsuo, T. Ohtani, Y. Yamada, K. Furihata, Y. Hayakawa, H. Seto, *J. Am. Chem. Soc.*, **2001**, *123*, 1262-1263.
28. A. D. Moorhouse, S. Haaider, M. Gunaratnam, D. Munnur, S. Neidle, J. E. Moses, *Mol. Bio. Syst.*, **2008**, *4*, 629-642.
29. M. Sumi, T. Tauchi, G. Sashida, A. Nakajima, A. Gotoh, K. Shin-Ya, J.H. Ohyashiki, K. Ohyashiki, *Int. J. Oncol.*, **2004**, *24*, 1481-1487.
30. S. Needle, *Therapeutic Applications of Quadruplex Nucleic Acids*, edited by Elsevier, **2012**, Ch.7.
31. T. Shalaby, A.O. von Bueren, M.L. Hürlimann, G. Fiaschetti, D. Casteletti, T. Masayuki, K. Nagasawa, A. Arcaro, I. Jelesarov, K. Shin-ya, M. Grotzer, *Mol. Cancer Ther.*, *9*, **2010**, 167-179.
32. W. Duan, A. Rangan, H. Vankayalapati, M.Y. Kim, Q. Zeng, D. Sun, H. Han, O.Y. Fedoroff, D. Nishioka, S.Y. Rha, E. Izbicka, D.D. Von Hoff, L.H. Hurley, *Mol. Cancer Ther.*, **2001**, *1*, 103-120.
33. D. Drygin, A. Siddiqui-Jain, S. O'Brien, M. Schwaebe, A. Lin, J. Bliesath, *Cancer Res.* **2009**, *71*, 1418-1430.

34. A.M. Zahler, J.W. Williamson, T.R. Cech, D.M. Prescott, *Nature*, **1991**, 350, 718-720.
35. S. Neidle, *Therapeutic Applications of Quadruplex Nucleic acids*, Elsevier, London, 1st Ed., **2012**, Ch. 4.
36. S. Neidle, *FEBS Journal*, **2010**, 277, 1118-1125.
37. S.M. Gowan, J.R. Harrison, L. Patterson, *Mol. Pharmacol.*, **2002**, 61, 1154-1162.
38. F. Cuenca, O. Greciano, M. Gunaratnam, S. Haider, D. Munnur, R. Nanjunda, W.D Wilson, S. Neidle, *Bioorg. Med. Chem. Lett.*, **2008**, 18, 1668-1673.
39. S.M. Hampel, A. Sidibe, M. Gunaratnam, J.F. Riou, S. Neidle, *Bioorg. Med. Chem. Lett.*, **2010**, 20, 6459-6463.
40. M. Gunaratnam, M. de la Fuente, S.M. Hampel, A.K. Todd, A.P. Reszka, A. Schätzlein, S. Neidle, *Bioorg. Med. Chem.*, **2011**, 19, 7151-7157.
41. G.W. Collie, R. Promontorio, S.M. Hampel, M. Micco, S. Neidle, GN. Parkinson, *J. Am. Chem. Soc.*, **2012**, 134, 2723-2731.
42. M. Micco, G.W. Collie, A.G. Dale, S.A. Ohnmacht, I. Pazitna, M. Gunaratnam, AP. Reszka, S. Neidle, *J. Med. Chem.*, **2013**, 56, 2959-2974.
43. F. Chaignon, M. Falkenström, S. Karlsson, E. Blart, F. Obodel, L. Hammarström, *Chem. Commun.*, **2007**, 7, 64-66.
44. M. Sasikumar, Y.V. Suseela, T. Govindaraju, *Asian J. Org. Chem.*, **2013**, 2, 779-785.
45. K.E. Sapsford, L. Berti, I.L. Medintz, *Angew. Chem. Int. Ed. Engl.*, **2006**, 45, 4562-4589.
46. J.L. Mergny, J.C. Maurizot, *Chem. Biochem.*, **2001**, 2, 124-132.
47. X. Lu, W. Zhu, Y. Xie, X. Li, Y. Gao, F. Li, H. Tian, *Chemistry - A European Journal*, **2010**, 16, 8355-8364.
48. M. Gunaratnam, S. Swank, S.M. Haider, K. Galesa, A.P. Reszka, M. Beltran, F. Cuenca, J.A. Fletcher, S. Neidle, *J. Med. Chem.*, **2009**, 52, 3774-3783.

DISCOVERY OF NEW G-QUADRUPLEX BINDING CHEMOTYPES (SCHOOL OF PHARMACY, UCL)

INTRODUCTION

During the months spent at the UCL School of Pharmacy, I have been involved in a collaboration concerning the synthesis of new G-quadruplex binding chemotypes, which was object of a publication [1]. In particular, I have dealt with the high-throughput 96-well FRET (Fluorescence Resonance Energy Transfer) assay of some acyclic furan- and thiophene based compounds (**1-6**), in order to evaluate the ability to stabilize G-quadruplex sequences.

G-quadruplexes are high-order nucleic acid arrangements involving a core π - π stacked guanine-quartets (G-quartets) [2]. The targeting of quadruplex DNA sequences in telomers and in oncogene promoter regions is emerging as a novel approach to anticancer therapy, mainly because the existence of quadruplex DNA with nucleic acid motifs distinct from double stranded DNA has been validated at genomic level [3].

A large number of small molecules have been reported as G-quadruplex binding ligands [4, 5, 6]. Only few small molecules that interact with G-quadruplex DNA have achieved *in vivo* studies in models of human cancer, such as quarfloxacin, a fluoroquinolone derivative which has reached clinical trials [7].

RESULTS AND DISCUSSIONS

Thirty-eight members of a large chemical library from the anti-parasitic drug discovery programme at Georgia State University (several hundred compounds) [8, 9] with very different scaffolds and functional groups, were screened using a high-throughput 96-well FRET (Fluorescence Resonance Energy Transfer) assay [10]. G4 stabilization was initially evaluated using dual-labelled F21T (human telomeric 21-mer) and c-KIT2 (a tyrosine kinase oncogene) G-quadruplex sequences, as well as a duplex DNA sequence (T-loop). The ten most active compounds were subsequently screened against an expanded panel of fluorescently-labelled promoter G4-forming sequences, with Hsp90A, Hsp90B (heat shock protein 90 promoter sequences), Kras21 (in the promoter of the k-RAS oncogene) and AR, a G-quadruplex sequence recently identified in the promoter of the androgen receptor (involved in prostate cancer development) [11]. Six acyclic furan- and thiophene-based compounds **1-6** showed high ΔT_m values (>15 °C) (Fig. 1).

Figure 1. Structures of compounds **1-6**, a control compound **7** and tetra-substituted naphthalene diimide **10d**.

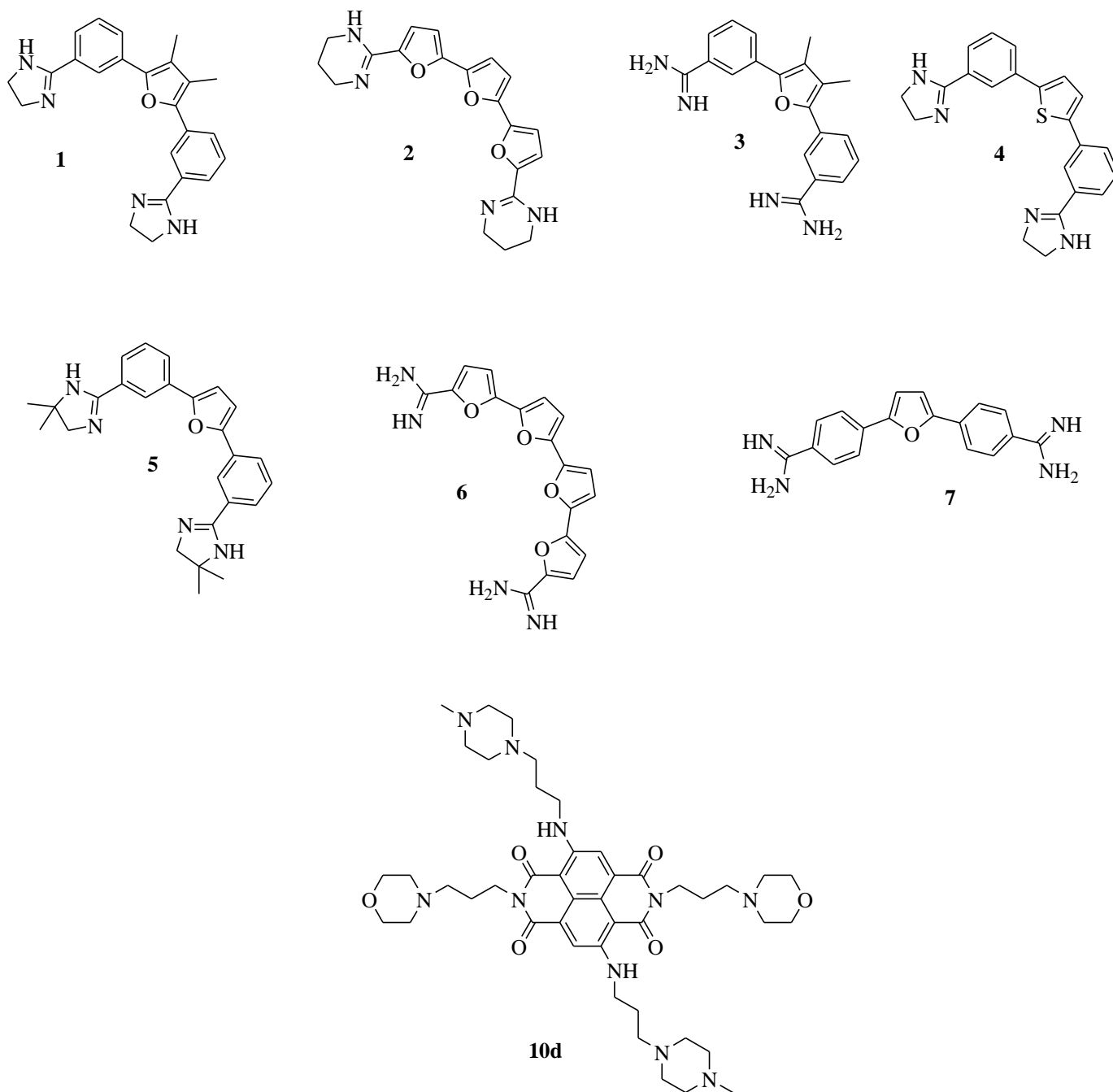


Table 1. FRET G4 stabilization (ΔT_m at 1 μ M in $^{\circ}$ C). Compound **7**, a negative control, is a *para* analogue of the mono-furan compounds. Compound **10d** is a tetra-substituted naphthalene diimide derivative used here as a G4 control [12].

| Compd | Mol. Wt | F21T | c-KIT2 | Hsp90A | Hsp90B | Kras21R | AR | T-Loop |
|------------|---------|------|--------|--------|--------|---------|------|--------|
| 1 | 384.5 | 22.3 | 16.8 | 27.7 | 23.7 | 19.6 | 15.4 | <2 |
| 2 | 364.4 | 20.4 | 16.3 | 26.0 | 22.0 | 18.5 | 13.8 | <2 |
| 3 | 330.5 | 17.6 | 17.8 | 21.2 | 18.1 | 15.1 | 11.9 | 2.2 |
| 4 | 372.5 | 18.0 | 13.9 | 22.5 | 19.1 | 15.9 | 10.2 | <2 |
| 5 | 412.5 | 22.6 | 18.5 | 26.6 | 22.7 | 18.3 | 14.7 | <2 |
| 6 | 350.3 | 18.6 | n/a | 20.6 | 16.2 | 13.4 | 10.1 | <2 |
| 7 | 302.5 | 14.4 | 12.2 | 19.0 | 15.7 | 16.6 | 9.9 | 3.4 |
| 10d | 830.6 | 26.6 | 22.0 | 33.1 | 28.6 | n/a | 15.9 | 4.9 |

All six compounds showed potent G-quadruplex stabilizing properties, as demonstrated by the large ΔT_m values for the selected G-quadruplex sequences. In particular, the bis-phenyl-mono-furan compounds **1** and **5** had very high ΔT_m values, widely comparable to those reported for tetra-substituted naphthalene diimides [12]. The tri-furan compound **2** is much more active in stabilizing the G-quadruplex than the polyfuran compound **6**.

Generally, F21T and the two Hsp90 G-quadruplex sequences have been most stabilized by compound **1-6**.

Comparing the stabilizing properties against AR G-quadruplex sequence of compounds **1-6** with the tetra-substituted naphthalene diimides already published [11], it is possible to observe that compound **1-6** exhibited only moderate ΔT_m values, which are generally lower than with the other G-quadruplexes. Compounds **1-6** produced slightly reduced but still significant stabilization of c-KIT2 and Kras21 G-quadruplexes, suggesting that these compounds have the ability to act simultaneously on multiple G-quadruplex sequences (G4-poly-targeting). In general for all the compounds the stabilization of the duplex DNA sequence (T-Loop) was not significant at the biologically relevant concentrations employed (1 μ M) and compounds **1** and **5** exhibited a particular selectivity for G-quadruplexes *versus* duplex DNA. A control compound **7**, an established duplex DNA minor groove binder, also showed a significant stabilization, although with higher effects on the duplex DNA.

In conclusion, these compounds are structurally-simple, chemically readily accessible with MW <400 Da. They have G-quadruplex stabilisation ability comparable to those previously observed with polycyclic heteroaromatic compounds [12] (such as compound **8**, showed in Table 1), but with low duplex DNA affinity.

EXPERIMENTAL DATA

CHEMISTRY

Synthesis was performed at Georgia State University.

BIOPHYSICAL STUDIES: FRET ASSAY

The ability of the compounds to stabilize DNA sequences was investigated using a fluorescence resonance energy transfer (FRET) assay modified to be used as a high-throughput screen in a 96-well format. Several quadruplex sequences were studied (including the human telomeric G-quadruplex DNA sequence 5'-FAM-d(GGG[TTAGGG]₃)-TAMRA-3' and the duplex sequence 5'-FAM-dTATAGCTATA-HEG-TATAGCTATA-TAMRA-3' (HEG linker: [(-CH₂-CH₂-O-)]₆).

The labelled oligonucleotides have attached to them the donor fluorophore FAM: 6-carboxyfluorescein and the acceptor fluorophore TAMRA: 6-carboxytetramethylrhodamine. The FRET probe sequences were diluted from stock to the correct concentration (400 nM) in a 60 mM potassium cacodylate buffer (pH 7.4) and then annealed by heating to 85 °C for 10 min, followed by cooling to room temperature in the heating block. The compound was stored as a 10 mM stock solution in DMSO; final solutions (at 2 × concentration) were prepared using 10 mM HCl in the initial 1:10 dilution, after which 60 mM potassium cacodylate buffer (pH 7.4) was used in all subsequent steps. The maximum HCl concentration in the reaction volume (at a ligand concentration of 20 μM) is thus 200 μM, well within the range of the buffer used. Relevant controls were also performed to check for interference with the assay. 96-Well plates (MJ Research, Waltham, MA) were prepared by aliquoting 50 μl of the annealed DNA into each well, followed by 50 μl of the compound solutions. Measurements were made on a DNA Engine Opticon (MJ Research) with excitation at 450-495 nm and detection at 515-545 nm. Fluorescence readings were taken at intervals of 0.5 °C in the range 30-100 °C, with a constant temperature being maintained for 30 s prior to each reading to ensure a stable value. Final analysis of the data was carried out using a script written in the program Origin 7.0 (OriginLab Corp., Northampton, MA). The advanced curve-fitting function in Origin 7.0 was used for calculation of ΔT_m values. All determinations were performed in triplicate or better. Esds in ΔT_m are ± 0.1 °C.

REFERENCES

1. S.A. Ohnmacht, E. Varavipour, R. Nanjunda, I. Pazitna, G. Di Vita, M. Gunaratnam, A. Kumar, M. A. Ismail, D.W. Boykin, W. D. Wilson, S. Neidle, *Chem. Commun.*, **2014**, *50*, 960-963.
2. S. Burge, G.N. Parkinson, P. Hazel, A.K. Todd, S. Neidle, *Nucleic Acids Res.*, **2006**, *34*, 5402-5415.
3. K.P. Bhabak, C. Arenz, *Bioorg. Med. Chem.*, **2013**, *21*, 6162-6170.
4. D. Monchard, M.P. Teulade-Fichou, *Org. Biomol. Chem.*, **2008**, *6*, 627-636.
5. T.M. Ou, Y.J. Lu, J.H. Tan, Z.S. Huang, K.Y. Wong, L.Q. Gu, *Chem. Med. Chem.*, **2008**, *3*, 690-713.
6. D.Z. Yang, K. Okamoto, *Future Med. Chem.*, **2010**, *2*, 619-646.
7. D. Drygin, A. Siddiqui-Jain, S. O'Brien, M. Schwaebe, A. Lin, J. Bliesath, C.B. Ho, C. Proffitt, K. Trent, J.P. Whitten, J.K. Lim, D. Von Hoff, K. Anderes, W.G. Rice, *Cancer Res.*, **2009**, *69*, 7653-7661.
8. B. Nguyen, C. Tardy, C. Bailly, P. Colson, C. Houssier, A. Kumar, D.W. Boykin, W.D. Wilson, *Biopolymers*, **2002**, *63*, 281-297.
9. R. Nanjunda, C. Musetti, A. Kumar, M. A. Ismail, A.A. Farahat, S. Wang, C. Sissi, M. Palumbo, D.W. Boykin, W.D. Wilson, *Curr. Pharm. Des.*, **2012**, *18*, 1934-1947.
10. B. Guyen, C.M. Schultes, P. Hazel, J. Mann, S. Neidle, *Org. Biomol. Chem.*, **2004**, *2*, 981-988.
11. T. Mitchell, A. Ramos-Montoya, M. Di Antonio, P. Murat, S. Ohnmacht, M. Micco, S. Jurmeister, L. Fryer, S. Balasubramanian, S. Neidle, D. E. Neal, *Biochemistry*, **2013**, *26*, 1429-1436.
12. M. Micco, G.W. Collie, A.G. Dale, S.A. Ohnmacht, I. Pazitna, M. Gunaratnam, A.P. Reszka, S. Neidle, *J. Med. Chem.*, **2013**, *56*, 2959-2974.